VIBRATION AND BUCKLING ANALYES OF TAPERED COMPOSITE BEAMS USING CONVENTIONAL AND ADVANCED FINITE ELEMENT FORMULATIONS

Abolghassem Zabihollah

A Thesis

in

The Department

Of

Mechanical and Industrial Engineering

Presented in Partial Fulfillment of the Requirements

for the Degree of Master of Applied Science at

Concordia University

Montreal, Quebec, Canada

June 2003

Your file Votre référence
ISBN: 0-612-83891-9
Our file Notre référence
ISBN: 0-612-83891-9

ABSTRACT

Vibration and buckling analyses of tapered composite beams using conventional and advanced finite element formulations

Abolghassem Zabihollah

Tapered composite beams are being used in various engineering applications such as helicopter yoke, robot arms and turbine blade in which the structure needs to be stiff at one location and flexible at another locations. Laminated tapered beams can be manufactured by terminating some plies at discrete locations. Different types of ply drop-off can be achieved depending on the application. Due to the variety of tapered composite beams and complexity of the analysis, no analytical solution is available at present and therefore finite element method has been used for the calculation of response. In the present thesis, the free vibration response and buckling of different types of tapered composite beams are analyzed first using conventional finite element formulation. Conventional finite element formulation requires a large number of elements to obtain acceptable results. In addition, continuity of curvature at element interfaces can not be guaranteed with the use of conventional formulation. As a result, stress distribution across the thickness is not continuous at element interfaces. In order to overcome these limitations, an advanced finite element formulation is developed in the present thesis for vibration and buckling analysis of tapered composite beams based on classical laminate theory and first-order shear deformation theory. The developed formulation is applied to

the analysis of various types of tapered composite beams. The efficiency and accuracy of the developed formulation are established in comparison with available solutions, where applicable, as well as with the results obtained using conventional formulation. A detailed parametric study has been conducted on various types of tapered composite beams, all made of NCT / 301 graphite-epoxy, in order to investigate the effects of boundary conditions, laminate configuration, taper angle, the ratio of the length of the thick section to the length of the thin section and the ratio of the height of the thick section, to the height of thin section.

ACKNOWLEDGMENTS

I wish to express my heartfelt and profound gratitude to my supervisor Dr. Rajamohan Ganesan for his invaluable guidance, assistance and inspiration throughout the span of this work and for his helpful financial support.

I would also like to express my deep appreciation to my wife. Without her love and encouragement this work would not have been possible.

CONTENTS

List of Figures

List of Tables

Nomenclature

φ_x	Rotation about y-axis
w	Displacement in thickness direction
b	Width of the beam
M_x	Bending moment per unit width
N_x^i	Initial axial force per unit width
$q(x)$	Lateral load per unit width
ρ_s	Density of the laminate per unit width
t	Time variable
B_{ij}	Coefficients of bending-stretching coupling matrix
u_o	Mid-plane displacement in x-direction
v_o	Mid-plane displacement in y-direction
D_{11}	The first coefficient of bending stiffness matrix of composite beam
σ_z	Stress in thickness direction
h	Thickness of the laminate
ρ_k	Density of individual ply of the laminate
E	Modulus of elasticity of isotropic material
I	Moment of inertia
A	Cross-section area
l	Length of finite element
Q_i	Secondary variable in the weak form

φ_i Rotation at i^{th} node

v Weight function for the finite element

w_i^e Degrees of freedom for the finite element e

W^e Deflection of the finite element e

c_i^e Variables for deflection of beam element in Euler-Bernoulli beam theory

Γ A matrix defined to simplify equation (2.16)

N_j Interpolation functions for the deflection in Euler-Bernoulli beam theory

K_{ij}^e Coefficients of the element stiffness matrix

G_{ij}^e Coefficients of the element geometric stiffness matrix

M_{ij}^e Coefficients of the element mass matrix

F_i^e Coefficients of the force vector

$[K]$ Stiffness matrix

$[G]$ Geometric stiffness matrix

$[M]$ Mass matrix

$\{w\}$ Vector containing nodal displacements and rotations

$\bullet$ Differentiation with respect to time

λ eigenvalue associated with the free vibration problem

P eigenvalue associated with the buckling problem

L Length of the beam

ζ Parameter in equation (2.35)

ξ Parameter in equation (2.37)

$[\overline{G}]$	$\frac{1}{N_x^i}[G]$
P_{cr}	Critical buckling load
σ_x	Stress in x-direction
z	Thickness direction in laminated beam
ε_x	Strain in x-direction
$\overline{Q}_{11}$	Coefficient of the transformed ply stiffness matrix
κ_x	Curvature of the beam in x-direction
ε_x^o	Strain in x-direction of the reference point
ϕ	Taper angle in tapered beam
$\varepsilon_{x'}$	Strain in taper direction
h_k'	Distance to the top surface of k^{th} ply in tapered beam from the mid-plane
h_{k-1}'	Distance to the lower surface of k^{th} ply in tapered beam from the mid-plane
t_k	Thickness of the k^{th} ply of the laminate
m	Slope in tapered beam
c	The intercept of the centerline of the ply from the mid-plane
g	The intercept of the upper surface of the laminated beam from the mid-plane
R	Parameter in equation (2.76)
$\overline{Q}_{11-p}$	$\overline{Q}_{11}$ of the drop-off ply
$\overline{Q}_{11-r}$	$\overline{Q}_{11}$ of the resin layers
φ	Total rotation of the cross-section in Euler-Bernoulli beam
ψ	Total rotation of the cross-section in Timoshenko beam

γ	The mean value of the shear deformation
Q_x	The transverse shear stress per unit width
I_{xy}	Rotational inertia
F_{55}	Variable introduced in equation (3.4)
$\overline{C}_{55}$	Transformed variable given by equation (3.5)
G_{23}	Out-of-plane shear modulus
G_{13}	In-plane shear modulus
C_{44}	G_{23}
C_{55}	G_{13}
μ	Shear correction factor used in Timoshenko beam theory
H_{55}	μF_{55}
a_i	Variables for deflection approximation in Timoshenko beam
b_i	Variables for rotation approximation in Timoshenko beam
Ψ_i	Interpolation functions corresponding to deflection in Timoshenko beam element
Φ_i	Interpolation functions corresponding to rotation in Timoshenko beam element
K_b^e	Bending term of the stiffness matrix in Timoshenko beam element
K_{st}^e	Shear term of the stiffness matrix in Timoshenko beam element
Θ	Rotation as a function of displacement in Timoshenko beam element
M_i	Bending moment at i^{th} node in advanced finite element formulation
F_i	Shear force at i^{th} node in advanced finite element formulation

Δ_i Flexural rigidity at i^{th} node in advanced finite element formulation

$[d]$ Matrix of nodal displacements

$[\ ]^{-1}$ Inverse of the matrix

u_j Generalized coordinates in advanced finite element formulation

ν Poisson's ratio

E_1 Modulus of elasticity in fiber direction

E_2 Modulus of elasticity in transverse direction

ω Natural frequency of the beam

Chapter 1

Introduction, Literature Survey and Scope of the Thesis

1.1 Vibration analysis in mechanical design

Mechanical vibration deals with the interaction of inertia and restoring forces. The former is due to the effect of mass of an object, while the latter is due to the elastic deformation capability of the object. The inertia force tends to maintain the current state of the object. The restoring force tends to push the object back to its equilibrium position. Obviously this is a time-dependent phenomenon. Time-dependent problems are of great concern in almost all mechanical engineering applications.

Undesired vibrations in equipment cause loss of accuracy as in the case of measuring equipment, fatigue failure and discomfort for human beings as in the case of aircrafts and cars. If the frequency of exciting force gets close to the frequency band of the natural frequencies of the structure, the mechanical component experiences severe vibration due to resonance. The resonance will decrease the lifetime of the structure and causes unpredictable failures. Dynamic analysis in mechanical design is of great importance to control the vibration in order to maintain the operating performance and to prevent sudden failures in structures.

1.2 Buckling analysis in mechanical design

Change in the geometry of a structure or a mechanical component under compression results in the loss of its ability to resist loading. Stability of structures under compression can be grouped into two categories: (1) instability associated with a bifurcation of equilibrium; (2) Instability that is associated with a limit of maximum load. The first category is characterized by the fact that as the compressive load increases, the member or system that originally deflects in the direction of applied force, suddenly deflects in a different direction. This phenomenon is called buckling. The point of transition from the usual deflection mode under load to an alternative deflection mode is refereed to as the point of bifurcation of equilibrium. The lowest load at the point of bifurcation is called critical buckling load.

Buckling analysis is basically a subtopic of non-linear rather than linear mechanics. In linear mechanics of deformable bodies, displacements are proportional to the loads. In buckling, disproportional increase in displacement occurs due to a small increase in the load. The instability due to buckling can lead to a catastrophic failure of a structure and it must be taken into account when one designs a structure.

1.3 Composite materials and structures

Development of composite materials is one of the great technological advances of the last half of the twentieth century [1]. By the term composite we usually refer to materials created by the synthetic assembly of two or more organic or inorganic components, in order to obtain specific characteristics and properties such as high strength, high modulus and low weight. Selected materials to create a composite material

are a reinforcing component and a compatible matrix binder. Composite materials are subdivided into the following classes on the basis of the form of the structural constituents: (i) laminar: composed of layers or laminar constituents; (ii) particulate: the dispersed phase consists of small particles; (iii) fibrous: the dispersed phase consists of fibers; (iv) flake: the dispersed phase consists of flat flakes.

Fiber reinforced composite materials are the engineering materials which are most commonly used in modern industries, such as aerospace, construction and automotive industries. In fibrous composite materials, the fibers provide virtually all strength and stiffness. The purpose of the matrix is to bind the reinforcements together and keep them in proper orientation, transfer the load to and between them and distribute it evenly, protect the fibers from hazardous environments and handling, provide resistance to crack propagation and damage, provide all the inter-laminar shear strength of the composite, and offer protection from high temperature and corrosion. The key point behind the fibrous composite is that the individual fibers are stiffer and stronger than the same material in bulk form whereas matrix materials have their usual bulk-form properties [2]. By changing the orientation of the fibers, we can optimize the composite material for strength, stiffness, fatigue, heat and moisture resistance. Fiber reinforced composite materials for structural applications are often made in the form of a thin layer, which is called *lamina.*

The structural elements, such as bars, beams and plates are made by stacking together many plies of fiber reinforced layers in different angles to achieve the desired

properties. The different layers of lamina are permanently bonded together under heat and pressure using a hot press or autoclave. Fiber orientation in each lamina and stacking sequences of layers can be chosen so as to achieve the desired strength and stiffness for specific applications.

Helicopter yoke, robot arms, turbine blade and satellite antennas are specific applications of composite structures that need to be stiff at one location and flexible at another location. Such structures can be made by terminating some plies at discrete locations to reduce the stiffness of the beam. This results in a tapered shape. Different techniques have been developed to create a tapered section. Some of the most common types of tapered sections are shown in Figure 1.1. One of the main objectives of this thesis is to investigate the vibration and buckling behavior of different types of tapered beams.

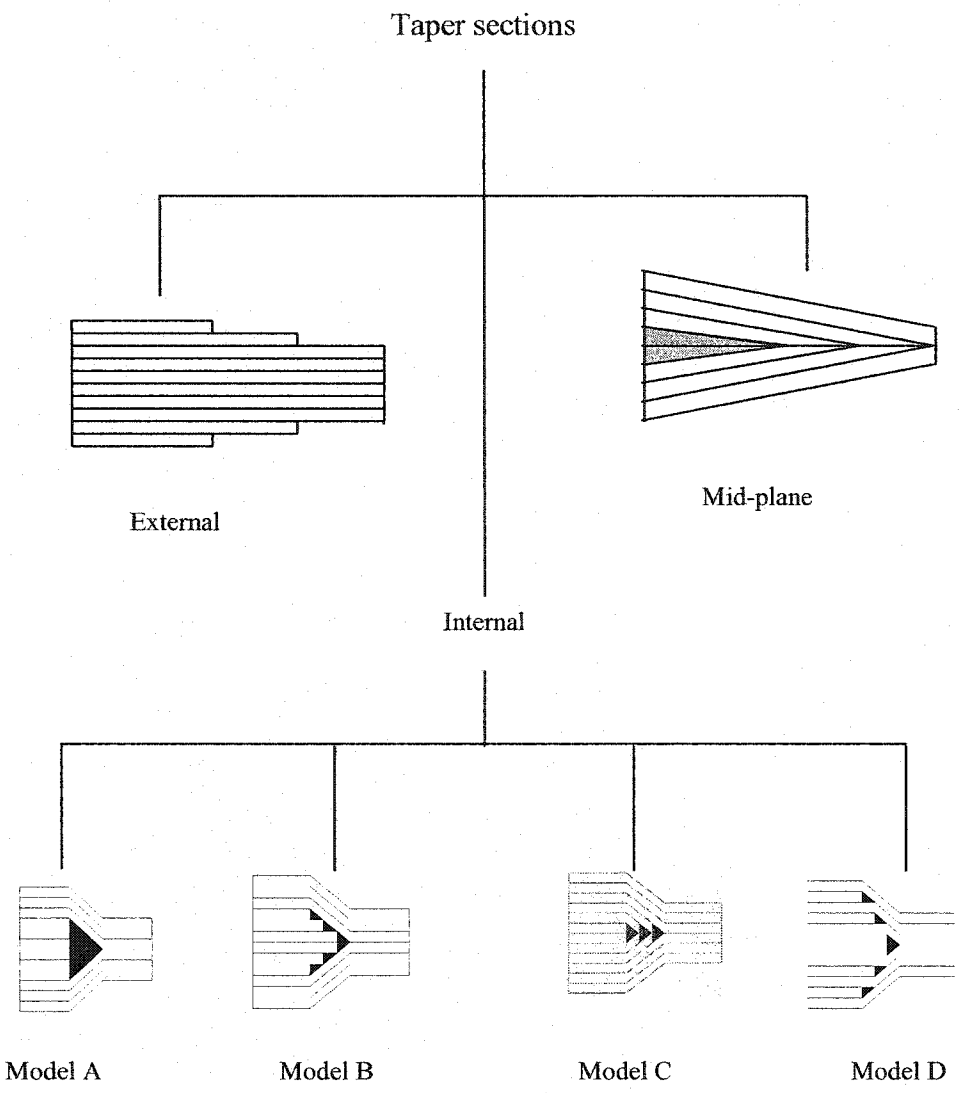

Figure 1.1 Schematic illustration of tapered sections

1.4 Finite element method

Structural analysis of complex designs relies heavily on the use of computer models. In analyzing the modern structures, it is no longer possible to treat structures as a series of black boxes being acted upon by various forces. Engineers must consider both

microscopic and macroscopic points of view in mechanical design. Finite element method (FEM) is one of the most powerful tools in engineering for the analysis of complex structures such as tapered composite beams. The speed of convergence and accuracy of the results obtained by finite element methods are strongly dependent on the element types, which are selected for the analysis. In conventional FEM, a beam element is modeled using two nodes at the ends where each node has two degrees of freedom. In conventional FEM the beam should be divided into a large number of elements to achieve an accurate result. Advanced FEM considers four degrees of freedom per node (eight degrees of freedom per element). The present thesis investigates the capability of the advanced FEM to provide the desired accuracy and speed of convergence for vibration and buckling analysis of tapered composite beams. It will be shown that the advanced FEM gives better accuracy and rapid convergence compared to conventional FEM.

1.5 Literature survey

In this section a comprehensive literature survey is presented on the vibration and buckling of composite beams, and on the application of the finite element method to composite beams. The literature survey is limited to the works available in English language and mostly published in the last two decades. The work done relevant to each topic is chronicled.

1.5.1 Vibration analysis of composite beams

Most of the works on composite beams have concentrated on delamination and failure analysis of composite beams. There are a few research works that deal with vibration analysis of laminated beams.

Abarcar and Cunniff [3] obtained experimental results for natural frequencies and the mode shapes of cantilever graphite-epoxy and boron-epoxy composite beams. Their work clearly indicated the interaction between bending and twisting for 15 degree and 30 degree laminated beams. Noor [4] obtained the natural frequencies for simply supported symmetric laminated plate by using classical laminate theory. Miller and Adams [5] studied the vibration characteristic of orthotropic fixed-free beams using the classical laminate theory. Chen and Yang [6] investigated the static and dynamic response of symmetrically laminated beams. Chandrashekhara *et al* [7] analyzed the free vibrations of composite beams including the effects of rotary inertia and shear deformation. A paper by Hodges *et al* [8] deals with the free vibration of composite beams using exact integration method and mixed finite element method. They discuss the influences of laminate configuration on the natural frequencies. Krishnaswamy *et al* [9] obtained the analytical solutions to vibration of laminated composite beams. Reddy and Khdeir [10] studied free vibration behavior of cross-ply composite laminates under various boundary conditions. The study concludes that shear deformation laminate theory accurately predicts the behavior of the composite laminate, whereas the classical laminate theory over predicts natural frequencies of the laminate. Exact solutions for free vibrations of composite beams including the rotary inertia and shear deformation were obtained by Abramovich [11]. Abramovich and Livshits [12] obtained analytical solutions for free vibration of

non-symmetric cross-ply laminated beams. Hjela and Teboub [13] use symbolic computations to analyze generally orthotropic composite beams. Eisenberger *et al* [14] obtained the dynamic stiffness of laminated beams by applying first order shear deformation theory. Marur and Kant [15] applied higher order theory and finite element for free vibration of composite beams. Teoh and Huang [16] obtained the analytical results for vibration of fiber reinforced composite beams. In this work both shear and rotary inertia are included.

Song and Waas [17] treat effects of shear deformation on free vibration of composite beams for different boundary conditions. Banerjee [18] uses dynamic stiffness to obtain natural frequencies of a Timoshenko composite beam under axial loading. Shi and Lam [19] present the free vibration analysis of composite beams based on the third order beam theory. By using Hamilton's principle, they derived the variation consistent equations of motion in matrix form. This work also studied the influences of the mass component resulting from higher-order displacement on the flexural vibration of composite beams. They proposed linear bending strain expressions to formulate accurate element with the same number of degrees of freedom. Ganapathi *et al* [20] used a three-node beam element to obtain natural frequencies of laminated composite beams. The formulation is general in the sense that it includes anisotropy, transverse shear deformation, in-plane and rotary inertia effects. Exact solutions for free vibrations of laminated composite beams have been given by many authors [2, 21, 22, and 23]. Matsunaga [24] presents the vibration of multi-layer composite beams according to higher order deformation theories. He uses the method of power series expansion of

displacement components. Rao *et al* [25] use mixed theory for vibration analysis of laminated beams.

Few researchers have investigated non-uniform and tapered composite beams. Rao and Ganesan [26] investigated the harmonic response of tapered composite beams using finite element method based on a higher order shear deformation theory. The tapered model in this investigation consists of individual tapered plies that are laid up in the width axis. Free vibration of stepped Timoshenko composite beams was studied by Farghaly and Gadelrab [27]. They obtained natural frequencies for a steeped composite beam based on Timoshenko beam theory. Tong *et al* [28] consider a linear-tapered beam for free vibration analysis. Polyzois *et al* [29] present dynamic analysis for linear tapered poles by applying finite element method. A complete review of different models of tapered composite beams has been presented by He *et al* [30]. Recently, Abd EL-Maksoud [31] presents the dynamic analysis of uniform and mid-plane tapered composite beams by using a higher order finite element formulation. Nigam [32] presents the dynamic analysis of laminated composite beams using Hierarchical Finite Element Method (HFEM).

1.5.2 Buckling analysis of composite beams

There are few works available on buckling analysis of composite beams in the literature. Khdeir and Reddy [33] used various plate theories to study the buckling of laminated plates. Banerjee and Williams [34] obtained critical buckling loads for columns by considering shear deformation effects. Khdeir and Reddy [35] discussed buckling behavior of cross-ply rectangular composite beams with different boundary conditions.

They present analytical solution for composite beams with different boundary conditions. Song and Waas [17] discussed the effects of shear deformation on the buckling of composite beams. They use simple higher-order theory, which assumes a cubic distribution for the displacement field through the thickness of the beam. Chen and Peng [36] studied the stability of rotating composite beams subjected to axial compressive load. Kim *et al* [37] conducted the buckling analysis of cross-ply laminate with one-dimensional through-the-width delaminations. Matsunaga [38] studied the buckling of multi-layer composite beams using higher-order deformation theories. Lee *et al* [39] presented a general analytical model based on the classical laminate theory to study the lateral buckling of a laminated composite beam with I-section. They consider different laminate configurations and boundary conditions. The exact solutions for critical buckling loads based on classical laminate theory for different boundary conditions are given by Bertholet [21], Reddy [2] and Whitney [22]. Abd EL-Maksoud [31] used an advanced finite element formulation to study the buckling of laminated beams. Recently, Cortinez and Piovan [40] discussed buckling of thin-walled composite beams. Lee and Kim [41] treated the lateral buckling of channel section composite beams.

1.5.3 Finite element vibration analysis

The idea of finite element method is to divide the domain of interest into some smaller sub-domains called *finite elements.* Various procedures have been developed to achieve more accuracy and rapid convergence of solutions. The most common procedure is to increase the number of elements while keeping the degrees of freedom of each element fixed. This technique has been applied for vibration analysis of beams by many researchers including Zienkiewicz [42], Cook [43] and Reddy [44]. They considered a

beam element with two nodes at the ends and two degrees of freedom that are, the deflection and rotation per node. Thomas and Dokumaci [45] presented an internal node element considering the total deflection and bending slope as the co-ordinates at the two terminal node and two internal nodes giving eight degrees of freedom to the element. Thomas and Abbas [46] presented a finite element model for Timoshenko beam element by considering total deflection, total slope, bending slope and the first derivative of bending slope as degrees of freedom. They raise the order of element matrices to the eighth-order. Dawe [47] presented a Timoshenko beam element with three nodes having two degrees of freedom, namely, the lateral deflection and the cross-sectional rotation per node. Nickel and Secor [48] derived stiffness and mass matrices of Timoshenko beams by using deflection, total slope and bending slope as the nodal co-ordinates for the end nodes and the bending slope at the mid-point, giving rise to matrices of order seven. Kapur [49] improved this model by taking bending deflection; shear deflection, bending slope and shear slope as nodal co-ordinates. To [50] considered four degrees of freedom per node and two nodes at the ends to obtain stiffness and mass matrices for tapered beams based on the Euler-Bernoulli beam element. In this model, the deflection, rotation, curvature and gradient of curvature are considered as degrees of freedom. Houmat [51] investigated the vibration of Timoshenko beams considering four-node element with variable degrees of freedom. In this model both the element transverse displacement and cross-sectional rotations are described by a cubic polynomial plus a variable number of trigonometric sine terms. Addition of trigonometric terms to the base polynomial function is known as *Hierarchical* finite element method. Shi *et al* [52] presented a finite element model for higher order plate theories. Gupta and Rao [53] applied finite element method

for the analysis of rotating Timoshenko beams. Ramtekkar *et al* [54] used a six-node element to obtain natural frequencies of laminated beams. The transverse stress components have been invoked as the nodal degrees of freedom by applying elasticity relations.

Finite element method has been used for vibration analysis of tapered beams in many works. Gupta and Rao [55] used finite element with two nodes at the ends and two degrees freedom per node to obtain the stiffness and mass matrices for linearly tapered and twisted beams. Cleghorn and Tabarrok [56] presented a finite element model for free vibration of lineary-tapered beams. Rao and Ganesan [57] applied conventional finite element formulation to determine natural frequencies of linearly tapered beams. Most recently Abd El-Maksoud [31] applied an advanced finite element model similar to the one presented by To [50] for vibration analysis of tapered composite beams. Nigam [32] used hierarchical finite element method to investigate the dynamic response of laminated composite beams.

1.6 Objectives of the Thesis

The objectives of the present thesis are: (1) to investigate the vibration response and buckling of composite beams with different types of taper configurations; (2) to develop and evaluate a finite element model with eight degrees of freedom that incorporates the essential (deflection and slope) and natural (bending moment and shear force) boundary conditions in the formulation for the vibration and buckling analyses of tapered composite beams; and (3) to conduct a detailed parametric study of the tapered composite beams.

This thesis presents advanced finite element models with eight nodal degrees of freedom that are based on classical laminate theory (Euler-Bernoulli beam element) and shear deformation theory (Timoshenko beam element). The advanced finite element formulation is applied to the vibration and buckling analyses of different types of tapered beams.

The advanced formulation gives more accurate results by using fewer elements, which is a good advantage in terms of computational expenses and discretization errors. The analysis is performed for different types of tapered beams to assess the superiority of each type of tapered beams with respect to natural frequencies and critical buckling load. Finally a detailed parametric study on tapered composite beams is conducted.

1.7 Layout of the Thesis

The present Chapter provided a brief introduction and literature survey on vibration and buckling analysis of composite beams that have uniform and variable thickness, as well as on higher order finite element method.

In Chapter 2, the conventional finite element formulation based on Euler-Bernoulli beam theory is developed. The methodology is applied to determine the natural frequencies and the critical buckling load of uniform thickness, mid-plane tapered and internally tapered composite beams. Detailed comparison has been made between different types of tapered beams.

In Chapter 3 the conventional finite element formulation based on Timoshenko beam element is developed. The effects of shear deformation and rotary inertia are considered. The developed formulation is applied to vibration analysis of uniform thickness and tapered composite beams.

Chapter 4 gives the development of a higher order finite element beam element by considering four degrees of freedom per node. The formulation is called as *Advanced* Finite Element Formulation. The advanced model is applied to the vibration and buckling analyses of different types of tapered composite beams. This chapter also introduces a higher order finite element model with four degrees of freedom per node based on Timoshenko beam element.

Chapter 5 is devoted to the parametric study on tapered composite beam taking into consideration the lengths of the thick and thin sections, laminate configurations, taper angle and boundary conditions. The parametric study is conducted to determine natural frequencies and critical buckling loads of tapered composite beams.

The thesis ends with Chapter 6, which provides the overall conclusions of the present work and some recommendations for future work.

Chapter 2

Analyses of composite beams based on classical laminate theory using conventional finite element formulation

2.1 Introduction

Composite structures are increasingly being used in a variety of structural components in aerospace and automobile industries due to their high strength to weight and stiffness to weight ratios. Interest in laminated beams as movable elements of machines that have uniform and non-uniform configurations, and tapered and stepped configurations, is growing as they are finding a number of applications in modern industries, such as turbine blades, helicopter blades and robot arms. Understanding the vibration and stability characteristics of laminated beams is essential to control the functionality of the beam component during operation.

In this chapter, buckling and vibration analysis of laminated beams are conducted using conventional finite element formulation. Section 2.2 discusses the one-dimensional analysis of laminated plate. In Section 2.3 finite element formulation for uniform composite beams has been developed. In Section 2.4 the formulation for the mid-plane tapered beams is developed and the element properties, namely, stiffness, mass and

geometric stiffness matrices are obtained. Finally, the formulation for the mid-plane tapered beam model will be modified so as to be applied to the analysis of a variety of internally-tapered configurations. The chapter ends with example applications involving different types of tapered beams.

2.2 One-dimensional analysis of laminated plates

Most of the composite structures are designed and constructed as laminations of n successive layers to create a laminated plate as shown in Figure 2.1. Thus, the theory of plates is applied for the analysis of the laminated plates. The elementary theory of plates assumes that, the normal stress (in z-direction) is negligible within the volume of the plate relative to the other stress components.

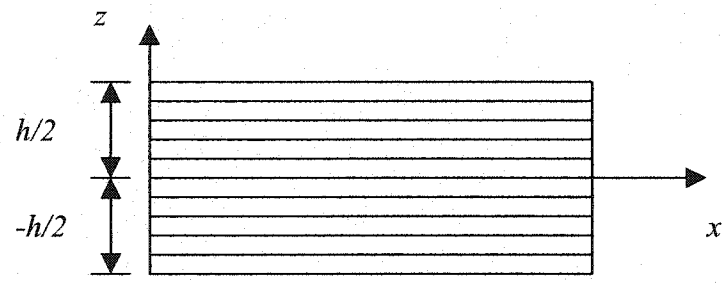

Figure 2.1 Schematic illustration of a laminated plate

Analysis of laminated plates reduces to one-dimensional analysis in the following two cases: (1) laminated beams, and (2) cylindrical bending of plate strip.

1) Laminated beams

In this case, the width of the laminated plate (along y-axis) is very small compared to the length (along x-axis). Therefore, changes in the width direction (y-axis) are negligible.

As a result, the equation of the plate reduces to one-dimensional equation as a function of x only.

2) Cylindrical bending

Consider a laminated plate shown in Figure 2.2 that is very long along the y direction and has a finite dimension, l, along the x-axis. Assume that the transverse load $q(x)$ is uniformly distributed at any section parallel to the x-axis. In this case the deformation of the plate can be considered to be independent of the coordinate along the length of the plate. In such a case the deflection w and the displacements along the x-axis and y-axis are functions of x only, and also all derivatives with respect to y-axis are zero. A beam element can be considered as a strip of such a plate with length l and width b as shown in Figure 2.2.

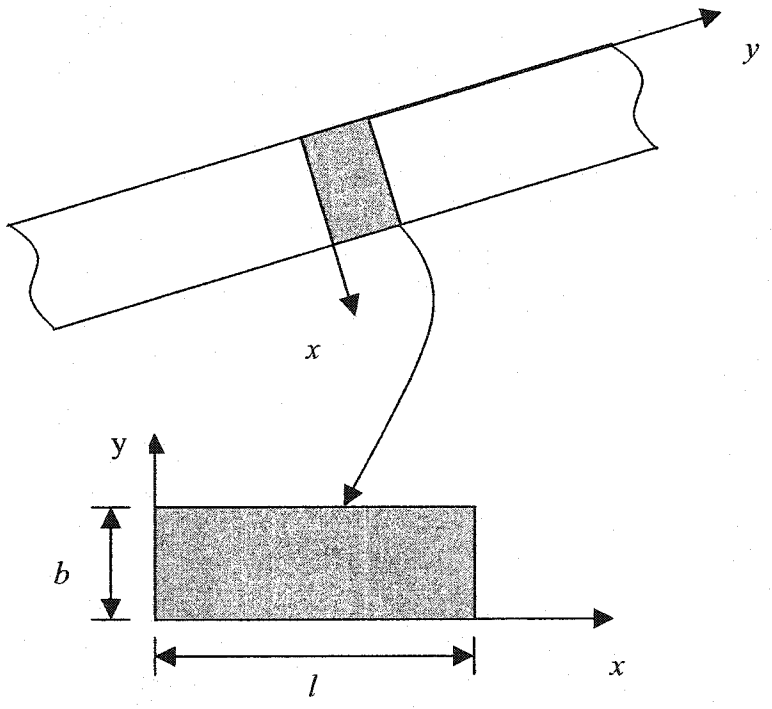

Figure 2.2 Schematic illustration of laminated plate in cylindrical bending

2.3 Vibration and buckling analysis of uniform thickness-composite beams based on Classical Laminated Plate Theory (CLPT)

Classical laminated plate theory states that the transverse shear stresses through the thickness of the laminate are negligible and further, the normal to the middle plane remains normal after deformation. Therefore, the rotation of the mid-plane about y-axis (clockwise positive) can be expressed as:

$$\varphi_x(x) = -\frac{\partial w}{\partial x} \tag{2.1}$$

where w and φ_x denote the deformation in the thickness direction and the rotation about y-axis respectively. Neglecting rotational inertia, the equation of motion of a uniform-thickness laminated beam based on classical laminate theory is given by [21]:

$$b\frac{\partial^2 M_x}{\partial x^2} + bN_x^i \frac{\partial^2 w}{\partial x^2} + bq(x) = b\rho_s \frac{\partial^2 w}{\partial t^2} \tag{2.2}$$

where b and N_x^i denote the width of the beam and the initial axial force per unit width along x-axis respectively. M_x denotes the bending moment about the y-axis per unit width. Considering the beam element as a plate strip in cylindrical bending, M_x is given by [21]:

$$M_x = B_{11}\frac{\partial u_o}{\partial x} + B_{16}\frac{\partial v_o}{\partial x} - D_{11}\frac{\partial^2 w}{\partial x^2} \tag{2.3}$$

where u_o and v_o denote the deformation of the reference point in the mid-plane in x and y directions, respectively. B_{ij} (i =1, j =1, 6) and D_{11} represent the coefficients of coupling stiffness and bending stiffness matrices, respectively. In the case of mid-plane symmetric laminated beams, $B_{11} = B_{16} = 0$ and Equation (2.3) reduces to the following equation:

$$M_x = -D_{11}\frac{\partial^2 w}{\partial x^2} \tag{2.4}$$

The term $q(x)$ denotes the distributed transverse load on the laminated beam and is defined as follows [21]:

$$q(x) = \sigma_z\left(z = \frac{h}{2}\right) - \sigma_z\left(z = -\frac{h}{2}\right) \tag{2.5}$$

where σ_z and h are the stress in the thickness direction and the thickness of the laminated beam, respectively.

The term ρ_s denotes the mass per unit length per unit width of the laminated beam and is defined as [21]:

$$\rho_s = \sum_{k=1}^{n} \rho_k (h_k - h_{k-1}) \tag{2.6}$$

where ρ_k is the density of each ply and, h_k and h_{k-1} denote the height of the upper and lower surfaces of each ply with respect to the mid-plane [21]. In the case of constant density, ρ, for all plies, equation (2.6) reduces to:

$$\rho_s = \rho h \tag{2.7}$$

Combining Equation (2.4) and Equation (2.2), the Equation of motion for a laminated beam is obtained as follows:

$$b\frac{\partial^2}{\partial x^2}\left(D_{11}\frac{\partial^2 w}{\partial x^2}\right) - bN_x^i\frac{\partial^2 w}{\partial x^2} - bq(x) + b\rho_s\frac{\partial^2 w}{\partial t^2} = 0 \tag{2.8}$$

It is worth noting that by replacing bD_{11} and $b\rho_s$ with EI and ρA, respectively, in Equation (2.8) one may obtain the equation of motion of beams made of isotropic materials based on Euler-Bernoulli beam theory. When classical laminate theory is applied for beam analysis, it is common in the literature to call it as Euler-Bernoulli beam theory.

2.3.1 Finite element model

The finite element model for the laminated beam is constructed using the three-step procedure given in reference [23]. First the domain (i.e., the length of the beam) is divided into a set of sub-domains as shown in Figure 2.3. The ub-domains are called beam elements and interfaces of the elements at the ends are called nodes.

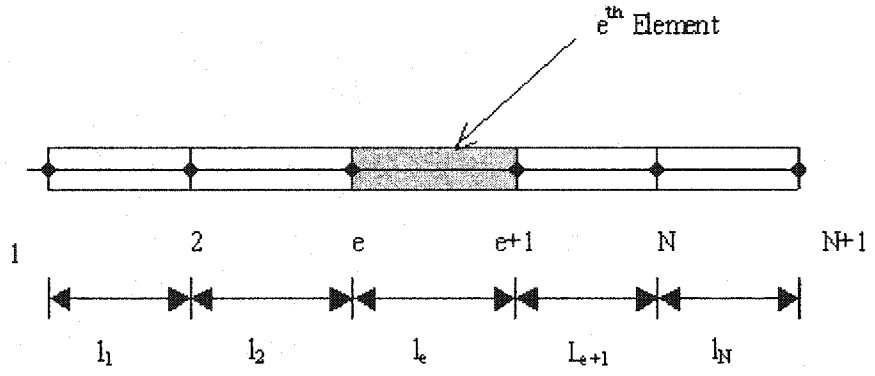

Figure 2.3 Finite element model of a beam

2.3.1.1 Weak form formulation based on Euler-Bernoulli beam theory

A typical element is isolated from the domain as shown in Figure 2.4 and its structural behavior is modeled. We use the weak form of the governing Equation (2.8) to construct the finite element model. In the weak form, w and φ, that are respectively the deflection and rotation as shown in Figure 2.4 are the primary variables. Q_i $(i = 1, 2, 3, 4)$ represent secondary variables corresponding to the primary variables. To construct the weak form of Equation (2.8), a function v is chosen as the weight function.

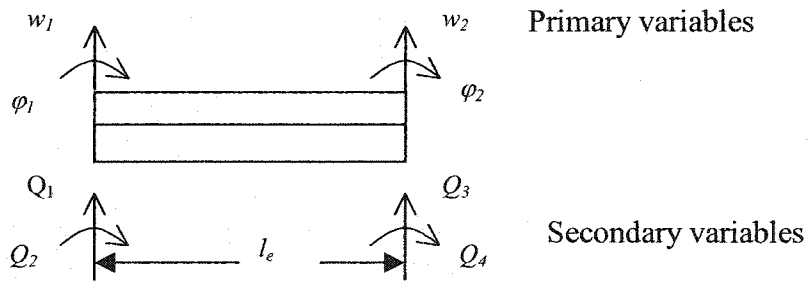

Figure 2.4 A typical finite element of uniform beam

Multiplying equation (2.8) by weight function v and integrating over the element:

$$\int_0^l \left[vb\frac{d^2}{dx^2}\left(D_{11}\frac{\partial^2 w}{\partial x^2}\right) - vbN_x^i\frac{\partial^2 w}{\partial x^2} - vbq(x) + vb\rho_s\frac{\partial^2 w}{\partial t^2}\right] dx = 0 \tag{2.9}$$

Integrating the first term of Equation (2.9) by parts twice and the second term once, the weak form is obtained as follows:

$$\int_0^l \left(bD_{11}\frac{d^2 v}{dx^2}\frac{\partial^2 w}{\partial x^2} + bN_x^i\frac{dv}{dx}\frac{\partial w}{\partial x} + vbq(x) + vb\rho_s\frac{\partial^2 w}{\partial t^2}\right) dx + v\frac{d}{dx}\left(bD_{11}\frac{\partial^2 w}{\partial x^2}\right)\Bigg|_{x=l}$$

$$- v\frac{d}{dx}\left(bD_{11}\frac{\partial^2 w}{\partial x^2}\right)\Bigg|_{x=0} - \frac{dv}{dx}\left(bD_{11}\frac{\partial^2 w}{\partial x^2}\right)\Bigg|_{x=l} + \frac{dv}{dx}\left(bD_{11}\frac{\partial^2 w}{\partial x^2}\right)\Bigg|_{x=0}$$

$$- vbN_x^i\frac{\partial w}{\partial x}\Bigg|_{x=l} + vbN_x^i\frac{\partial w}{\partial x}\Bigg|_{x=0} = 0 \tag{2.10}$$

The secondary variables are defined as follows:

$$Q_1^e = \left[\frac{d}{dx}\left(bD_{11}\frac{\partial^2 w}{\partial x^2}\right) - bN_x^i\frac{\partial w}{\partial x}\right]_{x=0}$$

$$Q_3^e = -\left[\frac{d}{dx}\left(bD_{11}\frac{\partial^2 w}{\partial x^2}\right) - bN_x^i\frac{\partial w}{\partial x}\right]_{x=l} \tag{2.11}$$

$$Q_2^e = \left(bD_{11}\frac{\partial^2 w}{\partial x^2}\right)_{x=0}$$

$$Q_4^e = -\left(bD_{11}\frac{\partial^2 w}{\partial x^2}\right)_{x=l}$$

Using Equation (2.11), we can rewrite Equation (2.10) as follows:

$$\int_0^l \left[bD_{11} \frac{\partial^2 v}{\partial x^2} \frac{\partial^2 w}{\partial x^2} + bN_x^i \frac{\partial v}{\partial x} \frac{\partial w}{\partial x} + vb\rho_s \frac{\partial^2 w}{\partial t^2} - bvq(x) \right] dx - Q_1^e v(0) - Q_3^e v(l) -$$

$$Q_2^e \left(-\frac{\partial v}{\partial x} \right)\Bigg|_{x=0} - Q_4^e \left(-\frac{\partial v}{\partial x} \right)\Bigg|_{x=l} = 0 \tag{2.12}$$

The third step is to develop finite element model based on the weak form given by equation (2.12). Since, deflection, w, and slope, φ_x, must be continuous everywhere in the domain, they should be continuous at each and every interface between two elements. For convenience sake, we define $\varphi_x = \varphi$. The deflection W and slope, φ, at nodes 1 and 2 are given as:

$$W^e(0,t) = w_1^e$$
$$W^e(l,t) = w_3^e$$
$$\varphi(0,t) = -\frac{dW^e}{dx}\Bigg|_{x=0} = w_2^e \tag{2.13}$$
$$\varphi(l,t) = -\frac{dW^e}{dx}\Bigg|_{x=l} = w_4^e$$

Since there are four boundary conditions per element, we need a fourth-order polynomial as follows:

$$W^e(x,t) = c_1^e + c_2^e x + c_3^e x^2 + c_4^e x^3 \tag{2.14}$$

To determine the coefficients, c_i^e, one can write boundary conditions (2.13) using Equation (2.14):

$$
\begin{aligned}
w_1^e &= c_1^e \\
w_2^e &= -c_2^e \\
w_3^e &= c_1^e + c_2^e l + c_3^e l^2 + c_4^e l^3 \\
w_4^e &= -c_2^e - 2c_3^e l - 3c_4^e l^2
\end{aligned}
\tag{2.15}
$$

Rewriting Equation (2.15) in matrix form, we get the following matrix equation:

$$
\begin{Bmatrix} w_1^e \\ w_2^e \\ w_3^e \\ w_4^e \end{Bmatrix} = \begin{bmatrix} 1 & 0 & 0 & 0 \\ 0 & -1 & 0 & 0 \\ 1 & l & l^2 & l^3 \\ 0 & -1 & -2l & -3l^2 \end{bmatrix} \begin{Bmatrix} c_1^e \\ c_2^e \\ c_3^e \\ c_4^e \end{Bmatrix}
\tag{2.16}
$$

In short form Equation (2.16) can be written as:

$$\{w\} = [\Gamma]\{c\} \tag{2.17}$$

By inverting $[\Gamma]$ and pre-multiplying $\{w\}$ with $[\Gamma]$, one can obtain $\{c\}$ as follows:

$$\{c\} = [\Gamma]^{-1}\{w\} \tag{2.18}$$

Substituting $\{c\}$ from Equation (2.18) into Equation (2.14), one can approximate the deflection of the beam by the following Equation:

$$w(x,t) \approx W^e(x,t) = w_1^e N_1 + w_2^e N_2 + w_3^e N_3 + w_4^e N_4 \tag{2.19}$$

where N_j (j =*1,2,3,4*) denote the interpolation functions. The essential requirements for the interpolation functions are: (1) They must be such that $W^e(x,t)$ satisfies the boundary conditions given by equation (2.15); (2) The first and second derivatives of N_j with respect to x are not equal to zero; (3) They should be complete and include all lower order terms in the polynomial leading to the highest term.

The interpolation functions have been obtained using MATLAB ® software as follows: (See *fen1.m* function in Appendix-B)

$$
\begin{aligned}
N_1^e &= 1-3\frac{x^2}{l^2}+2\frac{x^3}{l^3} \\
N_2^e &= -x+2\frac{x^2}{l}-\frac{x^3}{l^2} \\
N_3^e &= 3\left(\frac{x}{l}\right)^2-2\left(\frac{x}{l}\right)^3 \\
N_4^e &= \frac{x^2}{l}-\frac{x^3}{l^2}
\end{aligned}
\tag{2.20}
$$

Then substituting w from Equation (2.19) into Equation (2.12) and considering $v = N_1^e, N_2^e, N_3^e, N_4^e$ (because there are four unknowns, w_i^e), the i^{th} Equation is obtained as:

$$
0 = \int_0^l \left[bD_{11}\frac{d^2N_i}{dx^2}\left(\sum_{j=1}^{4} w_j^e \frac{d^2N_j}{dx^2}\right) + bN_x^i \frac{dN_i}{dx}\left(\sum_{j=1}^{4} w_j^e \frac{dN_j}{dx}\right) + b\rho_s N_i \left(\sum_{j=1}^{4} N_j \frac{d^2w_j^e}{dt^2}\right)\right] dx -
$$

$$\int_0^l bN_i q(x)dx - Q_1^e N_i(0) - Q_3^e N_i(l) - Q_2^e\left(-\frac{dN_i}{dx}\right)_{x=0} - Q_4^e\left(-\frac{dN_i}{dx}\right)_{x=l}$$

(2.21)

Equation (2.21) can be simplified as follows:

$$0 = \sum_{j=1}^{4}\int_0^l \left[\left(bD_{11}\frac{d^2N_i}{dx^2}\frac{d^2N_j}{dx^2} + bN_x^i\frac{dN_i}{dx}\frac{dN_j}{dx}\right)w_j^e b\rho_s N_i N_j\frac{d^2w_j^e}{dt^2}\right]dx - \int_0^l bN_i q(x)dx$$

$$- Q_1^e N_i(0) - Q_3^e N_i(l) - Q_2^e\left(-\frac{dN_i}{dx}\right)_{x=0} - Q_4^e\left(-\frac{dN_i}{dx}\right)_{x=l} \qquad (2.22)$$

The following coefficients are introduced:

$$K_{ij}^e = \int_0^l bD_{11}\frac{d^2N_i}{dx^2}\frac{d^2N_j}{dx^2}dx \qquad (2.23)$$

$$G_{ij}^e = \int_0^l bN_x^i\frac{dN_i}{dx}\frac{dN_j}{dx}dx \qquad (2.24)$$

$$M_{ij}^e = \int_0^l b\rho_s N_i N_j dx \qquad (2.25)$$

$$q_i^e = \int_0^l bN_i q(x)dx \qquad (2.26)$$

$$F_i^e = q_i^e + Q_1^e N_i(0) + Q_3^e N_i(l) + Q_2^e\left(-\frac{dN_i}{dx}\right)_{x=0} + Q_4^e\left(-\frac{dN_i}{dx}\right)_{x=l} \qquad (2.27)$$

Substituting Equations (2.23)-(2.27) into Equation (2.22), the i th Equation of the finite element is obtained as:

$$\sum_{j=1}^{4}\left[\left(K_{ij}^{e}+G_{ij}^{e}\right)w_{j}^{e}+M_{ij}^{e}\frac{d^{2}w_{j}^{e}}{dt^{2}}\right]-F_{i}^{e}=0 \tag{2.28}$$

For convenience sake, hereafter the superscript e is removed from the equations. In matrix form equation (2.28) can be written as:

$$\left([K]+[G]\right)\{w\}+[M]\{\ddot{w}\}=\{F\} \tag{2.29}$$

where $[K]$,$[G]$ and $[M]$ represent stiffness, geometric stiffness and mass matrices respectively, and $\{F\}$ is a force vector.

2.3.1.2 Element properties of uniform-thickness composite beam

The element properties (namely, stiffness, mass and geometric stiffness) of a uniform-thickness laminated composite beam have been obtained by performing the integrations of Equations (2.23) to (2.25) by MATLAB® software. The results are given as follows: (See the results obtained from program *fen1.m* in Appendix-B).

$$[K]=\frac{2bD_{11}}{l^{3}}\begin{bmatrix} 6 & -3l & -6 & -3l \\ & 2l^{2} & 3l & l^{2} \\ & & 6 & 3l \\ sym & & & 2l^{2} \end{bmatrix} \tag{2.30}$$

$$[M]=\frac{b\rho_{s}}{420}\begin{bmatrix} 156 & -22l & 54 & 13l \\ & 4l^{2} & -13l & -3l^{2} \\ & & 156 & 22l \\ sym & & & 4l^{2} \end{bmatrix} \tag{2.31}$$

$$[G]=\frac{bN_x^i}{30l}\begin{bmatrix} 36 & -3l & -36 & -3l \\ & 4l^2 & 3l & -l^2 \\ & & 36 & 3l \\ sym & & & 4l^2 \end{bmatrix} \tag{2.32}$$

2.3.2 Free vibration analysis of uniform-thickness composite beam

In natural vibration, the initial axial force $N_x^i = 0$ and $q(x) = 0$. The nodal values are given as:

$$w_j(t) = W_j e^{i\omega t} \qquad i = \sqrt{-1} \tag{2.33}$$

Substituting Equation (2.33) into Equation (2.29) and considering $N_x^i = 0$, we will obtain:

$$([K]-\omega^2[M])\{W\} = \{0\} \tag{2.34}$$

where ω represents natural frequency of vibration.

Considering $\lambda = \omega^2$, Equation (2.34) is an eigenvalue problem in the form:

$$([K]-\lambda[M])\{W\} = \{0\} \tag{2.35}$$

where λ and W represent the eigenvalue and the eigenvector respectively. In order to determine the natural frequencies of uniform-thickness composite beam, MATLAB® software has been used to solve the equation (2.35). (See *unib2.m* in Appendix-B)

The exact solutions corresponding to the Euler-Bernoulli beam theory, for transverse vibrations of uniform mid-plane symmetric composite beams, having different boundary conditions are listed bellow [21]. The following nomenclature is used for all cases;

ω_n : Natural frequency of the n^{th} mode; L : length of the beam;

A : area of cross-section of the beam; b : width of the beam

ρ : density of the composite material ; D_{11} : bending stiffness coefficient

1) Simply supported beam

$$\omega_n = \left(\frac{n\pi}{L}\right)^2 \sqrt{\frac{bD_{11}}{\rho A}} \qquad n=1, 2, 3... \tag{2.36}$$

2) Fixed-fixed beam

$$\omega_n = \left(\frac{\zeta_n}{L}\right)^2 \sqrt{\frac{bD_{11}}{\rho A}} \qquad n=1, 2, 3... \tag{2.37}$$

For the first three modes, the values of ζ_n are given as:

$\zeta_1 = 4.732$ $\zeta_2 = 7.853$ $\zeta_3 = 10.996$

3) Fixed-free beam

$$\omega_n = \frac{\xi_n}{(L^2)}\sqrt{\frac{bD_{11}}{\rho A}} \qquad n=1, 2, 3 \tag{2.38}$$

For the first three modes, the values of ξ_n are given as:

$$\xi_1 = 3.516 \qquad \xi_2 = 22.034 \qquad \xi_3 = 61.701$$

2.3.3 Buckling analysis of uniform-thickness composite beam

In the study of buckling problem, we consider an axial compressive load as:

$$N_x^i = -P \tag{2.39}$$

Further, only the static case with no external transverse load is considered. Considering Equation (2.39) and the static case as mentioned in the above, Equation (2.29) reduces to:

$$\left([K] - P[\overline{G}]\right)\{W\} = \{0\} \tag{2.40}$$

where matrix $[\overline{G}]$ is defined as:

$$[\overline{G}] = \frac{1}{N_x^i}[G] \tag{2.41}$$

Substituting Equation (2.32) into Equation (2.41), matrix $[\overline{G}]$ is given by:

$$[\overline{G}] = \frac{b}{30l}\begin{bmatrix} 36 & -3l & -36 & -3l \\ & 4l^2 & 3l & -l^2 \\ & & 36 & 3l \\ sym & & & 4l^2 \end{bmatrix} \tag{2.42}$$

Equation (2.40) is an eigenvalue problem where P represents the eigenvalue. The system represented by equation (2.40) has N eigenvalues where N represents the total degrees of freedom. The smallest eigenvalue will be the critical buckling load.

The exact solutions corresponding to the Euler-Bernoulli beam theory for critical buckling loads of uniform mid-plane symmetric composite beams, having different boundary conditions are listed below [21]. The following nomenclature is used for all cases;

P_{cr} - critical buckling load; L- length of the beam;

D_{11} - bending stiffness coefficient. b-width of the beam

1) Simply supported beam

$$P_{cr} = \frac{\pi^2 b D_{11}}{L^2} \tag{2.43}$$

2) Fixed-fixed beam

$$P_{cr} = \frac{4\pi^2 b D_{11}}{L^2} \tag{2.44}$$

3) Fixed-free beam

$$P_{cr} = \frac{\pi^2 b D_{11}}{4L^2} \tag{2.45}$$

2.3.4 Free vibration analysis of laminated beam-column

A beam under compressive axial load is well known as beam-column since it exhibits behaviors of both the beam and column. For a beam-column the Equation (2.29) changes to the following form:

$$\left([K]-P[\overline{G}]-\lambda[M]\right)\{W\}=\{0\} \tag{2.46}$$

where P is the prescribed axial load and $P < P_{cr}$. One may note that compressive axial load reduces the total stiffness of the element. Equation (2.46), again is an eigenvalue problem where $\lambda = \omega^2$. Here ω represents the natural frequencies of the beam-column.

2.4 Finite element analysis of tapered composite beam

In general, there are three types of tapered beams, externally-tapered, mid-plane tapered and internally-tapered beams. Externally-tapered beams as shown in Figure 2.5 can be modeled as combinations of elements with different thickness. The thickness for each element is constant. Thus, each element can be considered as uniform beam.

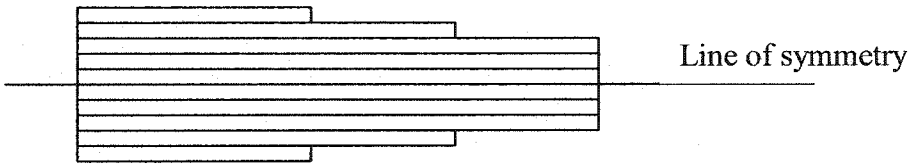

Figure 2.5 Schematic illustration of externally-tapered beam

Mid-plane tapered beams are in the form of Figure 2.6. In this case the centerline of each ply is not a straight line instead it is a function of x along the length of the element.

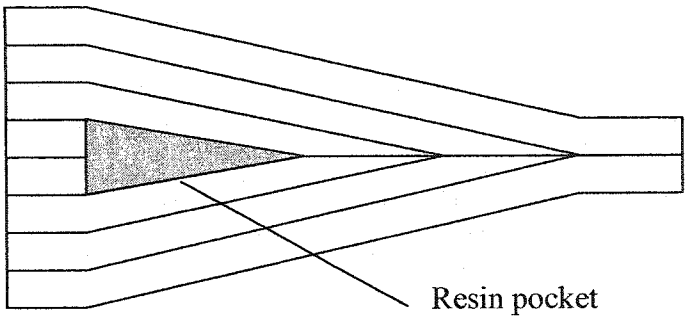

Figure 2.6 Schematic illustration of mid-plane tapered beam

Internally-tapered beams have been designed and developed in different types as shown in Figure 2.7.

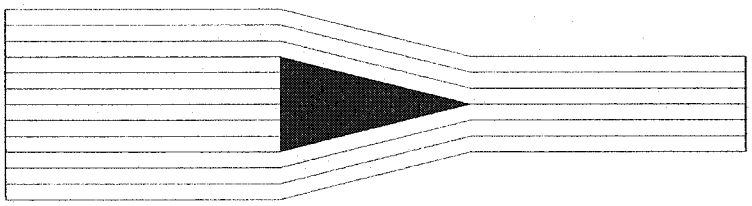

Model A

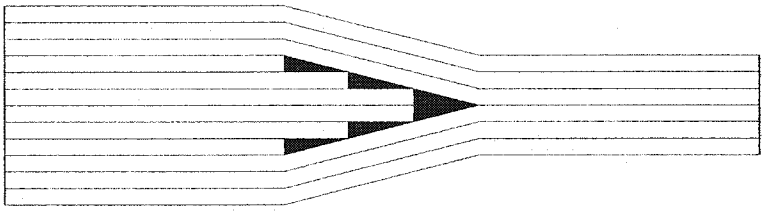

Staircase arrangement of multiple dropped plies (Model B)

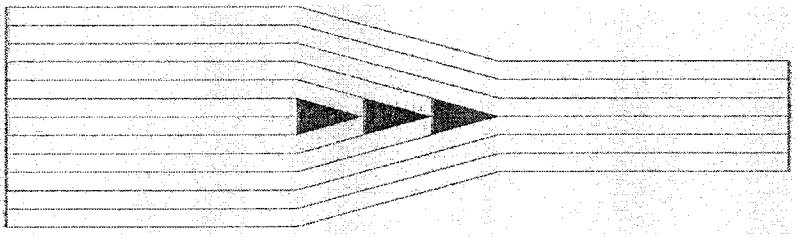

Overlapping dropped plies (Model C)

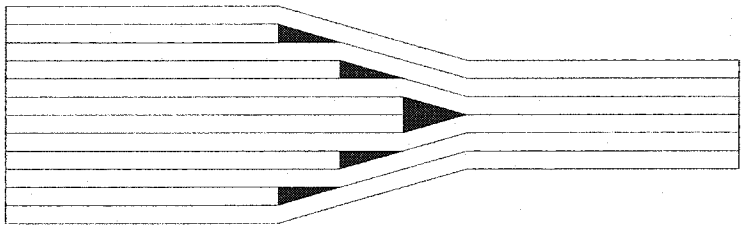

Continuous plies interspersed (Model D)

Figure 2. 7 Tapered beam models, A, B, C and D

2.4.1 Governing equation for mid-plane tapered beam

In this Section, the Equation of motion of a tapered beam is derived. The constitutive equation for laminated beam is given by Equation (2.2):

$$b\frac{\partial^2 M_x}{\partial x^2} + bN_x^i \frac{\partial^2 w}{\partial x^2} + bq(x) = b\rho_s \frac{\partial^2 w}{\partial t^2} \tag{2.2}$$

where M_x is the bending moment per unit length about y-axis given by [21]:

$$M_x = \sum_{k=1}^{n} \int_{h_{k-1}}^{h_k} z\sigma_x dz \tag{2.47}$$

where n represents the total number of plies in the laminate, and h_{k-1} and h_k are the distances to the lower and upper surfaces of each individual ply with respect to x axis. σ_x denotes the stress along the x direction. For a ply, the relation between stress and strain is given by [21]:

$$\sigma_x = \overline{Q}_{11}\varepsilon_x \tag{2.48}$$

where $\overline{Q}_{11}$ is the first coefficient of the transformed ply stiffness matrix and ε_x is the total strain along x axis which is given by [21]:

$$\varepsilon_x = \varepsilon_x^o + zk_x \tag{2.49}$$

ε_x^o and k_x denote the strain of the reference point and the curvature of the beam in the x-direction. In a tapered beam, all plies rotate by angle ϕ with respect to the x-direction.

Hence, the transformed strain along the taper axis (x') can be determined by neglecting strain in the thickness direction and shear strain as follows:

$$\varepsilon_{x'} = \varepsilon_x \cos^2(\phi) \tag{2.50}$$

Since x' lies on the two-dimensional plane of the individual ply, $\overline{Q}_{11}$ relates $\sigma_{x'}$ and $\varepsilon_{x'}$ as:

$$\sigma_{x'} = \overline{Q}_{11}\varepsilon_{x'} \tag{2.51}$$

In order to obtain the bending moment along x-axis, we must consider the effect of $\sigma_{x'}$ in the x-direction, which can be obtained by transformation of $\sigma_{x'}$ by the angle of ϕ and neglecting $\sigma_{y'}$ and $\gamma_{x'y'}$. Therefore we have:

$$\sigma_x = \sigma_{x'} \cos^2(\phi) = \overline{Q}_{11}\varepsilon_{x'} \cos^2(\phi) = \overline{Q}_{11}\varepsilon_x \cos^4(\phi) \tag{2.52}$$

Considering Equations (2.47), (2.51) and (2.52), the bending moment for the laminated beam along x-axis is derived as:

$$M_x = \sum_{k=1}^{n} \int_{h'_{k-1}}^{h'_k} \cos^4(\phi)\left[z\overline{Q}_{11}\varepsilon_x^o + z^2\overline{Q}_{11}k_x\right]dz \tag{2.53}$$

As one can see from Figure 2.8 the distances to the lower and upper surfaces of the k^{th} ply with respect to the x'-axis that are denoted by h'_{k-1} and h'_k are related to the ply thickness by the following relation:

$$(h'_k - h'_{k-1})\cos(\phi) = t_k \tag{2.54}$$

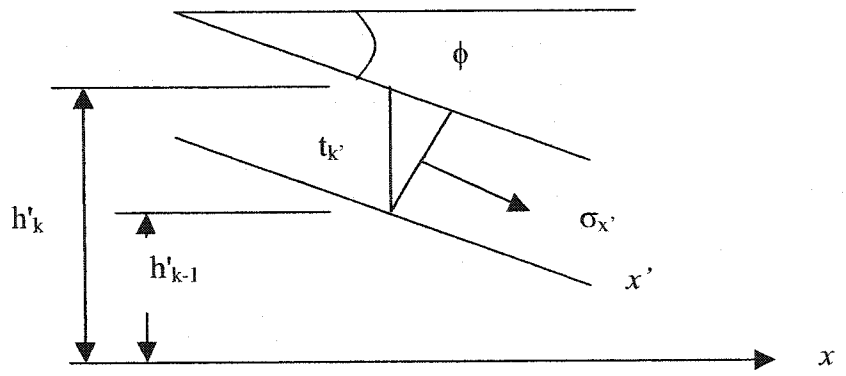

Figure 2.8 The k^{th} ply of the mid-plane tapered beam

Performing integration of the Equation (2.53), the bending moment of the laminated tapered beam is obtained as follows:

$$M_x = \sum_{k=1}^{n}\left[\frac{z^2}{2}\overline{Q}_{11}\varepsilon_x^o\cos^4(\phi)+\frac{z^3}{3}\cos^4(\phi)\overline{Q}_{11}k_x\right]_{h'_{k-1}}^{h'_k} \tag{2.55}$$

Equation (2.55) can be simplified to the following equation:

$$M_x = \sum_{k=1}^{n}\left[\left(\frac{h_k'^2-h_{k-1}'^2}{2}\right)\cos^4(\phi)\overline{Q}_{11}\varepsilon_x^o+\left(\frac{h_k'^3-h_{k-1}'^3}{3}\right)\cos^4(\phi)\overline{Q}_{11}k_x\right] \tag{2.56}$$

Equation (2.56) is simplified to the following form:

$$M_x = B_{11}(x)\varepsilon_x^o\cos^4(\phi)+D_{11}(x)\cos^4(\phi)k_x \tag{2.57}$$

where

$$B_{11}(x)=\sum_{k=1}^{n}\frac{1}{2}\left(h_k'^2-h_{k-1}'^2\right)\overline{Q}_{11} \tag{2.58}$$

$$D_{11}(x)=\sum_{k=1}^{n}\frac{1}{3}\left(h_k'^3-h_{k-1}'^3\right)\overline{Q}_{11} \tag{2.59}$$

According to classical laminate theory, curvature is given by:

$$k_x=-\frac{\partial^2 w}{\partial x^2} \tag{2.60}$$

For a mid plane symmetric laminate $B_{11} = 0$ [21]. Thus the bending moment reduces to:

$$M_x=-D_{11}(x)\cos^4(\phi)\frac{\partial^2 w}{\partial x^2} \tag{2.61}$$

Substituting these equations into Equation (2.2), the equation of motion for a tapered beam is obtained as:

$$\frac{\partial^2}{\partial x^2}\left(bD_{11}(x)\cos^4(\phi)\frac{\partial^2 w}{\partial x^2}\right)-bN_x^i\frac{\partial^2 w}{\partial x^2}-bq(x)+b\rho_s\frac{\partial^2 w}{\partial t^2}=0 \tag{2.62}$$

After redoing the derivation explained in Section 2.3.1, one can get the element properties for a mid-plane tapered beam as follows:

$$K_{ij}=\int_0^l bD_{11}(x)\cos^4(\phi)\frac{d^2N_i}{dx^2}\frac{d^2N_j}{dx^2}dx \tag{2.63}$$

$$G_{ij}=\int_0^l bN_x^i\frac{dN_i}{dx}\frac{dN_j}{dx}dx \tag{2.64}$$

$$M_{ij} = \int_0^l b\rho_s N_i N_j dx \tag{2.65}$$

2.4.2 Element properties for mid-plane tapered beam

To construct the stiffness and mass matrices for a tapered beam, one should note that in tapered case, the cross-section area and the value of D_{11} are not constant through the length of the beam. D_{11} can be written by the following Equation [21].

$$D_{11}(x) = \sum_{k=1}^{n}\left[t'_k \bar{z}_k^2 + \frac{t_k'^3}{12}\right](\overline{Q}_{11})_k \tag{2.66}$$

where t'_k for each ply is given by:

$$t'_k = h'_k - h'_{k-1} = \frac{t_k}{\cos(\phi)} \tag{2.67}$$

The term $(\overline{Q}_{11})_k$ denotes the first coefficient of the transformed ply stiffness matrix of individual ply, which is given by [21]:

$$\overline{Q}_{11} = \cos^4(\theta)Q_{11} + \sin^4(\theta)Q_{22} + 2\cos^2(\theta)\sin^2(\theta)Q_{12} + 4\cos^2(\theta)\sin^2(\theta)Q_{33} \tag{2.68}$$

where θ is the fiber orientation angle and Q_{ij} are the coefficients of the ply stiffness matrix for each ply which are given in reference [21]. $\bar{z}_k$ is the distance between the centerline of the tapered ply and the mid-plane of the laminate.

For the ply k, $\bar{z}_k$ is a function of x as shown in Figure 2.8.

$$\bar{z}_k = mx + c \tag{2.69}$$

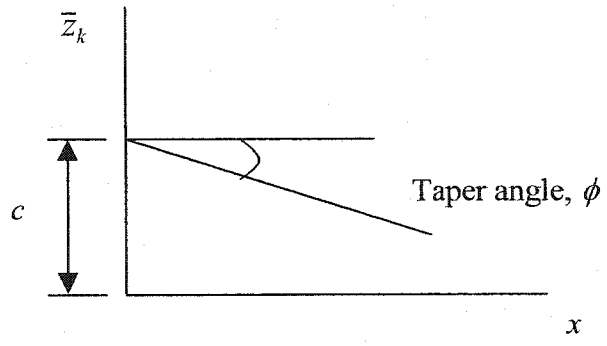

Figure 2.9 Centerline of a tapered ply

where c is the intercept of the centerline of the ply from the mid-plane line and m is the slope of the line that is given as:

$$m = -\tan(\phi) \tag{2.70}$$

ϕ denotes the taper angle of the laminated beam. Substituting Equation (2.69) and (2.67) into Equation (2.66), we can get:

$$D_{11}(x) = \sum_{k=1}^{n}\left[\frac{t_k}{\cos(\phi)}(mx+c)_k^2 + \frac{t_k^3}{12\cos^3(\phi)}\right](\bar{Q}_{11})_k \tag{2.71}$$

Substituting Equation (2.71) into Equation (2.63) it can be shown that:

$$K_{ij}^e = \int_0^l b\cos^4(\phi)\left[\sum_{k=1}^{n}\left(\frac{t_k}{\cos(\phi)}(mx+c)_k^2\right) + \frac{t_k^3}{12\cos^3(\phi)}\right](\bar{Q}_{11})_k \frac{d^2N_i}{dx^2}\frac{d^2N_j}{dx^2}dx \tag{2.72}$$

The stiffness matrix $[K]$ is obtained by substituting the shape functions into Equation (2.72) and performing the integration as specified by Equation (2.72). Integration has

been performed using MATLAB® software to determine the stiffness matrix for symmetric mid-plane tapered beams. (See *fen1.m* in Appendix-B).

$$\left[K^e\right] = \cos^3(\phi)\begin{bmatrix} K_{11}^e & K_{12}^e & K_{13}^e & K_{14}^e \\ K_{12}^e & K_{22}^e & K_{23}^e & K_{24}^e \\ K_{13}^e & K_{23}^e & K_{33}^e & K_{34}^e \\ K_{14}^e & K_{24}^e & K_{34}^e & K_{44}^e \end{bmatrix} \tag{2.73}$$

where the coefficients of the stiffness matrix are given as follows:

$$K_{11}^e = \sum_{k=1}^{n} b\left(\overline{Q}_{11}\right)_k t_k \frac{24m^2l^2 + 60clm + 60c^2 + 5t_k'^2}{5l^3}$$

$$K_{12}^e = \sum_{k=1}^{n} b\left(\overline{Q}_{11}\right)_k t_k \left(-\frac{1}{10}\right)\frac{14m^2l^2 + 40clm + 60c^2 + 5t_k'^2}{l^2}$$

$$K_{13}^e = \sum_{k=1}^{n} b\left(\overline{Q}_{11}\right)_k t_k \left(-\frac{1}{5}\right)\frac{14m^2l^2 + 40clm + 60c^2 + 5t_k'^2}{l^2}$$

$$K_{14}^e = \sum_{k=1}^{n} b\left(\overline{Q}_{11}\right)_k t_k \left(-\frac{1}{10}\right)\frac{34m^2l^2 + 80clm + 60c^2 + 5t_k'^2}{l^2}$$

$$K_{22}^e = \sum_{k=1}^{n} b\left(\overline{Q}_{11}\right)_k t_k \frac{8m^2l^2 + 30clm + 60c^2 + 5t_k'^2}{15l}$$

$$K_{23}^e = \sum_{k=1}^{n} b\left(\overline{Q}_{11}\right)_k t_k \left(\frac{1}{10}\right)\frac{14m^2l^2 + 40clm + 60c^2 + 5t_k'^2}{l^2}$$

$$K_{24}^e = \sum_{k=1}^{n} b\left(\overline{Q}_{11}\right)_k t_k \frac{26m^2l^2 + 60clm + 60c^2 + 5t_k'^2}{30l}$$

$$K_{33}^e = \sum_{k=1}^{n} b\left(\overline{Q}_{11}\right)_k t_k \frac{24m^2l^2 + 60clm + 60c^2 + 5t_k'^2}{5l^3}$$

$$K_{34}^e = \sum_{k=1}^{n} b\left(\overline{Q}_{11}\right)_k t_k \left(\frac{1}{10}\right)\frac{34m^2l^2 + 80clm + 60c^2 + 5t_k'^2}{l^2}$$

$$K_{44}^{e} = \sum_{k=1}^{n} b\left(\overline{Q}_{11}\right)_k t_k \frac{38m^2l^2 + 90clm + 60c^2 + 5t_k'^2}{15l}$$

(2.74)

The geometric stiffness matrix $[G]$ does not change by tapering the laminate. Also, the only change in mass matrix is due to the change in cross-section between thick and thin sections. The geometric stiffness matrix is given by:

$$[G] = \frac{bN_x^i}{30l}\begin{bmatrix} 36 & -3l & -36 & -3l \\ & 4l^2 & 3l & -l^2 \\ & & 36 & 3l \\ sym & & & 4l^2 \end{bmatrix} \tag{2.75}$$

The mass matrix for tapered laminated beam is obtained as (See *fen1.m* in Appendix-B):

$$[M] = \rho bl\begin{bmatrix} \frac{1}{35}(3ml+13g) & -\frac{1}{420}l(7ml+22g) & \frac{9}{140}(ml+2g) & \frac{1}{420}(6ml+13g) \\ & \frac{1}{840}l^2(3ml+8g) & -\frac{1}{420}l(7ml+13g) & -\frac{1}{280}l^2(ml+2g) \\ & & \frac{1}{35}(10ml+13g) & \frac{1}{420}l(15ml+22g) \\ sym & & & \frac{1}{840}l^2(5ml+8g) \end{bmatrix}$$

(2.76)

where g denotes the distance to the upper surface of the laminated beam from the mid-plane.

2.4.3 Finite element modeling for taper models A and C

Models A and C have the same geometry except that in model A all dropped-off plies are replaced by resin pocket. Also each finite element of model C can be considered for model A. Here model C is analyzed in full detail and the results are extended to model A. Since all models are symmetric, consider the upper half of the beam made with models A and C as shown in Figure 2.10.

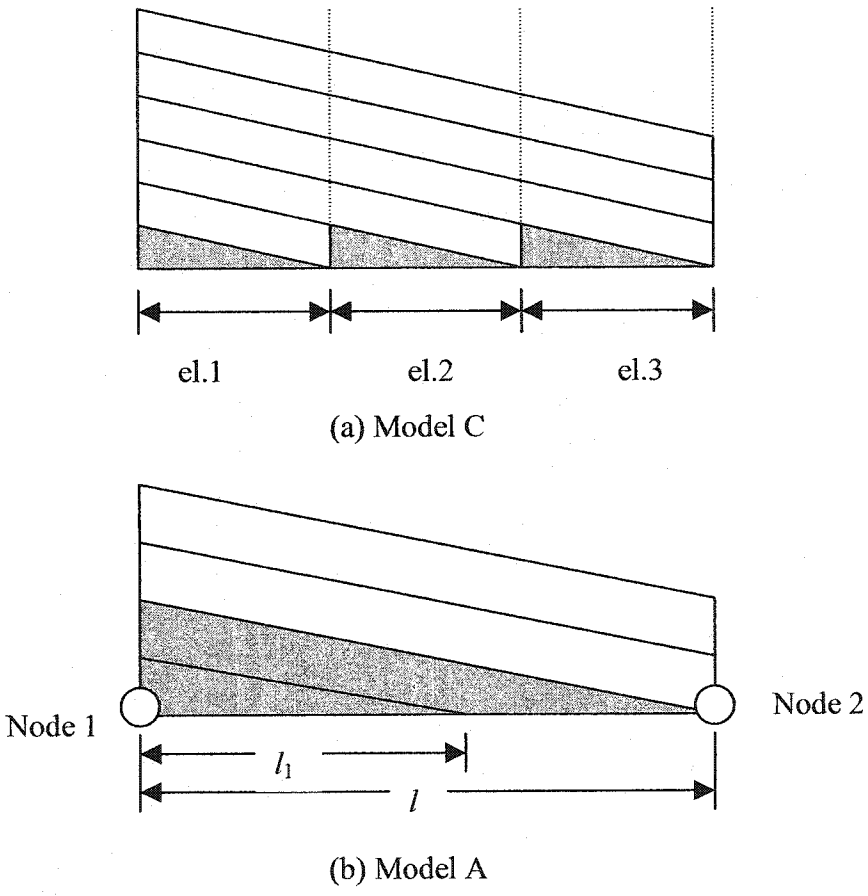

Figure 2.10 Schematic illustration of finite element for (a) model C and (b) model A

Although the resin pocket is not laminated, in order to proceed with the formulations as in the case of the laminated composite, let us consider the resin pocket to be made of imaginary layers with the same thickness as the other layers in laminated element.

As it is seen in Figure 2.10 the lengths of the layers in resin section are not equal. Therefore, the integration can not be performed from $x = 0$ to $x = l$ and it should be the summation of integrations for each segment. For convenience sake the following notations are used:

$$R = \frac{d^2 N_i}{dx^2} \frac{d^2 N_j}{dx^2} \tag{2.77}$$

For an element with the length l, K_{ij}^e is given by:

$$K_{ij}^e = \int_0^l bD_{11}(x)Rdx = \int_0^{l1} bD_{11}(x)Rdx + \int_{l1}^l bD_{11}(x)Rdx \tag{2.78}$$

One should note that in this case, to calculate $D_{11}(x)$, the plies located at resin pocket should be taken into account. Therefore we have:

$$D_{11}(x) = \sum_{k=1}^{n1} \left(\frac{t_k}{\cos(\phi)} \bar{z}_k^2 + \frac{t_k^3}{12\cos^3(\phi)} \right) \left(\overline{Q}_{11-p} \right)_k + \sum_{k=n1}^{n2} \left(\frac{t_k}{\cos(\phi)} \bar{z}_k^2 + \frac{t_k^3}{12\cos^3(\phi)} \right) \left(\overline{Q}_{11-r} \right)_k \tag{2.79}$$

where n*1* and *n2* denote the number of drop-off plies and number of imaginary plies considered together as resin pocket respectively. Notations *r* and *p* are used to indicate the imaginary resin layer and composite material prepreg.

The coefficients of the element matrices for tapered beams designated as model A and model C have been computed numerically by using MATLAB® software. (See *kmidA.m* and *kmidC.m* in Appendix-B)

2.4.4 Finite element modeling for taper models B and D

Finite element model for typical models B and D are shown in Figures 2.11. For convenience, each model is meshed by three elements. As one can see each element in model B is similar to the corresponding element in model D except that in model B the drop-off plies above resin pocket are the same for all elements in the mesh but in model D the plies above resin pocket are different for each element mesh.

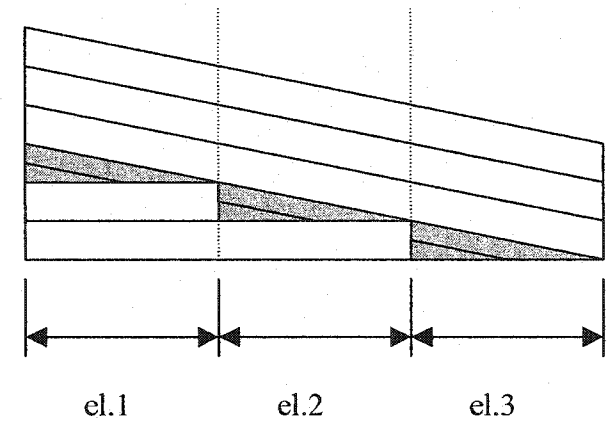

(a) Model B

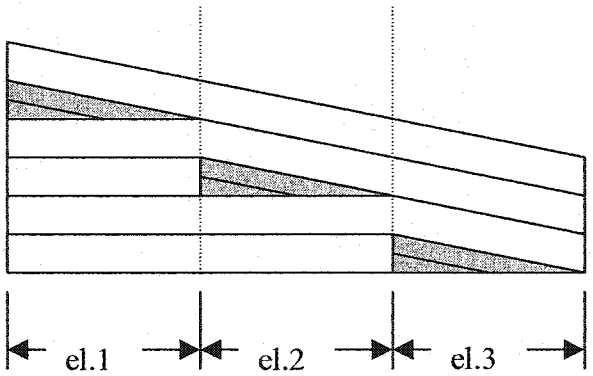

(b) Model D

Figure 2.11 FEM model for tapered beams: (a) model B and (b) model D

To explain the procedure, we consider a typical element of model D as shown in Figure 2.12. The resin pocket is considered as lamination of some plies with different lengths. One can see that the area above uniform layers is similar to a mid-plane taper. Thus the coefficients of stiffness matrix given by Equation (2.74) should be calculated as the summation of integrations of each sub-section:

$$\left(K_{ij}^{e}\right)_{0-L} = \left(K_{ij}^{e}\right)_{0-L_1} + \left(K_{ij}^{e}\right)_{L_1-L_2} + \left(K_{ij}^{e}\right)_{L_2-L} \tag{2.80}$$

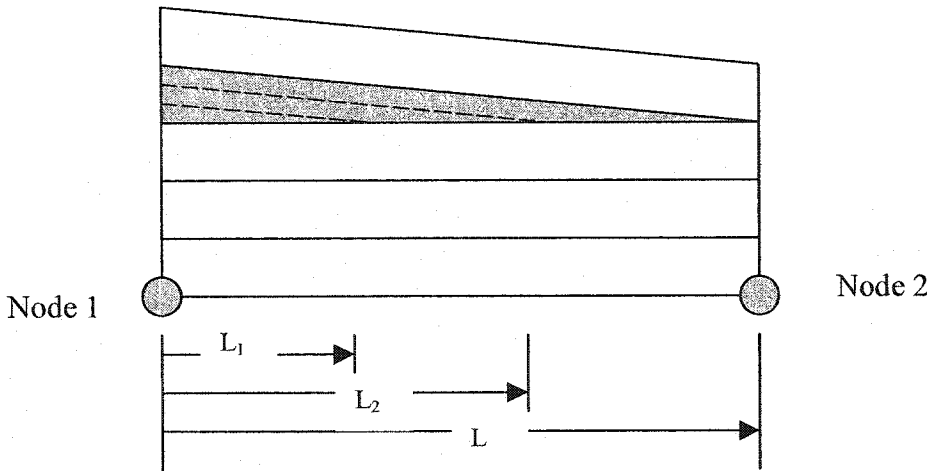

Figure 2.12 First part of finite element model D

where K_{ij}^{e} are computed using Equation (2.74). As shown in Figure 2.12 layers below the resin pocket are laid up uniformly. Therefore for these layers the taper angle should be set as zero. Individual routines have been developed using MATLAB ® software to calculate stiffness and mass matrices for internally-tapered beams, models A, B, C and D. The programs and routines have been listed in the next section.

2.5 Computer program and flowchart

In this Section the important routines developed for vibration and buckling analyses of uniform-thickness and tapered composite beams are listed. The flowchart shown in Figure 2.11 summarizes the procedures of the main computer programs in MATLAB ® software. Listing of routines and programs are provided in Appendix-B.

- **Dmat** This function calculates D matrix for a laminate composite
- **Qmat** This function calculates Q matrix for a laminate composite
- **Elindex** Calculates index for assembling matrices
- **Sycbc** Apply system boundary condition
- **Kmmat_b1** Stiffness and mass matrices for isotropic uniform Euler – Bernoulli beam
- **Kmmat_b2** Stiffness and mass matrices for laminated composite uniform Euler –Bernoulli beam
- **Kmmat_ba** Stiffness and mass matrices for laminated composite Euler-Bernoulli beam made with model A
- **Kmmat_bb** Stiffness and mass matrices for laminated composite Euler-Bernoulli beam made with model B
- **Kmmat_bc** Stiffness and mass matrices for laminated composite Euler-Bernoulli beam made with model C
- **Kmmat_bd** Stiffness and mass matrices for laminated composite Euler Bernoulli beam made with model D

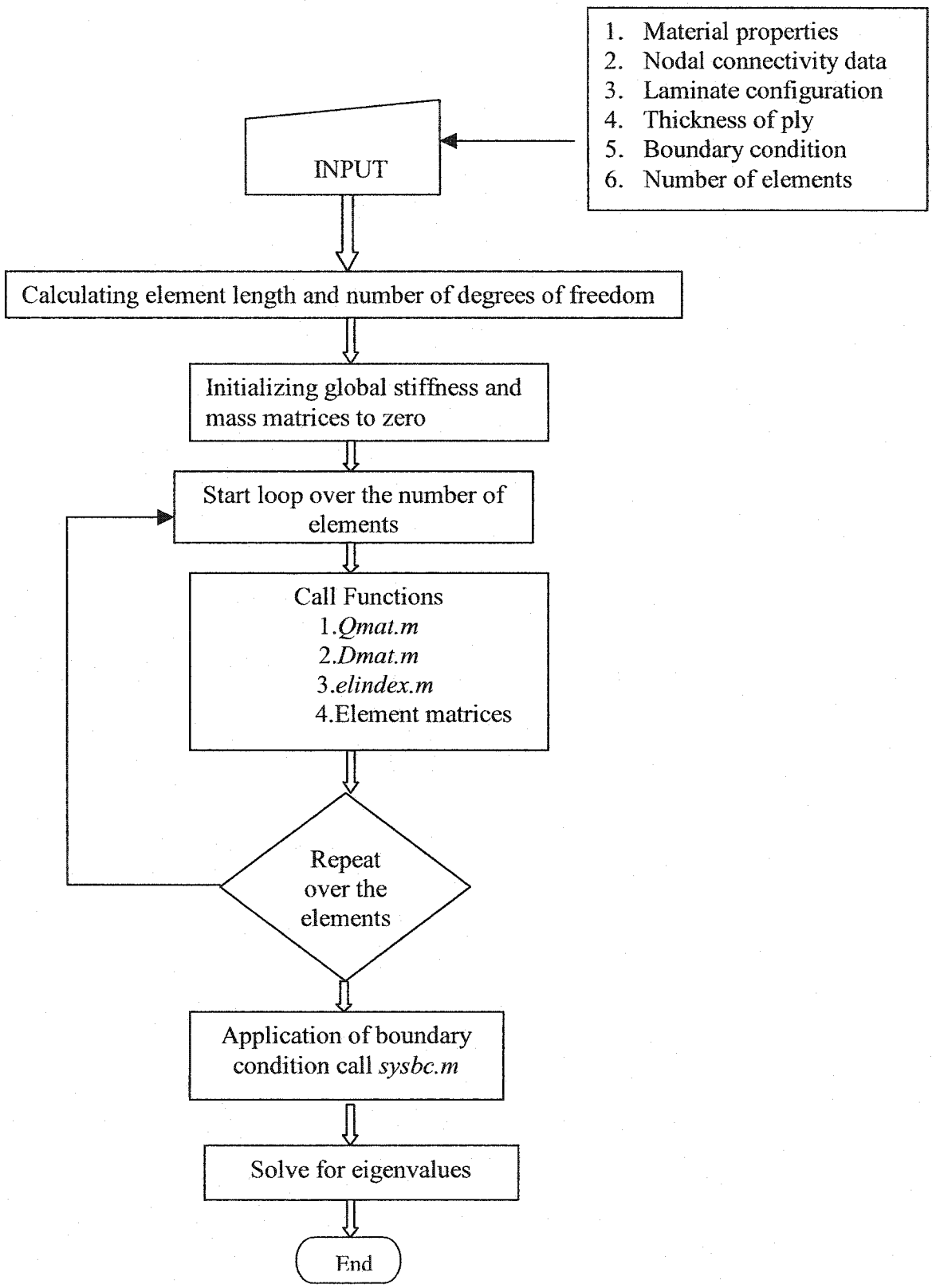

Figure 2.11 Flowchart of the main computer program

2.6 Example applications

In this Section a set of problems are solved for free vibration and buckling analyses of composite beams and free vibration of composite beam-columns to validate the formulations presented. The problems are solved for laminated beams in cylindrical bending. The results are compared with the exact solution in the case of uniform beams.

2.6.1 Uniform-thickness composite beam

2.6.1.1 Vibration analysis of uniform-thickness composite beam

Example 2.6.1.1

Problem description

A uniform-thickness composite beam with simply supported boundary condition made up of 144 plies is to be analyzed for free vibration. Mechanical properties are: E_1 is 144 GPa, E_2 is 12.14 GPa, ν_{12} is 0.21, ν_{21} is 0.288, G_{12} is 4.48 GPa, ρ is 1660.80 kg/m^3.

The geometric properties of the beam are: length (L) is 219.5 mm, individual ply thickness (t_k) is 0.1542 mm and the laminate configuration is $[0_4/\pm 45_4/\pm 45_{20}/-45_{20}]_s$.

The problem is solved using different number of elements to obtain the desired accuracy. The results are compared with the exact solution as well as with the results given in reference [32].

Table 2.1 The lowest three natural frequencies ($\times 10^3$ rad/sec) of a simply supported beam

Mode	Exact solution	2E(4DOF)	3E(6DOF)	4E(8DOF)	Ref. [32]
1	7.937	7.968	7.943	7.939	7.84
2	31.748	35.238	32.124	31.874	31.3
3	71.434	88.574	79.286	72.739	70.5

Example 2.6.1.2

Problem description

Uniform-thickness composite beams with (a) simply supported, (b) fixed-fixed and (c) fixed-free boundary conditions as shown in Figure.2.12 made up of 36 plies of NCT/301 graphite-epoxy are to be analyzed for free vibration. Mechanical properties are: E_1 is 113.9 GPa, E_2 is 7.9856 GPa, ν_{21} is 0.0178, ν_{12} is 0.288, G_{12} is 3.138 GPa, ρ is 1480 kg/m^3.

The geometric properties of the beams are: length (L) is 25 cm, individual ply thickness (t_k) is 0.125 mm and the laminate configuration is $(0/90)_{9s}$.

The problem is solved using different number of elements to obtain the desired accuracy.

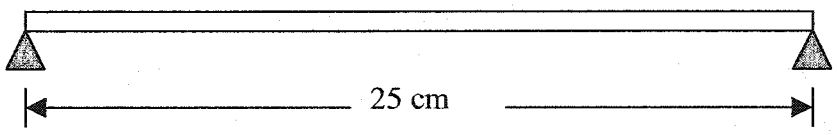

(a) Simply supported uniform composite beam

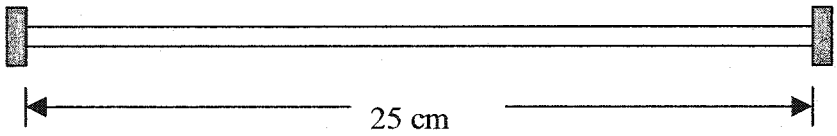

(b) Fixed-Fixed uniform composite beam

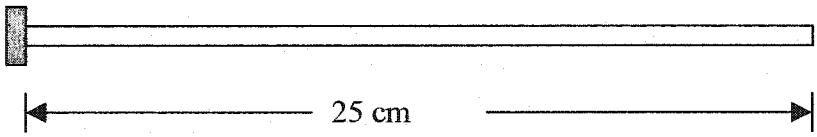

(c) Fixed-Free uniform composite beam

Figure 2.14 Uniform-thickness composite beams (example 2.6.1.2)

The results are compared with the exact solution given by Equations (2.35)-(2.37). Tables 2.1 to 2.3 give respectively the natural frequencies for the simply supported, fixed-fixed and fixed-free beams for mid-plane symmetric composite laminated beams.

Table 2.2 The lowest three natural frequencies ($\times 10^3$ rad/sec) of a simply supported beam

Mode	Exact solution	1E(2DOF)	2E(4DOF)	3E(6DOF)	4E(8DOF)
1	1.366	1.516	1.372	1.368	1.367
2	5.466	6.951	6.068	5.531	5.49
3	12.300	-	15.252	13.652	12.52

Table 2.3 The lowest three natural frequencies ($\times 10^3$ rad/sec) of fixed- fixed beam

Mode	Exact solution	1E(0DOF)	2E(2DOF)	3E(4DOF)	4E(6DOF)
1	3.100	-	3.148	3.111	3.102
2	8.539	-	11.352	8.711	8.619
3	16.743	-	-	20.259	17.100

Table 2.4 The lowest three natural frequencies ($\times 10^2$ rad/sec) of fixed-free beam

Mode	Exact solution	1E(2DOF)	2E(4DOF)	3E(6DOF)	4E(8DOF)
1	4.868	4.892	4.87	4.87	4.87
2	30.511	48.199	30.77	30.61	30.5
3	85.439	-	104.07	86.50	86.1

One observes that by increasing the number of elements to 4, the results for all the above boundary conditions get close enough to the corresponding exact solutions. Another interesting observation is that the natural frequencies for fixed-free boundary condition are the smallest compared to the cases of simply supported and fixed-fixed boundary conditions and the largest natural frequencies are for fixed-fixed boundary conditions.

2.6.1.2 Buckling analysis of uniform-thickness composite beam

Example 2.6.1.2 is considered to solve for critical buckling load. The mechanical properties and the geometry of the beams remain the same as example 2.6.1.2. The critical buckling load is obtained using FEM formulation explained in Section 2.3.2 and the results are compared with the exact solution given by Equations (2.58)-(2.60).

Table 2.4 gives respectively the critical buckling loads for the simply supported, fixed-fixed and fixed-free beams based on the cylindrical bending theory for mid-plane symmetric composite laminated beams.

Table 2.5 Critical buckling loads ($\times 10^3$N) for uniform composite beam with different boundary conditions

Boundary conditions	Exact solution	1 element	2 elements	3 elements	4 elements
Simply supported	39.38	47.89	39.68	39.52	39.40
Fixed-Fixed	157.54	-	159.62	159.01	158.70
Fixed-Free	9.847	9.921	9.852	9.847	9.847

Table 2.4 shows that by using 3 elements for fixed-free and simply supported boundary conditions the results obtained by MATLAB® are accurate enough compared to exact solutions whereas in fixed-fixed boundary condition we need more elements to have an accurate result. This is due to constraining four degrees of freedom in fixed-fixed case whereas for simply supported and fixed-free boundary conditions only two degrees of freedom are constrained.

2.6.1.3 Vibration analysis of uniform-thickness beam-column

Example 2.6.1.2 is considered for vibration analysis of a beam-column. In this case, the beams are loaded with a compressive axial load. The axial load is increased gradually as percentages of the critical buckling load to investigate the effects of axial load on the natural frequencies of beam-columns. Figure 2.15 illustrates that the ratio of natural frequency of beam-column under axial compressive load to natural frequency of the same beam without axial load (ω/ω_1) vs. the percentage of critical buckling load, P_{cr}, for simply supported, fixed-fixed and fixed-free composite beams. One should note that P_{cr} in Figure 2.15 is related to the corresponding boundary conditions for each case.

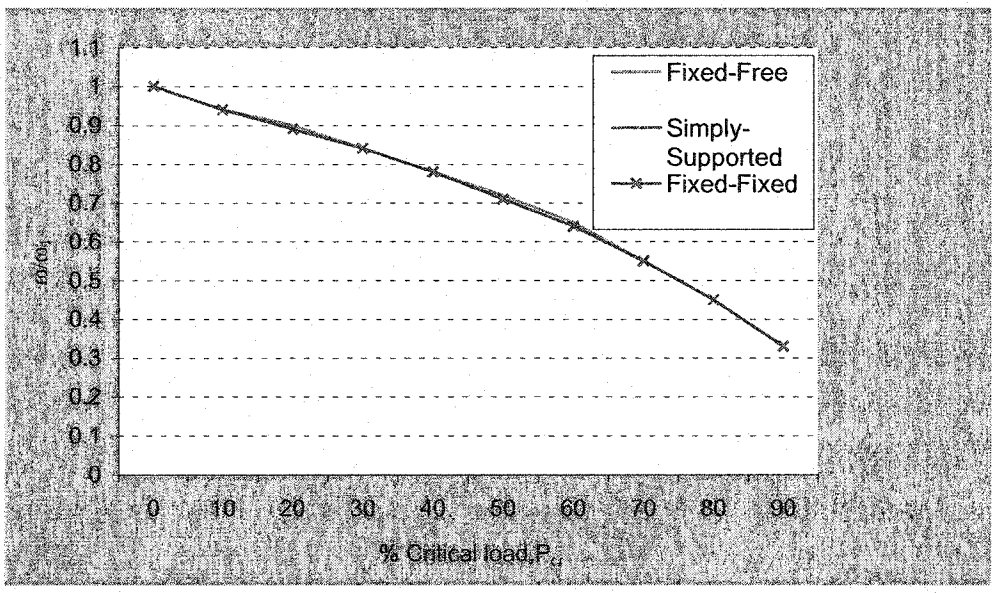

Figure 2.15 Frequency ratios vs. the percentage of critical buckling load for laminated beam-columns

Figure 2.15 shows that for all the above boundary conditions, the natural frequency decreases with the increase in the percentage of the corresponding buckling loads.

Another interesting result is that the rate of change of the natural frequencies for all boundary conditions is almost the same.

2.6.2 Tapered composite beam

Example 2.6.2.1

A mid-plane tapered composite beam as shown in Figure 2.6 has the following geometric properties: height is 1.219 mm; length is 12.2 mm (taper section). The configuration of the thick section is $[\pm 45_2]_s$ and that of the thin section is $[\pm 45]_s$. There are 8 plies in the thick section and 4 plies in the thin section. The angle of taper is equal to 1.43°. The thick section is fixed and thin section is free. The beam is meshed with two equal-length elements. The mechanical properties are the same as the mechanical properties of example 2.6.1.1. In Table 2.6, the results of the formulation obtained in the present chapter have been compared with the results of the same example given in reference [32].

Table 2.6 The lowest three natural frequencies ($\times 10^5$ rad/sec) of fixed-free beam

Mode No.	Reference [32]	Present
1	0.453	0.4430
2	2.29	2.1987
3	6.69	6.4743

2.6.2-1 Free vibration analysis of tapered beam model A

Example 2.6.2.2

Tapered beam made of model A as shown in Figure 2.10 is considered with 36 and 12 plies at thick and thin sections respectively, which results in 24 drop-off plies. The

configuration of the thick section is $(0/90)_{9s}$ and that of the thin section is $(0/90)_{3s}$. The problem is solved for different taper angles while the height ratio of thick and thin sections remains constant. As a result, the lengths of the beams change according to Table 2.7. The mechanical properties of the composite material are the same as in example 2.6.2.2. The thickness of each individual ply is 0.125 mm. The mechanical properties of the epoxy resin are given as: Elastic Modulus (E) is 3.93 GPa, Shear Modulus (G) is 1.034 GPa and Poisson's Ratio (ν) is 0.37. The beam is meshed by using three elements. The problem is solved for free vibration and the results for simply supported, fixed-free and fixed-fixed laminated beams are listed in Tables 2.8-2.10, respectively.

Table 2.7 The angles and length of the tapered beams

Angle ^{o}	0.1	0.5	0.75	1.0	1.5	2.0	2.5	3.0
L, m	0.8594	0.1719	0.1146	0.08594	0.0573	0.0430	0.0344	0.0286
L/h	190	38	25.46	19	12.7	9.54	7.36	6.36

Table 2.8 Natural frequencies ($\times 10^4$ rad/sec) of simply supported laminated beam of model A

Taper angle ^{o}	Mode 1	Mode 2	Mode 3	Mode 4
0.1	0.0068	0.0286	0.0654	0.1279
0.5	0.1712	0.7172	1.6355	3.1977
0.75	0.3852	1.6138	3.6800	7.1948
1.0	0.6848	2.8690	6.5422	12.7907
1.5	1.5408	6.4552	14.7195	28.7783
2.0	2.7391	11.4754	26.1669	51.1592
2.5	4.2797	17.9293	40.8835	79.9317
3.0	6.1624	25.8165	58.8683	115.0936

Table 2.9 Natural frequencies ($\times 10^4$ rad/sec) of fixed-free laminated beam of model A

Taper angle °	Mode 1	Mode 2	Mode 3	Mode 4
0.1	0.0040	0.0180	0.0470	0.0947
0.5	0.1023	0.4508	1.1769	2.3673
0.75	0.2303	1.0143	2.6481	5.3264
1.0	0.4094	1.8032	4.7078	9.4692
1.5	0.9213	4.0571	10.5922	21.3050
2.0	1.6378	7.2124	18.8298	37.8740
2.5	2.5590	11.2697	29.4200	59.1748
3.0	3.6847	16.2259	42.3618	85.2058

Table 2.10 Natural frequencies ($\times 10^4$ rad/sec) of fixed-fixed laminated beam of model A

Taper angle °	Mode 1	Mode 2	Mode 3	Mode 4
0.1	0.0159	0.0472	0.1069	0.2217
0.5	0.3994	1.1812	2.6736	5.5440
0.75	0.8987	2.6577	6.0157	12.4740
1.0	1.5974	4.7249	10.6947	22.1764
1.5	3.5946	10.6306	24.0618	49.8941
2.0	6.3901	18.8980	42.7746	88.6968
2.5	9.9840	29.5265	66.8315	138.5809
3.0	14.3760	42.5152	96.2307	199.5425

2.6.2.2 Free vibration analysis of tapered beam model B

The tapered beam of example 2.6.2.2 is considered to be made as model B. The beam is meshed with three equal-length elements. As it is seen in Figure 2.11, in the first and second elements, there are 16 and 8 uniform plies respectively. The problem is

solved for free vibration and the results obtained for simply supported, fixed- free and fixed-fixed boundary conditions are listed in Tables 2.11-2.13 respectively.

Table 2.11 Natural frequencies ($\times 10^4$ rad/sec) of simply supported laminated beam model B

Taper angle ^{o}	Mode 1	Mode 2	Mode 3	Mode 4
0.1	0.0164	0.0342	0.0673	0.1313
0.5	0.4107	0.8571	1.6839	3.2836
0.75	0.9242	1.9286	3.7888	7.3882
1.0	1.6431	3.4287	6.7356	13.1345
1.5	3.6976	7.7151	15.1550	29.5522
2.0	6.5749	13.7169	26.9417	52.4536
2.5	10.2760	21.4348	42.0954	82.0860
3.0	14.8021	30.8698	60.6156	118.2004

Table 2.12 Natural frequencies ($\times 10^4$ rad/sec) of fixed-free laminated beam model B

Taper angle ^{o}	Mode 1	Mode 2	Mode 3	Mode 4
0.1	0.0081	0.0218	0.0490	0.0961
0.5	0.2032	0.5468	1.2257	2.4049
0.75	0.4573	1.2303	2.7579	5.4110
1.0	0.8130	2.1874	4.9029	9.6196
1.5	1.8295	4.9219	11.0301	21.6436
2.0	3.2531	8.7506	19.6115	38.4765
2.5	5.0842	13.6742	30.6426	60.1173
3.0	7.3234	19.6930	44.1247	86.5651

Table 2.13 Natural frequencies ($\times 10^4$ rad/sec) of fixed-fixed laminated beam model B

Taper angle ^{o}	Mode 1	Mode 2	Mode 3	Mode 4
0.1	0.0208	0.0494	0.1098	0.2327
0.5	0.5221	1.2359	2.7456	5.8169
0.75	1.1749	2.7809	6.1775	13.0881
1.0	2.0888	4.9438	10.9823	23.2678
1.5	4.7001	11.1236	24.7098	52.3525
2.0	8.3566	19.7752	43.9278	93.0709
2.5	13.0589	30.8985	68.6354	145.2286
3.0	18.8078	44.4935	98.8319	209.4080

As one can observe the frequencies for all the boundary conditions and taper angles of model B are higher than the results for tapered beam of model A. This result was expected because the tapered section of model A is less stiff than the model B and it is due to a large pocket of resin in model A and due to the fact that the stiffness of resin material is lower than the stiffness of the fibers. In both cases the frequency is increased as the taper angles increased. The reason for this behavior is that increasing the angles results in decreasing the length and the beam becomes shorter and therefore the frequency of vibration increased.

2.6.2.3 Free vibration analysis of tapered beam model C

The tapered beam of example 2.6.2.2 is considered to be made as model C. The beam is modeled with 3 equal-length elements. As one can see the total volume of the resin pocket for models C and B are the same but they are distributed at different locations in each model. The problem is solved for free vibration and the results obtained for simply supported, fixed- free and fixed-fixed boundary conditions are listed in Tables 2.14 -2.16 respectively.

Table 2.14 Natural frequencies ($\times 10^4$ rad/sec) of simply supported laminated beam model C

Taper angle °	Mode 1	Mode 2	Mode 3	Mode 4
0.1	0.0071	0.0305	0.0690	0.1363
0.5	0.1790	0.7628	1.7269	3.4083
0.75	0.4028	1.7165	3.8854	7.6687
1.0	0.7160	3.0511	6.9073	13.6330
1.5	1.6110	6.8689	15.5410	3.0673
2.0	2.8638	12.2037	27.6273	54.5283
2.5	4.4745	19.0672	43.1653	85.1957
3.0	6.4429	27.4549	62.1538	122.6735

Table 2.15 Natural frequencies ($\times 10^4$ rad/sec) of fixed-free laminated beam model C

Taper angle $^\circ$	Mode 1	Mode 2	Mode 3	Mode 4
0.1	0.0045	0.0193	0.0504	0.0998
0.5	0.1148	0.4843	1.2607	2.4972
0.75	0.2583	1.0897	2.8366	5.6188
1.0	0.4593	1.9374	5.0428	9.9889
1.5	1.0333	4.3589	11.3460	22.4744
2.0	1.8370	7.7489	20.1699	39.9527
2.5	2.8701	12.1071	31.5137	62.4227
3.0	4.1327	17.4339	45.3767	89.8825

Table 2.16 Natural frequencies ($\times 10^4$ rad/sec) of fixed-fixed laminated beam model C

Taper angle $^\circ$	Mode 1	Mode 2	Mode 3	Mode 4
0.1	0.0172	0.0510	0.1139	0.2404
0.5	0.4307	1.2749	2.8487	6.0101
0.75	0.9692	2.8689	6.4103	13.5223
1.0	1.7253	5.1050	11.3951	24.0399
1.5	3.8763	11.4739	25.669	54.0881
2.0	6.8910	20.3972	45.5748	96.1524
2.5	10.7666	31.8688	71.2066	150.0229
3.0	15.5028	45.8880	102.5305	216.3160

2.6.2.4 Free vibration analysis of tapered beam model D

The tapered beam of example 2.6.2.2 is considered to be made as model D. The problem is solved for free vibration and the results obtained for simply supported, fixed free and fixed-fixed boundary conditions are listed in Table 2.17-2.19 respectively.

Table 2.17 Natural frequencies ($\times 10^4$ rad/sec) of simply supported laminated beam model D

Taper angle ^{o}	Mode 1	Mode 2	Mode 3	Mode 4
0.1	0.0196	0.0380	0.0758	0.1462
0.5	0.4915	0.9526	1.8957	3.6559
0.75	1.1059	2.1435	4.2654	8.2258
1.0	1.9662	3.8107	7.5829	14.6236
1.5	4.4245	8.5748	17.0616	32.9030
2.0	7.8670	15.2455	30.3317	58.4937
2.5	12.2948	23.8239	47.3930	91.3956
3.0	17.7089	34.3114	68.2454	131.6081

Table 2.18 Natural frequencies ($\times 10^4$ rad/sec) of fixed-free laminated beam model D

Taper angle ^{o}	Mode 1	Mode 2	Mode 3	Mode 4
0.1	0.0817	0.0480	0.05085	0.1077
0.5	0.2044	0.6201	1.2712	2.6928
0.75	0.4601	1.3953	2.8603	6.0588
1.0	0.8180	2.4806	5.0850	10.7711
1.5	1.8408	5.5818	11.4412	24.2348
2.0	3.2731	9.9242	20.3397	43.0833
2.5	5.1154	15.5087	31.7801	67.3163
3.0	7.3683	22.3360	45.7622	96.9329

Table 2.19 Natural frequencies ($\times 10^4$ rad/sec) of fixed-fixed laminated beam model D

Taper angle ^{o}	Mode 1	Mode 2	Mode 3	Mode 4
0.1	0.0240	0.0506	0.1935	0.2532
0.5	0.6022	1.2655	2.9838	6.3309
0.75	1.3551	2.8473	6.7135	14.2447
1.0	2.4090	5.0620	11.9353	25.3239
1.5	5.4211	11.3893	26.8542	51.6979
2.0	9.6387	20.2474	47.7405	101.2974
2.5	15.0627	31.6361	74.5939	158.2789
3.0	21.6944	45.5551	107.4141	227.9245

The fundamental frequencies of different types of tapered beam are compared in Figure 2.16. As one can observe the fundamental frequency for model D is higher than the others, this result was expected for model D because the number of uniform plies in model D are 12 in the first element and 8 in the second element, whereas, in model B there are 8 uniform plies in first element and 4 in the second one. As it is observed in tapered formulation, the slope decreases D_{11}, bending stiffness. Another feature of importance is that the value of the frequencies of models A and C are almost the same. This shows that the effect of tapering on the frequency are more than the effect of resin material.

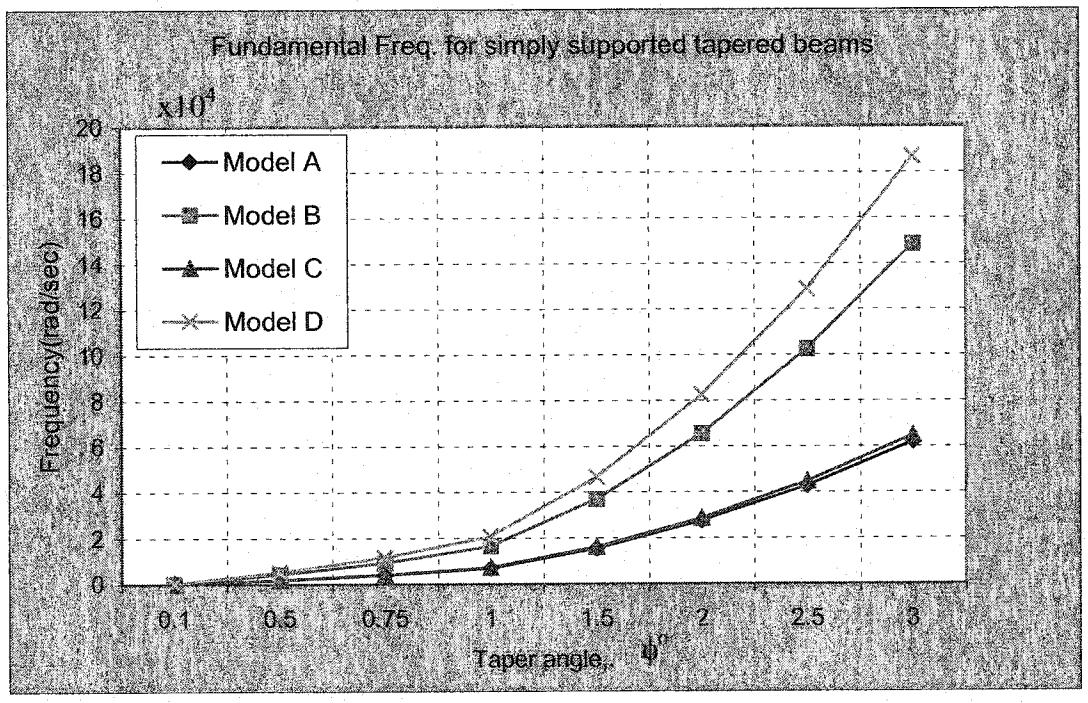

Figure 2.16 Fundamental frequencies for simply supported tapered beam models, A, B, C and D

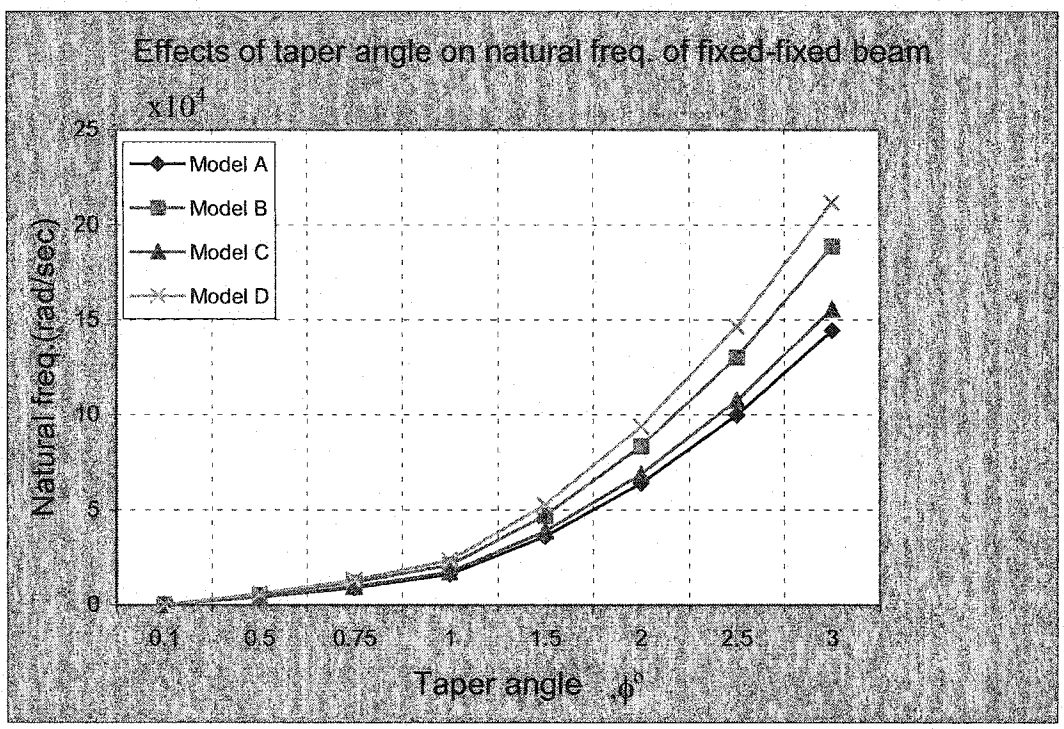

Figure 2.17 Fundamental frequencies for fixed-fixed tapered beam models, A, B, C and D

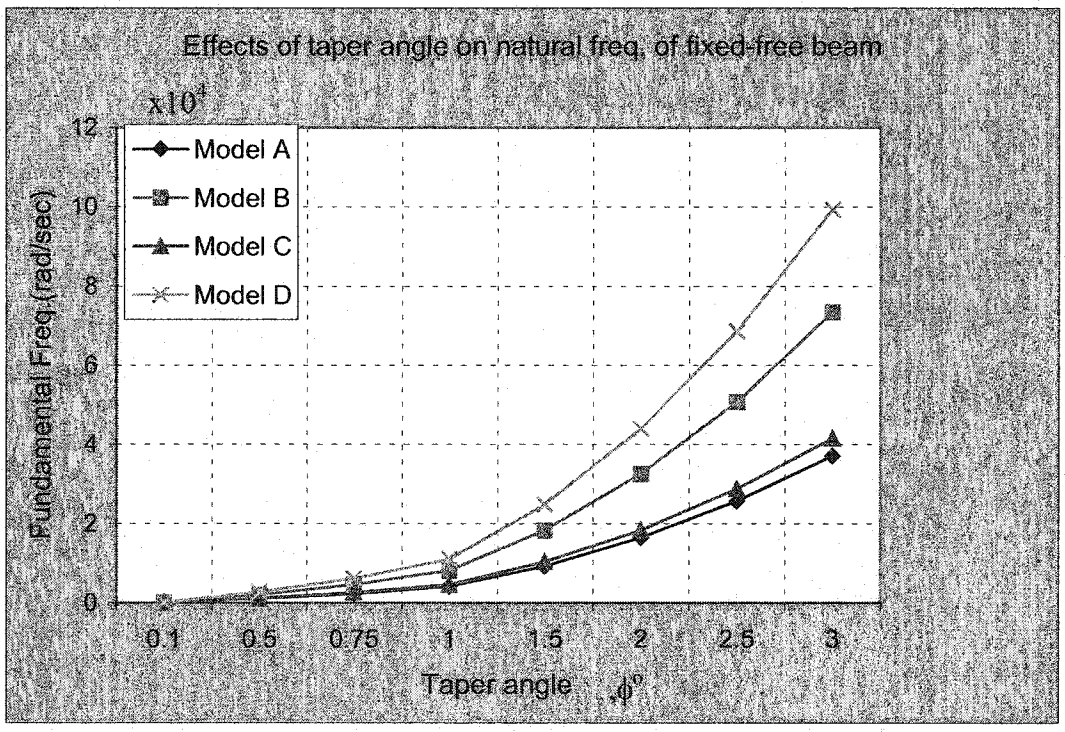

Figure 2.18 Fundamental frequencies for fixed-free tapered beam models, A, B, C and D

2.6.2.5 Buckling analysis of tapered composite beam

The tapered beams described in the example 2.6.2.2 are considered for buckling analysis. The critical buckling loads obtained for simply supported, fixed-free and fixed-fixed boundary conditions are listed in Tables 2.20-2.23.

Table 2.20 Critical buckling load ($\times 10^4$ N) of tapered laminated beam model A

Taper angle ^{o}	Simply supported	Fixed-free	Fixed- fixed
0.1	0.1399	0.0565	0.5556
0.5	3.4995	1.4146	13.8915
0.75	7.8733	3.1827	31.2535
1.0	13.9955	5.6576	55.5557
1.5	31.4799	12.7256	124.9608
2.0	55.9394	22.6133	222.0540
2.5	87.3554	35.3131	346.7614
3.0	125.7041	50.8153	498.9880

Table 2.21 Critical buckling load ($\times 10^4$ N) of tapered laminated beam model B

Taper angle ^{o}	Simply supported	Fixed-free	Fixed- fixed
0.1	0.4504	0.1030	0.8284
0.5	11.2596	2.5771	20.7094
0.75	25.3332	5.7983	46.5941
1.0	45.0341	10.3073	82.8287
1.5	101.3099	23.1867	186.3302
2.0	180.0644	41.2088	331.1684
2.5	281.2660	64.3647	517.2791
3.0	404.8741	92.6427	744.5802

Table 2.22 Critical buckling load ($\times 10^4$ N) of tapered laminated beams model C

Taper angle ^{o}	Simply supported	Fixed-free	Fixed- fixed
0.1	0.1490	0.0650	0.6164
0.5	3.7225	1.6254	15.4100
0.75	8.3810	3.6570	34.6719
1.0	14.8979	6.5006	61.6322
1.5	33.5098	14.6218	138.6287
2.0	59.5466	25.9828	246.3420
2.5	92.9887	40.5750	384.6906
3.0	135.8107	58.3874	553.5693

Table 2.23 Critical buckling load ($\times 10^4$ N) of tapered laminated beam model D

Taper angle ^{o}	Simply supported	Fixed-free	Fixed- fixed
0.1	0.4534	0.0866	0.9294
0.5	11.3346	2.1662	23.2341
0.75	25.5014	4.8737	52.2739
1.0	45.3320	8.6371	92.9240
1.5	101.9722	19.4884	209.0315
2.0	181.2222	34.6340	371.4933
2.5	283.0359	54.0913	580.2208
3.0	407.3539	77.8487	835.1000

As one can see the critical buckling loads increase by increasing taper angle for all types of boundary conditions and taper models. Figure 2.19 shows the effects of taper angle on the critical buckling load for a simply supported tapered beam model D. As it is seen for all taper angles, taper beam model D gives the highest value of critical buckling load. The lowest values of critical buckling load belong to the tapered beam model A.

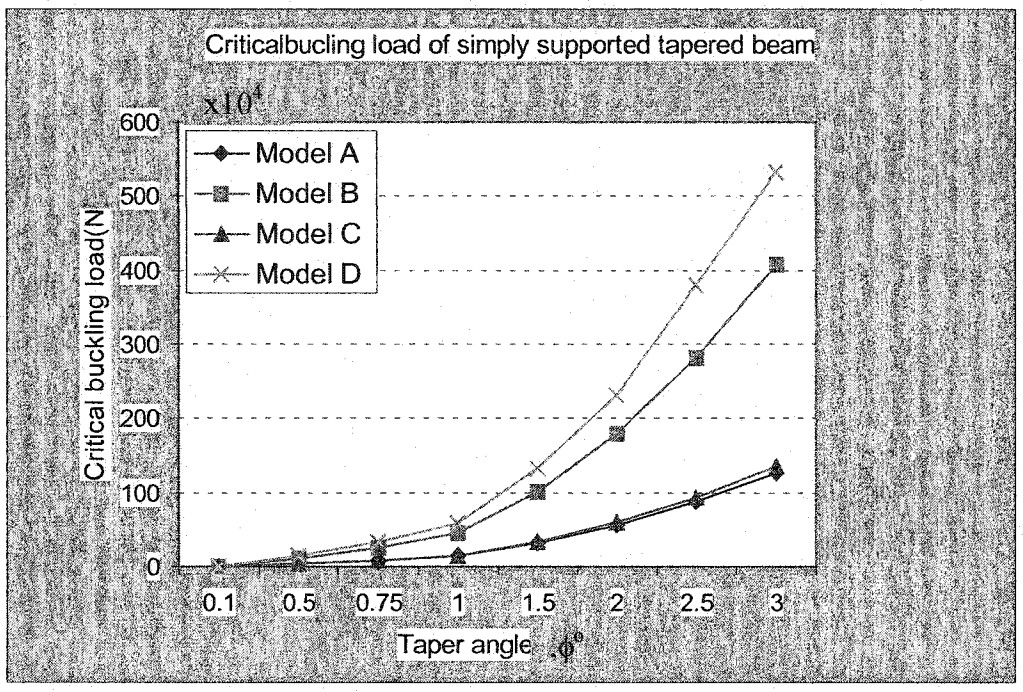

Figure 2.19 Critical buckling load for simply supported tapered beam

2.7 Conclusions and discussions

In this Chapter, the conventional finite element model was developed for the vibration and buckling analysis of uniform-thickness and tapered composite beams based on classical laminate theory. In the conventional formulation, we considered two nodes per beam element. Two degrees of freedom, deflection and rotation, are considered for each node. The formulation has been applied to obtain natural frequencies and critical buckling load of uniform-thickness and tapered composite beams. In the case of uniform-thickness beams, the results obtained have been compared with the exact solutions.

Finite element model was developed for analysis of tapered composite beams. Various types of tapered composite beams, viz. model A, staircase (model B), overlapped (model C) and continuous plies interspersed (model D) have been investigated for natural

frequencies and critical buckling loads under different boundary conditions. Tapered beam made with model D has the highest stiffness, model B and C take the second and third ranks respectively. Model A has the lowest stiffness. Therefore the natural frequencies and critical buckling loads of model D are the highest and consequently models B, C and D occupy the second, third and forth positions. Natural frequencies of model D are about three times more than the corresponding results for model A.

Observation of the results obtained for different boundary conditions for uniform beams as well as non-uniform beams reveals that the natural frequencies for fixed-fixed support are the highest. Simply supported and fixed-free supports take the second and third positions.

By increasing taper angles while keeping the thickness constant, the natural frequencies and critical buckling loads increase for all types of tapered beams.

Chapter 3

Vibration analysis of laminated composite beams based on First-order Shear Deformation Theory (FSDT)

3.1 Introduction

The classical theory of laminate describes, with a good precision, the mechanical behavior of thin laminate. In the case of thick laminate (ratio of the length to thickness less than 10), the results derived using the classical laminate theory show significant difference with the experimental results [2]. Also in composite materials the ratio of Young's modulus in fiber direction to the in-plane shear modulus is very high. This leads to a larger influence of shear deformation.

The first-order shear deformation theory (FSDT) improves the classical laminate theory by introducing the effects of transverse shear deformation. The first-order shear deformation theory, when considered for beams, is called as Timoshenko beam theory. The basic assumptions in Timoshenko beam theory are similar to classical laminate theory except that in Timoshenko theory, the transverse normal does not remain perpendicular to the mid surface after deformation. Figure 3.1 illustrates schematically the rotation of the cross-section in Timoshenko beam element. In Figure 3.1, φ represents the total rotation corresponding to Euler-Bernoulli beam element and ψ represents the

total rotation of the cross-section in the Timoshenko beam element. As it is seen the value of φ is different from ψ due to the effects of the shear deformation. $\gamma = \varphi - \psi$ is used as the mean value of the shear deformation. One should note that in Figure 3.1, $\varphi = \frac{\partial w}{\partial x}$

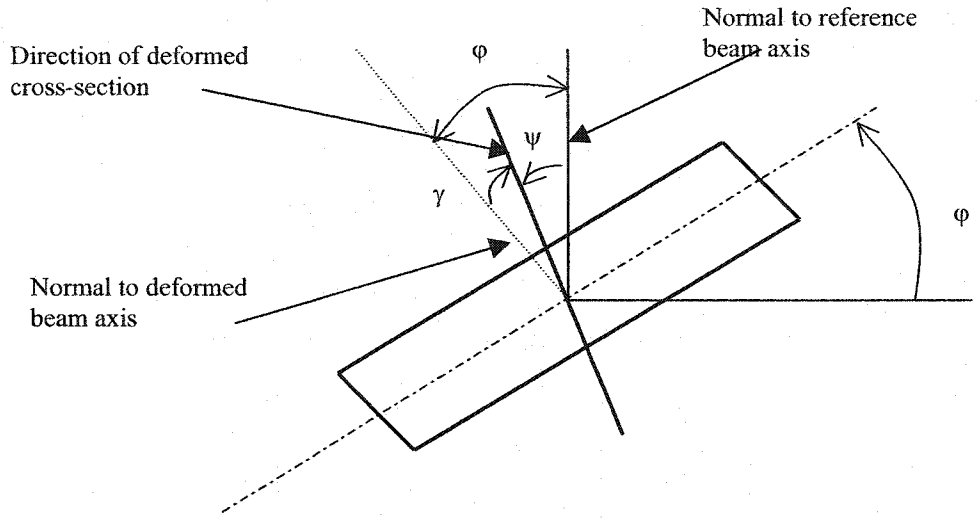

Figure 3.1 Definition of section rotation in the Timoshenko beam model

3.2 Vibration analysis of uniform-thickness laminated beam

3.2.1 Equation of motion for Timoshenko beam

The basic Equations for mid-plane symmetric composite beams in cylindrical bending are given as [3]:

$$b\frac{\partial Q_x}{\partial x} + bN_x^i \frac{\partial^2 w}{\partial x^2} + bq(x) = b\rho_s \frac{\partial^2 w}{\partial t^2} \tag{3.1}$$

$$b\frac{\partial M_x}{\partial x} - bQ_x = bI_{xy}\frac{\partial^2 \psi}{\partial t^2} \tag{3.2}$$

where Q_x denotes the transverse shear force per unit width which is given by [21]:

$$Q_x = F_{55}\left(\frac{\partial w}{\partial x} - \psi\right) \tag{3.3}$$

where F_{55} is given by:

$$F_{55} = \sum_{k=1}^{n}(h_k - h_{k-1})(\overline{C}_{55})_k = \sum_{k=1}^{n}(t_k)(\overline{C}_{55})_k \tag{3.4}$$

In Equation (3.4), n represents the total number of plies in the laminate, t_k the thickness of individual ply, and h_k and h_{k-1} are the distances to the upper and lower surfaces of k^{th} ply from the mid-plane. $\overline{C}_{55}$ is computed using the following relation:

$$\overline{C}_{55} = C_{44}\sin^2(\theta) + C_{55}\cos^2(\theta) \tag{3.5}$$

where θ is the angle between fiber orientation and the reference axis and the values of C_{44} and C_{55} are given by:

$$C_{44} = G_{23} \qquad C_{55} = G_{13} \tag{3.6}$$

where G_{13} and G_{23} denote the shear modulus values in relevant planes.

In first-order shear deformation theory, the transverse strains are considered constant through the laminate thickness; as a result the transverse shear stress will also be constant. In fact, the transverse shear stress is not constant through the thickness. This difference is corrected by considering a shear correction factor. Here the shear correction factor is denoted by μ. For most applications of the isotropic materials the value of μ is considered 5/6 but for laminated beams, the value of shear correction factor depends on the laminate configuration and the number of plies. The value of the shear correction factor has been computed for different laminate configurations and number of plies by Raman and Davalos [59]. Considering the shear correction factor, the transverse shear stress is given by:

$$Q_x = H_{55}\left(\frac{\partial w}{\partial x} - \psi\right) \tag{3.7}$$

where

$$H_{55} = \mu F_{55} \tag{3.8}$$

where I_{xy}, the rotational inertia is given by:

$$I_{xy} = \int_{-h/2}^{h/2} \rho z^2 dz \tag{3.9}$$

where h is the thickness of the laminate, z denotes the axis along the laminate thickness and ρ is the mass density of individual ply.

The bending moment is given by [21]:

$$M_x = D_{11}\kappa_x \tag{3.10}$$

where κ_x denotes the curvature along x-axis which is given by:

$$\kappa_x = \frac{\partial \psi}{\partial x} \tag{3.11}$$

Considering Equation (3.11), Equation (3.10) can be written as follows:

$$M_x = D_{11}\frac{\partial \psi}{\partial x} \tag{3.12}$$

D_{11}, ρ_s, $q\ (x)$ and N_x^i have been detailed in chapter 2 and are used here. Substituting Equations (3.12) and (3.7) into Equations (3.1) and (3.2) respectively, the differential equations for mid-plane symmetric laminated beams based on Timoshenko beam model are obtained as follows:

$$bH_{55}\left(\frac{\partial^2 w}{\partial x^2} - \frac{\partial \psi}{\partial x}\right) + bN_x^i\frac{\partial^2 w}{\partial x^2} + bq(x) - b\rho_s\frac{\partial^2 w}{\partial t^2} = 0 \tag{3.13}$$

$$\frac{\partial}{\partial x}\left(bD_{11}\frac{\partial \psi}{\partial x}\right) - bH_{55}\left(\frac{\partial w}{\partial x} - \psi\right) - bI_{xy}\frac{\partial^2 \psi}{\partial t^2} = 0 \tag{3.14}$$

where b denotes the width of the beam.

3.2.2. Weak form of the governing equations

To construct the weak forms of Equations (3.13) and (3.14), one can use the three- step procedure introduced in reference [2] that has been used in Chapter 2. In Timoshenko beam element there are two coupled differential equations for deflection and rotation. Therefore we require two weight functions, v_1 and v_2 to construct the weak forms of the differential Equations. Multiplying Equation (3.13) by v_1:

$$0=\int_0^l\left[v_1 bH_{55}\left(\frac{\partial^2 w}{\partial x^2}-\frac{\partial \psi}{\partial x}\right)+v_1 bN_x^i\frac{\partial^2 w}{\partial x^2}+v_1 bq(x)-v_1 b\rho_s\frac{\partial^2 w}{\partial t^2}\right]dx \tag{3.15}$$

Integration by parts of the first and second terms results in the following Equation:

$$0=\int_0^l\left[bH_{55}\frac{dv_1}{dx}\left(\frac{\partial w}{\partial x}-\psi\right)+\int_0^l bN_x^i\frac{dv_1}{dx}\frac{\partial w}{\partial x}-v_1 bq(x)+v_1 b\rho_s\frac{\partial^2 w}{\partial t^2}\right]dx$$

$$-\left[v_1 bH_{55}\left(\frac{\partial w}{\partial x}-\psi\right)\right]_{x=0}^{x=l}-v_1 bN_x^i\frac{\partial w}{\partial x}\Big|_{x=0}^{x=l} \tag{3.16}$$

Introducing the following notations for secondary variables:

$$Q_1^e=-\left[bH_{55}\left(\frac{\partial w}{\partial x}-\psi\right)+bN_x^i\frac{\partial w}{\partial x}\right]_{x=0} \tag{3.17}$$

$$Q_3^e=\left[bH_{55}\left(\frac{\partial w}{\partial x}-\psi\right)+bN_x^i\frac{\partial w}{\partial x}\right]_{x=l} \tag{3.18}$$

Considering Equations (3.17) and (3.18), the Equation (3.16) is obtained as:

$$0=\int_0^l\left[bH_{55}\frac{dv_1}{dx}\left(\frac{\partial w}{\partial x}-\psi\right)+bN_x^i\frac{dv_1}{dx}\frac{\partial w}{\partial x}+v_1b\rho_s\frac{\partial^2 w}{\partial t^2}-v_1bq(x)\right]dx-Q_1^e v_1(0)-Q_3^e v_1(l) \tag{3.19}$$

Similarly, multiplication of Equation (3.14) by v_2 results in the following relation:

$$0=\int_0^l(v_2\frac{\partial}{\partial x}\left(bD_{11}\frac{\partial\psi}{\partial x}\right)-v_2bH_{55}\left(\frac{\partial w}{\partial x}-\psi\right)-v_2bI_{xy}\frac{\partial^2\psi}{\partial t^2})dx \tag{3.20}$$

Introducing the secondary variables by:

$$Q_2^e=-\left[bD_{11}\frac{\partial\psi}{\partial x}\right]_{x=0} \tag{3.21}$$

$$Q_4^e=\left[bD_{11}\frac{\partial\psi}{\partial x}\right]_{x=l} \tag{3.22}$$

Integrating by parts the first term of equation (3.20) and using Equations (3.21) and (3.22), the Equation (3.20) can be written as:

$$0=\int_0^l\left[bD_{11}\frac{dv_2}{dx}\frac{\partial\psi}{\partial x}+v_2bH_{55}\left(\frac{\partial w}{\partial x}-\psi\right)+v_2bI_{xy}\frac{\partial^2\psi}{\partial t^2}\right]dx-Q_2^e v_2(0)-Q_4^e v_2(l) \tag{3.23}$$

3.2.3 Generation of finite element model

Considering primary variables at the end nodes:

$$w(0)=w_1^e \qquad w(l)=w_2^e \qquad \psi(0)=\psi_1^e \qquad \psi(l)=\psi_2^e \tag{3.24}$$

choosing a linear approximation for displacement and the cross-section rotation as follows:

$$w = a_1 + a_2 x \tag{3.25}$$

$$\psi = b_1 + b_2 x \tag{3.26}$$

and substituting boundary conditions from Equation (3.24), one can get:

$$w_1^e = a_1, \qquad w_2^e = a_1 + a_2 l \tag{3.27}$$

$$\psi_1^e = b_1, \qquad \psi_2^e = b_1 + b_2 l \tag{3.28}$$

Solving Equations (3.27) and (3.28) the variables a_1, a_2, b_1 and b_2 are determined as follows:

$$a_1 = w_1^e, \qquad a_2 = \frac{w_2^e - w_1^e}{l} \tag{3.29}$$

$$b_1 = \psi_1^e, \qquad b_2 = \frac{\psi_2^e - \psi_1^e}{l} \tag{3.30}$$

Substituting a_1, a_2, b_1 and b_2 into Equations (3.25) and (3.26), we will obtain:

$$w^e = w_1^e \Psi_1 + w_2^e \Psi_2 \tag{3.31}$$

$$\psi^e = \psi_1^e \Phi_1 + \psi_2^e \Phi_2 \tag{3.32}$$

where Ψ_1, Ψ_2, Φ_1 and Φ_2 are interpolation functions which are given as:

$$\Psi_1 = 1 - \frac{x}{l} \tag{3.33}$$

$$\Psi_2 = \frac{x}{l} \tag{3.34}$$

$$\Phi_1 = 1 - \frac{x}{l} \tag{3.35}$$

$$\Phi_2 = \frac{x}{l} \tag{3.36}$$

Now, considering $v_1 = \Psi_i$ and $v_2 = \Phi_i$ (for $i = 1,2$), from Equation (3.19) the following Equation is obtained:

$$\int_0^l \left[-bH_{55} \frac{d\Psi_i}{dx} \left(\sum_{j=1}^{2} \psi_j \Phi_j \right) + bH_{55} \frac{d\Psi_i}{dx} \left(\sum_{j=1}^{2} \frac{d\Psi_j}{dx} w_j \right) + bN_x^i \frac{d\Psi_i}{dx} \left(\sum_{j=1}^{2} \frac{d\Psi_j}{dx} w_j \right) \right] dx$$

$$- \int_0^l \Psi_i bq(x) dx + \int_0^l \Psi_i \rho_s b \left(\sum_{j=1}^{2} \Psi_j \frac{d^2 w_j}{dt^2} \right) - Q_1^e \Psi_i(0) - Q_3^e \Psi_i(l) = 0 \tag{3.37}$$

Similarly the i^{th} Equation of Equation (3.23) is obtained as:

$$\int_0^l \left[bD_{11} \left(\sum_{j=1}^{2} \frac{d\Phi_j}{dx} \frac{d\Phi_i}{dx} \psi_j \right) - \Phi_i bH_{55} \left(\sum_{j=1}^{2} \Phi_j \psi_j \right) + \Phi_i bH_{55} \left(\sum_{j=1}^{2} \frac{d\Psi_j}{dx} w_j \right) + \Phi_i bI_{xy} \left(\sum_{j=1}^{2} \frac{d^2 \psi_j}{dt^2} \Phi_j \right) \right] dx$$

$$- Q_2^e \Phi_i(0) - Q_4^e \Phi_i(l) = 0 \tag{3.38}$$

Introducing the following notations:

$$K_{ij}^{11} = \int_0^l bH_{55} \frac{d\Psi_i}{dx} \frac{d\Psi_j}{dx} dx \tag{3.39}$$

$$K_{ij}^{12} = \int_0^l bH_{55} \frac{d\Psi_i}{dx} \Phi_j dx \tag{3.40}$$

$$K_{ij}^{12} = K_{ji}^{21} \tag{3.41}$$

$$K_{ij}^{22} = \int_0^l \left[bD_{11} \frac{d\Phi_i}{dx} \frac{d\Phi_j}{dx} + bH_{55} \Phi_i \Phi_j \right] dx \tag{3.42}$$

$$G_{ij} = \int_0^l bN_x^i \frac{d\Psi_i}{dx} \frac{d\Psi_j}{dx} dx \tag{3.43}$$

$$M_{ij}^{11} = \int_0^l b\rho_s \Psi_i \Psi_j dx \tag{3.44}$$

$$M_{ij}^{22} = \int_0^l bI_{xy} \Phi_i \Phi_j dx \tag{3.45}$$

$$F_i^1 = Q_2^e \Phi_i(0) + Q_4^e \Phi_i(l) \tag{3.46}$$

$$F_i^2 = \int_0^l \Psi_i bq dx + Q_1^e \Psi_i(0) + Q_3^e \Psi_i(l) \tag{3.47}$$

Substituting Equations (3.39)-(3.47) into Equations (3.37) and (3.38), the finite element model for a laminated composite beam can be obtained by the following two equations:

$$\sum_{j=1}^{2}\left(K_{ij}^{11}+G_{ij}\right)w_j^e-\sum_{j=1}^{2}K_{ij}^{12}\psi_j^e+\sum_{j=1}^{2}M_{ij}^{11}\frac{d^2w_j^e}{dt^2}-F_i^2=0 \tag{3.48}$$

$$\sum_{j=1}^{2}K_{ij}^{22}\psi_j^e+\sum_{j=1}^{2}K_{ij}^{21}w_j^e+\sum_{j=1}^{2}M_{ij}^{22}\frac{d^2\psi_j^e}{dt^2}-F_i^1=0 \tag{3.49}$$

The element Equations (3.48) and (3.49) can be rewritten in matrix form as follows:

$$\begin{bmatrix}[K^{11}] & [K^{12}]\\ [K^{21}] & [K^{22}]\end{bmatrix}\begin{bmatrix}[w]\\ [\psi]\end{bmatrix}+\begin{bmatrix}[G] & [0]\\ [0] & [0]\end{bmatrix}\begin{bmatrix}[w]\\ [\psi]\end{bmatrix}+\begin{bmatrix}[M^{11}] & [0]\\ [0] & [M^{22}]\end{bmatrix}\begin{bmatrix}[\ddot{w}]\\ [\ddot{\psi}]\end{bmatrix}=\begin{bmatrix}[F^2]\\ [F^1]\end{bmatrix} \tag{3.50}$$

Considering Equation (3.50), the element properties, namely the stiffness, mass and geometric stiffness are introduced by Equations (3.51), (3.52) and (3.53) respectively.

$$[K^e]=\begin{bmatrix}[K^{11}] & [K^{12}]\\ [K^{21}] & [K^{22}]\end{bmatrix} \tag{3.51}$$

$$[M^e]=\begin{bmatrix}[M^{11}] & [0]\\ [0] & [M^{22}]\end{bmatrix} \tag{3.52}$$

$$[G^e]=\begin{bmatrix}[G] & [0]\\ [0] & [0]\end{bmatrix} \tag{3.53}$$

Here, one should note that when both deflection and rotation are approximated using linear interpolation functions such as Equations (3.31) and (3.32), the element becomes very stiff in the case of thin beam. Recalling that for a thin beam, the transverse shear

strain γ is neglected and using Equation (3.25) and Equation (3.26) for a thin beam, the shear strain is determined by:

$$\gamma = \frac{\partial w}{\partial x} - \psi = a_2 - b_1 - b_2 x \tag{3.54}$$

Neglecting shear strain, Equation (3.54) results in $a_2 - b_1 = 0$ and $b_2 = 0$, which itself results in a constant value for bending energy. In finite element literature, this phenomenon is well known as *shear locking*. One may see reference [2] for more details on shear locking. To overcome locking, we use reduced integration to evaluate the stiffness coefficients associated with the transverse shear strain in the element stiffness matrix (second term in Equation (3.42)). All other coefficient matrices are evaluated using full integration. Here, we use one point Gauss-quadrature to evaluate the term associated with the shear strain and two point Gauss quadrature to evaluate the other coefficients. Integration using Gauss-quadrature method has been explained in details in reference [67].

3.2.4 Element properties for uniform-thickness laminated beam

In the case of uniform thickness, bD_{11} is constant. All coefficients of the matrices in Equation (3.42) are evaluated using full integration except the coefficients associated with transverse shear strain (i.e., the second term of K^{22}), which are evaluated using reduced integration. Integration has been performed in MATLAB® (Appendix-B) and the results are given as:

$$[K^e] = \frac{bH_{55}}{4l}\begin{bmatrix} 4 & -2l & -4 & -2l \\ & l^2+\delta & 2l & l^2-\delta \\ & & 4 & 2l \\ sym & & & l^2+\delta \end{bmatrix} \tag{3.55}$$

where

$$\delta = \frac{4D_{11}}{H_{55}} \tag{3.56}$$

The Equation (3.55) can be divided into two terms corresponding to bending stiffness and shear stiffness as follows:

$$[K_b^e] = \frac{bH_{55}}{4l}\begin{bmatrix} 4 & -2l & -4 & -2l \\ & l^2 & 2l & l^2 \\ & & 4 & 2l \\ sym & & & l^2 \end{bmatrix} \tag{3.57}$$

$$[K_{st}^e] = \frac{4bD_{11}}{l}\begin{bmatrix} 0 & 0 & 0 & 0 \\ & 1 & 0 & -1 \\ & & 0 & 0 \\ sym & & & 1 \end{bmatrix} \tag{3.58}$$

where the subscripts b and st are assigned for bending stiffness and shear stiffness respectively. For convenience sake, the superscript e is removed in the following equations. The stiffness matrix for laminated Timoshenko beam is given by:

$$[K]=[K_b]+[K_{st}] \tag{3.59}$$

The mass matrix is given by:

$$[M]=\frac{l}{6}\begin{bmatrix} 2\rho_s & 0 & \rho_s & 0 \\ & 2I_{xy} & 0 & I_{xy} \\ & & 2 & 0 \\ sym & & & 2I_{xy} \end{bmatrix} \tag{3.60}$$

ρ_s denotes the mass inertia of the laminate which is given by:

$$\rho_s = \int_{-h/2}^{h/2} \rho dz \tag{3.62}$$

Replacing for I_{xy} and ρ_s from Equations (3.9) and (3.62) respectively, the mass matrix is obtained as:

$$[M]=\frac{lA\rho}{6}\begin{bmatrix} 2 & 0 & 1 & 0 \\ & \frac{h^2}{12} & 0 & \frac{h^2}{6} \\ & & 2 & 0 \\ sym & & & \frac{h^2}{12} \end{bmatrix} \tag{3.63}$$

Note that $bh = A$ where A is cross-section area.

The geometric stiffness matrix is obtained as follows:

$$\left[G^e\right]=\frac{bN_x^i}{l}\begin{bmatrix} 1 & 0 & -1 & 0 \\ & 0 & 0 & 0 \\ & & 1 & 0 \\ sym & & & 0 \end{bmatrix} \tag{3.64}$$

3.2.5 Free vibration analysis of laminated beam

In free vibration analysis, we consider [2]:

$$w(x,t)=W(x)e^{i\omega t} \qquad i=\sqrt{-1} \tag{3.65}$$

$$\psi(x,t)=\Theta(x)e^{i\omega t} \tag{3.66}$$

Therefore Equation (3.50) reduces to:

$$\left(\left[K^e\right]-\omega^2\left[M^e\right]\right)\begin{bmatrix}[W]\\ [\Theta]\end{bmatrix}=\begin{bmatrix}[0]\\ [0]\end{bmatrix} \tag{3.67}$$

The exact solution for simply supported laminated beam based on Timoshenko beam theory is given by [2]:

$$\omega_n=\left(\frac{n\pi}{L}\right)^2\sqrt{\frac{bD_{11}}{\rho h}}\sqrt{\frac{bH_{55}}{bH_{55}+\left(\frac{n\pi}{L}\right)^2 bD_{11}}} \tag{3.68}$$

where ω_n denotes the n^{th} natural frequency of the beam.

3.2.6 Free vibration analysis of laminated beam-column

The free vibration of a beam with axial compressive load is a special problem of beam, which is called beam-column, due to its capability to resist buckling like a column as well as lateral loading like a beam. Considering $N_x^i = -P$, Equation (3.50) changes to the following form:

$$\left([K]-P[\overline{G}]-\omega^2[M^e]\right)\begin{bmatrix}[W]\\[\Theta]\end{bmatrix}=\begin{bmatrix}[0]\\[0]\end{bmatrix} \tag{3.69}$$

where $[\overline{G}]=\frac{1}{N_x^i}[G]$

3.3. Vibration analysis of tapered composite beam

3.3.1 Mid-plane tapered beam

In the case of a beam with non-uniform thickness, as it was explained in the previous chapter, D_{11} is a function of x coordinate, which is given by Equation (2.70). This equation is also used in this chapter.

Examination of the Equations (3.57), (3.58), (3.63) and (3.64) for uniform beam shows that only the Equation (3.58) is a function of D_{11}. Therefore, Equation (3.70) should be used in integration of $[K_{st}]$, Equation (3.58). Integration of Equation (3.58) has been performed using MATLAB® software. The coefficients of the matrix given by Equation (3.58) have been determined as follows:

$$K_{11} = \sum_{k=1}^{n} \frac{b(Q_{11})_k}{12l\cos(\phi)}\left(4t_k m^2 l^2 + 12t_k cml + 12t_k c^2 + t_k'^3\right) \tag{3.71}$$

$$K_{12} = -K_{21} \tag{3.72}$$

$$K_{22} = K_{11} \tag{3.73}$$

The coefficients m and c have already been defined in chapter 2 in Section 2.4.2. Using Equations (3.71)-(3.73) in the Equation (3.58) for the stiffness matrix of a uniform beam, the Equation (3.58) has been modified for a tapered beam as follows:

$$[K_{st}] = K_{11}\begin{bmatrix} 0 & 0 & 0 & 0 \\ & 1 & 0 & -1 \\ & & 0 & 0 \\ sym & & & 1 \end{bmatrix} \tag{3.74}$$

3.3.2 Analysis of tapered beam models A and C

As it is seen in Figure 2.10, tapered beam models A and C have some similarities in terms of geometry. Tapered beam model C is constructed by adding some elements made with model A. Analysis of models A and C has been already detailed in section 2.4.3. In Timoshenko beam element we use the symbolic expression derived for mid-plane tapered beam to compute the stiffness matrix of model A. One should note that the element coefficients of the plies located in the resin pocket should be computed by using the material properties of resin.

Individual routines have been developed in MATLAB® software (Appendix-B) in order to compute the stiffness and mass matrices for tapered beam models A and C for

Timoshenko beam element. For example the routines for stiffness matrices for models A and C are named as *kmidAT.m* and *kmidCT.m* respectively.

3.3.3 Analysis of tapered beam, models B and D

Tapered beams made with models B and D are illustrated in Figure 2.11. The analysis of tapered beam models B and D proceeds in the same way as the procedure described in Section 2.4.4. Again for these cases the element coefficients can be computed by using the relations obtained for mid-plane tapered beams. To illustrate the computing procedure, the first element of model D is isolated in Figure 2.10. The integration in Equation (3.58) should be considered as the summation of integrations from L_1 to L_2 and from L_2 to L. In Timoshenko beam element only Equation (3.58) is a function of D_{11}. One should note that in order to compute the element properties for layers located in resin pocket, the material properties of resin should be considered. The stiffness and mass matrices for tapered beam models B and D have been computed numerically by using MATLAB® software (Appendix-B). The routines for stiffness matrices for models A and C are named as *kmidBT.m* and *kmidDT.m* respectively.

3.4 Example applications

In this Section the formulations developed in the previous Sections have been applied to free vibration analysis of uniform and tapered composite beams. The results obtained by MATLAB® software will be compared with the exact solution given by Equation (3.68) in the case of uniform beam. Various types of internally-tapered beams

will be investigated. In the case of tapered beams, the results are validated by choosing a very small taper angle and comparing the results with uniform beams.

3.4.1 Uniform-thickness composite beams

Problem description

A uniform-thickness composite beam with simply supported boundary conditions as shown in Figure 3.2 made up of 72 plies of NCT/301 graphite-epoxy is to be analyzed for free vibration. Mechanical properties are: E_1 is 113.9 GPa, E_2 is 7.9856 GPa, ν_{21} is 0.0178, ν_{12} is 0.288, G_{23} is 2.856 GPa, G_{12} is 3.138 GPa and ρ is 1480 kg/m^3.

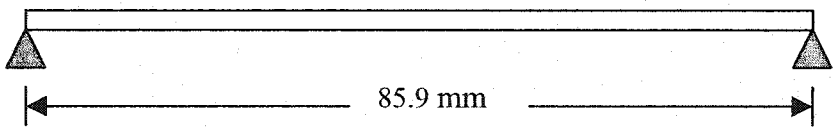

Figure 3.2 Simply supported beam of example 3.1

The geometric properties of the beam are, length (L) is 85.9 mm; thickness (h) is 9.0 mm (L/H =9.5); individual ply thickness (t_k) is 0.125 mm and the laminate configuration is $(0/90)_{9\,s}$. The problem is solved using different number of elements to obtain the desired accuracy. The results are compared with the exact solution given by equation (3.68). Table 3.1 gives the lowest three natural frequencies for the simply supported beam based on the cylindrical bending theory for mid-plane symmetric composite laminated beams.

Table 3.1 The lowest three natural frequencies ($\times 10^4$ rad/sec) for a simply supported beam

Mode	Exact solution	4 Elements	6 Elements	8 Elements	9 Elements
1	2.052	2.197	2.115	2.087	2.079
2	6.572	8.099	7.216	6.926	6.850
3	11.694	16.114	13.785	12.852	12.603

Comparison of results given in Table 3.1 with the results obtained in Table 2.1 indicates that in order to achieve an accurate result for a Timoshenko beam element, the beam should be divided into many elements.

3.4.1.1 Effects of laminate configuration on natural frequencies

We now intend to explore the effects of laminate configuration on the natural frequencies. The above example is considered to determine the natural frequencies for $[0/90]_{18\,s}$, $[\pm 45]_{18\,s}$ and $[0_4/\pm 45_{16}]_s$.

Table 3.2 The lowest three natural frequencies ($\times 10^4$ rad/sec) for a simply supported beam with different laminate configurations

Ply orientation	Mode No.1	Mode No.2	Mode No.3
$[0/90]_{18\,s}$	2.087	6.926	12.852
$[\pm 45]_{18\,s}$	1.619	5.845	11.620
$[0_4/\pm 45_{16}]_s$	2.021	6.797	12.733

Effects of laminate configuration on stiffness of the element in Timoshenko beam element can be seen by considering Equations (3.4), (3.5) as well as Equations (2.64) and (2.65) where one can see that theses Equations are a function of laminate configuration.

3.4.2 Tapered composite beams

Example 3.4.2.1

As the first example we consider a symmetric tapered beam with a very small taper angle of 0.251°. With such a small angle tapered beam can be compared with uniform beam. The beam consists of 48 plies at the thick section and 40 plies at the thin section. That means we have only 8 plies that are cut-off. The tapered beam is modeled with model C as shown in Figure 2.8(a). The configuration of the thick section is $(0/90)_{12s}$ and that of the thin section is $(0/90)_{10s}$. The beam is meshed using four equal-length elements. The material properties of graphite-epoxy are the same as in the problem described in section 3.4.1. The mechanical properties of the epoxy resin are given as: Elastic Modulus (E) is 3.93 GPa, Shear Modulus (G) is 1.034 GPa and Poisson's Ratio (ν) is 0.37. The lowest three natural frequencies have been determined for both uniform and tapered beams using 4 elements. The results for uniform beam are determined for simply supported boundary condition as 1.628×10^4 rad/sec, 7.640×10^4 rad/sec and 20.860×10^4 rad/sec respectively and the results for tapered beam are obtained as 1.489×10^4 rad/sec, 7.130×10^4 rad/sec and 20.368×10^4 rad/sec. As seen the results for uniform and tapered beams are close enough to validate the formulations developed for tapered beam.

Example 3.4.2.2

A tapered beam made with model A as shown in Figure 2.8 (b) is considered with 48 plies at thick section and 24 plies at thin section. As a result there is a large amount of resin pocket in this model. The mechanical properties are as detailed in example 3.4.1.

The problem is analyzed considering various taper angles. The relation between the length and the taper angles is given in Table 3.3. The thickness of individual ply is as considered in example 3.4.2.1. The configuration of the thick section is $[\pm 45]_{12s}$ and that of the thin section is $[\pm 45]_{6s}$. The material properties of the graphite-epoxy and resin are the same as in the problem described in Section 3.4.1.

Table 3.3 Relation between the length and taper angle in example 3.4.2.2

Taper angle, °	1	2	3	4	5
Length, m	0.0859	0.0429	0.0286	0.0214	0.0171

Natural frequencies for the above problem are given in Table 3.4.

Table 3.4 The natural frequencies ($\times 10^4$ rad/sec) for simply supported laminated beam model A of example 3.4.2.2

Taper angle °	Mode No.1	Mode No.2	Mode No.3
1	0.860	4.331	13.930
2	3.380	15.526	39.442
3	7.372	30.261	65.754
4	12.568	46.295	91.726
5	18.683	62.656	117.433

From the results given in Table 3.4, we conclude that the higher the taper angle is the higher the natural frequencies are. This result was expected when we examine the Equations (3.71)-(3.73) where we see that the taper angle has a direct effect on the stiffness of the beam. On the other hand from Table 3.3 we see that the taper angle affects the length of the beam which itself affects the stiffness of the beam. The above problem

has been solved for different laminate configurations to investigate the effects of laminate configuration. Figure 3.3 illustrates the fundamental frequencies for tapered beam model A with different laminate configurations that are: (i) LC (1) that has $[0/90]_{12s}$ configuration at thick section and $[0/90]_{6s}$ configuration at thin section; (ii) LC (2) that has $[\pm 45]_{12s}$ configuration at thick section and $[\pm 45]_{6s}$ configuration at thin section; (iii) LC (3) that has $[0_4/\pm 45_{10}]_s$ configuration at thick section and $[0_4/\pm 45_4]_s$ configuration at thin section. The lowest four natural frequencies are determined for different boundary conditions and for the laminate configurations LC (1), LC (2) and LC (3). As one can see the results given by Figure 3.3 are similar to the results obtained for uniform thickness beam. The influence of the laminate configuration on the stiffness matrix has been discussed in example 3.4.2.1.

Another feature of importance is that by increasing taper angle, the natural frequencies increase. This result can be expected by observation of Equation 3.71 and Table 3.3 where one can see that the slope of the beam has a direct effect on the stiffness matrix of the element. On the other hand Table 3.3 indicates that increasing the taper angle while keeping the thickness as constant, decreases the length of the beam.

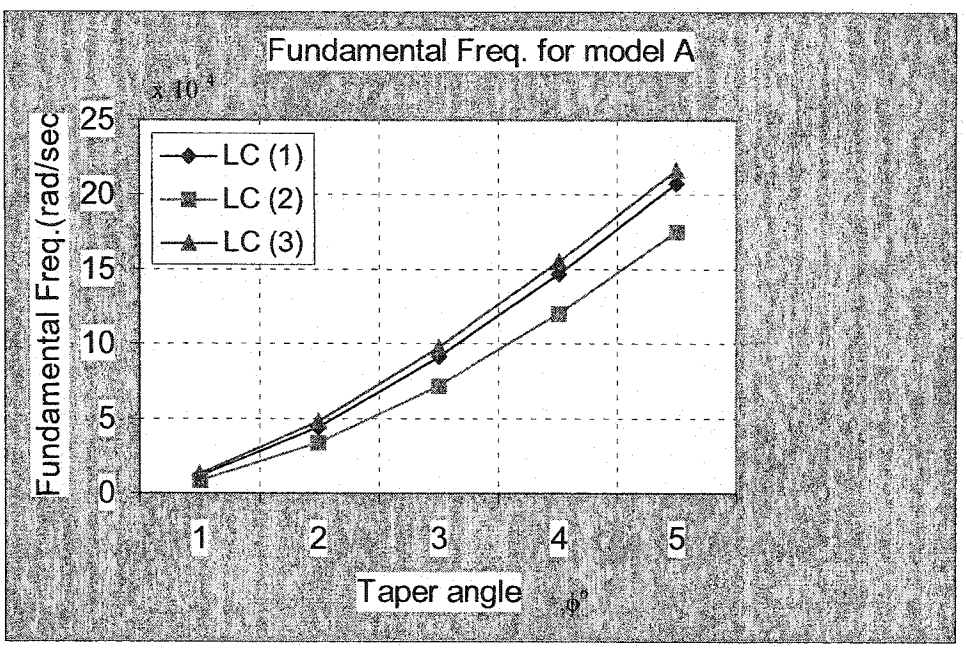

Figure 3.3 Fundamental frequencies for tapered beam model A for different laminate configurations

Example 3.4.2.3

Problem described in example 3.4.2.2 is considered as a tapered beam made with model B as shown in Figure 2.11. In this case eight plies have been dropped off in each element. The beam is meshed with three equal-length elements. The first and second elements consist of 16 and 8 uniform plies respectively. Table 3.5 gives the natural frequencies obtained for the above problem.

Table 3.5 The natural frequencies ($\times 10^4$ rad/sec) for simply supported laminated beam model B with LC (2) configuration

Taper angle °	Mode No.1	Mode No.2	Mode No.3
1	0.896	4.527	14.341
2	3.624	16.464	40.341
3	8.066	32.043	66.807
4	13.916	48.646	92.842
5	20.786	65.294	118.606

Problem 3.4.2.3 has been solved for different laminate configurations. Figure 3.4 shows the results for various taper angles. As one can see the general form of these results are similar to the results determined for model A except that in tapered beam model B the value of the natural frequencies are higher than those given for model A. This is due to the existence of uniform plies in the tapered beam model B which cause a stiffer element compared to the tapered beam model A.

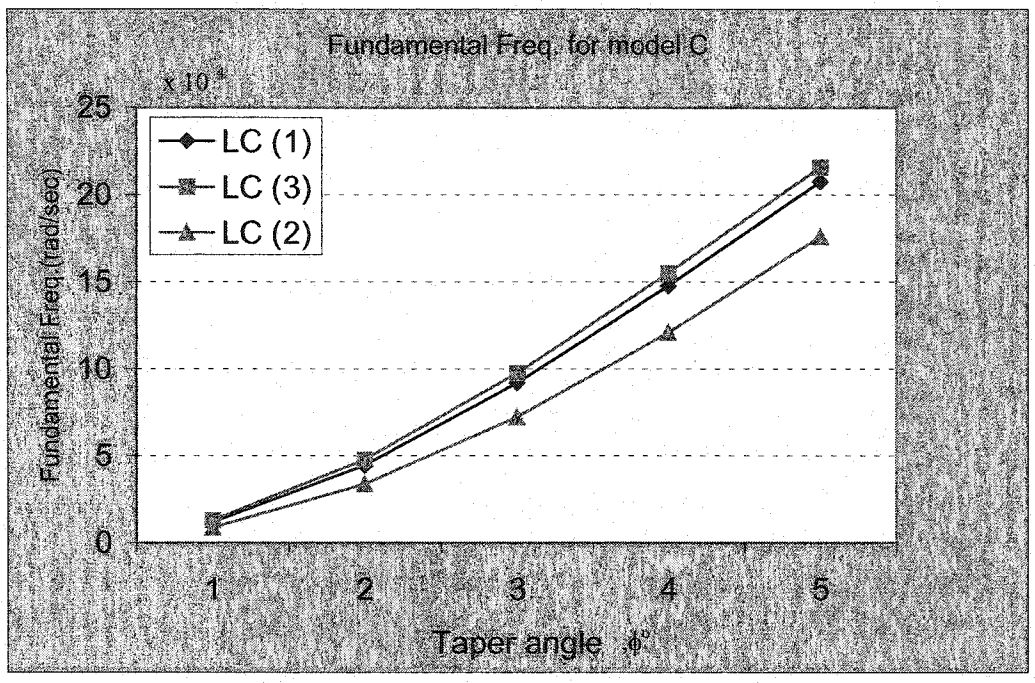

Figure 3.4 Fundamental frequencies for tapered beam model B for different laminate configurations

Example 3.4.2.4

Problem described in example 3.4.2.2 is considered as a tapered beam made with model C as shown in Figure 2.10(a). This model is similar to model A except that here the volume of the resin pocket is smaller than the resin pocket of model A. In this case eight

plies have been dropped off in each element. The beam is meshed with three equal-length elements. Table 3.6 gives the natural frequencies obtained for the above problem.

Table 3.6 The natural frequencies ($\times 10^4$ rad/sec) for simply supported laminated beam model C with LC (2) configuration

Taper angle °	Mode No.1	Mode No.2	Mode No.3
1	0.872	4.410	14.184
2	3.427	15.760	39.773
3	7.470	30.628	66.173
4	12.726	46.753	92.239
5	18.901	63.180	118.051

As it was expected the results obtained for model C are slightly higher than the results given for tapered beam model A. Therefore we conclude that the resin pocket has not much effect on the stiffness value. This problem has been solved for different laminate configurations. Figure 3.5 illustrates these results. The effects of taper angle and laminate configuration on natural frequencies have been already discussed in the previous examples.

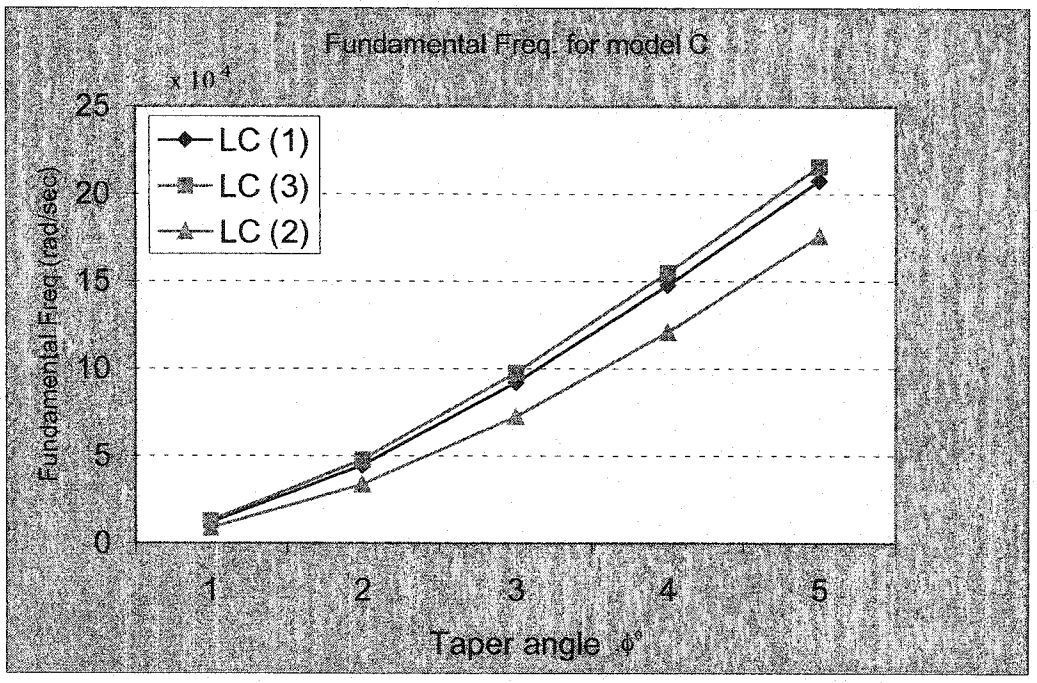

Figure 3.5 Fundamental frequencies for tapered beam model C for different laminate configurations

Example 3.4.2.5

Problem described in example 3.4.2.3 is considered as a tapered beam made with model D as shown in Figure 2.11(b). This model is similar to model B except that here there are 28 and 12 uniform plies in the first and second elements respectively. The beam is meshed with three elements. Table 3.7 gives the natural frequencies obtained for the above problem.

Table 3.7 The natural frequencies ($\times 10^4$ rad/sec) for simply supported laminated beam model D with LC (2) configuration

Taper angle °	Mode No.1	Mode No.2	Mode No.3
1	0.941	4.693	13.932
2	3.926	16.729	36.966
3	8.760	31.115	59.635
4	14.868	45.531	81.920
5	21.648	59.663	104.178

As we expected the natural frequencies for tapered beam model D are higher than that of the other tapered models. This is due to the existence of more number of uniform plies in the element. The above problem has been solved for different laminate configurations and various taper angles to have a better comparison between the results for different tapered models. Figure 3.6 shows these results in graphical form. Fundamental frequencies for simply supported beam made with all types of tapered models under investigation have been determined and illustrated in Figure 3.7. Based on the results illustrated in Figure 3.7, one can conclude that the natural frequencies for tapered beam model D is the highest and consequently models, B, C and A take the other positions. This conclusion is valid for all taper angles and laminate configurations.

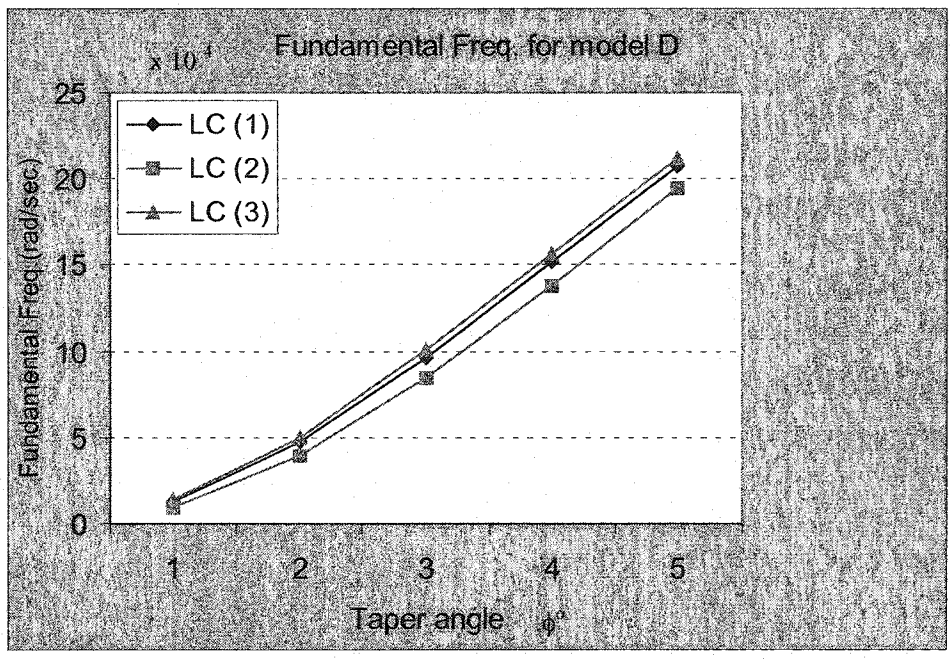

Figure 3.6 Fundamental frequencies for tapered beam model D for different laminate configurations

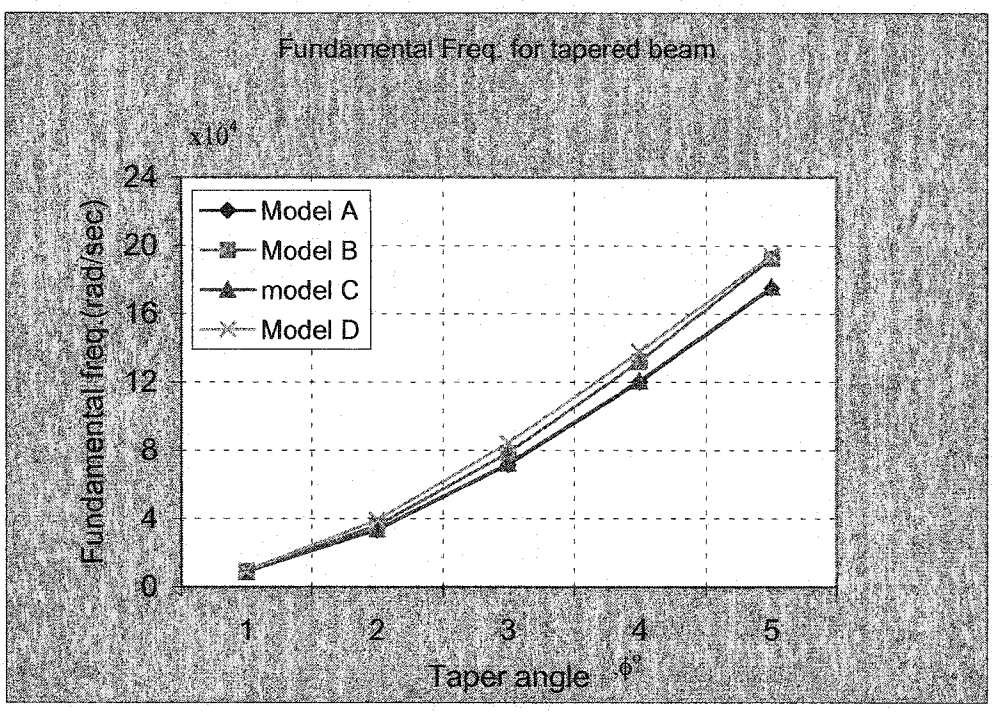

Figure 3.7 Fundamental frequencies for simply supported tapered beams with LC (2) configuration vs. taper angle

3.4 Conclusions and discussions

In this Chapter, the conventional finite element formulation based on Timoshenko beam theory was developed for analysis of uniform-thickness and tapered composite beams. The developed formulation was used to analyze the uniform-thickness beam and various types of tapered beams viz. models A, B, C and D. In the case of uniform-thickness beams, the results obtained have been compared with the exact solutions.

Based on the results obtained in this Chapter, it is shown that the tapered beam made with model D has the highest stiffness; models B and C take the second and third ranks, respectively. Model A has the lowest stiffness. Therefore, the natural frequencies of

model D are the highest and consequently models B, C and D take the second, third and fourth positions. Natural frequencies of model D are about three times that of model A.

With regard to the boundary conditions, we conclude that the natural frequencies for fixed-fixed support are the highest. Simply supported and fixed-free supports take the second and third positions.

According to the results given for different taper angles, we conclude that by increasing the taper angle while keeping the thickness constant, the natural frequencies increase for all types of tapered beams.

Chapter 4

Vibration and buckling analyses of composite beams using advanced finite element formulation

4.1 Introduction

In the conventional FEM formulation, in order to get a result with acceptable accuracy, the beam has to be divided into many elements. Furthermore, in general, finite element model based on low degree polynomial displacement functions incorporates only crude curvature distributions and usually yields discontinuous bending moments across element interfaces. It has been shown that accurate results can be obtained more efficiently by increasing the number of degrees of freedom in the element rather than increasing the number of elements that have the same or lower degrees of freedom [51].

4.2 Analysis of uniform-thickness laminated beam based on CLPT

In this Section, an advanced finite element formulation for the analysis of composite beams is established. In this model, a beam element with two nodes at the ends and four degrees of freedom per node is considered. The transverse displacement w, the slope $\frac{\partial w}{\partial x}$, the curvature $\frac{\partial^2 w}{\partial x^2}$, and the gradient of curvature $\frac{\partial^3 w}{\partial x^3}$ are considered as the

degrees of freedom for each node. Thus a seventh degree polynomial displacement function is required to satisfy boundary conditions. This element represents all the physical situations involved in any combinations of displacement, rotation, bending moment and shear force. In the following sub-sections, the stiffness, geometric stiffness and mass matrices of uniform-thickness composite beam will be derived using the advanced finite element beam model.

4.2.1. Governing equations

The Equation of motion for a composite beam is given by [21]:

$$b\frac{\partial^2 M_x}{\partial x^2} + bN_x^i \frac{\partial^2 w}{\partial x^2} + bq(x) = b\rho_s \frac{\partial^2 w}{\partial t^2} \tag{2.2}$$

where b and N_x^i denote the width of the beam and initial axial force along x-axis, respectively, and M_x denotes the bending moment along x-axis per unit width and is given by:

$$M_x = B_{11}\frac{\partial u_o}{\partial x} + B_{16}\frac{\partial v_o}{\partial x} - D_{11}\frac{\partial^2 w}{\partial x^2} \tag{2.3}$$

Further, $q(x)$ and ρ_s are transversely distributed load and density of the laminated beam per unit length, respectively. $q(x)$ and ρ_s are given by Equations (2.5) and (2.6) respectively. In the case of mid-plane symmetric laminated beam, $B_{11} = B_{16} = 0$ and M_x reduces to the following equation:

$$M_x = -D_{11}\frac{\partial^2 w}{\partial x^2} \tag{4.1}$$

where

$$D_{11} = \sum_{k=1}^{n}\left[t_k \bar{z}_k^2 + \frac{t_k^3}{12}\right](\overline{Q}_{11})_k \tag{4.2}$$

where t_k denotes the thickness of each ply and $(\overline{Q}_{11})_k$ denotes the first coefficient of the transformed stiffness matrix of the lamina which is given by:

$$\overline{Q}_{11} = \cos^4(\theta)Q_{11} + \sin^4(\theta)Q_{22} + 2\cos^2(\theta)\sin^2(\theta)Q_{12} + 4\cos^2(\theta)\sin^2(\theta)Q_{33} \tag{4.3}$$

where θ is the fiber orientation angle and the coefficients of ply stiffness Q_{ij}, are given in reference [21]. $\bar{z}_k$ denotes the distance from the centre line of each ply to the mid-plane of the laminate. Combining Equation (4.1) and Equation (2.2), the constitutive Equation of symmetric composite beams in cylindrical bending has been obtained as:

$$\frac{d^2}{dx^2}\left(bD_{11}\frac{\partial^2 w}{\partial x^2}\right) - bN_x^i\frac{\partial^2 w}{\partial x^2} - bq(x) + b\rho_s\frac{\partial^2 w}{\partial t^2} = 0 \tag{4.4}$$

One should note that for uniform thickness laminated beam bD_{11} has a constant value.

4.2.2 Weak form

The weak form corresponding to the Equation (4.4) has been obtained in Sub-section 2.3.1.1 by following the three-step procedure presented in reference [45]:

$$\int_0^l \left(bD_{11}\frac{d^2v}{dx^2}\frac{\partial^2 w}{\partial x^2} + bN_x^i \frac{dv}{dx}\frac{\partial w}{\partial x} + bq(x) + vb\rho_s \frac{\partial^2 w}{\partial t^2} \right) dx \quad + v\frac{d}{dx}\left(bD_{11}\frac{\partial^2 w}{\partial x^2} \right)\Bigg|_{x=l}$$

$$- v\frac{d}{dx}\left(bD_{11}\frac{\partial^2 w}{\partial x^2} \right)\Bigg|_{x=0} - \frac{dv}{dx}\left(bD_{11}\frac{\partial^2 w}{\partial x^2} \right)\Bigg|_{x=l} + \frac{dv}{dx}\left(bD_{11}\frac{\partial^2 w}{\partial x^2} \right)\Bigg|_{x=0}$$

$$- vbN_x^i \frac{\partial w}{\partial x}\Bigg|_{x=l} + vbN_x^i \frac{\partial w}{\partial x}\Bigg|_{x=0} = 0 \tag{4.5}$$

The following notations introduce the secondary variables:

$$Q_1^e = \left[\frac{d}{dx}\left(bD_{11}\frac{d^2 w}{dx^2} \right) - bN_x \frac{dw}{dx} \right]_{x=0} \tag{4.6}$$

$$Q_3^e = -\left[\frac{d}{dx}\left(bD_{11}\frac{d^2 w}{dx^2} \right) - bN_x \frac{dw}{dx} \right]_{x=l} \tag{4.7}$$

$$Q_2^e = \left(bD_{11}\frac{d^2 w}{dx^2} \right)_{x=0} \tag{4.8}$$

$$Q_4^e = -\left(bD_{11}\frac{d^2 w}{dx^2} \right)_{x=l} \tag{4.9}$$

Substituting Equations (4.6)-(4.9) into Equation (4.5), we obtain:

$$\int_0^l \left[bD_{11}\frac{\partial^2 v}{\partial x^2}\frac{\partial^2 w}{\partial x^2} + bN_x^i \frac{\partial v}{\partial x}\frac{\partial w}{\partial x} + vb\rho_s \frac{\partial^2 w}{\partial t^2} - vbq(x) \right] dx$$

$$- Q_1^e v(0) - Q_3^e v(l) - Q_2^e \left(-\frac{\partial v}{\partial x} \right)\Bigg|_{x=0} - Q_4^e \left(-\frac{\partial v}{\partial x} \right)\Bigg|_{x=l} = 0 \tag{4.12}$$

4.2.3 Finite element model

In this model, four degrees of freedom are considered for each node; shear force and bending moment as natural boundary conditions, and deflection and slope as geometric boundary conditions. Thus there are eight degrees of freedom per element. A finite element model of a uniform beam with four degrees of freedom per node is shown in Figure 4.1.

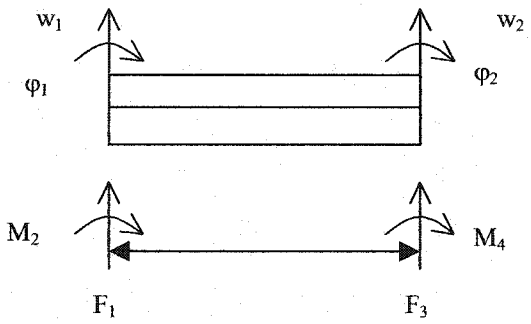

Figure 4.1 Finite element model of a uniform beam with four degrees of freedom per node.

The deflection, W, should be approximated by a seventh-order polynomial as follows:

$$W(x) = c_0 + c_1 x + c_2 x^2 + c_3 x^3 + c_4 x^4 + c_5 x^5 + c_6 x^6 + c_7 x^7 \tag{4.11}$$

Then, rotation, shear force and bending moment as a function deflection W are given as follows:

$$\varphi(x) = -\frac{dW(x)}{dx} = -c_1 - 2c_2 x - 3c_3 x^2 - 4c_4 x^3 - 5c_5 x^4 - 6c_6 x^5 - 7c_7 x^6 \tag{4.12}$$

$$F(x) = bD_{11}\frac{d^3 W(x)}{dx^3} = bD_{11}\left[6c_3 + 24c_4 x + 60c_5 x^2 + 120c_6 x^3 + 210c_7 x^4\right] \tag{4.13}$$

$$M(x) = -bD_{11}\frac{d^2W(x)}{dx^2} = -bD_{11}\left[2c_2 + 6c_3x + 12c_4x^2 + 20c_5x^3 + 30c_6x^4 + 42c_7x^5\right] \quad (4.14)$$

To evaluate the above relations at the two ends of the element, one can choose the first node at $x = 0$ and the second node at $x = l$. One may consider the value of bD_{11} at the ends as follows:

$$\Delta_1 = bD_{11}\big|_{x=0} \quad (4.17)$$

$$\Delta_2 = bD_{11}\big|_{x=l} \quad (4.18)$$

It should be noted that Δ_1 and Δ_2 have the same values for uniform beam ($\Delta_1 = \Delta_2 = \Delta$).

To evaluate the coefficients c_i, one can use the following boundary conditions:

$$W(0) = w_1^e = c_0 \quad (4.19)$$

$$\varphi(0) = \varphi_1 = -\frac{dW}{dx} = -c_1 \quad (4.20)$$

$$F(0) = F_1 = 6\Delta_1 c_3 \quad (4.21)$$

$$M(0) = M_1 = -2\Delta_1 c_2 \quad (4.22)$$

$$W(l) = w_2^e = c_0 + c_1 l + c_2 l^2 + c_3 l^3 + c_4 l^4 + c_5 l^5 + c_6 l^6 + c_7 l^7 \quad (4.23)$$

$$\varphi(l) = \varphi_2 = -(c_1 + 2c_2 l + 3c_3 l^2 + 4c_4 l^3 + 5c_5 l^4 + 6c_6 l^5 + 7c_7 l^6) \quad (4.24)$$

$$F(l) = F_2 = \Delta_2\left[6c_3 + 24c_4 l + 60c_5 l^2 + 120c_6 l^3 + 210c_7 l^4\right] \quad (4.25)$$

$$M(l) = M_2 = -\Delta_2\left[2c_2 + 6c_3 l + 12c_4 l^2 + 20c_5 l^3 + 30c_6 l^4 + 42c_7 l^5\right] \quad (4.26)$$

In matrix form, the Equations (4.17)-(4.24) can be written as:

$$\begin{Bmatrix} w_1 \\ \varphi_1 \\ F_1 \\ M_1 \\ w_2 \\ \varphi_2 \\ F_2 \\ M_2 \end{Bmatrix} = \begin{bmatrix} 1 & 0 & 0 & 0 & 0 & 0 & 0 & 0 \\ 0 & -1 & 0 & 0 & 0 & 0 & 0 & 0 \\ 0 & 0 & 0 & 6\Delta_1 & 0 & 0 & 0 & 0 \\ 0 & 0 & -2\Delta_1 & 0 & 0 & 0 & 0 & 0 \\ 1 & l & l^2 & l^3 & l^4 & l^5 & l^6 & l^7 \\ 0 & -1 & -2l & -3l^2 & -4l^3 & -5l^4 & -6l^5 & -7l^7 \\ 0 & 0 & 0 & 6\Delta_2 & 24\Delta_2 l & 60\Delta_2 l^2 & 120\Delta_2 l^3 & 210\Delta_2 l^4 \\ 0 & 0 & -2\Delta_2 & -6bD_{11}l & -12\Delta_2 l^2 & -20\Delta_2 l^3 & -30\Delta_2 l^4 & -42\Delta_2 l^5 \end{bmatrix} \begin{Bmatrix} c_1 \\ c_2 \\ c_3 \\ c_4 \\ c_5 \\ c_6 \\ c_7 \\ c_8 \end{Bmatrix} \tag{4.25}$$

In short form the Equation (4.25) can be rewritten by:

$$\{d\} = [\Gamma]\{c\} \tag{4.26}$$

Using interpolation functions $W(x)$ can be approximated as:

$$\{W\} = [N]\{d\} \tag{4.27}$$

where $[N]$ is a vector containing interpolation functions. Substituting for $\{d\}$, from equation (4.26) into Equation (4.27), we have:

$$\{W\} = [N][\Gamma]\{c\} \tag{4.28}$$

Substituting for $\{c\}$ from equation (4.11) into Equation (4.28), we get:

$$[I] = [N][\Gamma][X]^{-1} \tag{4.29}$$

where $[X]$ is a vector which is given by:

$$[X] = \begin{bmatrix} 1 & x & x^2 & x^3 & x^4 & x^5 & x^6 & x^7 \end{bmatrix} \tag{4.30}$$

Finally, interpolation functions can be obtained by solving the following equation:

$$[N] = [\Gamma]^{-1}[X] \tag{4.31}$$

By using MATLAB® software, the interpolation functions are obtained as follows: (See *Nad.m* in Appendix-B):

$$N_1 = 1 - 35\frac{x^4}{l^4} + 84\frac{x^5}{l^5} - 70\frac{x^6}{l^6} + 20\frac{x^7}{l^7} \tag{4.32}$$

$$N_2 = -x + 20\frac{x^4}{l^3} - 45\frac{x^5}{l^4} + 36\frac{x^6}{l^5} - 10\frac{x^7}{l^6} \tag{4.33}$$

$$N_3 = \left(\frac{1}{\Delta_1}\right)\left(\frac{x^3}{6} - \frac{2x^4}{3l} + \frac{x^5}{l^2} - \frac{2x^6}{3l^3} + \frac{x^7}{6l^4}\right) \tag{4.34}$$

$$N_4 = \left(\frac{1}{\Delta_1}\right)\left(\frac{-x^2}{2} + \frac{5x^4}{l^2} - \frac{10x^5}{l^3} + \frac{15x^6}{2l^4} - \frac{2x^7}{l^5}\right) \tag{4.35}$$

$$N_5 = \frac{35x^4}{l^4} - \frac{84x^5}{l^5} + \frac{70x^6}{l^6} - \frac{20x^7}{l^7} \tag{4.36}$$

$$N_6 = \frac{15x^4}{l^3} - \frac{39x^5}{l^4} + \frac{34x^6}{l^5} - \frac{10x^7}{l^6} \tag{4.37}$$

$$N_7 = \left(\frac{1}{\Delta_2}\right)\left(\frac{-x^4}{6l} + \frac{x^5}{2l^2} - \frac{x^6}{2l^3} + \frac{x^7}{6l^4}\right) \tag{4.38}$$

$$N_8 = \left(\frac{1}{\Delta_2}\right)\left(\frac{-5x^4}{2l^2} + \frac{7x^5}{l^3} - \frac{13x^6}{2l^4} + \frac{2x^7}{l^5}\right) \tag{4.39}$$

One may note that in the case of uniform beam, both Δ_1 and Δ_2 have the same values i.e. $\Delta_1 = \Delta_2 = \Delta = bD_{11}$. The interpolation functions which are given by Equations (4.32)-(4.39) satisfy the following interpolation properties:

$$N_1\big|_{x=0} = 1 \qquad N_i\big|_{x=0} = 0 \qquad (i \neq 1) \tag{4.40}$$

$$N_5\big|_{x=l} = 1 \qquad N_i\big|_{x=l} = 0 \qquad (i \neq 5) \tag{4.41}$$

$$-\frac{dN_2}{dx}\bigg|_{x=0} = 1 \qquad -\frac{dN_i}{dx}\bigg|_{x=0} = 0 \qquad (i \neq 2) \tag{4.42}$$

$$-\frac{dN_6}{dx}\bigg|_{x=l} = 1 \qquad -\frac{dN_i}{dx}\bigg|_{x=l} = 0 \qquad (i \neq 6) \tag{4.43}$$

$$-\Delta_1 \frac{d^2N_4}{dx^2}\bigg|_{x=0} = 1 \qquad -\Delta_1 \frac{d^2N_i}{dx^2}\bigg|_{x=0} = 0 \qquad (i \neq 4) \tag{4.44}$$

$$-\Delta_2 \frac{d^2N_8}{dx^2}\bigg|_{x=l} = 1 \qquad -\Delta_2 \frac{d^2N_i}{dx^2}\bigg|_{x=l} = 0 \qquad (i \neq 8) \tag{4.45}$$

$$\Delta_1 \frac{d^3N_3}{dx^3}\bigg|_{x=0} = 1 \qquad \Delta_1 \frac{d^3N_i}{dx^3}\bigg|_{x=0} = 0 \qquad (i \neq 3) \tag{4.46}$$

$$\Delta_2 \frac{d^3N_7}{dx^3}\bigg|_{x=l} = 1 \qquad \Delta_2 \frac{d^3N_i}{dx^3}\bigg|_{x=l} = 0 \qquad (i \neq 7) \tag{4.47}$$

Introducing the generalized displacement u by the following relations:

$$u_1 = W(0) \tag{4.48}$$

$$u_5 = W(l) \tag{4.49}$$

$$u_2 = -\frac{dW}{dx}\bigg|_{x=0} \tag{4.50}$$

$$u_3 = F(0) = \Delta_1 \frac{d^3W}{dx^3}\bigg|_{x=0} \tag{4.51}$$

$$u_4 = M(0) = -\Delta_1 \frac{d^2W}{dx^2}\bigg|_{x=0} \tag{4.52}$$

$$u_6 = -\left.\frac{dW}{dx}\right|_{x=l} \tag{4.53}$$

$$u_7 = F(l) = -\Delta_2 \left.\frac{d^3W}{dx^3}\right|_{x=l} \tag{4.54}$$

$$u_8 = M(l) = -\Delta_2 \left.\frac{d^2W}{dx^2}\right|_{x=l} \tag{4.55}$$

Considering $v = N_i^e$ where, $i = 1,2,...,8$. Substituting u and v in weak form obtained by Equation (4.12), the i^{th} Equation is obtained as:

$$0 = \int_0^l \left[bD_{11} \frac{d^2N_i}{dx^2} \left(\sum_{j=1}^{8} u_j^e \frac{d^2N_j}{dx^2} \right) + bN_x^i \frac{dN_i}{dx} \left(\sum_{j=1}^{8} u_j^e \frac{dN_j}{dx} \right) + b\rho_s N_i \left(\sum_{j=1}^{8} N_j \frac{d^2u_j^e}{dt^2} \right) - bN_i q(x) \right] dx$$

$$-Q_1^e N_i(0) - Q_3^e N_i(l) - Q_2^e \left(-\frac{dN_i}{dx} \right)_{x=0} - Q_4^e \left(-\frac{dN_i}{dx} \right)_{x=l} \tag{4.56}$$

Equation (4.58) can be simplified as:

$$= \sum_{j=1}^{8} \int_0^l \left[\left(bD_{11} \frac{d^2N_i}{dx^2} \frac{d^2N_j}{dx^2} + bN_x^i \frac{dN_i}{dx} \frac{dN_j}{dx} \right) u_j^e + b\rho_s N_i N_j \frac{d^2u_j^e}{dt^2} \right] dx - \int_0^l bN_i q(x) dx$$

$$-Q_1^e N_i(0) - Q_3^e N_i(l) - Q_2^e \left(-\frac{dN_i}{dx} \right)_{x=0} - Q_4^e \left(-\frac{dN_i}{dx} \right)_{x=l} = 0 \tag{4.57}$$

Introducing the following coefficients:

$$K_{ij} = \int_0^l bD_{11} \frac{d^2 N_i}{dx^2} \frac{d^2 N_j}{dx^2} dx \tag{4.58}$$

$$G_{ij} = \int_0^l bN_x^i \frac{dN_i}{dx} \frac{dN_j}{dx} dx \tag{4.59}$$

$$M_{ij} = \int_0^l b\rho_s N_i N_j dx \tag{4.60}$$

$$F_i^e = q_i^e + Q_1^e N_i(0) + Q_3^e N_i(l) + Q_2^e \left(-\frac{dN_i}{dx} \right)_{x=0} + Q_4^e \left(-\frac{dN_i}{dx} \right)_{x=l} \tag{4.61}$$

$$q_i^e = \int_0^l bN_i q(x) dx \tag{4.62}$$

Substituting Equations (4.58) - (4.60) into Equation (4.57), the i^{th} Equation is obtained as:

$$\sum_{j=1}^{8} \left[\left(K_{ij}^e + G_{ij}^e \right) u_j^e + M_{ij}^e \frac{d^2 u_j^e}{dt^2} \right] - F_i^e = 0 \tag{4.63}$$

In short form Equation (3.65) can be written as:

$$\left([K] + [G] \right) [u] + [M] \, [\ddot{u}] = [F] \tag{4.64}$$

$[K]$, $[M]$ and $[G]$ denote respectively the stiffness, mass and geometric stiffness matrices, for individual element.

4.2.4 Element properties of uniform thickness laminated beam

Substituting interpolation functions from Equations (4.32) - (4.39) in Equations (4.58)-(4.60) and performing integration through the length of the beam, the stiffness, mass and geometric stiffness matrices are given by Equations (4.65) - (4.67) respectively. (See *fen2.m* in Appendix-B)

$$[K]=\frac{\Delta}{l^3}\begin{bmatrix}
\frac{280}{11} & \frac{140l}{11} & -\frac{l^3}{22\Delta} & \frac{40l^2}{33\Delta} & -\frac{280}{11} & \frac{140l}{11} & \frac{l^3}{22\Delta} & \frac{40l^2}{33\Delta} \\
 & \frac{600l^2}{77} & -\frac{8l^4}{231\Delta} & \frac{379l^3}{462\Delta} & -\frac{140l}{11} & \frac{380l^2}{77} & \frac{5l^4}{462\Delta} & \frac{181l^3}{462\Delta} \\
 & & \frac{2l^6}{3465\Delta^2} & -\frac{l^5}{99\Delta^2} & \frac{l^3}{22\Delta} & \frac{5l^4}{462\Delta} & \frac{l^6}{4620\Delta^2} & \frac{5l^5}{2772\Delta^2} \\
 & & & \frac{50l^3}{231\Delta^2} & \frac{-40l^2}{33\Delta} & \frac{181l^3}{462\Delta} & \frac{-5l^5}{2772\Delta^2} & \frac{l^5}{462\Delta^2} \\
 & & & & \frac{280}{11} & \frac{-140l}{11} & \frac{-l^3}{22\Delta} & \frac{-40l^2}{33\Delta} \\
 & & & & & \frac{600l^2}{77} & \frac{8l^4}{231\Delta} & \frac{379l^3}{462\Delta} \\
 & & & & & & \frac{2l^6}{3465\Delta^2} & \frac{l^5}{99\Delta^2} \\
sym & & & & & & & \frac{50l^4}{231\Delta^2}
\end{bmatrix} \tag{4.65}$$

$$[M]=\frac{b\rho_s l}{420}\begin{bmatrix}
\frac{72940}{429} & \frac{4530l}{143} & \frac{-383l^2}{2574\Delta} & \frac{1370l^2}{429\Delta} & \frac{17150}{429} & \frac{-1905l}{143} & \frac{-521l^3}{5148\Delta} & \frac{-775l^2}{429\Delta} \\
 & \frac{100l}{143} & \frac{-6l^4}{143\Delta} & \frac{245l^3}{286\Delta} & \frac{1905l}{143} & \frac{-1865l^2}{429} & \frac{-5l^4}{156\Delta} & \frac{-995l^3}{1716\Delta} \\
 & & \frac{l^6}{3861\Delta^2} & \frac{-l^5}{198\Delta^2} & \frac{-521l^3}{5148\Delta} & \frac{5l^4}{156\Delta} & \frac{7l^6}{30888\Delta^2} & \frac{43l^5}{10296} \\
 & & & \frac{43l^4}{429\Delta^2} & \frac{775l^2}{429\Delta} & \frac{-995l^3}{1716\Delta} & \frac{-43l^5}{10296\Delta^2} & \frac{-131l^4}{1716\Delta^2} \\
 & & & & \frac{72940}{429} & \frac{-4530l}{143} & \frac{-383l^2}{2574\Delta} & \frac{-1370l^2}{429\Delta} \\
 & & & & & \frac{100l^2}{13} & \frac{6l^4}{143\Delta} & \frac{245l^3}{286\Delta} \\
 & & & & & & \frac{l^6}{3861\Delta^2} & \frac{l^5}{198\Delta^2} \\
 & & & & & & & \frac{43l^4}{429\Delta^2} \\
sym & & & & & & &
\end{bmatrix}$$

(4.66)

$$[G]=bN_x^i\begin{bmatrix}
\frac{700}{429l} & \frac{271}{858} & \frac{-5l^2}{5148\Delta} & \frac{23l}{858\Delta} & \frac{-700}{429l} & \frac{271}{858} & -\frac{5l^2}{5148\Delta} & -\frac{23l}{858\Delta} \\
 & \frac{300l}{1001} & \frac{-25l^3}{18018\Delta} & \frac{123l^2}{4004\Delta} & \frac{-271}{858} & \frac{97l}{6006} & \frac{5l^3}{12012\Delta} & \frac{47l^2}{1201\Delta} \\
 & & \frac{l^5}{90090\Delta^2} & \frac{-37l^4}{180180\Delta^2} & \frac{5l^2}{5148\Delta} & \frac{5l^3}{12012\Delta} & -\frac{l^5}{144144\Delta^2} & -\frac{73l^4}{720720\Delta^2} \\
 & & & \frac{73l^3}{18018\Delta^2} & \frac{-23l}{858\Delta} & \frac{-47l^2}{12012\Delta} & \frac{-73l^4}{720720\Delta^2} & \frac{7l^3}{5148\Delta^2} \\
 & & & & \frac{700}{429l} & \frac{-271}{858} & \frac{5l^2}{5148\Delta_2} & \frac{23l}{858\Delta_2} \\
 & & & & & \frac{300l}{1001} & -\frac{25l^3}{18018\Delta} & -\frac{123l^2}{4004\Delta} \\
 & & & & & & \frac{l^5}{90090\Delta^2} & \frac{37l^4}{180180\Delta^2} \\
 & & & & & & & \frac{73l^3}{18018\Delta^2} \\
sym & & & & & & &
\end{bmatrix}$$

(4.67)

4.2.5 Free vibration analysis of laminated composite beam

In free vibration, the axial force is set to zero, $N_x^i = 0$, and the nodal values are given by:

[2]

$$u_j^e(t) = U_j^e e^{i\omega t} \quad , \quad i = \sqrt{-1} \tag{4.68}$$

Substituting Equation (4.70) into Equation (4.64) and considering $N_x^i = 0$, we will obtain:

$$\left([K] - \omega^2 [M]\right)\{U\} = [0] \tag{4.69}$$

where ω represents natural frequency of vibration. Considering $\lambda = \omega^2$, one can see that Equation (4.71) is an eigenvalue problem in the form:

$$\left([K] - \lambda [M]\right)\{U\} = [0] \tag{4.70}$$

where λ represents the eigenvalue and U^e, the eigenvector. Equation (4.70) has been solved using MATLAB ® to determine the natural frequencies of free vibration of a uniform- thickness composite beam.

The exact solution for the free vibration of the mid-plane symmetric laminated composite beam using cylindrical bending theory has been given by Equations (2.36) - (2.38).

4.2.6 Buckling analysis of laminated composite beam

In the study of buckling problem, we consider an axial compressive load on the beam as:

$$N_x^i = -P \tag{4.71}$$

In the absence of lateral force and by using Equation (4.71), Equation (4.64) reduces to:

$$\left([K] - P[\overline{G}]\right)[U] = [0] \tag{4.72}$$

where matrix $[\overline{G}]$ is defined as:

$$[\overline{G}] = \frac{1}{N_x^i}[G] \tag{4.73}$$

Equation (4.73) is an eigenvalue problem where P is the eigenvalue and the smallest eigenvalue is the critical buckling load.

The exact solution for critical buckling load of mid-plane symmetric laminated composite beam using cylindrical bending theory is given by Equations (2.43)-(2.45).

4.2.7 Free vibration analysis of laminated beam-column

In the case of free vibration with compressive axial load, Equation (4.64) changes to the following form:

$$\left([K] - P[\overline{G}] - \lambda[M]\right)\{U\} = \{0\} \tag{4.74}$$

Equation (4.74), again is an eigenvalue problem where λ is the natural frequency of the composite beam-column.

4.3 Analysis of tapered beam based on CLPT

4.3.1. Governing equations

The differential equation of motion for mid-plane symmetric laminated tapered beam has been obtained in Chapter 2 by the following equation:

$$\frac{\partial^2}{\partial x^2}\left(bD_{11}(x)\cos^4(\phi)\frac{\partial^2 u}{\partial x^2}\right)-bN_x^i\frac{\partial^2 u}{\partial x^2}-bq(x)+b\rho_s\frac{\partial^2 u}{\partial t^2}=0 \tag{4.75}$$

Following the same procedure as in Section 4.2 for uniform beam, the weak form is obtained as:

$$=\sum_{j=1}^{8}\int_0^l\left[\left(bD_{11}(x)\cos^4(\phi)\frac{d^2N_i}{dx^2}\frac{d^2N_j}{dx^2}+bN_x^i\frac{dN_i}{dx}\frac{dN_j}{dx}\right)u_j^e+b\rho_s N_i N_j\frac{d^2u_j^e}{dt^2}-N_i bq(x)\right]dx$$

$$-Q_1^e N_i(0)-Q_3^e N_i(l)-Q_2^e\left(-\frac{dN_i}{dx}\right)_{x=0}-Q_4^e\left(-\frac{dN_i}{dx}\right)_{x=l}=0 \tag{4.78}$$

For drop-off plies, the value of bending stiffness is a function of x and is expressed by:

$$D_{11}(x)=\sum_{k=1}^{n}\left[t_k'\bar{z}_k^2+\frac{t_k'^3}{12}\right](\overline{Q}_{11})_k \tag{2.66}$$

where $\bar{z}_k$ is the distance between ply centerline and the mid-plane surface. In tapered laminate, $\bar{z}_k$ is a function of x as shown in Figure 2.9 and is shown in Figure 4.5 for convenience.

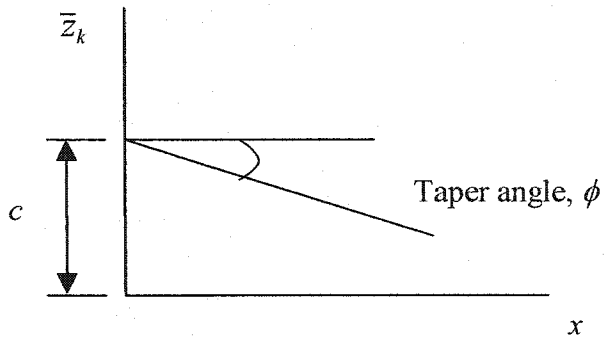

Figure 4.2 Centerline of the tapered laminate as function of x

$$\bar{z}_k = mx + c \tag{2.69}$$

Considering Equation (2.66), the coefficients of the stiffness, geometric stiffness and the mass matrices are given by the following equations:

$$K_{ij}^e = \int_0^l bD_{11}(x)\cos^4(\phi)\frac{d^2N_i}{dx^2}\frac{d^2N_j}{dx^2}dx \tag{4.79}$$

$$G_{ij}^e = \int_0^l bN_x^i\frac{dN_i}{dx}\frac{dN_j}{dx}dx \tag{4.80}$$

$$M_{ij}^e = \int_0^l b\rho_s N_i N_j dx \tag{4.81}$$

where $i = 1,2,....,8$, $j = 1,2,....,8$

4.3.2 Element properties of mid-plane tapered beam

The stiffness matrix for mid-plane symmetric laminated tapered beam is obtained by performing the integration in Equation (4.79) in MATLAB ® software as follows:

$$\left[K^e\right]=\cos^2(\phi)\begin{bmatrix} K_{11}^e & K_{12}^e & K_{13}^e & K_{14}^e & K_{15}^e & K_{16}^e & K_{17}^e & K_{18}^e \\ & K_{22}^e & K_{23}^e & K_{24}^e & K_{25}^e & K_{26}^e & K_{27}^e & K_{28}^e \\ & & K_{33}^e & K_{34}^e & K_{35}^e & K_{36}^e & K_{37}^e & K_{38}^e \\ & & & K_{44}^e & K_{45}^e & K_{46}^e & K_{47}^e & K_{48}^e \\ & & & & K_{55}^e & K_{56}^e & K_{57}^e & K_{58}^e \\ & & & & & K_{66}^e & K_{67}^e & K_{68}^e \\ & & & & & & K_{77}^e & K_{78}^e \\ sym & & & & & & & K_{88}^e \end{bmatrix} \tag{4.82}$$

The coefficients of stiffness matrix are long algebraic expressions, which are given in Appendix-A. Here the first and the last coefficients are presented to give an idea of such expressions.

$$K_{11}^e=\sum_{k=1}^{n}\frac{70}{429l^3}\left(\overline{Q}_{11}\right)_k t_k\left(156c^2+156cml+48m^2l^2+13t_k'^2\right) \tag{4.83}$$

$$K_{88}^e=\sum_{k=1}^{n}\frac{1}{18018\Delta_2^2}l\left(\overline{Q}_{11}\right)_k t_k\left(3900c^2+5460cml+2134m^2l^2+325t_k'^2\right) \tag{4.84}$$

Similarly the mass matrix for tapered mid-plane symmetric laminated beam is obtained by performing the integration in Equation (4.81) in MATLAB ® software as follows:

$$\left[M^e\right]=\begin{bmatrix} M_{11}^e & M_{12}^e & M_{13}^e & M_{14}^e & M_{15}^e & M_{16}^e & M_{17}^e & M_{18}^e \\ & M_{22}^e & M_{23}^e & M_{24}^e & M_{25}^e & M_{26}^e & M_{27}^e & M_{28}^e \\ & & M_{33}^e & M_{34}^e & M_{35}^e & M_{36}^e & M_{37}^e & M_{38}^e \\ & & & M_{44}^e & M_{45}^e & M_{46}^e & M_{47}^e & M_{48}^e \\ & & & & M_{55}^e & M_{56}^e & M_{57}^e & M_{58}^e \\ & & & & & M_{66}^e & M_{67}^e & M_{68}^e \\ & & & & & & M_{77}^e & M_{78}^e \\ sym & & & & & & & M_{88}^e \end{bmatrix} \tag{4.85}$$

where each coefficient of mass matrix is a long algebraic expression which is shown in Appendix-A. For example the first and the last expressions are given here:

$$M_{11}^e=\frac{1}{2574}\rho bl(235ml+1042g) \tag{4.86}$$

$$M_{88}^e=\frac{1}{360360\Delta_2^2}\rho bl^5(51ml+86g) \tag{4.87}$$

where g denotes the intercept of the upper surface of the laminated beam measured from the mid-plane.

The geometric stiffness matrix is computed by Equation (4.67) given for uniform symmetric beams except that in tapered beam, one should note that the values of Δ_1 and Δ_2 are computed at the respective ends of the tapered beam and therefore they have different values whereas in uniform beam both Δ_1 and Δ_2 have the same values.

4.3.3 Element properties of tapered beam models A and C

As it is seen in Figure 2.8, tapered beam models A and C have similar geometry. Geometrically the model C consists of a number of elements, which have been made using model A (Here, we use three elements of model A to construct model C). On the other hand model A can be considered as a mid-plane tapered beam. In this case, the resin pocket is divided into imaginary plies. Therefore, the element properties of tapered beam model A can be obtained by using the symbolic relations given for mid-plane tapered beams. As one can see the plies in the laminate have unequal lengths. Thus the integrations should be performed with different limits. That is instead of integrating from zero to l for all plies, one should perform the integration from zero to l_1, plus l_1 to l, etc. One should note that the element coefficients of the plies located in resin pocket should be computed by using the material properties of resin.

Individual routines have been developed in MATLAB® software to compute the stiffness, mass and geometric stiffness matrices for tapered beam models A and C.

4.3.4 Element properties of tapered beam models B and D

Another two important models for constructing tapered beams are shown in Figure 2.9. These two models have some similarities. Each element in both models consists of some drop-off plies, some imaginary plies in resin pocket and some plies, which are laid up uniformly. Obviously the number of the plies is different for each model. Again for these cases the element coefficients can be computed by using the relations obtained for mid-plane tapered beams. To illustrate the computing procedure, the first part of finite element of model D is isolated in Figure 4.3. The integrations are

the summation of integrations from L_1 to L_2, and L_2 to L. One should note that to compute the element properties for plies located in resin pocket, the material properties of resin should be considered.

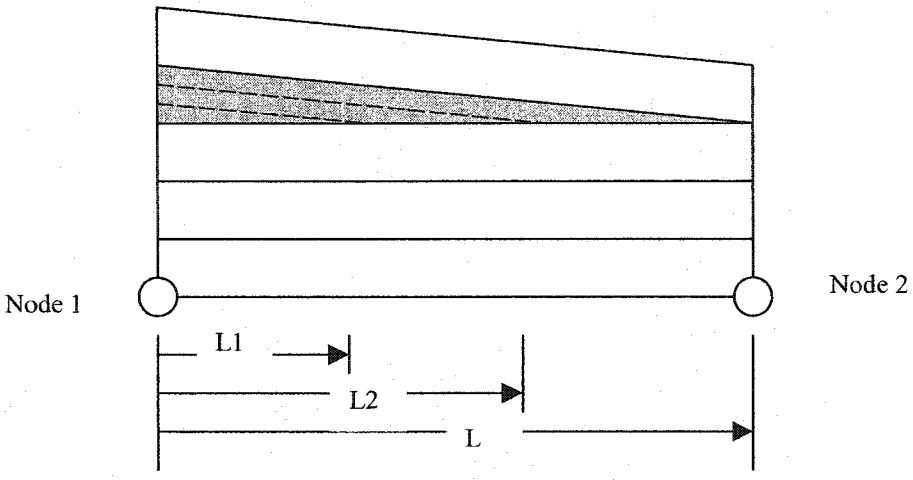

Figure 4.3 First part of finite element of model D

4.4 Advanced finite element formulation for vibration analysis of composite beam based on FSDT

The Euler-Bernoulli beam theory neglects the effects of shear deformation. Thus for bending vibration, this gives higher frequency than those obtained by experiment and for thick beams these values for lower modes are not accurate. Timoshenko theory improves the Euler-Bernoulli beam theory by including the effects of shear deformation. Various finite element formulations have been presented for the analysis of Timoshenko beam. Chapter 3 dealt with the analysis of Timoshenko beam using conventional finite element formulation where four degrees of freedom (rotations and deflections at the ends) have been considered per element. The results obtained in chapter 3 showed that in

conventional finite element formulation, a large number of elements should be considered to achieve an accurate result.

In this section an advanced finite element model for analysis of Timoshenko beams has been established based on the finite element model presented by Thomas and Abbas [47] for isotropic materials. In this model, four degrees of freedom, total deflection, w, first derivative of deflection, w', slope, ψ and first derivative of slope, ψ' are considered for each node, as a result, for a two-node element, there are eight degrees of freedom.

4.4.1 Governing equations

The equations of motion of laminated beam based on Timoshenko beam theory have been determined as in Equations (3.13) and (3.14) and are given here for convenience.

$$bH_{55}\left(\frac{\partial^2 w}{\partial x^2}-\frac{\partial \psi}{\partial x}\right)+bN_x^i\frac{\partial^2 w}{\partial x^2}+bq(x)-b\rho_s\frac{\partial^2 w}{\partial t^2}=0 \tag{3.13}$$

$$\frac{\partial}{\partial x}\left(bD_{11}\frac{\partial \psi}{\partial x}\right)-bH_{55}\left(\frac{\partial w}{\partial x}-\psi\right)-bI_{xy}\frac{\partial^2 \psi}{\partial t^2}=0 \tag{3.14}$$

4.4.2 Weak form

The weak forms of the governing equations have been determined by Equations (3.19) and (3.23) as follows:

$$0=\int_0^l\left[bH_{55}\frac{dv_1}{dx}\left(\frac{\partial w}{\partial x}-\psi\right)+bN_x^i\frac{dv_1}{dx}\frac{\partial w}{\partial x}+v_1b\rho_s\frac{\partial^2 w}{\partial t^2}-v_1bq(x)\right]dx-Q_1^e v_1(0)-Q_3^e v_1(l)$$

(4.88)

$$0=\int_0^l\left[bD_{11}\frac{dv_2}{dx}\frac{\partial\psi}{\partial x}+v_2bH_{55}\left(\frac{\partial w}{\partial x}-\psi\right)+v_2bI_{xy}\frac{\partial^2\psi}{\partial t^2}\right]dx-Q_2^e v_2(0)-Q_4^e v_2(l) \tag{4.89}$$

4.4.3 Interpolation functions

To construct the finite element model, we have four degrees of freedom per element corresponding to deflection and four degrees of freedom corresponding to rotations. Therefore to satisfy the boundary conditions we consider cubic polynomial expressions for w and ψ of the forms:

$$w=a_o+a_1x+a_2x^2+a_3x^3 \tag{4.90}$$

$$\psi=b_o+b_1x+b_2x^2+b_3x^3 \tag{4.91}$$

Here, we define the generalized co-ordinates, w, w', ψ and ψ' at nodes 1 and 2.

$$W^e(0,t)=w_1^e\ ,\ W^e(l,t)=w_3^e\ ,\quad \left.\frac{\partial W^e}{\partial x}\right|_{x=0}=w_2^e,\quad \left.\frac{\partial W^e}{\partial x}\right|_{x=l}=w_4^e \tag{4.92}$$

$$\psi^e(0,t)=\psi_1^e\ ,\psi^e(l,t)=\psi_3^e,\quad \left.\frac{\partial\psi^e}{\partial x}\right|_{x=0}=\psi_2^e,\quad \left.\frac{\partial\psi^e}{\partial x}\right|_{x=l}=\psi_4^e \tag{4.93}$$

Substituting approximation expression (4.90) into boundary conditions (4.92) involving deflection, we have:

$$w_1^e=a_o^e, \tag{4.94}$$

$$w_2^e=a_1^e \tag{4.95}$$

$$w_3^e = a_o^e + a_1^e l + a_2^e l^2 + a_3^e l^3 \tag{4.96}$$

$$w_4^e = a_1^e + 2a_2^e l + 3a_3^e l^2 \tag{4.97}$$

Similarly substituting approximation expression (4.91) into boundary conditions (4.93) involving rotations, we have:

$$\psi_1^e = b_o^e \tag{4.98}$$

$$\psi_2^e = b_1^e \tag{4.99}$$

$$\psi_3^e = b_o^e + b_1^e l + b_2^e l^2 + b_3^e l^3 \tag{4.100}$$

$$\psi_4^e = b_1^e + 2b_2^e l + 3b_3^e l^2 \tag{4.101}$$

Determining the coefficients a_i and b_i ($i = 0, 1, 2, 3$) from Equations (4.94)-(4.101) and substituting them in Equations (4.91) and (4.92), one may write the following approximation expressions for w and φ:

$$W^e = \sum_{i=1}^{4} w_i^e \Psi_i \quad , \quad \psi^e = \sum_{i=1}^{4} \psi_i^e \Phi_i \tag{4.102}$$

where, Ψ_i and Φ_i denote the interpolation functions for w and ψ that are obtained as:

$$\Psi_1^e = \Phi_1^e = 1 - 3\frac{x^2}{l^2} + 2\frac{x^3}{l^3} \tag{4.103}$$

$$\Psi_2^e = \Phi_2^e = -x + 2\frac{x^2}{l} - \frac{x^3}{l^2} \tag{4.104}$$

$$\Psi_3^e = \Phi_3^e = 3\left(\frac{x}{l}\right)^2 - 2\left(\frac{x}{l}\right)^3 \tag{4.105}$$

$$\Psi_4^e = \Phi_4^e = \frac{x^2}{l} - \frac{x^3}{l^2} \tag{4.106}$$

4.4.4 Element matrices

The stiffness and mass matrices for Timoshenko beam element are given by the following equations:

$$\left[K^e\right] = \begin{bmatrix} \left[K^{11}\right] & \left[K^{12}\right] \\ \left[K^{12}\right]^T & \left[K^{22}\right] \end{bmatrix} \tag{4.107}$$

$$\left[M^e\right] = \begin{bmatrix} \left[M^{11}\right] & [0] \\ [0] & \left[M^{22}\right] \end{bmatrix} \tag{4.108}$$

where,

$$K_{ij}^{11} = \int_0^l bH_{55} \frac{d\Psi_i}{dx} \frac{d\Psi_j}{dx} dx \tag{4.109}$$

$$K_{ij}^{12} = \int_0^l bH_{55} \frac{d\Psi_i}{dx} \Phi_j dx \tag{4.110}$$

$$K_{ij}^{12} = K_{ji}^{21} \tag{4.111}$$

$$K_{ij}^{22} = \int_0^l \left[bD_{11} \frac{d\Phi_i}{dx} \frac{d\Phi_j}{dx} + bH_{55} \Phi_i \Phi_j \right] dx \tag{4.112}$$

$$M_{ij}^{11} = \int_0^l b\rho_s \Psi_i \Psi_j dx \tag{4.113}$$

$$M_{ij}^{22} = \int_0^l bI_{xy} \Phi_i \Phi_j dx \tag{4.114}$$

The stiffness and mass matrices of Timoshenko beams are obtained upon performing the integrations in the Equations (4.109)-(4.114).

$$\left[K^e\right] = bH_{55}\begin{bmatrix}
\frac{6}{5l} & \frac{1}{2} & \frac{1}{10} & \frac{l}{10} & \frac{-6}{5l} & \frac{1}{2} & \frac{1}{10} & \frac{-l}{10} \\
 & \frac{13}{35}+\frac{6}{5l}\delta & \frac{-l}{10} & \frac{11}{210}l^2+\frac{1}{10}\delta & \frac{-1}{2} & \frac{9l}{70}-\frac{6}{5l}\delta & \frac{l}{10} & \frac{-13}{420}l^2+\frac{1}{10}\delta \\
 & & \frac{2l}{15} & 0 & \frac{-1}{10} & \frac{1}{10} & \frac{-l}{30} & \frac{-l^2}{60} \\
 & & & \frac{1}{105}l^3+\frac{1}{10}\delta & \frac{-l}{10} & \frac{13}{420}l^2-\frac{1}{10}\delta & \frac{l^2}{60} & \frac{-1}{140}l^3-\frac{l}{30}\delta \\
 & & & & \frac{6}{5l} & \frac{-1}{2} & \frac{-1}{10} & \frac{l}{10} \\
 & & & & & \frac{13}{35}l+\frac{5}{6l}\delta & \frac{-1}{10} & \frac{-11}{210}l^2-\frac{1}{10}\delta \\
 & & & & & & \frac{2}{15}l & 0 \\
sym & & & & & & & \frac{1}{105}l^3+\frac{2l}{15}\delta
\end{bmatrix} \tag{4.115}$$

where

$$\delta = \frac{D_{11}}{H_{55}} \tag{4.116}$$

$$[M^e]=\frac{\rho l}{420}\begin{bmatrix} 156A & 0 & 22lA & 0 & 54A & 0 & -13Al & 0 \\ & 13h^3 & 0 & \frac{11}{6}lh^3 & 0 & \frac{27}{6}h^3 & 0 & \frac{-13}{12}lh^3 \\ & & 4l^2A & 0 & 13lA & 0 & -3l^2A & 0 \\ & & & \frac{l^2h^3}{3} & 0 & \frac{13}{12}lh^3 & 0 & \frac{-l^2h^3}{4} \\ & & & & 156A & 0 & -22lA & 0 \\ & & & & & 13h^3 & 0 & \frac{-11}{6}lh^3 \\ & & & & & & 4l^2A & 0 \\ sym & & & & & & & \frac{l^2h^3}{3} \end{bmatrix} \quad (4.117)$$

Note that the nodal displacement vector is considered as $\{w_1, \psi_1, w_1', \psi_1', w_2, \psi_2, w_2', \psi_2'\}$, where w and ψ denote the deflection and rotation, and w' and ψ' represent the first derivative of w and ψ, respectively.

4.5 Computer programming

Different programs and routines have been developed in MATLAB® software to perform the vibration and buckling analyses of uniform and tapered composite beams. The flowcharts of the main programs for uniform and tapered beams are as shown in Figure 2.11. The details of the programs are provided in Appendix-B. The nomenclature of the programs and routines are chosen such that one may get an idea of the functions of the programs. For example *kadA.m* is used for *k* matrix of tapered beam model A using advanced FEM and *ada.m* refers to analysis of tapered beam model A and so on.

4.6 Example applications

In this Section a set of problems has been solved for free vibration and buckling of composite beams, and for the free vibration of composite beam-columns to validate the formulations presented. The problems are solved considering cylindrical bending theory. Comparisons with existing results and the results obtained in the present work using conventional formulation are made wherever possible.

4.6.1 Uniform-thickness composite beams

Example 4.6.1

Uniform-thickness composite beams with (a) simply supported, (b) fixed-fixed and (c) fixed-free boundary conditions as shown in Figure 2.5 made up of 36 plies of NCT/301 graphite-epoxy with the following mechanical properties are to be analyzed for free vibration based on CLPT. E_1 is 113.9 GPa, E_2 is 7.9856 GPa, ν_{21} is 0.0178, ν_{12} is 0.288, G_{12} is 3.138 GPa, ρ=1480 kg/m^3. The geometric properties of the beams are: the length (L) of the beam is 25 cm; individual ply thickness (t_k) is 0.125 mm and the laminate configuration is $(0/90)_{9s}$.

The problem is solved using different number of elements to obtain the desired accuracy. The results are compared with the exact solution given by equations (2.36) to (2.38). Tables 4.1 to Table 4.3 give the natural frequencies for the simply supported, fixed-fixed and fixed-free beams based on the cylindrical bending theory for mid-plane symmetric composite laminated beams. In the following tables, *n*A and *n*C denote the number of

elements used in advanced formulation and conventional formulation, respectively, and *n*DOF denotes the total number of degrees of freedom.

Table 4.1 The natural frequencies ($\times 10^3$ rad/sec) of a simply supported beam

Mode	Exact solution	1A(6DOF)	2A(10DOF)	3C(6DOF)	4C(8DOF)
1	1.366	1.366	1.366	1.368	1.367
2	5.466	5.466	5.466	5.531	5.49
3	12.300	12.644	12.300	13.652	12.52

Table 4.2 The natural frequencies ($\times 10^3$ rad/sec) of a fixed-fixed beam

Mode	Exact solution	1A(4DOF)	2A(8DOF)	3C(4DOF)	4C(6DOF)
1	3.100	3.098	3.098	3.111	3.102
2	8.539	8.543	8.540	8.711	8.619
3	16.743	17.673	16.744	20.259	17.100

Table 4.3 The natural frequencies ($\times 10^3$ rad/sec) of a fixed-free beam

Mode	Exact solution	1A(6DOF)	2A(10DOF)	3C(6DOF)	4C(8DOF)
1	0.4868	0.486	0.486	0.487	0.487
2	3.051	3.051	3.051	3.061	3.051
3	8.543	8.553	8.543	8.650	8.610

The results of the Tables 4.1 to Table 4.3 show that the advanced formulation gives more accuracy and faster convergence than conventional formulation. The fast convergence is important when one needs to determine the higher modes of vibration. By using two advanced elements the percentage of error is about zero even for the third mode whereas the use of 4 conventional elements gives 0.72 % error for the third mode in all boundary conditions. Figure 4.4 shows the natural frequencies of a simply supported beam based on the results given in Table 4.1. As one can see, the results obtained using advanced formulation fully match the exact solutions.

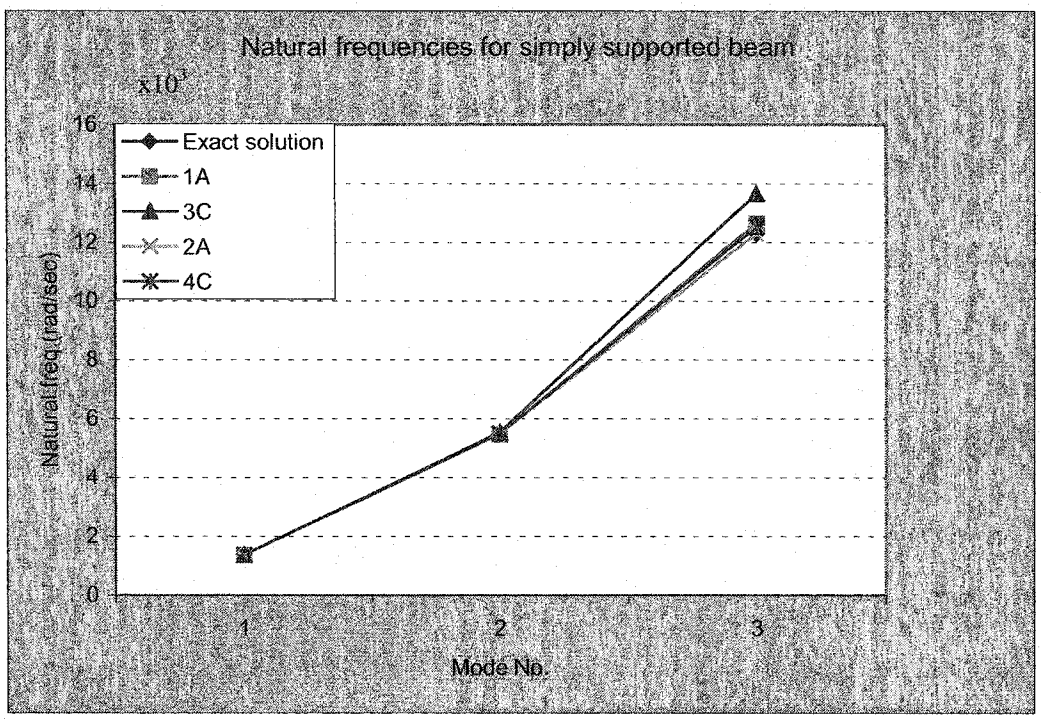

Figure 4.4 Natural frequencies of simply supported beam of example 4.6.1

Example 4.6.2

Example 4.6.1 is considered to solve for critical buckling load. The mechanical properties and the geometry of the beams remain the same in example 4.6.1. The critical buckling load is obtained using advanced formulation explained in section 4.2.5 and the results are compared with the exact solution given by Equations (2.43)-(2.45).

Table 4.4 gives the critical buckling loads for the simply supported, fixed-fixed and fixed-free beams based on the cylindrical bending theory for mid-plane symmetric composite laminated beams.

Table 4.4 Critical buckling loads ($\times 10^3$N) for beam of example 4.6.2 with different boundary conditions

Boundary conditions	Exact solution	1 A	2 A	3 C	4 C
Simply supported	39.38	39.38	39.38	39.54	39.43
Fixed-fixed	157.52	157.64	157.53	159.02	158.76
Fixed-free	9.847	9.847	9.847	9.859	9.848

The results of the Table 4.4 shows that for buckling analysis, the advanced formulation gives more accuracy by using fewer elements compared to conventional formulation. This is the same result as we experienced in dynamic analysis. Therefore we conclude that advanced formulation has better accuracy than conventional formulation for dynamic analysis as well as static analysis.

Example 4.6.3

Example 4.6.1 is considered for vibration analysis of a beam-column. In this case, the beam is loaded with a compressive axial load. The axial load is increased gradually as the percentage of the critical buckling load to investigate the effects of axial load on the natural frequencies of beam-column. Figure 4.5 shows the ratio of the natural frequency of free vibration with axial load P over the natural frequency of free vibration without axial load, $\frac{\omega}{\omega_1}$, vs. the percentage of critical buckling load for simply supported, fixed-fixed and fixed-free boundary conditions.

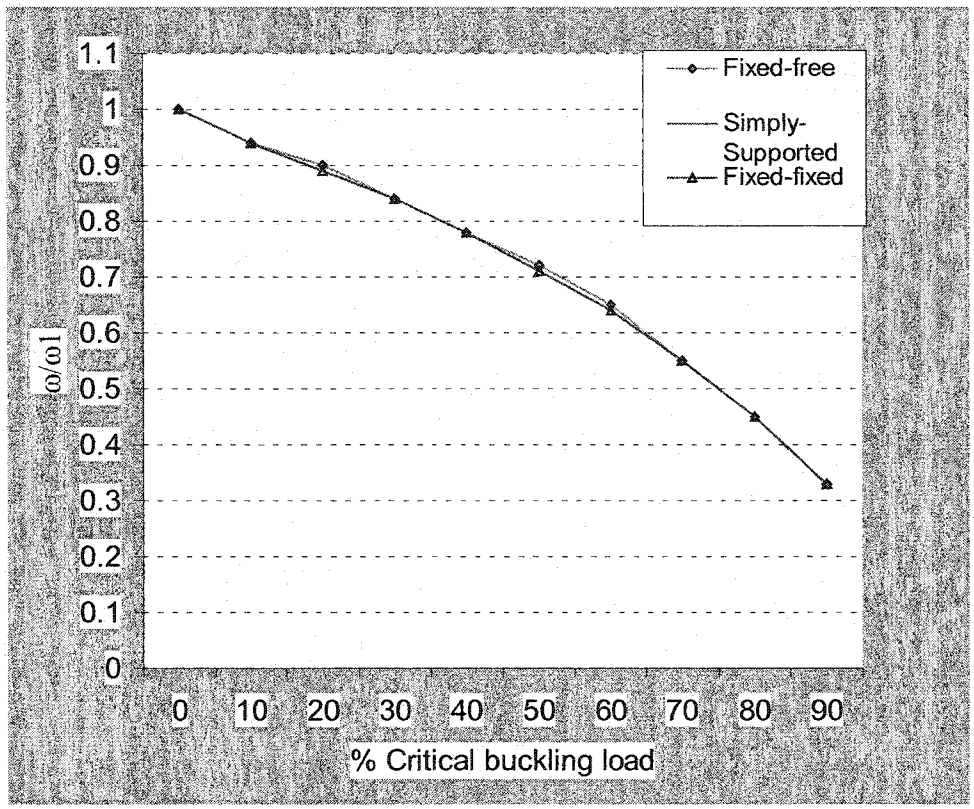

Figure 4.5 Effects of axial load on frequency ratio for laminated beams

Figure 4.5 shows that by increasing the axial load, the natural frequencies decrease. This result was expected from Equation (4.74) where one can conclude that the compressive axial load decreases the value of stiffness of the element. As it is seen in Figure 4.5 the rate of change of the frequency for fixed-fixed, fixed-free and simply supported cases are very close.

Example 4.6.4

A uniform-thickness composite beam with simply supported boundary conditions is considered to solve for natural frequencies based on Timoshenko beam model using advanced formulation. The mechanical properties are selected similar to the example

4.6.1. The laminate configuration is cross-ply. Total thickness is 0.018 m and number of plies are 144. The length of the beam is 0.0859 m.

Table 4.5 compares the results for example 4.6.4 using different number of advanced elements with the exact solution. To show the superiority of advanced formulation presented above the example 4.6.4 is solved using conventional formulation. The beam has been meshed by 5 elements. The results for the first three natural frequencies are 4.044×10^4 rad/sec, 13.117×10^4 rad/sec and 24.372×10^4 rad/sec, respectively.

Table 4.5 Natural frequencies ($\times 10^4$ rad/sec) of simply supported uniform beam based on Timoshenko beam element

Mode No.	Exact solution	1A(6 d.o.f)	2A(10 d.o.f)	3A(14 d.o.f)
1	3.86	5.293	4.461	3.802
2	11.541	17.687	12.708	12.125
3	19.693	78.471	22.252	19.059

Comparing the results given in Table 4.5 with the results obtained by using conventional formulation for Timoshenko beam element, one can see that advanced formulation offers faster convergence and more accurate results. These results become more important when determining higher modes of vibration. For example, the conventional formulation gives 23% of error in computing the third mode of vibration while for advanced formulation there is only 3% of error.

4.6.2 Tapered beams

4.6.2.1 Effects of taper types on vibration response

Example 4.6.2.1

Example 2.6.1.2 is solved using advanced formulation and the results are compared with the results given in reference [32] determined using Hierarchical finite element formulation.

Table 4.6 Natural frequencies ($\times 10^5$ rad/sec) for fixed-free laminated tapered beam of example 4.6.2.1

Mode No.	Reference [32]	Present
1	0.453	0.4430
2	2.29	2.1987
3	6.69	6.4743

Example 4.6.2.2

Problem description

Various tapered beams made of models A and C as shown in Figure 2.10 and models B and D as shown in Figure 2.9 are considered with 36 and 12 plies at thick and thin sections respectively that results in 24 drop-off plies. The stacking sequence of the laminate at thick section is $(0/90)_{9s}$ and at thin section is $(0/90)_{3s}$. Hereafter this laminate configuration will be referred as LC (1). The beam is meshed with three equal-length elements for all tapered beams. The problem is solved for different taper angles while the height ratio of thick and thin sections remains constant. As a result, the length of the

beam changes according to Table 2.5. The mechanical properties of the composite material are the same as in example 4.6.1 and the thickness of each individual ply is 0.125 mm. The mechanical properties of the epoxy resin are: Elastic Modulus (E) is 3.93 GPa, Shear Modulus (G) is 1.034 GPa, and Poisson's Ratio (ν) is 0.37.

Tapered beam model A

To make a tapered beam with model A, 24 plies have been dropped off which results in a large resin pocket. The problem is solved for free vibration. The results for simply supported, fixed-free and fixed-fixed laminated beams are listed in Tables 4.6 to 4.8 respectively.

Table 4.7 Natural frequencies ($\times 10^4$ rad/sec) for simply supported laminated tapered beam model A

Taper angle ^{o}	Mode 1	Mode 2	Mode 3	Mode 4
0.1	0.0068	0.0280	0.0613	0.1105
0.5	0.1702	0.7005	1.5342	2.7640
0.75	0.3831	1.5763	3.4520	6.2193
1.0	0.6811	2.8025	6.1371	11.0567
1.5	1.5326	6.3060	13.8094	24.8765
2.0	2.725	11.2111	24.5522	44.2339
2.5	4.2583	17.5203	38.3673	69.1234
3.0	6.1328	25.2328	55.2567	99.5517

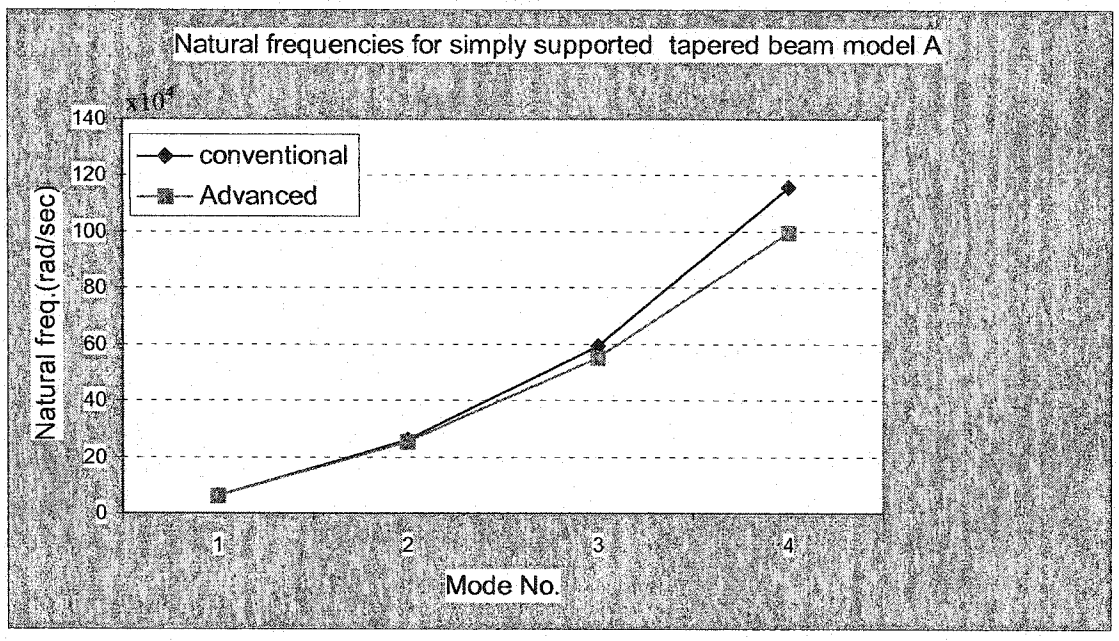

Figure 4.6 Natural frequencies for tapered beam model A with taper angle of 3 °

Figure 4.6 compares the results obtained using conventional and advanced formulations for the lowest four natural frequencies of a simply supported tapered beam model A. As it is seen the results obtained by advanced formulation are always lower than the results given by conventional formulation.

Table 4.8 Natural frequencies ($\times 10^4$ rad/sec) of fixed-free laminated beam model A

Taper angle °	Mode 1	Mode 2	Mode 3	Mode 4
0.1	0.0040	0.0179	0.04566	0.0855
0.5	0.1018	0.4485	1.1448	2.1388
0.75	0.2291	1.0093	2.5760	4.8124
1.0	0.4074	1.7943	4.5797	8.5557
1.5	0.91684	4.0375	10.3051	19.2512
2.0	1.6300	7.1785	18.3218	34.2275
2.5	2.5473	11.2178	28.6311	53.4867
3.0	3.6686	16.1559	41.2346	77.0316

Table 4.9 Natural frequencies ($\times 10^4$ rad/sec) of fixed- fixed laminated beam model A

Taper angle ^{o}	Mode 1	Mode 2	Mode 3	Mode 4
0.1	0.0154	0.0433	0.8278	0.1384
0.5	0.3864	1.0831	2.0831	3.4601
0.75	0.8695	2.4372	4.6578	7.7854
1.0	1.5459	4.3329	8.2780	13.2841
1.5	3.4785	9.7496	18.6329	31.1445
2.0	6.1845	17.3342	33.1281	55.3730
2.5	9.6644	27.0879	51.7686	86.5304
3.0	13.9188	39.01206	74.5573	124.6213

Tapered beam model B

Tapered beam model B as shown in Figure 2.9 is made by dropping off eight plies in each element. Thus, the resin pocket in this case is distributed at different locations. The beam is meshed with three equal-length elements. As it is seen in Figure 2.9, in the first and second elements, there are 16 and 8 uniform plies respectively. The problem is solved for free vibration and the results for simply supported, fixed-free and fixed-fixed laminated beams are listed in Tables 4.9 to 4.11 respectively.

Table 4.10 Natural frequencies ($\times 10^4$ rad/sec) of simply supported laminated beam model B

Taper angle ^{o}	Mode 1	Mode 2	Mode 3	Mode 4
0.1	0.0072	0.0318	0.0660	0.1157
0.5	0.1811	0.7969	1.6506	2.8946
0.75	0.4075	1.7931	3.7140	6.8946
1.0	0.7244	3.1879	6.6029	11.5791
1.5	1.6301	7.1732	14.8571	26.0548
2.0	2.8983	12.7536	26.4158	46.3237
2.5	4.5291	19.9297	41.2794	72.3892
3.0	6.5228	28.7029	59.4507	104.2551

Table 4.11 Natural frequencies ($\times 10^4$ rad/sec) of fixed -free laminated beam model B

Taper angle ^{o}	Mode 1	Mode 2	Mode 3	Mode 4
0.1	0.0050	0.0199	0.0532	0.1004
0.5	0.1258	0.4998	1.3305	2.5114
0.75	0.2832	1.1247	2.9937	5.6508
1.0	0.5035	1.9996	5.3223	10.0462
1.5	1.1330	4.4994	11.9760	22.6054
2.0	2.0145	7.9997	21.2927	40.1910
2.5	3.1480	12.5011	33.2736	62.8057
3.0	4.5338	18.0041	47.9208	90.4529

Table 4.12 Natural frequencies ($\times 10^4$ rad/sec) of fixed - fixed laminated beam model B

Taper angle ^{o}	Mode 1	Mode 2	Mode 3	Mode 4
0.1	0.0174	0.0502	0.0978	0.1544
0.5	0.4352	1.2571	2.4453	3.8613
0.75	0.9792	2.8286	5.5020	8.6881
1.0	1.7409	2.8286	5.5020	8.6881
1.5	3.9173	5.0288	9.7816	15.4459
2.0	6.9648	20.1183	39.1327	61.7931
2.5	10.8838	31.4385	61.1520	96.5629
3.0	15.6749	45.2778	88.0712	139.0701

Tapered beam model C

Tapered beam of model C, as shown in Figure 2.8 has been made by dropping off 8 plies in each element. The beam is modeled with 3 equal-length elements. As one can see the total volume of the resin pocket for models C and B are the same but they are distributed at different locations in each model. The problem is solved for free vibration and the results for simply supported, fixed-free and fixed-fixed boundary conditions are listed in Tables 4.12 to 4.14 respectively.

Table 4.13 Natural frequencies ($\times 10^4$ rad/sec) of simply supported laminated beam model C

Taper angle ^{o}	Mode 1	Mode 2	Mode 3	Mode 4
0.1	0.0071	0.0298	0.0653	0.1176
0.5	0.1782	0.7453	1.6337	2.9403
0.75	0.4011	1.6774	3.6759	6.6159
1.0	0.7131	2.9822	6.5352	11.7618
1.5	1.6047	6.7105	14.705	26.4658
2.0	2.8531	11.9308	26.1450	47.0546
2.5	4.4585	18.6441	40.8562	73.5313
3.0	6.4211	26.8513	58.8413	105.9001

Table 4.14 Natural frequencies ($\times 10^4$ rad/sec) of fixed -free laminated beam model C

Taper angle ^{o}	Mode 1	Mode 2	Mode 3	Mode 4
0.1	0.0045	0.0019	0.0048	0.0091
0.5	0.1148	0.4831	1.2224	2.2795
0.75	0.2583	1.0870	2.7505	5.1291
1.0	0.4593	1.9325	4.8900	9.1186
1.5	1.0334	4.3484	11.0032	20.5183
2.0	1.8374	7.7310	19.5629	36.4802
2.5	2.8713	12.0815	30.5707	57.0069
3.0	4.1353	17.3999	44.0279	82.1015

Table 4.15 Natural frequencies ($\times 10^4$ rad/sec) of fixed - fixed laminated beam model C

Taper angle ^{o}	Mode 1	Mode 2	Mode 3	Mode 4
0.1	0.0166	0.0463	0.0884	0.1474
0.5	0.4168	1.1592	2.2101	3.6868
0.75	0.9380	2.6083	4.9729	8.2955
1.0	1.6676	4.6371	8.8410	14.7480
1.5	3.7524	10.4342	19.8936	33.1851
2.0	6.6716	18.5514	35.3695	59.0011
2.5	10.4255	28.9899	55.2713	92.1999
3.0	15.0149	41.7513	79.6019	132.7865

Tapered beam model D

Tapered beam of model D as shown in Figure 2.9 is made by dropping off eight plies in each element. Thus, the resin pocket in this case is distributed at different locations. The beam is meshed with three equal-length elements. As it is seen in Figure 2.9, in the first and second elements, there are 28 and 12 uniform plies respectively. The problem is solved for free vibration and the results for simply supported, fixed-free and fixed-fixed laminated beams are listed in Tables 4.15 to 4.17 respectively.

Table 4.16 Natural frequencies ($\times 10^4$ rad/sec) of simply supported laminated beam model D

Taper angle °	Mode 1	Mode 2	Mode 3	Mode 4
0.1	0.0082	0.0333	0.0735	0.1314
0.5	0.2068	0.8349	1.8376	3.2853
0.75	0.4653	1.8786	4.1347	7.3922
1.0	0.8272	3.3399	7.3508	13.1419
1.5	1.8614	7.5153	16.5405	29.5713
2.0	3.3094	13.3617	29.4080	52.5760
2.5	5.1716	20.8801	45.9553	82.1594
3.0	7.4481	30.0715	66.1849	118.3261

Table 4.17 Natural frequencies ($\times 10^4$ rad/sec) of fixed-free laminated beam model D

Taper angle °	Mode 1	Mode 2	Mode 3	Mode 4
0.1	0.0036	0.0195	0.0532	0.1017
0.5	0.0902	0.4887	1.3321	2.5447
0.75	0.2030	1.0997	2.9972	5.7257
1.0	0.3610	1.9551	5.3286	10.1793
1.5	0.8123	4.3993	11.9902	22.9050
2.0	1.4442	7.8217	21.3178	40.7237
2.5	2.2564	12.2228	33.3128	63.6381
3.0	3.2504	17.6034	47.9772	91.6517

Table 4.18 Natural frequencies ($\times 10^4$ rad/sec) of fixed-fixed laminated beam model D

Taper angle ^{o}	Mode 1	Mode 2	Mode 3	Mode 4
0.1	0.0182	0.05147	0.0996	0.1651
0.5	0.4559	1.2868	2.4905	4.1275
0.75	1.0258	2.8955	5.6038	9.2871
1.0	1.8238	5.1477	9.9628	16.5107
1.5	4.1038	11.5831	22.4174	37.1516
2.0	7.2963	20.5940	39.8567	66.0532
2.5	11.4018	32.1819	62.2833	103.2199
3.0	16.4210	46.3485	89.7006	148.6575

4.6.2.2 Effects of ply orientations on vibration response of tapered beams

Now we intend to study the effects of ply orientations on free vibration of tapered beam. Observation of the results presented in the previous section shows that the tapered beam model D gives higher natural frequencies for all types of boundary conditions, which means that the tapered beam model D is the stiffest model compared to the other tapered types. In this section the tapered beam model D is considered to investigate the effects of ply orientation on natural vibration of tapered beam. Tables 4.19 and 4.20 give the natural frequencies for laminate configuration LC (2) that has $(\pm 45)_{9s}$ at thick section and $(\pm 45)_{3s}$ at thin section and laminate configuration LC (3) that has $(0_4/\pm 45_7)_s$ at thick section and $(0_4/\pm 45)_s$ at thin section respectively.

Table 4.19 Natural frequencies ($\times 10^4$ rad/sec) for simply supported beam of model D with LC (2) configuration

Taper angle ^{o}	Mode 1	Mode 2	Mode 3	Mode 4
0.1	0.0059	0.0242	0.0522	0.0953
0.5	0.1499	0.6053	1.3306	2.3830
0.75	0.3372	1.3620	2.9939	5.3620
1.0	0.5996	2.4214	5.3226	9.5327
1.5	1.3492	5.4486	11.9766	21.4500
2.0	2.3989	9.6873	21.2937	38.1367
2.5	3.7488	15.1381	33.2753	59.5954
3.0	5.3990	21.8020	47.9232	85.8295

Table 4.20 Natural frequencies ($\times 10^4$ rad/sec) for simply supported beam of model D with LC (3) configuration

Taper angle ^{o}	Mode 1	Mode 2	Mode 3	Mode 4
0.1	0.0104	0.0411	0.0942	0.1641
0.5	0.2608	1.0296	2.2856	4.1040
0.75	0.5868	2.3168	5.1428	9.2342
1.0	1.0432	4.1188	9.1430	16.4168
1.5	2.3474	9.2680	20.5731	36.9402
2.0	4.1735	16.4779	36.5777	65.6773
2.5	6.5219	25.7497	57.1930	102.6325
3.0	9.3928	37.0848	82.3209	147.8117

Figure 4.7 compares the fundamental frequency obtained for laminate configurations LC (1), LC (2) and LC (3) for tapered beam of model D with different taper angles.

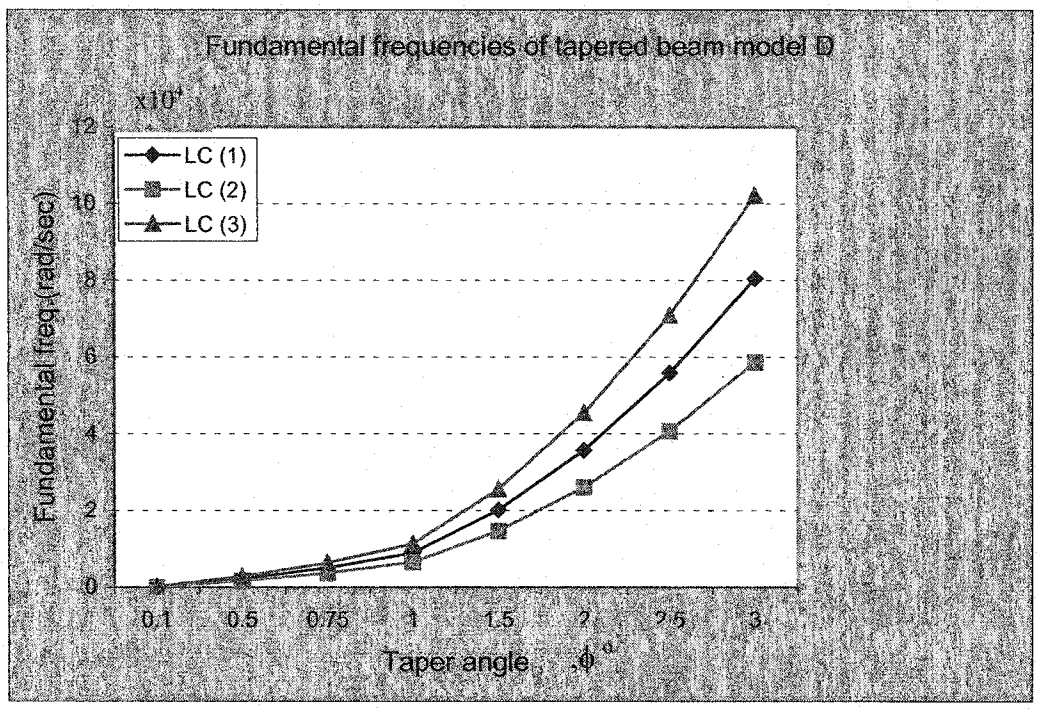

Figure 4.7 Fundamental frequency for simply supported tapered beam model D

Figure 4.7 shows that the tapered beam with LC (3) laminate configuration gives the highest natural frequency. The effects of ply orientations on free vibration can be determined by investigating the Equations (2.67) and (2.68) where one can see that beam stiffness D_{11} is a function of Q_{11} which itself is a function of ply orientation.

It can be seen from Figure 4.7 that by increasing taper angle the natural frequencies increase for all ply orientations under investigation. Recalling the geometric dimensions of tapered beams given in Table 2.5, one can see that the higher the taper angle is the smaller is the length of the beam. Equation (4.85) shows that the length of the beam has direct effects on stiffness matrix.

4.6.2.3 Effects of boundary conditions on vibration response of tapered beams

To see the effects of boundary conditions on natural frequencies, a tapered beam made with model D is considered. Taper angle of 3° is chosen and the laminate configuration is cross-ply. The first four natural frequencies are plotted in Figure 4.8. The effects of boundary conditions on natural frequencies for tapered beam are similar to the corresponding results obtained for uniform beams. As it is seen the natural frequencies for fixed-fixed support are the highest and the fixed-free support gives the lowest natural frequencies. This is due to the effects of restrained degrees of freedom. In fixed-fixed support there are four restrained degrees of freedom whereas for fixed-free support there are only two restrained degrees of freedom.

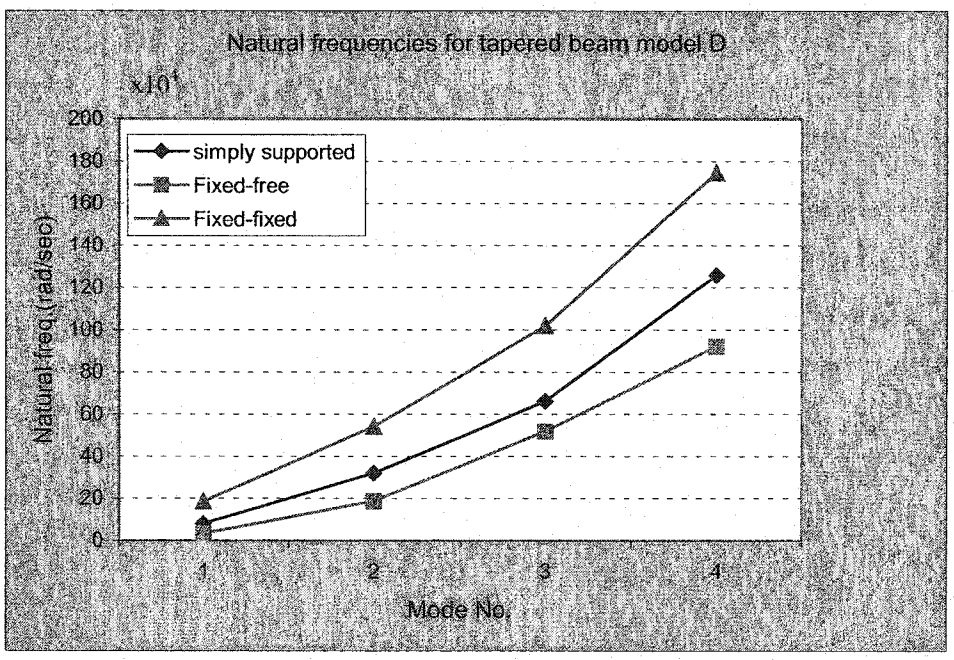

Figure 4.8 Natural frequencies for tapered beam of model D with LC (1) configuration and taper angle of 3 °

4.6.2.4 Effects of taper types on vibration response of tapered beams

To study the effects of types of the tapered beams on natural frequencies, different types of tapered beams that are simply supported have been considered. The natural frequencies have been computed for different taper angles. The results are shown in Figure 4.9. As it was expected the natural frequencies for tapered beam model D are the highest and tapered beam models, B, C and A take respectively the other positions. This is the same result that we saw in conventional formulation. The reason for this has already been discussed in Chapter 2.

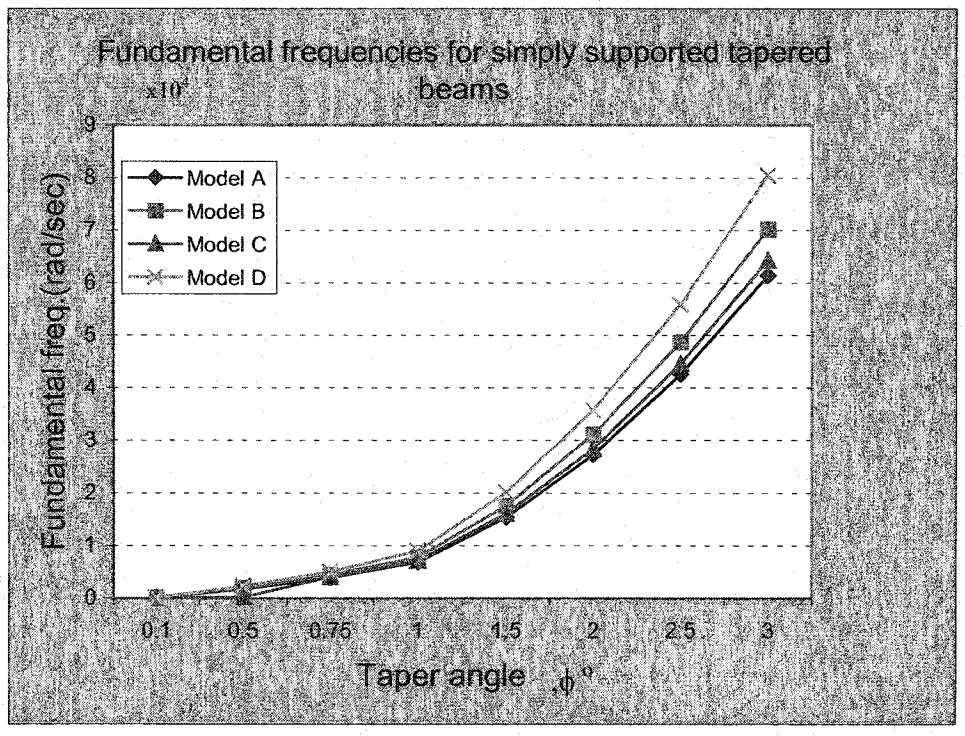

Figure 4.9 Fundamental frequencies for different tapered beams with LC (1) configuration and simply supported boundary condition

4.6.2.5 Effects of taper types on buckling of tapered beams

As we observed from the results given in example 4.6.2.2 the tapered beam with LC (3) configuration is the stiffest beam. To investigate the effects of the type of taper on buckling loads, we consider tapered beam models, A, B, C and D for different boundary conditions and different taper angles. Tables 4.21 to 4.24 give the critical buckling loads for tapered beam models A, B, C and D respectively. To have a clear observation, these results are plotted in Figure 4.10. As one can see in Figure 4.10, the tapered beam model D gives the highest value for critical buckling load. Consequently tapered beam models B, C and D take the other positions. This observation is similar to the results shown in Figure 4.9. This is due to the high stiffness of tapered beam model D that has been discussed in the previous section.

Table 4.21 Critical buckling load ($\times 10^4$ N) of tapered laminated beams of model A with LC (3) configuration

Taper angle ^{o}	Simply supported	Fixed-free	Fixed- fixed
0.1	0.2038	0.0826	0.7725
0.5	5.0956	2.0664	19.3136
0.75	11.4649	4.6492	43.4542
1.0	20.3811	8.2649	77.2485
1.5	45.8518	18.5938	173.7874
2.0	81.4999	33.0498	308.9008
2.5	127.3147	51.6286	482.5479
3.0	183.2822	74.3246	694.6761

Table 4.22 Critical buckling load ($\times 10^4$ N) of tapered laminated beams of model B with LC (3) configuration

Taper angle ^{o}	Simply supported	Fixed-free	Fixed- fixed
0.1	0.2119	0.0898	0.8194
0.5	5.2985	2.2463	20.4864
0.75	11.9213	5.0540	46.0931
1.0	21.1925	8.9845	81.9397
1.5	47.6773	20.2126	184.3411
2.0	84.7446	35.9271	327.6597
2.5	132.3834	56.1234	511.8521
3.0	190.5791	80.7952	736.8624

Table 4.23 Critical buckling load ($\times 10^4$ N) of tapered laminated beams of model C with LC (3) configuration

Taper angle ^{o}	Simply supported	Fixed-free	Fixed- fixed
0.1	0.2083	0.08716	0.7999
0.5	5.2081	2.1789	19.9977
0.75	11.7178	4.9024	44.9934
1.0	20.8308	8.7151	79.9847
1.5	46.8634	19.6065	179.9430
2.0	83.2980	34.8499	319.8422
2.5	130.1236	54.4400	499.6400
3.0	187.3259	78.3727	719.2820

Table 4.24 Critical buckling load ($\times 10^4$ N) of tapered laminated beams of model D with LC (3) configuration

Taper angle ^{o}	Simply supported	Fixed-free	Fixed- fixed
0.1	0.4139	0.1237	1.5400
0.5	10.3475	3.0930	38.5015
0.75	23.2813	6.9592	86.6257
1.0	41.3872	12.3714	153.9945
1.5	93.1095	27.8321	346.4437
2.0	165.4986	49.4706	615.7907
2.5	258.5326	77.2802	961.9535
3.0	372.1832	111.2525	138.4827

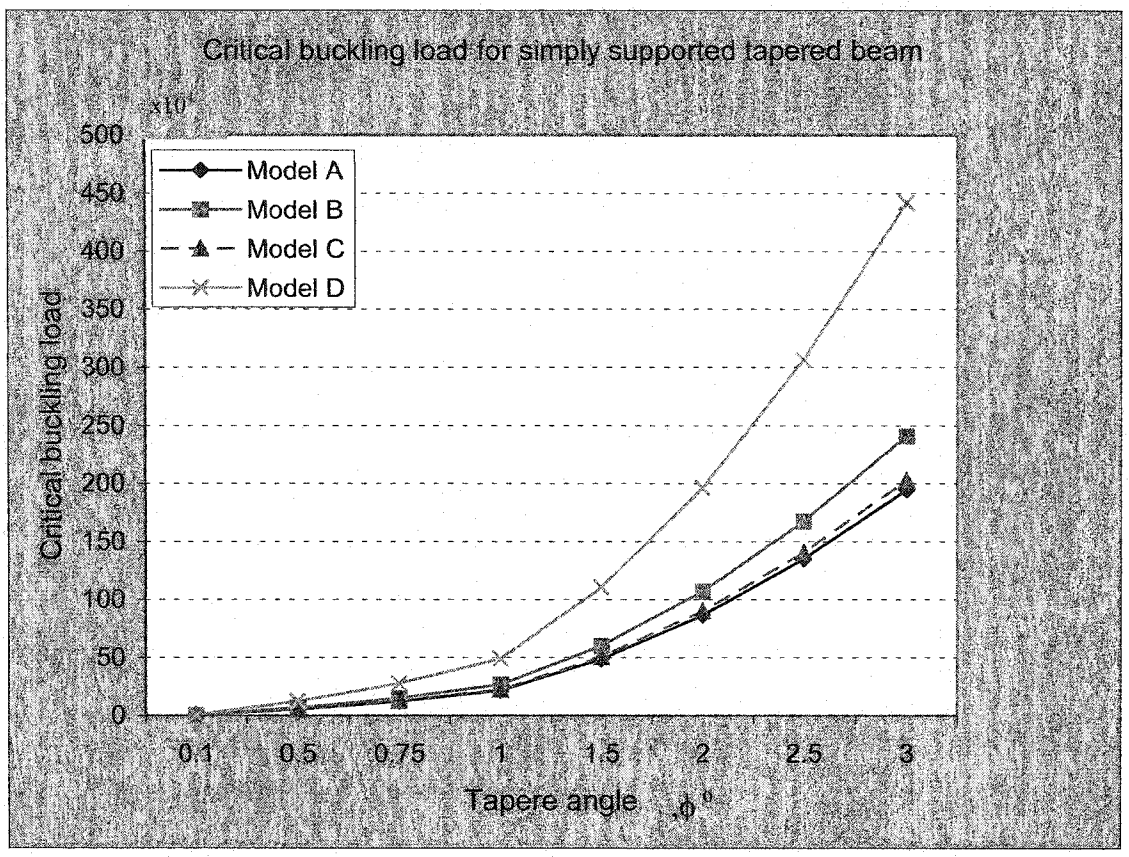

Figure 4.10 Critical buckling loads for simply supported tapered beam with LC (3) configuration

4.7 Conclusions and discussions

In this Chapter, the advanced finite element formulation has been developed for vibration and buckling analyses of uniform-thickness and tapered composite beams based on classical laminate theory. The formulation has been applied to obtain natural frequencies and critical buckling loads of uniform-thickness and tapered composite beams. In the case of uniform-thickness beams, the results obtained have been compared with the exact solutions.

The advanced finite element formulation has been applied for the analysis of tapered composite beams. Various types of tapered composite beams, viz. model A, staircase (model B), overlapped (model C) and continuous plies interspersed (model D) have been investigated for natural frequencies and critical buckling loads under different boundary conditions. Based on the results obtained in this chapter, it is shown that the tapered beam made with model D has the highest stiffness and that models B and C take the second and third ranks respectively. Model A has the lowest stiffness. Therefore the natural frequencies and critical buckling loads of model D are the highest and models B, C and A take the second, third and fourth positions. Natural frequencies of model D are about three times more than the corresponding results for model A. By comparing the results obtained using advanced formulation with the results obtained using conventional formulation, one can see that the results obtained using advanced formulation are always lower than the results obtained using conventional formulation.

With regard to the boundary conditions, we conclude that the natural frequencies for fixed-fixed support are the highest. Simply supported and fixed-free supports take the second and third positions.

According to the results given for different taper angles, we conclude that by increasing taper angles while keeping the thickness constant, the natural frequencies and critical buckling loads increase for all types of tapered beams.

Chapter 5

Parametric study on tapered composite beams

5.1 Introduction

In Chapters 2 and 3 different types of tapered sections were analyzed using conventional finite element formulation. In Chapter 4, advanced finite element formulation has been developed for uniform-thickness, mid-plane tapered and internally-tapered composite beams. The advanced formulation was applied to buckling analysis, vibration analysis and the analysis of laminated beam-columns. Four types of tapered sections were introduced as models A, B, C and D as shown in Figure 2.4.

The examples described in Chapters 2, 3 and 4 were designed so as to focus our study on the effects of different types of tapered sections on vibration response and buckling. Commonly used tapered beams consist of a thick section, a thin section and a tapered section as shown in Figure 5.1. The length of the tapered section depends on the taper angle and usually is much smaller than the lengths of the other two sections.

Major considerations in designing a tapered composite beam are ply orientations, taper angle and type of the tapered section, namely, external, mid-plane and internal

tapering. In terms of internal tapering, there are four choices that are called as models A, B, C and D.

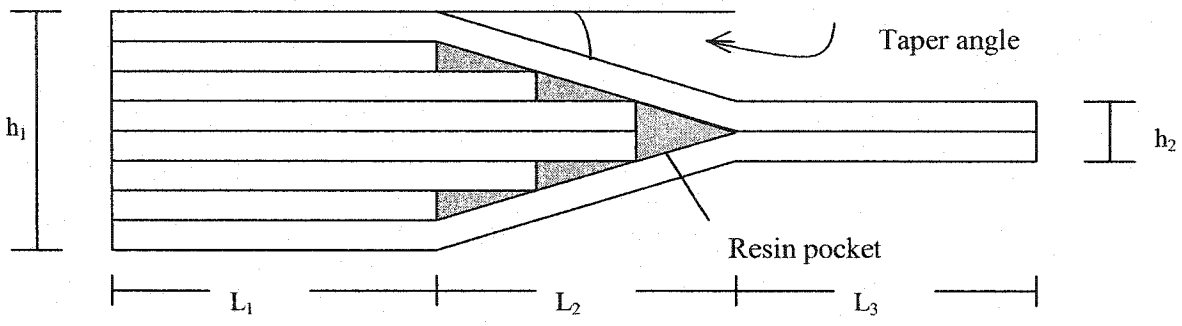

Figure 5.1 Schematic illustration of a tapered beam of model B

In this Chapter, the parametric study is conducted on the tapered beam shown in Figure 5.1. The material chosen is NCT/301 graphite-epoxy that is available in the laboratory of Concordia Centre for Composites. The properties of the material are listed in Table 5.1 and Table 5.2. The specifications of composite (ply orientations) and geometric properties (number of plies, taper angle, and length) are detailed in individual problems. In all cases the laminate is symmetric. All problems are solved using advanced finite element formulations. In some cases the results obtained using conventional formulation are given for comparison.

The tapered beams are analyzed for different types of internally tapered sections that are called as models A, B, C and D. Variations in the boundary conditions, stacking sequences and taper angles are considered for all cases. In general, there are two ways of changing the taper angle: (a) change the length of tapered section while keeping the

thickness of the thick and thin sections as constants. b) change the number of drop-off plies (i.e., change the thickness of thick and thin sections).

The free vibration and buckling problems are solved using advanced formulation. In some cases the results obtained using conventional formulation are given for comparison. The results are summarized in tables and where applicable, in plots. The results are compared and interpreted right after each problem.

5.2 Parametric study on the free vibration of tapered composite beams

Example 5.2.1

Problem Description

The tapered composite beam of Figure 5.1 has the following geometric properties: length of the thick section (L_1) is 135 mm; length of the thin section (L_3) is 135 mm; length of tapered section (L_2) is 28.6 mm; height at thick section (h_1) is 4.5 mm; height at thin section (h_2) is 1.5 mm; ply thickness (t_p) is 0.125 mm; stacking sequence for the thick section is $[0/90]_{9s}$ and for thin section is $[0/90]_{3s}$. Taper angle ϕ is 3°. There are 36 plies in the thick section ane 12 plies in the thin section. The mechanical properties of the graphite-epoxy and the resin are listed in Table 5.1 and Table 5.2 respectively. Tapered section is considered to be made of model C. The thick and thin sections are modeled using one element for each and the tapered section is modeled using three equal-length elements.

Table 5.1 Mechanical properties of unidirectional graphite-epoxy prepreg

Longitudinal Modulus (E_1)	113.9 GPa
Transverse Modulus (E_2)	7.985 GPa
(E_3) = (E_2)	7.985 GPa
In-Plane Shear Modulus (G_{12})	3.137 GPa
Out-of-Plane Shear Modulus (G_{23})	2.852 GPa
Density (ρ, Kg/m^3)	1480
Major Poisson's Ratio (v_{12})	0.288
Minor Poisson's Ratio (v_{21})	0.018

Table 5.2 Mechanical properties of resin material

Elastic Modulus (E)	3.93 GPa
Shear Modulus (G)	1.034 GPa
Poisson's Ratio (v)	0.37

5.2.1 Effects of boundary conditions on the natural frequencies

The lowest three natural frequencies for the above-mentioned problem are obtained using conventional and advanced finite element formulations. The results obtained using both the formulations are given in Table 5.3.

Before discussing about the results it is necessary to validate the results. In order to validate the results given in Table 5.3, the problem described in section 5.2 is solved for a very small angle (0.5 ^{o}) and numbers of plies in thick and thin sections are

considered as 36 and 32, respectively. In this case the tapered section is meshed by two equal-length elements. The total length remains the same (L = 298.6 mm). The results for this geometry can be compared with that for a uniform beam with the same length and 36 plies.

For example, for fixed-free condition, the lowest three natural frequencies for the tapered laminated beam described above with taper angle of 0.5 ° are obtained as: 3.30×10^2, 20.400×10^2 and 56.619×10^2, respectively. The corresponding results for a uniform beam are given as: 3.413×10^2, 21.45×10^2 and 60.63×10^2 respectively. For simply supported and fixed-fixed beams the fundamental frequencies for tapered beam with taper angle of 0.5° are obtained as: 8.998×10^2 and 20.467×10^2 respectively, and the corresponding results for uniform-thickness beams are given as: 9.58×10^2 and 21.805×10^2. Considering the fact that there is considerable change in the thin section length, it can be observed that the results for tapered beam and uniform-thickness beam are comparable thus validating the results given in Table 5.3.

Table 5.3 The lowest four natural frequencies of tapered beam of the beam described in example 5.2.1

Mode	Natural frequencies, $\times 10^2$ (rad/sec)		
	Simply supported	Fixed-free	Fixed-fixed
1	3.797(3.798)	4.108(4.110)	12.523(12.544)
2	23.701(23.841)	12.451(12.465)	35.666(36.051)
3	50.310(51.349)	35.391(35.598)	68.528(71.843)
4	85.111(94.318)	69.563(71.269)	107.002(126.873)

* The values in the parentheses have been obtained using conventional formulation

Observation of the results of Table 5.3 shows that changing the boundary condition results in a considerable variation in the natural frequencies. The natural frequencies for the fixed-fixed support are the highest and the second rank is for the simply supported case and the lowest values are for fixed-free support. Figure 5.2 gives the lowest four natural frequencies for different types of boundary conditions. Figure 5.2 shows the observation results of Table 5.3 in graphical form. It may be noted that for the finite element model, the modes are not continuous.

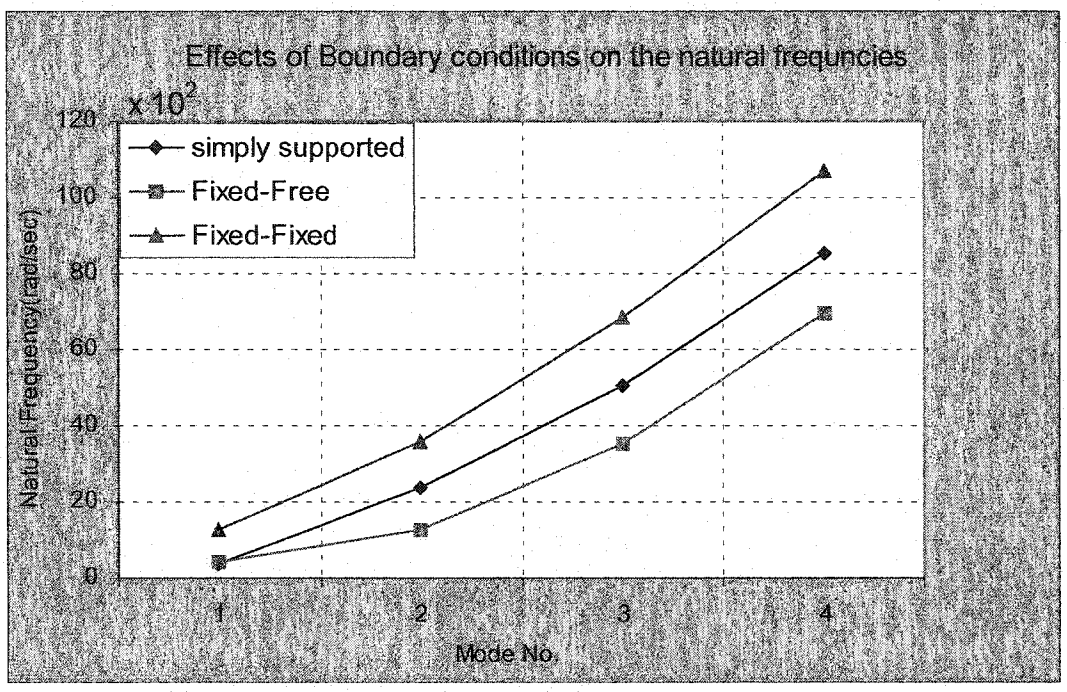

Figure 5.2 Effects of boundary conditions on natural frequencies of the beam described in example 5.2.1

5.2.2 Effects of laminate configuration on the natural frequencies

The problem described in example 5.2.1 is considered to investigate the effects of laminate configurations on the natural frequencies. The same material and geometric properties are used. The laminate configurations considered are: (i) LC (1) that has $[0/90]_{9s}$ configuration at thick section and $[0/90]_{3s}$ configuration at thin section ; (ii) LC (2) that has $[\pm 45]_{9s}$ configuration at thick section and $[\pm 45]_{3s}$ configuration at thin section; (iii) LC (3) that has $[0_4/\pm 45_7]_s$ configuration at thick section and $[0_4/\pm 45]_s$ configuration at thin section. The lowest four natural frequencies are determined for different boundary conditions and for the laminate configurations LC (1), LC (2) and LC (3). Table 5.4 and Table 5.5 give the values of the lowest four natural frequencies for the above cases.

Table 5.4 The natural frequencies of tapered beam with LC (2) configuration corresponding to different boundary conditions

Mode	Natural frequencies, $\times 10^2$ (rad/sec)		
	Simply supported	Fixed-Free	Fixed-Fixed
1	2.609 (2.609)	2.895 (2.896)	8.905 (8.916)
2	16.499 (16.597)	8.827 (8.836)	24.797 (25.064)
3	35.733 (36.565)	24.611 (24.746)	49.324 (51.239)
4	59.173 (65.552)	49.352 (50.794)	74.555 (88.570)

* The values in the parentheses have been obtained using conventional formulation

Table 5.5 The natural frequencies of tapered beam with LC (3) configuration corresponding to different boundary conditions

Mode	Natural frequencies, $\times 10^2$ (rad/sec)		
	Simply supported	Fixed-Free	Fixed-Fixed
1	4.604 (4.606)	4.723 (4.725)	14.254 (14.268)
2	27.940 (28.092)	14.255 (14.698)	42.190 (42.638)
3	57.203 (58.168)	41.859 (42.112)	79.057 (81.082)
4	101.093 (111.907)	79.099 (80.504)	126.719 (149.367)

*The values in the parentheses are obtained using conventional finite element formulation.

Figures 5.3, 5.4 and 5.5 show the effects of laminate configuration for simply supported, fixed-free and fixed-fixed boundary conditions respectively,

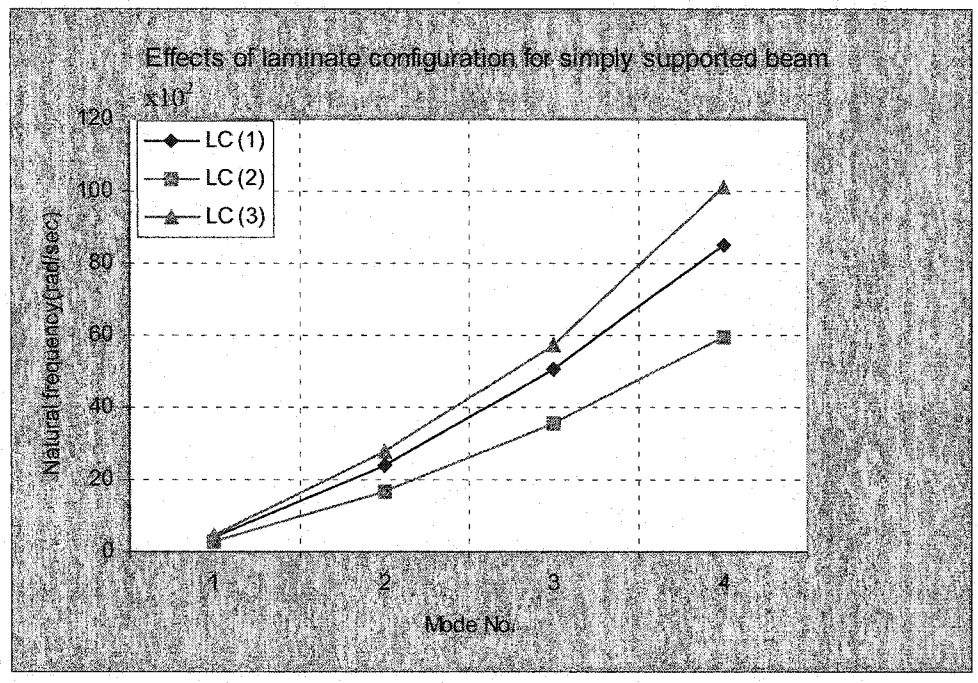

Figure 5.3 Natural frequencies of laminate configurations LC (1), LC (2) and LC (3) with simply supported boundary condition

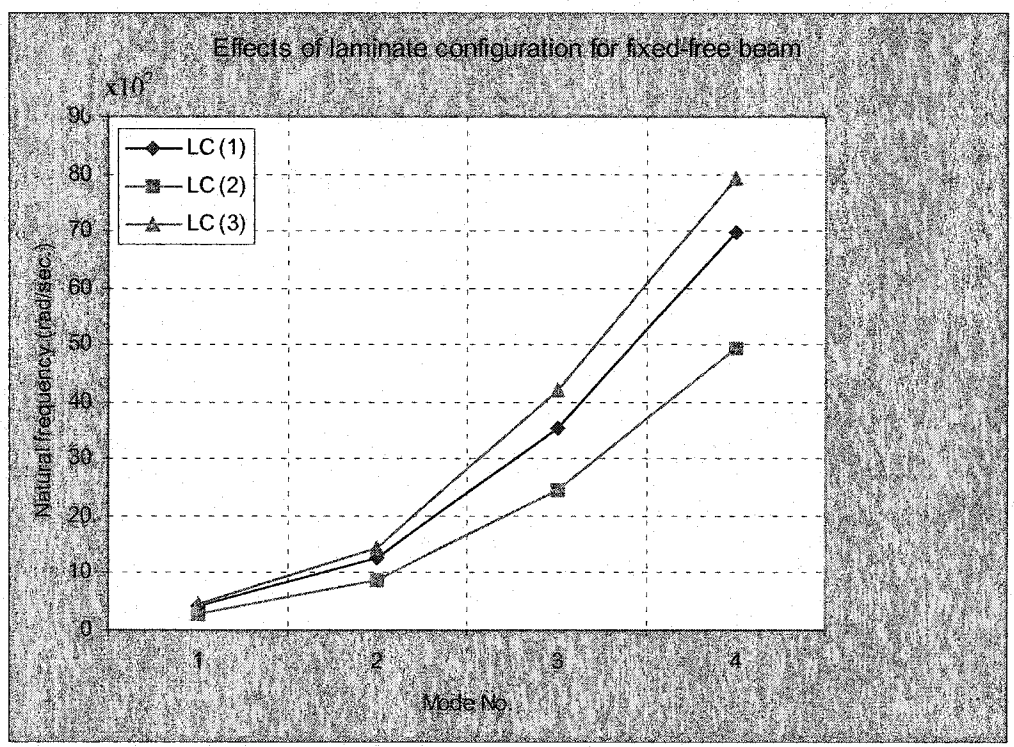

Figure 5.4 Natural frequencies of laminate configurations LC (1), LC (2) and LC (3) with fixed-free boundary condition

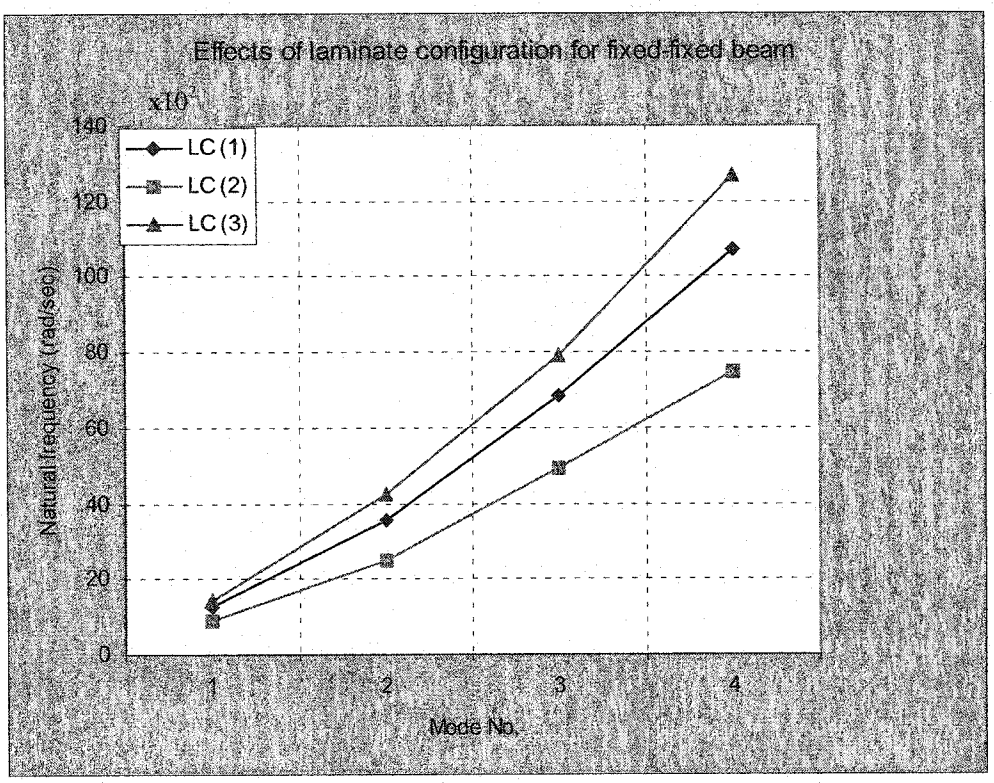

Figure 5.5 Natural frequencies of laminate configurations LC (1), LC (2) and LC (3) with fixed-fixed boundary condition

One can observe that for all types of boundary conditions, the natural frequencies for LC (3) laminate configuration are the highest and the lowest values belong to LC (2) laminate configuration. The changes in natural frequencies for different configurations are due to change in stiffness and mass matrices for each configuration. Recalling Equations (4.67) and (4.68), one can see that stiffness and mass matrices directly depend on the value of D_{11} which itself directly depends on Q_{11} as shown in Equation (4.2). Further, tapered beam of example 5.2.1 has been considered. The changes in the fundamental frequency corresponding to different ply orientation angles for the laminate with $[\pm\theta]$ ply group are plotted in Figure 5.6. As one can see the fundamental frequency drops significantly for ply orientation angles greater than 10^{o}.

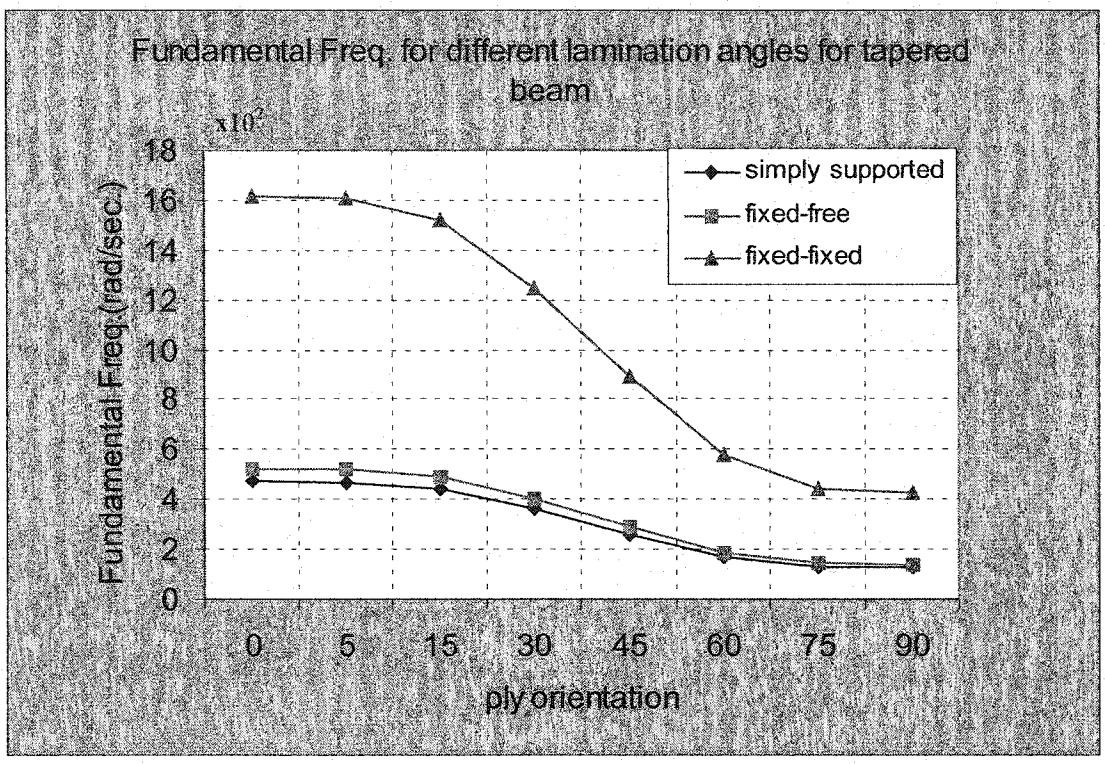

Figure 5.6 Fundamental frequencies of tapered beams with [±θ] ply group

5.2.3 Effects of the taper angle on the natural frequencies

To study the effects of taper angles on the natural frequencies, the tapered beam described in example 5.2.1 is considered. Taper angles have been increased from 1^{o} to 3^{o} to investigate the effects of taper angle on natural frequencies. The thickness ratio for all angles remains constant and therefore, increasing the taper angle results in decreasing the length of the tapered section. To have comparable results, the total length of the beam for all angles is kept constant and the change in the length of the tapered section is considered and correspondingly the lengths of the thick and thin sections are adjusted using equal increments.

Tables 5.6 to 5.8 give the values for the lowest three natural frequencies for simply supported, fixed-free and fixed-fixed supports respectively.

Table 5.6 Effects of taper angle on the natural frequencies ($\times 10^2$ rad/sec) for simply supported tapered beam with LC (1) configuration

Taper angle, ϕ°	1st mode	2 nd mode	3 rd mode
1	4.270	25.013	50.508
2	3.910	24.280	50.116
3	3.797	23.701	50.310

Observation of the results of Table 5.6 shows that increasing the taper angle leads to decreasing the natural frequencies. One should note that these results are obtained for realistic tapered beam, which consists of a thick section, a thin section and a tapered section. Decreasing the natural frequencies by increasing taper angle relates to the decreasing the value of D_{11}, which in turn results in decreasing stiffness and mass (matrices). Figure 5.6 shows that the rates of decreasing the natural frequencies for all types of tapered section are very close. The natural frequency shows significant drop between 1 and 2 degrees but after 2 degree the slope becomes less steep.

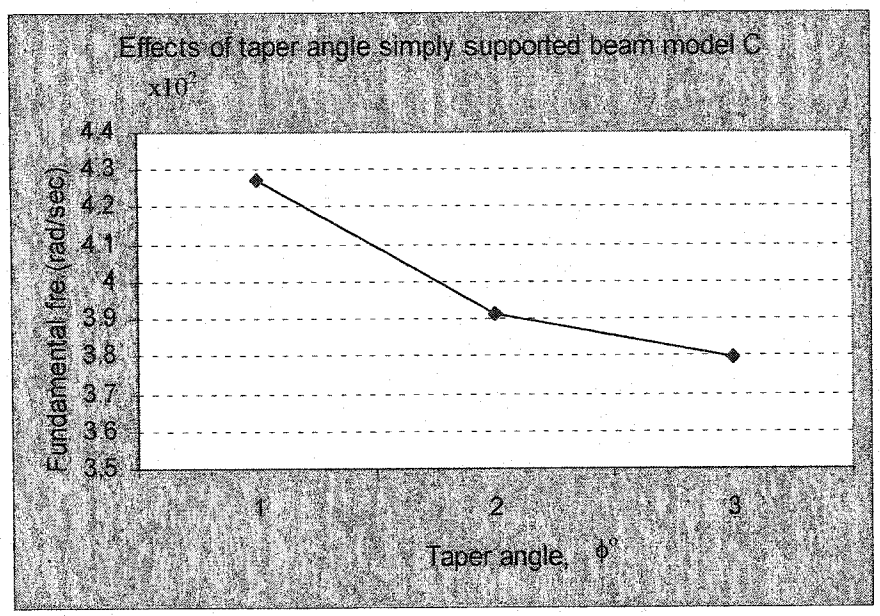

Figure 5.7 Effects of taper angle on the natural frequencies of tapered beam of model C with LC (1) configuration

Table 5.7 and Table 5.8 give the values of the lowest three natural frequencies for fixed-free and fixed -fixed supports for tapered beam with LC (1) laminate configuration. As expected from our discussion for simply supported beam (Table 5.6), the natural frequencies decrease by increasing taper angle for both fixed-free and fixed-fixed supports.

Table 5.7 Effects of taper angle on the natural frequencies ($\times 10^2$ rad/sec) for fixed-free tapered beam with LC (1) configuration

Taper angle, ϕ^o	1st mode	2 nd mode	3 rd mode
1	6.392	19.182	55.009
2	4.224	12.556	36.277
3	4.110	12.465	35.598

Table 5.8 Effects of taper angle on the natural frequencies ($\times 10^2$ rad/sec) for fixed-fixed tapered beam with LC (1) configuration

Taper angle, ϕ^o	1st mode	2 nd mode	3 rd mode
1	19.266	55.449	106.349
2	12.581	36.578	69.039
3	12.522	35.666	69.528

5.2.4 Effects of the length ratio of the thick and the thin sections on the natural frequencies

To see how the ratio of the lengths of thick and thin sections (L_1/L_3) affects the natural frequencies, the data input of the problem described in section 5.2 is used except that here the lengths of the thick section and the thin section are changed while the total length remains unchanged. In the first case the length of the thick section is considered as half of the length of the thin section and in the second case both thick and thin section have equal lengths and as the last case the length of the thick section is considered as

twice the length of the thin section. The values of the lowest three natural frequencies for simply supported, fixed-free and fixed-fixed supports are given in Tables 5.9 to 5.11 respectively. These results show that for simply supported and fixed-free supports, a longer thick section leads to higher natural frequencies whereas for fixed-fixed support a longer thin section leads to higher natural frequencies. This observation is shown graphically in Figure 5.7 for the fundamental frequencies for simply supported, fixed-free and fixed –fixed supports.

Table 5.9 The lowest three natural frequencies ($\times 10^2$ rad/sec) of tapered beam of model C with LC (1) configuration for simply supported boundary condition

L_1/L_3	1st mode	2 nd mode	3 rd mode
1/2	3.433	16.974	44.43
1	3.797	23.701	50.310
2	4.876	27.990	57.245

Table 5.10 The lowest three natural frequencies ($\times 10^2$ rad/sec) of tapered beam of model C with LC (1) configuration for fixed-free boundary condition

L_1/L_3	1st mode	2 nd mode	3 rd mode
1/2	2.828	13.965	28.787
1	4.110	12.465	35.598
2	4.883	14.555	41.994

Table 5.11 The lowest three natural frequencies ($\times 10^2$ rad/sec) of tapered beam of model C with LC (1) configuration for fixed-fixed boundary condition

L_1/L_3	1st mode	2 nd mode	3 rd mode
1/2	14.256	28.798	57.879
1	12.522	35.666	69.528
2	12.290	42.356	79.157

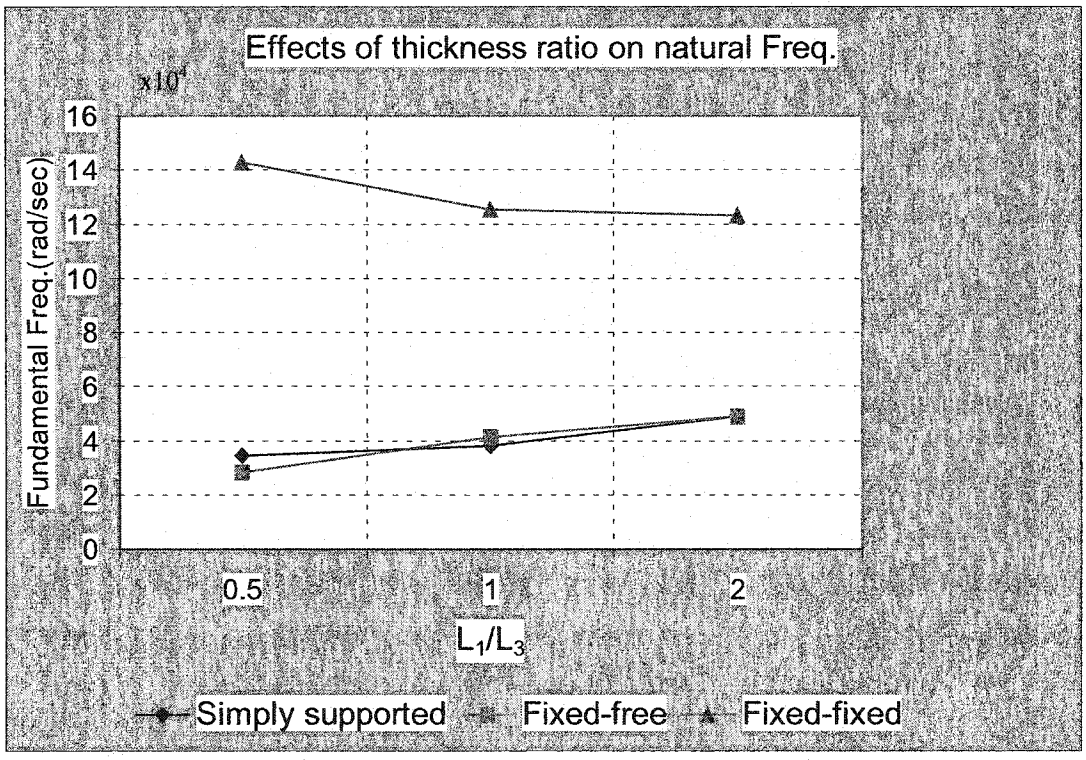

Figure 5.8 Effects of the length ratio on the fundamental frequency

5.2.5 Effects of the thickness ratio of the thick and the thin sections on the natural frequencies

The effects of the ratio of the thickness of the thick and thin sections (h_1/h_3) are investigated by considering the data input for the problem explained in section 5.2. There are 36 layers in the thick section for all cases and further, there are 24 layers in the thin section for the first case, 18 for the second case and 12 for the third case. The laminate configuration for all cases is LC (1). The values of the lowest three natural frequencies for simply supported, fixed-free and fixed-fixed supports are given in Tables 5.9 to 5.11 respectively. One can see that for simply supported and fixed-fixed cases, increasing the thickness ratio does increase the natural frequencies, which is due to corresponding changes in the mass and stiffness (matrices). For fixed-free support, the natural frequencies increase by increasing the thickness ratio from 1.5 to 2 but after that again decrease. This result is due to the location of the restrained degrees of freedom.

Table 5.12 The lowest three natural frequencies ($\times 10^2$ rad/sec) of tapered beam of model C with LC (1) configuration for simply supported boundary condition

h_1/h_3	1st mode	2 nd mode	3 rd mode
1.5	7.363	32.457	69.127
2	5.762	29.127	59.231
3	3.797	23.701	50.310

Table 5.13 The lowest three natural frequencies ($\times 10^2$ rad/sec) of tapered beam of model C with LC (1) configuration for fixed-free boundary condition

h_1/h_3	1st mode	2 nd mode	3 rd mode
1.5	3.930	17.616	50.197
2	4.183	15.052	44.440
3	4.108	12.451	35.391

Table 5.14 The lowest three natural frequencies ($\times 10^2$ rad/sec) of tapered beam of model C with LC (1) configuration for fixed-fixed boundary condition

h_1/h_3	1st mode	2 nd mode	3 rd mode
1.5	17.425	50.417	94.336
2	14.882	44.729	81.277
3	12.529	35.667	69.528

The fundamental frequencies for simply supported, fixed-free and fixed-fixed boundary conditions are plotted in Figure 5.8.

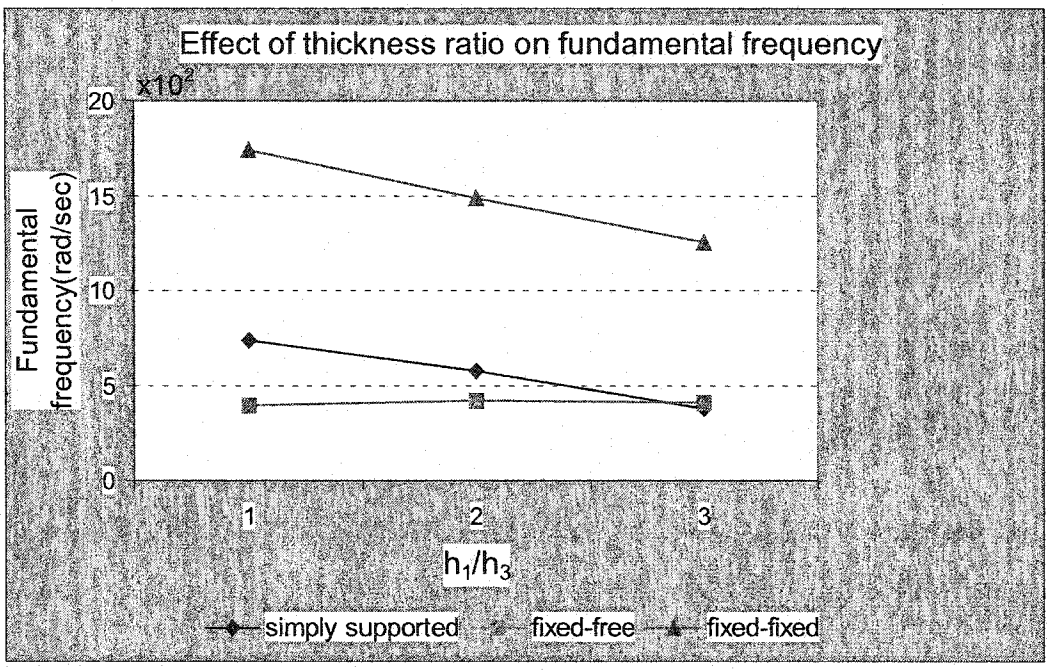

Figure 5.9 The effects of the thickness ratio on the fundamental frequency

5.2.6 Effects of different types of tapered section (A, B, C, and D)

To study the effects of different types of tapered section on the natural frequencies, the problem described in Section 5.2 is considered. The material and the geometric properties are as described in Section 5.2. Here, different types of tapered section (models A, B, C and D) are considered in tapered beam. The lowest three natural frequencies for simply supported, fixed-free and fixed-fixed boundary conditions for all types of tapered section and different laminate configurations are given in Tables 5.15 to 5.17.

Table 5.15 Effects of different types of tapered section on frequencies ($\times 10^2$ rad/sec) for simply supported beam with taper angle of 3 ^{o}

Laminate	Mode no.	Model A	Model B	Model C	Model D
LC (1)	1	3.785	3.810	3.797	3.835
	2	23.567	23.736	23.701	24.369
	3	50.288	50.323	50.310	49.637
LC (2)	1	2.614	2.715	2.609	2.739
	2	16.884	17.463	16.50	17.962
	3	35.205	35.854	35.733	35.417
LC (3)	1	4.619	4.680	4.604	4.849
	2	28.533	28.571	27.940	30.121
	3	56.410	57.306	57.203	56.984

Table 5.15 Effects of different types of tapered section on frequencies ($\times 10^2$ rad/sec) for fixed-free beam with taper angle of 3 °

Laminate	Mode No.	Model A	Model B	Model C	Model D
LC (1)	1	4.092	4.120	4.108	4.215
	2	12.445	12.468	12.451	12.308
	3	35.179	35.440	35.391	36.308
LC (2)	1	2.960	3.029	2.895	3.111
	2	8.671	8.905	8.827	8.811
	3	25.140	26.123	24.610	26.918
LC (3)	1	4.810	4.984	4.723	5.023
	2	14.070	15.045	14.255	14.421
	3	42.735	43.295	41.859	45.526

The first three natural frequencies of fixed-free beam with LC (3) laminate configuration for different types of tapered beams are shown in Figure 5.9. The taper angle for all types of tapered beam is 3 °.

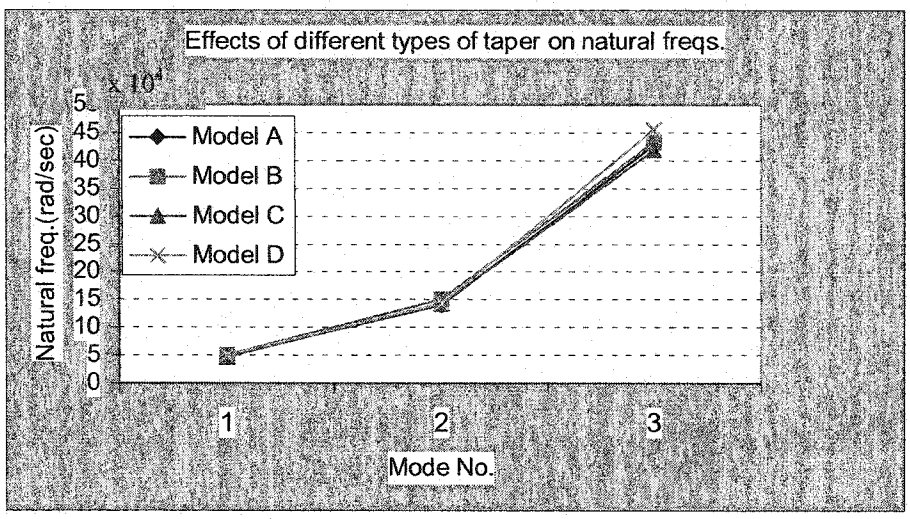

Figure 5.10 The effects of type of tapered section on the natural frequencies of fixed-free boundary conditions and LC (3) laminate configuration

Table 5.17 Effects of different types of tapered section on frequencies ($\times 10^2$ rad/sec) for fixed- fixed beam with taper angle of 3 °

Laminate	Mode No.	Model A	Model B	Model C	Model D
LC (1)	1	12.526	12.541	12.523	12.316
	2	35.452	35.717	35.666	36.678
	3	69.425	69.497	69.528	68.689
LC (2)	1	8.706	8.956	8.905	8.804
	2	25.348	26.330	24.798	27.061
	3	48.737	49.745	49.324	49.215
LC (3)	1	13.972	14.305	14.254	14.204
	2	43.118	43.243	42.191	45.817
	3	78.051	79.286	79.056	78.662

The results obtained for different types of tapered section show that the natural frequencies for tapered beam in which tapered section is made as model D gives the highest values for the natural frequencies. This result was expected from the geometry of the model D. Model D has more uniform layers in the tapered section. For example, in the problem explained in section 5.2, there are 36 plies in the thick section, which are dropped to 12 in the thin section through three equal-length elements. Therefore, in the first and second elements 24 and 12 plies are laid up uniformly (zero taper angle). Whereas in the model B the uniform plies in the first and second elements are 16 and 8 respectively. Recalling equation (4.2) and noting that $\bar{z}_k = \tan(-\phi)x + c$, one can see that increasing ϕ decreases the $\bar{z}_k$ and therefore decreases the value for D_{11}. Therefore, when the drop-off plies lower the value of D_{11} the lower is the stiffness of the tapered beam. Considering this reason, we expect to have lower value for the natural frequencies for model B. Observation of the results given in the Tables 5.11 to 5.13 confirms our expectation. The natural frequencies for models A and C are very close, which means that the resin does not considerably affect the stiffness of the beam and this is the same observation that was obtained from the investigation of the tapered beam in the previous chapters.

5.3 Parametric study on the critical buckling load of tapered composite beams

The parametric study on the critical buckling load is conducted using advanced formulation as we did for the parametric study on natural vibration. The problem described in example 5.2.1 is considered; the material and geometric properties explained in example 5.2.1 are used here to solve the problems for critical buckling load.

5.3.1 Effects of boundary conditions on critical buckling load

The problem described in Section 5.2 is considered to investigate the effects of boundary conditions on the critical buckling load. The thick and thin sections have equal length and laminate configuration is LC (1). All types of tapered section are taken into consideration and the problems are solved for simply supported, fixed-free and fixed-fixed boundary conditions. Table 5.18 gives the critical buckling load for simply supported, fixed-free and fixed-fixed supports. The critical buckling load for fixed-fixed support is the highest whereas the fixed-free support gives the lowest value for the critical buckling load. As expected (from our discussion in Section 5.2.3), the critical buckling loads for model D are the highest followed by models B, C and A.

Table 5.18 Effects of boundary conditions on critical buckling load for tapered beam

Model	Critical buckling load, $\times 10^3$ N		
	Simply supported	Fixed-Free	Fixed-Fixed
A	2.0489	1.180	14.339
B	2.066	1.193	14.350
C	2.055	1.186	14.358
D	2.133	1.246	14.361

5.3.2 Effects of laminate configuration on critical buckling load

The problem described in example 5.2.1 is considered to study the effects of laminate configuration on the critical buckling load. The input data of the example 5.2.1

is used here for the laminates LC (1), LC (2) and LC (3). All types of tapered sections are taken into consideration. Tables 5.19 to 5.21 give the critical buckling loads for simply supported, fixed-free and fixed-fixed supports respectively.

Table 5.19 Effects of laminate configuration on critical buckling load of simply supported beam

Laminate	Critical buckling load $\times 10^3$ N			
	Model A	Model B	Model C	Model D
LC (1)	2.0489	2.066	2.055	2.133
LC (2)	0.917	1.007	0.964	1.000
LC (3)	3.0513	3.077	3.055	3.180

Table 5.20 Effects of laminate configuration on critical buckling load of fixed-free beam

Laminate	Critical buckling load $\times 10^3$ N			
	Model A	Model B	Model C	Model D
LC (1)	1.180	1.193	1.186	1.246
LC (2)	0.559	0.518	0.562	0.590
LC (3)	1.723	1.743	1.727	1.822

Table 5.21 Effects of laminate configuration on critical buckling load of fixed-fixed beam

Laminate	Critical buckling load $\times 10^3$ N			
	Model A	Model B	Model C	Model D
LC (1)	14.339	14.350	14.358	14.361
LC (2)	7.069	7.124	7.081	7.091
LC (3)	19.295	19.306	19.299	19.317

The laminate LC (3) gives the highest value for the critical buckling load and the laminate LC (2) gives the lowest value. In fact, the value of the critical buckling load for the laminate LC (3) is about three times more than the corresponding value for the laminate LC (2) and about 30% more than corresponding value for laminate LC (1). These results were expected from our discussions in Section 5.2.2 where we discussed that the stiffness of the laminated beam is a function of laminate configuration due to the existence of the term D_{11} that is a function of Q_{11} (See equation 4.2). From Equation (4.3), one may see that the value of Q_{11} depends on fiber orientation.

5.3.3 Effects of the taper angle on critical buckling load

To see how the taper angle affects the critical buckling load, the tapered beam explained in Section 5.2.3 is considered except that here the tapered section is considered to be of model D with laminate configuration LC (3). This laminate configuration is selected because it is more common and we saw in the Section 5.3.2 that LC (3) laminate gives the highest value for the critical buckling load. Changing the taper angle is performed in

the same manner as we did in Section 5.2.3. Thicknesses of the thick and thin sections remain the same and therefore changing the taper angle leads to changing the length of the tapered section. The total length of the beam for all angles is kept constant and the change in the length of the tapered section is considered and correspondingly the lengths of the thick and thin sections are adjusted using equal increments.

Table 5.22 Effects of taper angle on critical buckling load for model D with LC (3) configuration

Taper angle, ϕ°	Critical buckling load, $\times 10^{2}$ N		
	Simply supported	Fixed-free	Fixed-fixed
1	3.793	2.185	20.167
2	3.375	1.956	19.422
3	3.180	1.822	19.317

Table 5.22 gives the critical buckling loads for simply supported, fixed-free and fixed-fixed boundary conditions for different taper angles. Table 5.22 shows that increasing the taper angle result in decreasing the critical buckling load for simply supported, fixed-free and fixed-fixed supports. One should note that these results have been obtained for a realistic tapered beam, which consists of a thick section, a thin section and a tapered section. As we discussed in section 5.2.2, increasing taper angle results in decreasing stiffness of the laminated beam and in turn results in decreasing critical buckling load. Figure 5.10 shows the changes in critical buckling loads vs. taper angle.

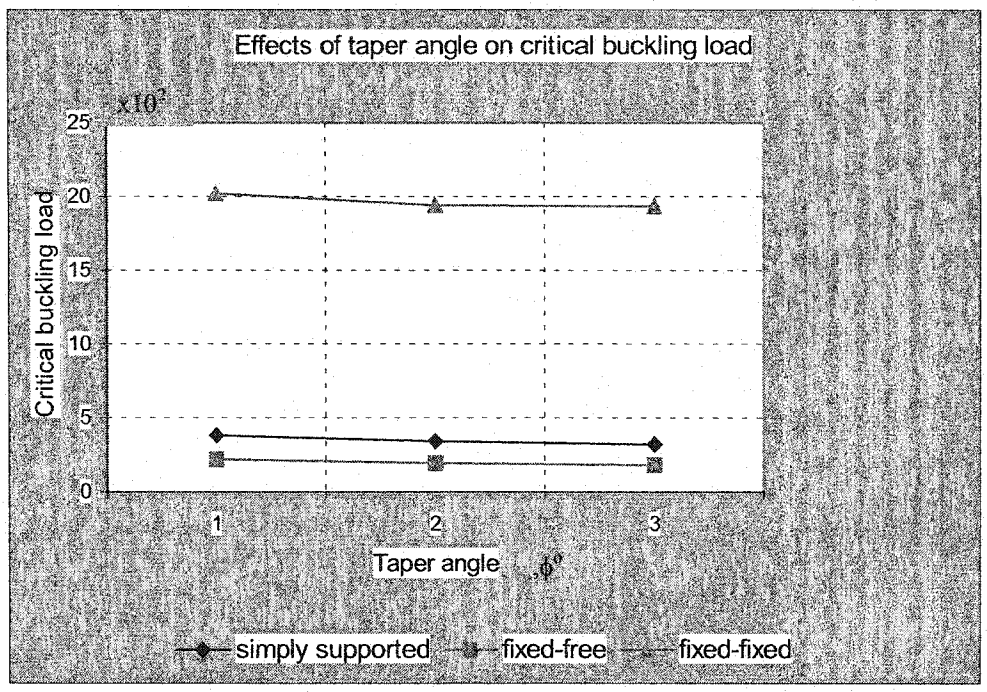

Figure 5.11 Effects of taper angle on the critical buckling load for a tapered beam

5.3.4 Effects of the length ratio of the thick and the thin sections on critical buckling load

The study of the effect of the ratio of the thick and thin section lengths is conducted by considering the problem explained in the previous section except that here the taper angle is 3 ° and the lengths of the thick and thin sections have been changed while keeping the total length of the beam constant. As the first case, the length of the thin section is considered as twice the length of the thick section and for the second case, both the thick and thin sections have equal length. As the last case, the length of thin section is half of the length of the thick section.

Table 5.23 gives the critical buckling load for tapered beam explained above for different length ratio values. One can see that increasing the length of the thick section

results in increasing the critical buckling load. This result is valid for all types of supports under investigation that are simply supported, fixed-free and fixed-fixed boundary conditions. This is due to increasing stiffness of the beams.

Table 5.23 Effects of L_1/L_3 on critical buckling load of model D with LC (3) configuration

L_1/L_3	Critical buckling load, $\times 10^3$ N		
	Simply supported	Fixed-free	Fixed-fixed
1/2	2.249	1.096	16.796
1	3.180	1.822	19.317
2	5.712	3.511	24.628

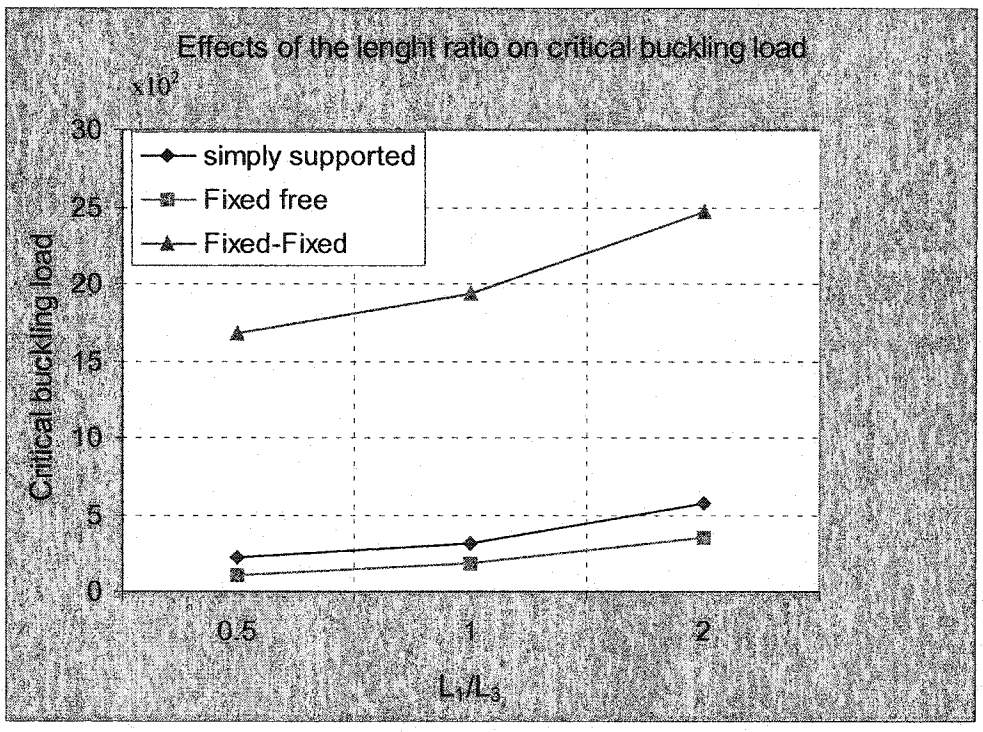

Figure 5.12 Effects of length ratio on the critical buckling load for a tapered beam

5.4 Conclusions and discussions

In this chapter a parametric study on vibration and buckling of tapered composite beams has been conducted. Different types of tapered sections have been considered in tapered beams. The problems have been solved for different boundary conditions, various taper angles and different laminate configurations. The effects of the length ratio of the thick and thin sections as well as thickness ratio of the thick and thin sections have been investigated.

We conclude that tapered beam having model D as tapered section provides the highest natural frequencies and critical buckling loads compared to the other tapered sections. Consequently tapered beams with models B, C and A as tapered section take the second, third and fourth positions. Increasing taper angle decreases the value of natural frequencies and critical buckling loads. One should note that these results are obtained for realistic tapered beam, which consists of a thick section, a thin section and a tapered section. Another feature of importance is that the higher the length of the thick section is the higher are the natural frequency and critical buckling loads.

Chapter 6

Conclusions and future work

In the present thesis the advanced finite element formulation has been developed for buckling and vibration analysis of tapered composite beams. Different configurations of tapered beams, mid-plane tapered as well as internally tapered beams have been investigated. The study on the vibration and buckling response has been conducted using conventional finite element formulation and advanced formulation for uniform-thickness and tapered composite beams.

The constitutive equation of motion of the tapered composite beams has been derived by taking into account the effect of taper angle. Based on the differential equation developed for tapered beams, the conventional and advanced finite element formulations have been improved for mid-plane and internally tapered beams.

The finite element model for the composite beams is considered based on conventional formulation with two degrees of freedom per node, namely deflection and slope. It was shown that the conventional FEM model for beams has some disadvantages: large number of elements are needed to achieve accurate results and the curvature varies linearly along the length of the element, which is not appropriate for tapered beams.

The conventional finite element model has been improved by introducing advanced finite element formulations for Euler-Bernoulli and Timoshenko beam elements. The advanced formulation based on the Euler-Bernoulli beam element considers four degrees of freedom per node, that are, displacement, slope, curvature and gradient of curvature. The advanced formulation based on the Timoshenko beam element considers displacement, rotation, the first derivative of displacement, and the first derivative of rotation per node. Thus, both the elements adequately represent all the physical situations involved in any combinations of displacement, rotation, bending moment and shearing force.

The symbolic computations and numerical results have been obtained using MATLAB ® software. The element properties, that are, stiffness, mass and geometric matrices have been computed numerically using individual sub-routines.

The parametric study is carried out for the tapered composite beams to see the effects of various changes in the laminate parameters on the natural frequencies and critical buckling loads. The effects of the length ratio (the length of the thick section over the length of the thin section), the thickness ratio (the ratio of the thickness of the thick and thin sections), and the taper angle are considered to see the effects of the geometry changes on the natural frequencies and critical buckling load. The effects of the changes in the boundary conditions and the changes in the laminate configurations are also considered in the parametric study. The work done in the present thesis has provided some conclusions on the performance of the advanced finite element formulation, and

manufacturing and design of the tapered composite beams. The most important conclusions on finite element formulation are:

- The accuracy can be obtained more efficiently and rapidly by increasing the number of degrees of freedom in the element rather than increasing the number of elements of the same or fewer degrees of freedom. This result has been achieved from comparisons of the conventional and advanced finite element formulations.
- The advanced formulation uses fewer elements to obtain accurate results which itself leads to less expensive computational processes. This result is very important in vibration analysis especially in the computation of higher frequencies.
- In general, the Euler-Bernoulli beam element needs less number of elements to arrive at an accurate result whereas the Timoshenko beam element uses more elements to give an accurate result. This conclusion is valid for both conventional and advanced finite element formulations.

In terms of manufacturing and design of tapered composite beams, the laminated beam with only a tapered section designed using different tapered configurations is not a practical one. A more realistic tapered beam consist of a thick section, a tapered section and a thin section. Both the cases have been investigated for their vibration and buckling response. The most important conclusions are:

- The tapered beam model D (staircase-dispersed), is the stiffest configuration, hence this model gives the highest natural frequencies and critical buckling loads for all types of boundary conditions, geometries and laminate configurations.
- The tapered beams designed using model A and model C (overlapped-grouped), are very similar in term of stiffness. This result shows that the resin pocket has no significant effect on the stiffness.
- In term of stiffness, the tapered beam model D is the stiffest model and the model A is the least-stiff model. Further models B and C take the second and third ranks.

The study on the vibration and buckling of the tapered laminates can be continued in the future based on the following recommendations:

1. The advanced finite element formulation presented in this thesis can be extended for the analysis of the forced vibration response of different types of laminated beams.
2. The advanced finite element formulation introduced for uniform-thickness Timoshenko beam element can be extended for tapered beams.
3. The effects of damping can be included in the vibration analysis for both Euler-Bernoulli and Timoshenko beam elements.
4. The advanced finite element formulation could be extended for the analysis of tapered laminated composite plates.

References

[1] Laarus, T. T. and Argyris, J., *Finite Element Analysis for Composite Structures,* 1998, Kluwer Academic Publishers, Netherlands.

[2] Reddy, J.N., *Mechanics of Laminated Composite Plates – Theory and Analysis,* 1997, CRC Press, U.S.A.

[3] Abararcar, R. B. and Cunniff, P. F., "The Vibration of Cantilevered Beam of Fiber Reinforced Materials", Journal of Composite Materials, Vol. 6, 1972, pp.504-516.

[4] Noor, Ahmed K., "Free Vibration of Multilayered Composite Plates", AIAA Journal, Vol. 11, 1973, pp. 1038-1039.

[5] Miller, A. K. and Adams, D. F., "An analytic Means of Determing the Flexural and Torsional Resonant Frequencies of Generally Orthotropic Beams", Journal of Sound and Vibration, Vol.41, 1975, pp.433-449.

[6] Chen, A. T. and Yang, T.Y., "Static and Dynamic Formulation of a Symmetrically Laminated beam Finite Element for a Microcomputer", Journal of Composite Materials, Vol.19, 1985, pp.459-475.

[7] Chandrashekhara, K., Krishnamurthy, K. and Roy, S., "Free Vibration of Composite beams including Rotary Inertia and Shear Deformation", Composite Structures, Vol. 14, 1990, pp.269-279.

[8] Hodges, Dewey H., Atilgan, Ali R., Fulton, Mark V. and Rehfield, L.W., "Free Vibration Analysis of Composite Beams", Journal of the American Helicopter Society, Vol. 36 (3), 1991, pp.36-47.

[9] Krishnaswamy, S., Chandrashekhara, K. and Wu, W. Z. B., "Analytical Solutions to Vibration of Generally Layered Composite Beams", Journal of Sound and Vibration, Vol.159 (1), 1992, pp.85-99.

[10] Khedeir, A. A. and Reddy, J. N., "Free Vibration of Cross-ply Laminated Beams with Arbitrary Boundary Conditions", International Journal of Engineering, Vol.32 (12), 1994, pp.1971-1980.

[11] Abramovich, A., "Shear Deformation and Rotary Inertia Effects of Vibrating Composite Beams", Composite Structures, Vol. 20, 1992, PP.165-173. Science, Vol. 32 (12), 1994, pp. 1971-1980.

[12] Abramovich, H. and Livshits, A., "Free Vibration of Non-Symmetric Cross-Ply Laminated Composite Beams", Journal of Sound and Vibration, Vol.176 (5), 1994, pp.596-612.

[13] Hjela, P. and Teboub, Y., "Free Vibration of Generally Layered Composite Beams using Symbolic Computations", Composite Structures, Vol. 33 (3), 1995. pp.123-134.

[14] Eisenberger, M., Abramovich, H., and Shulepov, O., "Dynamic Stiffness Analysis of Laminated Beams using a First Order Shear Deformation Theory", Composite Structures, Vol.31, 1995, pp. 265-271.

[15] Marur, S. R. and Kant, T., "Free Vibration Analysis of Fiber Reinforced Composite Beams using Higher Order Theories and Finite Element Modeling", Journal of Sound and Vibration, Vol.194 (3), 1996, pp. 337-351.

[16] Teoh, L. S. and Huang, C. C., "Vibration of Beams of Fiber Reinforced Material", Journal of Sound and Vibration, Vol.51 (22), 1997, pp. 467-473.

[17] Song, S. J. and Waas, A. M., "Effects of Shear Deformation on Buckling and Free Vibration of Laminated Composite Beams", Composite Structures, Vol. 37(1), 1997, pp. 33-43.

[18] Banerjee, J. R., "Free Vibration of Axially Loaded Composite Timoshenko Beams using the Dynamic Stiffness Matrix Method", Composite Structures, Vol. 69(2), 1998, pp. 197-208.

[19] Shi, G. and Lam, K. Y., "Finite Element Vibration Analysis of Composite Beams based on Higher-Order Beam Theories", Journal Sound and Vibration, Vol. 219 (4), 1999, pp. 707-721.

[20] Ganapathi, M. and Patel, B. P., and Touratier, M., "Influence of Amplitude of Vibration on Loss Factors of Laminated Composite Beams and Plates", Journal of Sound and Vibration, Vol.219 (4), 1999, pp. 730-738.

[21] Bertholet, J.M., *Composite Materials – Mechanical Behavior and Structural Analysis,* 1999, Springer Verlag, New York.

[22] Whitney, J.M., *Structural Analysis of Laminated Anisotropic Plates,* 1987, Technomic Publishing Company, Lancaster, Pa.

[23] Jones, R. M., *Mechanics of Composite Materials,* 1975, Scripta Book Co., Washington.

[24] Matsunaga, H., "Vibration and Buckling of Multilayered Composite Beams According to Higher Order Deformation Theories", Journal of Sound and Vibration, Vol. 246 (1), 2001, pp. 47-62.

[25] Rao, M. K., Desai, Y. M. and Chitins, M. R., "Free Vibration of Laminated Beams Using Mixed Theory", Composite Structures, Vol. 52(2), 2001, pp.149-160.

[26] Rao, Ramalingeswara, S., and Ganesan, N., "Dynamic Response of Non-Uniform Composite Beams", Journal of Sound and Vibration, Vol.200 (5), 1997, pp.563-577.

[27] Farghaly, S. H. and Gadelrab, R. M., "Free Vibration of a Stepped Composite Timoshenko Cantilevered Beam", Journal of Sound and Vibration, Vol. 187 (5), 1995, pp. 886-896.

[28] Tong, X., Tabarrok, B. and Yeh, K. Y., "Vibration Analysis of Timoshenko Beams with Non-homogeneity and Varying Cross-section", Journal of Sound and Vibration, Vol. 186 (5), 1995, pp.821-835.

[29] Polyzois, D. Raftoyiannis, I. G. and Ibrahim, S., "Finite Elements Method for the Dynamic Analysis of Tapered Composite Poles", Composite Structures, Vol. 43 (1), 1998, pp.25-34.

[30] He, K. Hoa, S. V. and Ganesan, R., "The Study of Tapered Laminated Composite Structures: a review", Composites Science and Technology, Vol. 60(14), 2000, pp.2643-2657.

[31] Abd EL-Maksoud, Mohamed A, "Dynamic Analysis and Buckling of Variable-Thickness Laminated Composite Beams using Conventional and Advanced Finite Element Formulations", M.A.Sc. Thesis, 2000, Concordia University.

[32] Nigam, Amit, "Dynamic Analysis of Composite Beams using Hierarchical Finite Element Method", M.A.Sc. Thesis, 2002, Concordia University.

[33] Khdeir, A. A. and Reddy, J.N., "Buckling and Vibration of Laminated Composite Plates using Various Plate Theories", AIAA Journal, Vol.27 (12), 1989, pp.1808-1817.

[34] Banerjee, J. R. and Williams, F. W., "The Effect of Shear Deformation on The Critical Buckling of Columns", Journal of Sound and Vibration, Vol.174 (5),1994, pp. 607-616.

[35] Khdeir, A. A. and Reddy, J.N., "Buckling of Cross-ply Laminated Beams with Arbitrary Boundary Conditions", Composite Structures, Vol. 37(1), 1997, pp. 1-3.

[36] Chen, L. W. and Peng, W. K., "The Stability Behavior of Rotating Composite Shafts under Axial Compressive Loads", Composite Structures, Vol. 41(3), 1998, pp. 253-263.

[37] Kim, C. G. Kyoung, W.M. and Hong, C. -S., "Buckling and Post Buckling Behavior of Composite Cross-ply Laminates with Multiple Delaminations", Composite Structures, Vol. 43(4), 1998, pp. 257-274.

[38] Matsunaga, H., "Vibration and Buckling of Deep Beams-Columns on Two-Parameter Elastic Foundations", Journal of Sound and Vibration, Vol. 228 (2), 1999, pp. 359-376.

[39] Lee, J. Kim, S. E. and Hong, K. "Lateral Buckling of I-section Composite Beams, Engineering Structures, Vol. 24 (7), 2002, pp.955-964.

[40] Cortinez, V. H. and Piovan, M. T., "Vibration and Buckling of Composite Thin-walled Beams with Shear Deformability", Journal of Sound and Vibration, Vol. 258 (4), 2002, pp. 701-723.

[41] Lee, J. and Kim, S. E., "Lateral Buckling Analysis of Thin-walled Laminated Channel-section Beams", Composite Structures, Vol.56 (4), 2002, pp.391-399.

[42] Zienkiewicz, O. C., *The Finite Element Method*, 1979, McGraw-Hill, New York.

[43] Cook, R.D., Malkus, D. S. and Plesha, M. E., *Concepts and Applications of FiniteElement Analysis,* 1989, Wiley Publishing Company, New York.

[44] Reddy, J.N., *An Introduction to the Finite Element Method,* 1993, McGraw-Hill, New York.

[45] Thomas, J. L. and Dokumaci, E., "Improved Finite Element for Vibration Analysis of Tapered Beams", Aeronautical Quarterly, Vol. 24, 1973, pp.39-46.

[46] Thomas, J. and Abbas, A. H., "Finite Element Model for Dynamic Analysis of Timoshenko Beam", Journal of Sound and Vibration, Vol. 41 (3), 1975, pp. 291-299.

[47] Dawe, D. J., "A Finite Element for the Vibration Analysis of Timoshenko Beams", Journal of Sound and Vibration, Vol.60 (1), 1978, pp.11-20.

[48] Nickel, R. and Secor, G., "Convergence of Consistently Derived Timoshenko Beam Finite Elements", International Journal of Numerical Methods in Engineering, Vol.5, 1972, pp. 243-253.

[49] Kapur, K., "Vibration of Timoshenko Beam using a Finite Element Approach", Journal of the Acoustical Society of America, Vol.40, 1966, pp.1058-1063.

[50] To, C. W. S., "Higher Order Tapered Beam Finite Element for Vibration Analysis", Journal of Sound and Vibration, Vol. 63 (1), 1979, pp. 33-50.

[51] Houmat, A., "Vibrations of Timoshenko Beams by Variable Order Finite Elements", Journal of Sound and Vibration, Vol. 187(5), 1995, pp. 841-849.

[52] Shi, G., and Lam, K. Y. and Tay, T. E., "On Efficient Finite Element Modeling of Composite Beams and Plates Using Higher Order Theories and an Accurate Composite Beam Element", Composite Structures, Vol. 41(2), 1998, pp.159-165.

[53] Gupta, R. S. and Rao, S.S., "Finite Element Vibration Analysis of Rotating Timoshenko Beams", Journal of Sound and Vibration, Vol. 242 (1), 2001, pp. 103-124.

[54] Ramtekkar, G. S., Desai, Y. M., and Shah, A. H., "Natural Vibration of Laminated Composite Beams by using Mixed Finite Element Modeling", Journal of Sound and Vibration, Vol. 257(4), 2002,pp. 635-651.

[55] Gupta, R. S. and Rao, S.S., "Finite Element Eigenvalue Analysis of Tapered and Twisted Timoshenko Beams", Journal of Sound and Vibration, Vol.56 (2),1978,pp.187-200.

[56] Cleghorn, W. L. and Tabarrok, B., "Finite Element Formulation of a Tapered Timoshenko Beam for Free Vibration Analysis", Journal of Sound and Vibration, Vol.152 (3), 1997, pp.461-470.

[57] Rao, Ramalingeswara, S. and Ganesan, N., "Dynamic Response of Tapered Composite Beams Using Higher Order Shear Deformation Theory", Journal of Sound and Vibration, Vol.187 (5), 1995, pp. 737-756.

[58] Kim, D. H., *Composite Structures for Civil and Architectural Engineering,* 1995, E & FN Spon, U.S.A.

[59] Raman, Prabhu Madabhusi and Davalos, Julio F., "Static Shear Correction Factor for Laminated Rectangular Beams", Composites: Part B, 27B, 1996, pp. 285-293.

[60] Chen, H., "Failure Analysis of Laminated Composite Beams". M.A.Sc. Thesis, 2001, Concordia University.

[61] Shames, I. H. and Dym, C. L., *Energy and Finite Element Methods in Structural Mechanics*, 1985, McGraw-Hill, New York.

[62] Ochoa, O. O. and Reddy, J. N., *Finite Element Analysis of Composite Laminates,* 1992, Kluwer Academic Publishers, Boston.

[63] Petyt, Maurice, *Introduction to Finite Element Vibration Analysis,* 1990, Cambridge University Press, New York.

[64] Cheung, Y. K. and Leung, A. Y. T., *Finite Element Methods in Dynamics,* 1991, Kluwer Academic Publishers, New York.

[65] Abrate, Serge, *Impact on Composite Structures,* 1998, Cambridge, Cambridge University Press, New York.

[66] Matthews, F. L., Davies, G. A. O., Hitchings, D. and Soutis, C., *Finite Element Modeling of Composite Materials and Structures,* 2000, CRC Press, Boca Raton, FL.

[67] Atkinson, Kendall E. *An Introduction to Numerical Analysis*, 1978, John Wiley & Sons, New York.

Appendix-A

The coefficients of stiffness and mass matrices of tapered composite beams using advanced finite element formulation

1.1 Coefficients of the stiffness matrix for tapered composite beams using advanced finite element formulations

$$K_{11}^{e}=\sum_{k=1}^{n}\frac{70}{429l^{3}}\left(\overline{Q}_{11}\right)_{k}t_{k}\left(156c^{2}+156cml+48m^{2}l^{2}+13t_{k}^{\prime 2}\right)$$

$$K_{12}^{e}=\sum_{k=1}^{n}\frac{5}{429l^{2}}\left(\overline{Q}_{11}\right)_{k}t_{k}\left(1092c^{2}+936cml+258m^{2}l^{2}+91t_{k}^{\prime 2}\right)$$

$$K_{13}^{e}=\sum_{k=1}^{n}-\frac{1}{3432\Delta_{1}}\left(\overline{Q}_{11}\right)_{k}t_{k}\left(156c^{2}+208cml+68m^{2}l^{2}+13t_{k}^{\prime 2}\right)$$

$$K_{14}^{e}=\sum_{k=1}^{n}\frac{1}{1287l\Delta_{1}}\left(\overline{Q}_{11}\right)_{k}t_{k}\left(1560c^{2}+1677cml+501m^{2}l^{2}+130t_{k}^{\prime 2}\right)$$

$$K_{15}^{e}=-K_{11}^{e}$$

$$K_{16}^{e}=\sum_{k=1}^{n}\frac{5}{429l^{2}}\left(\overline{Q}_{11}\right)_{k}t_{k}\left(1092c^{2}+1248cml+414m^{2}l^{2}+91t_{k}^{\prime 2}\right)$$

$$K_{17}^{e}=\sum_{k=1}^{n}-\frac{1}{3432\Delta_{2}}\left(\overline{Q}_{11}\right)_{k}t_{k}\left(156c^{2}+104cml+16m^{2}l^{2}+13t_{k}^{\prime 2}\right)$$

$$K_{18}^{e}=\sum-\frac{1}{1287l\Delta_{2}}\left(\overline{Q}_{11}\right)_{k}t_{k}\left(1560c^{2}+144cml+384m^{2}l^{2}+130t_{k}^{\prime 2}\right)$$

$$K_{22}^{e}=\sum_{k=1}^{n}\frac{10}{1001l}\left(\overline{Q}_{11}\right)_{k}t_{k}\left(780c^{2}+598cml+144m^{2}l^{2}+65t_{k}^{\prime 2}\right)$$

$$K_{23}^{e}=\sum_{k=1}^{n}-\frac{1}{9009l\Delta_{1}}\left(\overline{Q}_{11}\right)_{k}t_{k}\left(312c^{2}+351cml+99m^{2}l^{2}+26t_{k}^{\prime 2}\right)$$

$$K_{24}^{e}=\sum_{k=1}^{n}\frac{1}{72072\Delta_{1}}\left(\overline{Q}_{11}\right)_{k}t_{k}\left(59124c^{2}+56160cml+14652m^{2}l^{2}+24927t_{k}^{\prime 2}\right)$$

$$K_{25}^{e} = -K_{12}^{e}$$

$$K_{26}^{e} = \sum_{k=1}^{n} \frac{5}{3003l} \left(\overline{Q}_{11}\right)_k t_k \left(2964c^2 + 2964cml + 942m^2l^2 + 247t_k'^2\right)$$

$$K_{27}^{e} = \sum_{k=1}^{n} -\frac{1l}{72072\Delta_2} \left(\overline{Q}_{11}\right)_k t_k \left(780c^2 - 144m^2l^2 + 65t_k'^2\right)$$

$$K_{28}^{e} = \sum_{k=1}^{n} -\frac{1}{72072\Delta_2} \left(\overline{Q}_{11}\right)_k t_k \left(28236c^2 + 18720cml + 3888m^2l^2 + 2353t_k'^2\right)$$

$$K_{33}^{e} = \sum_{k=1}^{n} \frac{1}{270270\Delta_1^2} l^3 \left(\overline{Q}_{11}\right)_k t_k \left(156c^2 + 3900cml + 993m^2l^2 + 455t_k'^2\right)$$

$$K_{34}^{e} = \sum_{k=1}^{n} -\frac{1}{540540\Delta_1^2} l^2 \left(\overline{Q}_{11}\right)_k t_k \left(5460c^2 + 3900cml + 993m^2l^2 + 455t_k'^2\right)$$

$$K_{35}^{e} = \sum_{k=1}^{n} \frac{1}{3432\Delta_1} \left(\overline{Q}_{11}\right)_k t_k \left(156c^2 + 208cml + 68m^2l^2 + 13t_k'^2\right)$$

$$K_{36}^{e} = \sum_{k=1}^{n} -\frac{1}{72072\Delta_1} l \left(\overline{Q}_{11}\right)_k t_k \left(780c^2 + 1560cml + 636m^2l^2 + 65t_k'^2\right)$$

$$K_{37}^{e} = \sum_{k=1}^{n} -\frac{1}{720720\Delta_1\Delta_2} l^3 \left(\overline{Q}_{11}\right)_k t_k \left(156c^2 + 156cml + 50m^2l^2 + 13t_k'^2\right)$$

$$K_{38}^{e} = \sum_{k=1}^{n} -\frac{1}{2162160\Delta_1\Delta_2} l^2 \left(\overline{Q}_{11}\right)_k t_k \left(3900c^2 + 3120cml + 942m^2l^2 + 325t_k'^2\right)$$

$$K_{44}^{e} = \sum_{k=1}^{n} \frac{1}{180180\Delta_1^2} l \left(\overline{Q}_{11}\right)_k t_k \left(3900c^2 + 2340cml + 574m^2l^2 + 325t_k'^2\right)$$

$$K_{45}^{e} = \sum_{k=1}^{n} -\frac{1}{1287l\Delta_1} \left(\overline{Q}_{11}\right)_k t_k \left(1560c^2 + 1677cml + 501m^2l^2 + 130t_k'^2\right)$$

$$K_{46}^{e} = \sum_{k=1}^{n} \frac{1}{72072\Delta_1} \left(\overline{Q}_{11}\right)_k t_k \left(28236c^2 + 37752cml + 13404m^2l^2 + 2353t_k'^2\right)$$

$$K_{47}^{e} = \sum_{k=1}^{n} \frac{1}{2162160\Delta_1\Delta_2} l^2 \left(\overline{Q}_{11}\right)_k t_k \left(3900c^2 + 4680cml + 1722m^2l^2 + 325t_k'^2\right)$$

$$K_{48}^{e} = \sum_{k=1}^{n} -\frac{1}{72072\Delta_1\Delta_2} l \left(\overline{Q}_{11}\right)_k t_k \left(156c^2 + 156cml - 44m^2l^2 + 13t_k'^2\right)$$

$$K_{55}^{e} = K_{11}^{e}$$

$$K_{56}^e = K_{16}^e$$

$$K_{57}^e = -K_{17}^e$$

$$K_{58}^e = -K_{18}^e$$

$$K_{66}^e = \sum_{k=1}^{n} \frac{10}{1001l}\left(\overline{Q}_{11}\right)_k t_k \left(780c^2 + 962cml + 326m^2l^2 + 65t_k'^2\right)$$

$$K_{67}^e = \sum_{k=1}^{n} -\frac{1}{9009\Delta_2} l\left(\overline{Q}_{11}\right)_k t_k \left(312c^2 + 273cml + 60m^2l^2 + 26t_k'^2\right)$$

$$K_{68}^e = \sum_{k=1}^{n} -\frac{1}{72072\Delta_2}\left(\overline{Q}_{11}\right)_k t_k \left(59124c^2 + 62088cml + 17616m^2l^2 + 4927t_k'^2\right)$$

$$K_{77}^e = \sum_{k=1}^{n} \frac{1}{270270\Delta_2^2} l^3\left(\overline{Q}_{11}\right)_k t_k \left(156c^2 + 195cml + 69m^2l^2 + 13t_k'^2\right)$$

$$K_{78}^e = \sum_{k=1}^{n} \frac{1}{540540\Delta_2^2} l^2\left(\overline{Q}_{11}\right)_k t_k \left(5460c^2 + 7020cml + 2553m^2l^2 + 455t_k'^2\right)$$

$$K_{88}^e = \sum_{k=1}^{n} \frac{1}{18018\Delta_2^2} l\left(\overline{Q}_{11}\right)_k t_k \left(3900c^2 + 5460cml + 2134m^2l^2 + 325t_k'^2\right)$$

1.2 Coefficients of the mass matrix for tapered composite beams using advanced finite element formulations

$$M_{11}^e = \frac{1}{2574}\rho bl\left(235ml + 1042g\right)$$

$$M_{12}^e = \frac{1}{1600}\rho bl^2\left(139ml + 453g\right)$$

$$M_{13}^e = \frac{1}{1081080\Delta_1}\rho bl^4\left(143ml + 383g\right)$$

$$M_{14}^e = \frac{1}{72072\Delta_1}\rho bl^3\left(191ml + 548g\right)$$

$$M_{15}^e = \frac{245}{5148}\rho bl\left(ml + 2g\right)$$

$$M_{16}^e = -\frac{1}{36036}\rho bl^2\left(547ml + 1143g\right)$$

$$M_{17}^{e}=\frac{1}{2162160\Delta_2}\rho bl^4(235ml+321g)$$

$$M_{18}^{e}=\frac{1}{144144\Delta_2}\rho bl^3(287ml+620g)$$

$$M_{22}^{e}=\frac{1}{6006}\rho bl^3(39ml+110g)$$

$$M_{23}^{e}=\frac{1}{720720\Delta_1}\rho bl^5(29ml+72g)$$

$$M_{24}^{e}=\frac{1}{120120\Delta_1}\rho bl^4(94ml+245g)$$

$$M_{25}^{e}=\frac{1}{36036}\rho bl^2(596ml+1143g)$$

$$M_{26}^{e}=-\frac{373}{720720}\rho bl^3(ml+2g)$$

$$M_{27}^{e}=\frac{1}{720720\Delta_2}\rho bl^5(26ml+55g)$$

$$M_{28}^{e}=\frac{1}{720720\Delta_2}\rho bl^4(482ml+995g)$$

$$M_{33}^{e}=\frac{1}{259459\Delta_1^2}\rho bl^4(7ml+16g)$$

$$M_{34}^{e}=-\frac{1}{2162160\Delta_1^2}\rho bl^4(11ml+26g)$$

$$M_{35}^{e}=\frac{1}{2162160\Delta_1}\rho bl^4(286ml+521g)$$

$$M_{36}^{e}=\frac{1}{720720\Delta_1}\rho bl^5(29ml+35g)$$

$$M_{37}^{e}=\frac{1}{3706560\Delta_1}\rho bl^7(ml+2g)$$

$$M_{38}^{e}=-\frac{1}{4324320\Delta_1}\rho bl^6(22ml+43g)$$

$$M_{44}^{e}=\frac{1}{360360\Delta_1^2}\rho bl^5(35ml+86g)$$

$$M_{45}^{e}=\frac{1}{144144\Delta_1}\rho bl^3(333ml+620g)$$

$$M_{46}^{e}=-\frac{1}{720720\Delta_1}\rho bl^4(513ml+995g)$$

$$M_{47}^{e}=\frac{1}{4324320\Delta_2\Delta_1}\rho bl^{6}(21ml+43g)$$

$$M_{48}^{e}=\frac{131}{1441440\Delta_2\Delta_1}\rho bl^{5}(ml+2g)$$

$$M_{55}^{e}=\frac{1}{2574}\rho bl(807ml+1042g)$$

$$M_{56}^{e}=-\frac{1}{6006}\rho bl^{2}(314ml+453g)$$

$$M_{57}^{e}=\frac{1}{1081080\Delta_2}\rho bl^{4}(240ml+383g)$$

$$M_{58}^{e}=\frac{1}{72072\Delta_2}\rho bl^{3}(357ml+548g)$$

$$M_{66}^{e}=\frac{1}{6006}\rho bl^{3}(71ml+110g)$$

$$M_{67}^{e}=\frac{1}{720720\Delta_2}\rho bl^{5}(43ml+72g)$$

$$M_{68}^{e}=-\frac{1}{12020\Delta_2}\rho bl^{4}(151ml+245g)$$

$$M_{77}^{e}=\frac{1}{25945920\Delta_2^2}\rho bl^{7}(9ml+16g)$$

$$M_{78}^{e}=\frac{1}{2162160\Delta_2^2}\rho bl^{6}(15ml+26g)$$

$$M_{88}^{e}=\frac{1}{360360\Delta_2^2}\rho bl^{5}(51ml+86g)$$

Appendix-B

MATLAB ® programs

elindex

```
%This function makes an index for assembling
%stiffness and mass matrices
%nnel = number of nodes per element
%ndof = number of degree of freedom per element
%iel = element counter

function [index]=elindex(iel,nnel,ndof)
edof=nnel*ndof;
start=(iel-1)*(nnel-1)*ndof;
for i=1:edof
  index(i)=start+i;
end
```

---

elasmbl

```
% This function assembles the elements matrices
% kk = assembled stiffness matrix
% mm = assembled mass matrix
% k = element stiffness matrix
% m = element mass matrix
% index = refer to index for assembly which calculate
% in "elindex" function

function [kk,mm]=elasmbl(kk,mm,m,k,index)
edof=length(index);
for i=1:edof
  ii=index(i);
  for j=1:edof
    jj=index(j);
    kk(ii,jj)=kk(ii,jj)+k(i,j);
    mm(ii,jj)=mm(ii,jj)+m(i,j);
  end
end
```

---

symbc

```
% This function applies boundary conditions
```

```
% kk(i,j) for degree of freedom which are constrained is set as zero
% m(i,j) for degree of freedom which are constrained is set as zero
% bcdof refer to a vector contains the constrained DOF

function [kk,mm]=symbc(kk,mm,bcdof)
t=length(bcdof);
sdof=size(kk);
for i=1:t
  c=bcdof(i);
  for j=1:sdof
    kk(c,j)=0;
    kk(j,c)=0;
    mm(c,j)=0;
    mm(j,c)=0;
  end
  mm(c,c)=1;
end
```

Qmat

This function computes [Q] matrix for a laminate.

```
function [Q]=Qmat(E1,E2,G12,r12,r21)
Q(1,1)=E1/(1-r12*r21);
Q(1,2)=r12*E2/(1-r12*r21);
Q(2,1)=Q(1,2);
Q(2,2)=E2/(1-r12*r21);
Q(3,3)=G12;
Q=[ Q(1,1) Q(1,2)   0;
    Q(2,1) Q(2,2)   0;
    0      0        Q(3,3)];
```

---

abdmat

This function computes A, B and D matrices for a laminate.

```
function [A,d,D]=abdmat(teta,Q,h)
[num1,num]=size(teta);
zh=zeros(1,num+1);
for i=1:num+1
    zh(1,i)=-h/2+(i-1)*(h/num);
end


%Transformation of layer material matrix to xyz coordinate
% and get A, B and D Matrices
```

```
A=zeros(3,3);
B=zeros(3,3);
D=zeros(3,3);
for nlay=1:num
    Qbar=zeros(3,3);
    m=cos(teta(nlay));
    n=cos(pi/2-teta(nlay));
    Qbar(1,1)=Q(1,1)*m^4+2*(Q(1,2)+2*Q(3,3))*n^2*m^2+Q(2,2)*n^4;
    Qbar(1,2)=(Q(1,1)+Q(2,2)-4*Q(3,3))*n^2*m^2+Q(1,2)*(n^4+m^4);
    Qbar(2,1)=Qbar(1,2);
    Qbar(1,3)=(Q(1,1)-Q(1,2)-2*Q(3,3))*n*m^3+(Q(1,2)-
Q(2,2)+2*Q(3,3))*n^3*m;
    Qbar(3,1)=Qbar(1,3);
    Qbar(2,2)=Q(1,1)*n^4+2*(Q(1,2)+2*Q(3,3))*n^2*m^2+Q(2,2)*m^4;
    Qbar(2,3)=(Q(1,1)-Q(1,2)-2*Q(3,3))*n^3*m+(Q(1,2)-
Q(2,2)+2*Q(3,3))*n*m^3;
    Qbar(3,2)=Qbar(2,3);
    Qbar(3,3)=(Q(1,1)+Q(2,2)-2*Q(1,2)-
2*Q(3,3))*n^2*m^2+Q(3,3)*(n^4+m^4);

    for i=1:3
        for j=1:3
            A(i,j)=A(i,j)+Qbar(i,j)*(h/num);
%Axial Stiffness  Matrix
            B(i,j)=B(i,j)+0.5*Qbar(i,j)*(zh(nlay+1)^2-zh(nlay)^2);
%Axial-Bending Stiffness  Matrix
            D(i,j)=D(i,j)+1/3*Qbar(i,j)*(zh(nlay+1)^3-zh(nlay)^3);
%Bending Stiffness Matrix
        end
    end
end
```

---

kmmat_b2

This function gives the stiffness and mass matrices for a uniform laminated beam based on Euler-Bernoulli beam theory.

```
%el = Young modulus
%I = Moment of inertia
%l = length of each individual element
%Area = cross section area of each element
%ro = density of the material
%k refer to stiffness matrix
%m refer to mass matrix

function [k,m]=kmmat_b2(d,b,l,area,ro)
k=d*b/(l^3)*[12 6*l -12 6*l;
        6*l 4*l^2 -6*l 2*l^2;
        -12 -6*l 12 -6*l;
        6*l 2*l^2 -6*l 4*l^2];

m=(ro*area*l/420)*[156 22*l 54 -13*l;
   22*l 4*l^2 13*l -3*l^2;
   54 13*l 156 -22*l;
   -13*l -3*l^2 -22*l 4*l^2];
```

kmidA

This function creates stiffness matrix for tapered beam model A based on Euler-Bernoulli beam theory using conventional FEM

```
function
[k]=kmidA(E1,E2,NU12,NU21,G12,WID,TP,teta1,angle,AL,QXXi,npt,npm,npta,n
n,p);

n=tan(angle);
k=0;
Q11=E1/(1-(NU12*NU21));
Q33=G12;
Q12=Q11*NU21;
Q21=(NU12*E2)/(1-(NU12*NU21));
Q22=E2/(1-(NU12*NU21));
Q=[Q11,Q12,0;Q21,Q22,0;0,0,Q33];
TP1=TP/cos(angle);
for i=1:npta
   c=TP*(npt+0.5-i);
   teta=teta1(1,i);
   M=cos(teta);
   N=sin(teta);
   QXX=M^4*Q11+N^4*Q22+(2*M^2*N^2*Q12)+(4*M^2*N^2*Q33);
   QYY=(N^4*Q11)+(M^4*Q22)+(2*M^2*N^2*Q12)+(4*M^2*N^2*Q33);
   QXY=(M^2*N^2*Q11)+(M^2*N^2*Q22)+((M^4+N^4)*Q12)-(4*M^2*N^2*Q33);
   QXS=(M^3*N*Q11)-(M*N^3*Q22)+(((M*N^3)-(M^3*N))*Q12)+(2*((M*N^3)-
(M^3*N))*Q33);
   QYS=(M*N^3*Q11)-(M^3*N*Q22)+(((M^3*N)-(M*N^3))*Q12)+(2*((M^3*N)-
(M*N^3))*Q33);
   QSS=(M^2*N^2*Q11)+(M^2*N^2*Q22)-(2*M^2*N^2*Q12)+(((M^2-N^2)^2)*Q33);
   QT=[QXX,QXY,2*QXS;QXY,QYY,2*QXS;QXS,QYS,2*QSS];
   %
   %PLY PARAMETER
   %
   A=(24*n^2*AL^2+60*c*AL*n+60*c^2+5*TP1^2)/(AL^3);
   B=(14*n^2*AL^2+40*c*AL*n+60*c^2+5*TP1^2)/(AL^2);
   C=(34*n^2*AL^2+80*c*AL*n+60*c^2+5*TP1^2)/(AL^2);
   D=(8*n^2*AL^2+30*c*AL*n+60*c^2+5*TP1^2)/(15*AL);
   E=(26*n^2*AL^2+60*c*AL*n+60*c^2+5*TP1^2)/(30*AL);
   F=(38*n^2*AL^2+90*c*AL*n+60*c^2+5*TP1^2)/(15*AL);
   H=WID*QXX*TP*cos(angle)^3;
   % Tapered plies
   ks=H*[0.2*A,0.1*B,-0.2*A,0.1*C;
      0.1*B,D,-0.1*B,E;
      -0.2*A,-0.1*B,0.2*A,-0.1*C;
      0.1*C,E,-0.1*C,F];
   k=ks+k;
end
% Resin plies with equal length
for i=npta+1:npt-nn
   c=c-TP;
```

```
   A=(24*n^2*AL^2+60*c*AL*n+60*c^2+5*TP1^2)/(AL^3);
   B=(14*n^2*AL^2+40*c*AL*n+60*c^2+5*TP1^2)/(AL^2);
   C=(34*n^2*AL^2+80*c*AL*n+60*c^2+5*TP1^2)/(AL^2);
   D=(8*n^2*AL^2+30*c*AL*n+60*c^2+5*TP1^2)/(15*AL);
   E=(26*n^2*AL^2+60*c*AL*n+60*c^2+5*TP1^2)/(30*AL);
   F=(38*n^2*AL^2+90*c*AL*n+60*c^2+5*TP1^2)/(15*AL);
   H=WID*QXXi*TP*cos(angle)^3;
   ks=H*[0.2*A,0.1*B,-0.2*A,0.1*C;

      0.1*B,D,-0.1*B,E;
      -0.2*A,-0.1*B,0.2*A,-0.1*C;
      0.1*C,E,-0.1*C,F];
   k=ks+k;

end
% Resin plies with deducing length
L1(1)=0;
for i=1:nn
   j=i+1;
   L1(j)=-i*TP/n;
end
   for j=1:nn
      c=c-TP;
      a=0;
      jj=nn-j+1;
      b=L1(jj);
      tp=TP;
      alfa=angle;
      q=QXXi;
      l=AL;
      m=n;
      [ks]=kmidf(tp,q,l,m,c,a,b);

      k=ks+k;
      k=cos(angle)*k;
end



k=k-(p/10)*[12/AL 1 -12/AL 1;
   1 4*AL/3 -1 -AL/3;
   -12/AL -1 12/AL -1;
   1 -AL/3 -1 4*AL/3];
```

---

kmidB1

This function creates stiffness matrix for tapered beam model B based on Euler-Bernoulli beam theory using conventional FEM

```
function
[k]=kmidB1(E1,E2,NU12,NU21,G12,WID,TP,teta1,angle,AL,QXXi,npm,npta,npt,
th,nptm,npu,p);
```

```
m=tan(angle);
Q11=E1/(1-(NU12*NU21));
Q33=G12;
Q12=Q11*NU21;
Q21=(NU12*E2)/(1-(NU12*NU21));
Q22=E2/(1-(NU12*NU21));
Q=[Q11,Q12,0;Q21,Q22,0;0,0,Q33];
k=0;
TP1=TP/cos(angle);

for i=1:npta
   c=TP*(npt+0.5-i);
   teta=teta1(1,i);
      M=cos(teta);
   N=sin(teta);
        QXX=M^4*Q11+N^4*Q22+(2*M^2*N^2*Q12)+(4*M^2*N^2*Q33);
        QYY=(N^4*Q11)+(M^4*Q22)+(2*M^2*N^2*Q12)+(4*M^2*N^2*Q33);
        QXY=(M^2*N^2*Q11)+(M^2*N^2*Q22)+((M^4+N^4)*Q12)-
(4*M^2*N^2*Q33);
        QXS=(M^3*N*Q11)-(M*N^3*Q22)+(((M*N^3)-
(M^3*N))*Q12)+(2*((M*N^3)-(M^3*N))*Q33);
        QYS=(M*N^3*Q11)-(M^3*N*Q22)+(((M^3*N)-
(M*N^3))*Q12)+(2*((M^3*N)-(M*N^3))*Q33);
        QSS=(M^2*N^2*Q11)+(M^2*N^2*Q22)-(2*M^2*N^2*Q12)+(((M^2-
N^2)^2)*Q33);
        QT=[QXX,QXY,2*QXS;QXY,QYY,2*QXS;QXS,QYS,2*QSS];
        %PLY PARAMETER

        A=(24*m^2*AL^2+60*c*AL*m+60*c^2+5*TP1^2)/AL^3;
        B=(14*m^2*AL^2+40*c*AL*m+60*c^2+5*TP1^2)/(AL^2);
        C=(34*m^2*AL^2+80*c*AL*m+60*c^2+5*TP1^2)/(AL^2);
        D=(8*m^2*AL^2+30*c*AL*m+60*c^2+5*TP^2)/(15*AL);
        E=(26*m^2*AL^2+60*c*AL*m+60*c^2+5*TP1^2)/(30*AL);
        F=(38*m^2*AL^2+90*c*AL*m+60*c^2+5*TP1^2)/(15*AL);
        H=WID*QXX*TP*cos(angle)^3;
        ks=H*[0.2*A,0.1*B,-0.2*A,0.1*C;
           0.1*B,D,-0.1*B,E;
           -0.2*A,-0.1*B,0.2*A,-0.1*C;
           0.1*C,E,-0.1*C,F];
        k=ks+k;
     end
     L1(1)=0;
for i=1:npm
   j=i+1;
   L1(j)=-i*TP/m;
end
   for j=1:npm
      c=c-TP;
      a=0;
      jj=npm-j+1;
      b=L1(jj);
      tp=TP;

      q=QXXi;
      l=AL;
      [ks]=kmidf(tp,q,l,m,c,a,b);
```

```
      k=ks+k;
k=k*cos(angle);
end
     HT=npu*TP;
     D=0;
if npu~=0,
   for l=1:npu
        M=cos(teta1(1,l));
        N=sin(teta1(1,l));
        QXX=M^4*Q11+N^4*Q22+(2*M^2*N^2*Q12)+(4*M^2*N^2*Q33);
                HB=HT-TP;
        D=D+((1/3)*(HT^3-HB^3)*QXX);
        HT=HT-TP;
     end
  else
end

   ks=WID*D*[12/AL^3 6/AL^2 -12/AL^3 6/AL^2;
   6/AL^2 4/AL 6/AL^2 2/AL;
   -12/AL^3 6/AL^2 12/AL^3 6/AL^2;
   6/AL^2 2/AL 6/AL^2 4/AL];

   k=k+ks;

     k=k-(p/10)*[12/AL 1 -12/AL 1;
       1 4*AL/3 -1 -AL/3;
       -12/AL -1 12/AL -1;
       1 -AL/3 -1 4*AL/3];
```

kmidC1

This function creates stiffness matrix for tapered beam model C based on Euler-Bernoulli beam theory using conventional FEM

```
function
[k]=kmidC(E1,E2,NU12,NU21,G12,WID,TP,teta1,angle,AL,QXXi,npt,npm,npta,p
)

m=tan(angle);
Q11=E1/(1-(NU12*NU21));
Q33=G12;
Q12=Q11*NU21;
Q21=(NU12*E2)/(1-(NU12*NU21));
Q22=E2/(1-(NU12*NU21));
Q=[Q11,Q12,0;Q21,Q22,0;0,0,Q33];
k=0;
TP1=TP/cos(angle);
for i=1:npta
   c=TP*(npt-i+0.5);
   teta=teta1(1,i);
   M=cos(teta);
   N=sin(teta);

   QXX=M^4*Q11+N^4*Q22+(2*M^2*N^2*Q12)+(4*M^2*N^2*Q33);
```

```
   QYY=(N^4*Q11)+(M^4*Q22)+(2*M^2*N^2*Q12)+(4*M^2*N^2*Q33);
   QXY=(M^2*N^2*Q11)+(M^2*N^2*Q22)+((M^4+N^4)*Q12)-(4*M^2*N^2*Q33);
   QXS=(M^3*N*Q11)-(M*N^3*Q22)+(((M*N^3)-(M^3*N))*Q12)+(2*((M*N^3)-
(M^3*N))*Q33);
   QYS=(M*N^3*Q11)-(M^3*N*Q22)+(((M^3*N)-(M*N^3))*Q12)+(2*((M^3*N)-
(M*N^3))*Q33);
   QSS=(M^2*N^2*Q11)+(M^2*N^2*Q22)-(2*M^2*N^2*Q12)+(((M^2-N^2)^2)*Q33);
   QT=[QXX,QXY,2*QXS;QXY,QYY,2*QXS;QXS,QYS,2*QSS];

   A=(24*m^2*AL^2+60*c*AL*m+60*c^2+5*TP1^2)/AL^3;
   B=(14*m^2*AL^2+40*c*AL*m+60*c^2+5*TP1^2)/(AL^2);
   C=(34*m^2*AL^2+80*c*AL*m+60*c^2+5*TP1^2)/(AL^2);
   D=(8*m^2*AL^2+30*c*AL*m+60*c^2+5*TP1^2)/(15*AL);
   E=(26*m^2*AL^2+60*c*AL*m+60*c^2+5*TP1^2)/(30*AL);
   F=(38*m^2*AL^2+90*c*AL*m+60*c^2+5*TP1^2)/(15*AL);
   H=WID*QXX*TP*cos(angle)^3;
   ks=H*[0.2*A,0.1*B,-0.2*A,0.1*C;
      0.1*B,D,-0.1*B,E;
      -0.2*A,-0.1*B,0.2*A,-0.1*C;
      0.1*C,E,-0.1*C,F];
   k=ks+k;
end
L1(1)=0;
for i=1:npm
   j=i+1;
   L1(j)=-i*TP/m;
end
npta1=npta+1;
npt2=npta+npm;
   for j=1:npm
      c=c-TP;
      a=0;
      jj=npm-j+1;
      b=L1(jj);
      tp=TP;
      alfa=angle;
      q=QXXi;
      l=AL;
      [ks]=kmidf(tp,q,l,m,c,a,b);

      k=ks+k;
k=k*cos(angle);
end

k=k-(p/10)*[12/AL 1 -12/AL 1;
   1 4*AL/3 -1 -AL/3;
   -12/AL -1 12/AL -1;
   1 -AL/3 -1 4*AL/3];
```

---

kmidd

This function creates stiffness matrix for tapered beam model D based on Euler-Bernoulli beam theory using conventional FEM

```
function
[k]=kmidd1(E1,E2,NU12,NU21,G12,WID,TP,teta1,angle,AL,QXXi,npm,npta,npt,
th,nptm,npu,p);
m=tan(angle);
k=0;
Q11=E1/(1-(NU12*NU21));
Q33=G12;
Q12=Q11*NU21;
Q21=(NU12*E2)/(1-(NU12*NU21));
Q22=E2/(1-(NU12*NU21));
Q=[Q11,Q12,0;Q21,Q22,0;0,0,Q33];
TP1=TP/cos(angle);
for i=1:npta
   c=TP*(npt-i+0.5);
   teta=teta1(1,i);
   M=cos(teta);
   N=sin(teta);
   QXX=M^4*Q11+N^4*Q22+(2*M^2*N^2*Q12)+(4*M^2*N^2*Q33);
   QYY=(N^4*Q11)+(M^4*Q22)+(2*M^2*N^2*Q12)+(4*M^2*N^2*Q33);
   QXY=(M^2*N^2*Q11)+(M^2*N^2*Q22)+((M^4+N^4)*Q12)-(4*M^2*N^2*Q33);
   QXS=(M^3*N*Q11)-(M*N^3*Q22)+(((M*N^3)-(M^3*N))*Q12)+(2*((M*N^3)-
(M^3*N))*Q33);
   QYS=(M*N^3*Q11)-(M^3*N*Q22)+(((M^3*N)-(M*N^3))*Q12)+(2*((M^3*N)-
(M*N^3))*Q33);
   QSS=(M^2*N^2*Q11)+(M^2*N^2*Q22)-(2*M^2*N^2*Q12)+(((M^2-N^2)^2)*Q33);
   QT=[QXX,QXY,2*QXS;QXY,QYY,2*QXS;QXS,QYS,2*QSS];
   %PLY PARAMETER

   A=(24*m^2*AL^2+60*c*AL*m+60*c^2+5*TP1^2)/AL^3;
   B=(14*m^2*AL^2+40*c*AL*m+60*c^2+5*TP1^2)/(AL^2);
   C=(34*m^2*AL^2+80*c*AL*m+60*c^2+5*TP1^2)/(AL^2);
   D=(8*m^2*AL^2+30*c*AL*m+60*c^2+5*TP1^2)/(15*AL);
   E=(26*m^2*AL^2+60*c*AL*m+60*c^2+5*TP^2)/(30*AL);
   F=(38*m^2*AL^2+90*c*AL*m+60*c^2+5*TP1^2)/(15*AL);
   H=WID*QXX*TP*cos(angle)^3;
   ks=H*[0.2*A,0.1*B,-0.2*A,0.1*C;
      0.1*B,D,-0.1*B,E;
      -0.2*A,-0.1*B,0.2*A,-0.1*C;
      0.1*C,E,-0.1*C,F];
   k=ks+k;
end
 L1(1)=0;
for i=1:4
   j=i+1;
   L1(j)=-i*TP/m;
end
   for j=1:4
      c=c-TP;
      a=0;
      jj=4-j+1;
      b=L1(jj);
      tp=TP;
      q=QXXi;
      l=AL;
      [ks]=kmidf(tp,q,l,m,c,a,b);
        k=ks+k;
end
```

```
HT=npu*TP;
     D=0;
if npu~=0,
     for l=th:nptm
        M=cos(teta1(1,l));
        N=sin(teta1(1,l));
        QXX=M^4*Q11+N^4*Q22+(2*M^2*N^2*Q12)+(4*M^2*N^2*Q33);
        HB=HT-TP;
        D=D+((1/3)*(HT^3-HB^3)*QXX);
        HT=HT-TP;
     end
  else
end

  ks=WID*D*[12/AL^3 6/AL^2 -12/AL^3 6/AL^2;
     6/AL^2 4/AL 6/AL^2 2/AL;
     -12/AL^3 6/AL^2 12/AL^3 6/AL^2;
     6/AL^2 2/AL 6/AL^2 4/AL];

  k=k+ks;

  k=k-(p/10)*[12/AL 1 -12/AL 1;
     1 4*AL/3 -1 -AL/3;
     -12/AL -1 12/AL -1;
     1 -AL/3 -1 4*AL/3];
```

---

kmmat t2

```
%This function calculates stiffness and mass matrices for laminate
composite Timoshenko beam


function [k,m]=kmmat_t2(d,b,f55,area,l,ro,mu)
% Bending stiffness matrix
kb=(b*d/l)*[0  0 0  0;
            0  1 0 -1;
            0  0 0  0;
            0 -1 0  1];
%  Shear stiffness matrix
ks=(mu*f55*b/(4*l))*[4    2*l  -4    2*l;
                     2*l  l^2  -2*l  l^2;
                    -4    -2*l  4    -2*l;
                     2*l  l^2  -2*l  l^2];
% Summation of bending and shear matrices
k=ks+kb;
% Mass matrix
m=(ro*area*l/6)*[2 0 1 0;
             0 h 0 h;
             1 0 2 0;
             0 h^2 0 h^2];
```

---

kmidAT

This function creates stiffness matrix for tapered beam model A based on Timoshenko beam theory using conventional FEM

```
function
[k]=kmidAT1(E1,E2,NU12,NU21,G12,WID,TP,teta1,angle,AL,k,QXXi,npt,npm,np
ta,p,MO,nn,f55);

kb=zeros(4,4);
m=tan(angle);
k=zeros(4,4);
Q11=E1/(1-(NU12*NU21));
Q33=G12;
Q12=Q11*NU21;
Q21=(NU12*E2)/(1-(NU12*NU21));
Q22=E2/(1-(NU12*NU21));
Q=[Q11,Q12,0;Q21,Q22,0;0,0,Q33];

for i=1:npta
    c=TP*(npt+0.5-i);
    teta=teta1(1,i);
    M=cos(teta);
    N=sin(teta);
    QXX=M^4*Q11+N^4*Q22+(2*M^2*N^2*Q12)+(4*M^2*N^2*Q33);
    b=WID;
    A=QXX*(4*TP*m^2*AL^2+12*TP*c*m*AL+12*TP*c^2+TP^3)/(12);
    kb=(WID*A/AL)*[0 0 0 0;
        0 1 0 -1;
        0 0 0 0;
        0 -1 0 1];
    k=kb+k;
end
for i=npta+1:npt-nn
    c=c-TP;
    A=QXXi*(4*TP*m^2*AL^2+12*TP*c*m*AL+12*TP*c^2+TP^3)/(12);
    kb=(WID*A/AL)*[0 0 0 0;
        0 1 0 -1;
        0 0 0 0;
        0 -1 0 1];
    k=kb+k;
end
L1(1)=0;
for i=1:nn
    j=i+1;
    L1(j)=-i*TP/m;
end
for j=1:nn
    c=c-TP;
    a=0;
    jj=nn-j+1;
    b=L1(jj);
    t=TP;
    q=QXXi;
    l=AL;
```

```
    A1=1/3*q*t*m^2/l^2*(b^3-a^3)+q*t*c*m/l^2*(b^2-
a^2)+q*t*(c^2+1/12*t^2)/l^2*(b-a);
    kb=(WID*A1/AL)*[0 0 0 0;
        0 1 0 -1;
        0 0 0 0;
        0 -1 0 1];
    k=kb+k;
end

ks=(MO*f55/(4*AL))*[4 2*AL -4 2*AL;
    2*AL AL^2 -2*AL AL^2;
    -4 -2*AL 4 -2*AL;
    2*AL AL^2 -2*AL AL^2];
k=k+ks;

k=k-(p/10)*[12/AL 1 -12/AL 1;
   1 4*AL/3 -1 -AL/3;
   -12/AL -1 12/AL -1;
   1 -AL/3 -1 4*AL/3];
```

---

kmidBt1

This function creates stiffness matrix for tapered beam model B based on Timoshenko beam theory using conventional FEM

```
function
[k]=kmidBt1(E1,E2,NU12,NU21,G12,WID,TP,teta1,angle,AL,QXXi,npm,npta,npt
,th,nptm,npu,p,MO,f55)

m=tan(angle);
Q11=E1/(1-(NU12*NU21));
Q33=G12;
Q12=Q11*NU21;
Q21=(NU12*E2)/(1-(NU12*NU21));
Q22=E2/(1-(NU12*NU21));
Q=[Q11,Q12,0;Q21,Q22,0;0,0,Q33];
k=0;


for i=1:npta
   c=TP*(npt+0.5-i);
   teta=teta1(1,i);
   M=cos(teta);
   N=sin(teta);
   QXX=M^4*Q11+N^4*Q22+(2*M^2*N^2*Q12)+(4*M^2*N^2*Q33);
   b=WID;
   A=QXX*(4*TP*m^2*AL^2+12*TP*c*m*AL+12*TP*c^2+TP^3)/(12);
   kb=(WID*A/AL)*[0 0 0 0;0 1 0 -1;0 0 0 0;0 -1 0 1];
   k=kb+k;
end
L1(1)=0;
for i=1:npm
```

```
   j=i+1;
   L1(j)=-i*TP/m;
end
   for j=1:npm
      c=c-TP;
      a=0;
      jj=npm-j+1;
      b=L1(jj);
      t=TP;
      q=QXXi;
      l=AL;
   A1=1/3*q*t*m^2/l^2*(b^3-a^3)+q*t*c*m/l^2*(b^2-
a^2)+q*t*(c^2+1/12*t^2)/l^2*(b-a);
    kb=(WID*A1/AL)*[0 0 0 0;
      0 1 0 -1;
      0 0 0 0;
      0 -1 0 1];

      k=kb+k;
end
HT=npu*TP;
D=0;
if npu~=0,
   for l=th:nptm
       c=c-TP;
      M=cos(teta1(1,l));
      N=sin(teta1(1,l));
      QXX=M^4*Q11+N^4*Q22+(2*M^2*N^2*Q12)+(4*M^2*N^2*Q33);
      QYY=(N^4*Q11)+(M^4*Q22)+(2*M^2*N^2*Q12)+(4*M^2*N^2*Q33);
      QXY=(M^2*N^2*Q11)+(M^2*N^2*Q22)+((M^4+N^4)*Q12)-(4*M^2*N^2*Q33);
      QXS=(M^3*N*Q11)-(M*N^3*Q22)+(((M*N^3)-(M^3*N))*Q12)+(2*((M*N^3)-
(M^3*N))*Q33);
      QYS=(M*N^3*Q11)-(M^3*N*Q22)+(((M^3*N)-(M*N^3))*Q12)+(2*((M^3*N)-
(M*N^3))*Q33);
      QSS=(M^2*N^2*Q11)+(M^2*N^2*Q22)-(2*M^2*N^2*Q12)+(((M^2-
N^2)^2)*Q33);
      QT=[QXX,QXY,2*QXS;QXY,QYY,2*QXS;QXS,QYS,2*QSS];
      HB=HT-TP;
      D=D+((1/3)*(HT^3-HB^3)*QXX);
      HT=HT-TP;
   end

   kb=(WID*D/AL)*[0 0 0 0;
      0 1 0 -1;
      0 0 0 0;
      0 -1 0 1];

   k=kb+k;
else
end

ks=(MO*f55/(4*AL))*[4 2*AL -4 2*AL;
   2*AL AL^2 -2*AL AL^2;
   -4 -2*AL 4 -2*AL;
   2*AL AL^2 -2*AL AL^2];

k=k+ks;
```

```
k=k-(p/10)*[12/AL 1 -12/AL 1;
   1 4*AL/3 -1 -AL/3;
   -12/AL -1 12/AL -1;
   1 -AL/3 -1 4*AL/3];
```

---

kmidtC

This function creates stiffness matrix for tapered beam model C based on Timoshenko beam theory using conventional FEM

```
function
[k]=kmidtC1(E1,E2,NU12,NU21,G12,WID,TP,teta1,angle,AL,QXXi,npt,npm,npta
,p,MO,f55)

m=tan(angle);
Q11=E1/(1-(NU12*NU21));
Q33=G12;
Q12=Q11*NU21;
Q21=(NU12*E2)/(1-(NU12*NU21));
Q22=E2/(1-(NU12*NU21));
Q=[Q11,Q12,0;Q21,Q22,0;0,0,Q33];
k=0;

for i=1:npta
   c=TP*(npt+0.5-i);
   teta=teta1(1,i);
   M=cos(teta);
   N=sin(teta);
   QXX=M^4*Q11+N^4*Q22+(2*M^2*N^2*Q12)+(4*M^2*N^2*Q33);
   b=WID;
   A=QXX*(4*TP*m^2*AL^2+12*TP*c*m*AL+12*TP*c^2+TP^3)/(12);
   kb=(WID*A/AL)*[0 0 0 0;
      0 1 0 -1;
      0 0 0 0;
      0 -1 0 1];

      k=kb+k;
end
L1(1)=0;
for i=1:npm
   j=i+1;
   L1(j)=-i*TP/m;
end
   for j=1:npm
      c=c-TP;
      a=0;
      jj=npm-j+1;
      b=L1(jj);
```

```
      t=TP;
      q=QXXi;
      l=AL;
   A1=1/3*q*t*m^2/l^2*(b^3-a^3)+q*t*c*m/l^2*(b^2-
a^2)+q*t*(c^2+1/12*t^2)/l^2*(b-a);
    kb=(WID*A1/AL)*[0 0 0 0;
      0 1 0 -1;
      0 0 0 0;
      0 -1 0 1];

      k=kb+k;
end


ks=(MO*f55/(4*AL))*[4 2*AL -4 2*AL;
   2*AL AL^2 -2*AL AL^2;
   -4 -2*AL 4 -2*AL;
   2*AL AL^2 -2*AL AL^2];
k=k+ks;

k=k-(p/10)*[12/AL 1 -12/AL 1;
   1 4*AL/3 -1 -AL/3;
   -12/AL -1 12/AL -1;
   1 -AL/3 -1 4*AL/3]
```

---

kmiddt

This function creates stiffness matrix for tapered beam model D based on Timoshenko beam theory using conventional FEM

```
function
[k]=kmiddt1(E1,E2,NU12,NU21,G12,WID,TP,teta1,angle,AL,QXXi,npm,npta,npt
,th,nptm,npu,p,MO,f55);


m=tan(angle);
k=0;
Q11=E1/(1-(NU12*NU21));
Q33=G12;
Q12=Q11*NU21;
Q21=(NU12*E2)/(1-(NU12*NU21));
Q22=E2/(1-(NU12*NU21));
Q=[Q11,Q12,0;Q21,Q22,0;0,0,Q33];

for i=1:npta
        c=TP*(npt-i+0.5);
        teta=teta1(1,i);
        M=cos(teta);
        N=sin(teta);
        QXX=M^4*Q11+N^4*Q22+(2*M^2*N^2*Q12)+(4*M^2*N^2*Q33);
        A=QXX*(4*TP*m^2*AL^2+12*TP*c*m*AL+12*TP*c^2+TP^3)/(12);
```

```
        kb=(WID*A/AL)*[0 0 0 0;
        0 1 0 -1;
        0 0 0 0;
        0 -1 0 1];

     k=kb+k;
  end
  L1(1)=0;
  for i=1:npm
     j=i+1;
     L1(j)=-i*TP/m;
  end
  for j=1:npm
     c=c-TP;
     a=0;
     jj=npm-j+1;
     b=L1(jj);
     t=TP;
     q=QXXi;
     l=AL;
     A1=1/3*q*t*m^2/l^2*(b^3-a^3)+q*t*c*m/l^2*(b^2-
a^2)+q*t*(c^2+1/12*t^2)/l^2*(b-a);
     kb=(WID*A1/AL)*[0 0 0 0;
        0 1 0 -1;
        0 0 0 0;
        0 -1 0 1];

     k=kb+k;
  end

  HT=npu*TP;
     D=0;
if npu~=0,
   for l=th:nptm
       c=c-TP;
        M=cos(teta1(1,l));      %note instead of th in
M=cos(teta1(1,th)) ,it is changed to (1,l)
        N=sin(teta1(1,l));
        QXX=M^4*Q11+N^4*Q22+(2*M^2*N^2*Q12)+(4*M^2*N^2*Q33);
        HB=HT-TP;
        D=D+((1/3)*(HT^3-HB^3)*QXX);
        HT=HT-TP;
     end
     kb=(WID*D/AL)*[0 0 0 0;
        0 1 0 -1;
        0 0 0 0;
        0 -1 0 1];

     k=kb+k;
  else
  end

  ks=(MO*f55/(4*AL))*[4 2*AL -4 2*AL;
     2*AL AL^2 -2*AL AL^2;
     -4 -2*AL 4 -2*AL;
     2*AL AL^2 -2*AL AL^2];
```

```
k=k+ks;
```

uni b2

```
display('This program calculate modal vibration of a uniform')
display('orthotropic composite beam based on CLPT')

%e1=input('Enter E1 = ');
e1=113.9e9;
%e2=input('Enter E2 = ');
e2=7.9856e9;
%g12=input('Enter G12 = ');
g12=3.138e9;
%nu12=input('nu12 = ');
nu12=0.288;
%nu21=input('nu21 = ');
nu21=0.0178;
%tp=input('Enter thickness of each ply = ');
tp=0.000125;
%ro=input('density =');
ro=1480;
%np=input('Enter number of plies = ');
np=36;
np=np/2;
%lb=input('Enter lenght of the beam = ');
lb=0.2986;
%b=input('Enter width of the beam = ');
b=1;
nel=input('Enter number of elements= ');
ip=input('select boundary condition,1 = ss,2 = c-f,3 = c-c');
nnode=nel+1; % number of nodes
nnel=2; %numbe of nodes per element
ndof=2;                %number of DOF per node
sdof=nnode*ndof;       % system DOF
%
%-----------------------------------------
%nodal connectivity
%-----------------------------------------------

for i=1:nel
    nodes(i,1)=i;
   nodes(i,2)=i+1;
end
if ip==1
   bcdof=[1 sdof-1];
elseif ip==2
   bcdof=[1 2];
else
   bcdof=[1 2 sdof-1 sdof];
end

bcval=zeros(size(bcdof));
%intialization matrices
kk=zeros(sdof,sdof);
```

```
mm=zeros(sdof,sdof);
%k=zeros(4,4);
m=zeros(4,4);
for i=1:2:np
   ii=i+1;
   teta(i)=0;
   teta(ii)=90;
end
teta=teta*pi/180;
[q]=qmat(e1,e2,g12,nu12,nu21);
[D]=dmat(q,teta,np,tp);
area=b*np*tp;
for iel=1:nel
   d=D;
   l=lb/nel;
   [index]=elindex(iel,nnel,ndof);
   [k,m]=kmmat_b2(d,b,l,area,ro);
   [kk,mm]=elasmbl(kk,mm,m,k,index);
end
[kk,mm]=symbc(kk,mm,bcdof);
%
%solution of the system
%---------------------------------------------------------------
[ev,eq]=eig(kk,mm);
[lambda,item]=sort(diag(eq));
fr=sqrt(lambda);
nmod=sdof-length(bcdof);

for i=1:nmod
   frex1=(i*pi/lb)^2;
   frex2=sqrt(b*d/(ro*area));
   frex(i)=frex1*frex2;
   beta(i)=frex(i)*l^2/(sqrt(b*d/(ro*area)));
end
```

---

midA

```
% This program gives the natural freq. for model A using conventional
FEM

E1=113.9e9;E2=7.9856e9;NU12=0.288;NU21=0.0178;G12=3.138e9;G23=2.96e9;

WID=1.0;TP=0.000125;ro=1480;p=0;

npm=12;npta=12;angle=-1;angle=angle*pi/180;

L=-12*0.000125/tan(angle);
MO=0.833;
ip=1;
it=2;
%for II=1:4
 %teta1(II)=0;
%end
```

```
for II=1:2:36
  J=II+1;
  teta1(II)=45;
   teta1(J)=-45;
end
teta1=teta1*pi/180;
QXXi= 4.2869e9;

nel=4;                      %number of elements
nn=npm/nel;
nnode=nel+1;                % number of nodes
nnel=2;                     %number of nodes per element
ndof=2;                     %number of DOF per node
sdof=nnode*ndof;            % system DOF
%
%-----------------------------------------;

%nodal connectivity
%-----------------------------------------------
for i=1:nel
   nodes(i,1)=i;
   nodes(i,2)=i+1;
end
if ip==1
   bcdof=[1 sdof-1];
elseif ip==2
   bcdof=[1 2];
else
   bcdof=[1 2 sdof-1 sdof];
end

bcval=zeros(size(bcdof));
%intialization matrices
kk=zeros(sdof,sdof);
mm=zeros(sdof,sdof);
k=zeros(4,4);
m=zeros(4,4);
tp=TP;
g12=G12;
g23=G23;
teta=teta1;
f55=f55mat(tp,g12,g23,teta)
for iel=1:nel

   AL=L/nel;
   npt=npta+npm;
   index=feeldof1(iel,nnel,ndof);

   a1=npt*TP*WID;
   a2=(npt-nn)*TP*WID;
   area=(a1+a2)/2;
   if it==1

[k]=kmidA1(E1,E2,NU12,NU21,G12,WID,TP,teta1,angle,AL,QXXi,npt,npm,npta,
nn,p);
    m=mmidA(ro,area,AL);
   %k=k*2;  % for buckling
```

```
   %m=(1/10)*[12/AL 1 -12/AL 1;
   %1 4*AL/3 -1 -AL/3;
   %-12/AL -1 12/AL -1;
   %1 -AL/3 -1 4*AL/3];
elseif it==2

[k]=kmidAT1(E1,E2,NU12,NU21,G12,WID,TP,teta1,angle,AL,k,QXXi,npt,npm,np
ta,p,MO,nn,f55);
    [m]=(ro*area*AL/6)*[2 0 1 0;
   0 0 0 0;
   1 0 2 0;
   0 0 0 0];
end

   [kk,mm]=elasmbl(kk,mm,m,k,index);
   if iel~=nel,
      npm=npm-nn;
   else
   end
end
[kk,mm]=symbc(kk,mm,bcdof);
%solution of the system
%-----------------------------------------------------------------
[V,Q]=eig(kk,mm);
[LAMBDA,ITEM]=sort(diag(Q));
NEWV=V(:,ITEM);
fr=sqrt(LAMBDA)
```

---

mid B

```
% This program gives the natural frequencies for tapered beam model B
using conventional FEM

E1=113.9e9;E2=7.9856e9;NU12=0.288;NU21=0.0178;G12=3.138e9;G23=2.96e9;

WID=1.0;TP=0.000125;ro=1480;p=0;

npm=3;npta=12;nptm=24;npu=9;angle=-1;angle=angle*pi/180;

L=-12*0.000125/tan(angle);
ip=1;
it=2;       %it=1 for E_Bernoulli    it=2 for Timoshenko
MO=0.833;
%for II=1:4
    %teta1(II)=0;
    %end

for II=1:2:24
   J=II+1;
   teta1(II)=45;
   teta1(J)=-45;
end
teta1=teta1*pi/180;
QXXi=3.7e9/(1-0.37^2);
```

```
nel=4;                                  %number of elements
nnode=nel+1;                            % number of nodes
nnel=2;                                 %number of nodes per element
ndof=2;                                 %number of DOF per node
sdof=nnode*ndof;                        % system DOF
%
%-----------------------------------------
%nodal connectivity
%-----------------------------------------

for i=1:nel
   nodes(i,1)=i;
   nodes(i,2)=i+1;
end
if ip==1
   bcdof=[1 sdof-1];
elseif ip==2
   bcdof=[1 2];
else
   bcdof=[1 2 sdof-1 sdof];
end
bcval=zeros(size(bcdof));
%intialization matrices
kk=zeros(sdof,sdof);
mm=zeros(sdof,sdof);
k=zeros(4,4);
m=zeros(4,4);
tp=TP;
g12=G12;
g23=G23;
teta=teta1;
f55=f55mat(tp,g12,g23,teta);
th=npta+npm+1;
for iel=1:nel
   npt=npta+npm+npu;
   AL=L/nel;
   index=elindex(iel,nnel,ndof);
   a1=(npt)*TP*WID;
   a2=(npt-npm)*TP*WID;
   area=(a1+a2)/2;
    if it==1

[k]=kmidB1(E1,E2,NU12,NU21,G12,WID,TP,teta1,angle,AL,QXXi,npm,npta,npt,
th,nptm,npu,p);
 m=mmidA(ro,area,AL);

 elseif it==2

[k]=kmidBt1(E1,E2,NU12,NU21,G12,WID,TP,teta1,angle,AL,QXXi,npm,npta,npt
,th,nptm,npu,p,MO,f55);
        [m]=(ro*area*AL/6)*[2 0 1 0;
            0 0 0 0;
            1 0 2 0;
            0 0 0 0];
    end
    [kk,mm]=elasmbl(kk,mm,m,k,index);
    if iel~=nel,
```

```
        th=th+npm;
        npu=npu-npm;
    else
    end
end

[kk,mm]=symbc(kk,mm,bcdof);
%
%solution of the system
%--------------------------------------------------------------------
[V,Q]=eig(kk,mm);
[LAMBDA,ITEM]=sort(diag(Q));
NEWV=V(:,ITEM);
fr=sqrt(LAMBDA)
```

---

midC

```
%this program gives the natural freq. for model C using conventional
FEM
E1=113.9e9;E2=7.9856e9;NU12=0.288;NU21=0.0178;G12=3.138e9;G23=2.8526e9;

WID=1.0;TP=0.000125;ro=1480;p=0;

npm=3;npta=21;angle=-5;angle=angle*pi/180;
L=-12*0.000125/tan(angle);

ip=1;
it=2;                    % it=1 for E_Bernoulli   it=2 for Timoshenko
MO=0.833;
for II=1:4
   teta1(II)=0;
end

for II=5:2:24
   J=II+1;
   teta1(II)=45;
   teta1(J)=-45;
end
teta1=teta1*pi/180;
QXXi= 4.2869e9;
nel=4;                  %number of elements
nnode=nel+1;            % number of nodes
nnel=2;                 %number of nodes per element
ndof=2;                 %number of DOF per node
sdof=nnode*ndof;        % system DOF
%
%-----------------------------------------
%nodal connectivity
%-----------------------------------------
for i=1:nel
   nodes(i,1)=i;
   nodes(i,2)=i+1;
end
```

```
if ip==1
   bcdof=[1 sdof-1];
elseif ip==2
   bcdof=[1 2];
else
   bcdof=[1 2 sdof-1 sdof];
end
bcval=zeros(size(bcdof));
%intialization matrices
kk=zeros(sdof,sdof);
mm=zeros(sdof,sdof);
k=zeros(4,4);
m=zeros(4,4);
tp=TP;
g12=G12;
g23=G23;
teta=teta1;
f55=f55mat(tp,g12,g23,teta);

for iel=1:nel
   npt=npm+npta;

   AL=L/nel;
   index=elindex(iel,nnel,ndof);
     a1=(npt)*TP*WID;
   a2=(npt-npm)*TP*WID;
   area=(a1+a2)/2;
   if it==1

[k]=kmidC1(E1,E2,NU12,NU21,G12,WID,TP,teta1,angle,AL,QXXi,npt,npm,npta,
p);
 m=mmidA(ro,area,AL);
elseif it==2
[k]=kmidtC1(E1,E2,NU12,NU21,G12,WID,TP,teta1,angle,AL,QXXi,npt,npm,npta
,p,MO,f55);;
%[m]=mtimo(area,AL,ro,TP)
end
   [kk,mm]=elasmbl(kk,mm,m,k,index);
   if iel~=nel,
      npta=npta-npm;
   else
   end
end
[kk,mm]=symbc(kk,mm,bcdof);

%
%solution of the system
%-------------------------------------------------------------
[V,Q]=eig(kk,mm);
[LAMBDA,ITEM]=sort(diag(Q));
NEWV=V(:,ITEM);
fr=sqrt(LAMBD)
```

midD

```
% This program gives the natural freq. for model D using conventional
FEM

E1=113.9e9;E2=7.9856e9;NU21=0.0178;NU12=0.288;G12=3.138e9;G23=2.96e9;

WID=1.0;TP=0.000125;ro=1480;p=0;MO=5/8;
npm=3;npta=3;nptm=24;npu=18;angle=-1;
angle=angle*pi/180;
L=-12*0.000125/tan (angle);
ip=1;
it=2;
%for II=1:4
   %teta1(II)=0;
%end

for II=1:2:24
    J=II+1;
    teta1(II)=45;
    teta1(J)=-45;
 end
teta1=teta1*pi/180;

QXXi=3.7e9/(1-0.37^2);
nel=4;                    %number of elements
nnode=nel+1;              % number of nodes
nnel=2;                   %number of nodes per element
ndof=2;                   %number of DOF per node
sdof=nnode*ndof;          % system DOF
%
%-----------------------------------------
%
%nodal connectivity
%-----------------------------------------------

for i=1:nel
    nodes(i,1)=i;
   nodes(i,2)=i+1;
end
if ip==1
   bcdof=[1 sdof-1];
elseif ip==2
   bcdof=[1 2];
else
   bcdof=[1 2 sdof-1 sdof];
end
bcval=zeros(size(bcdof));


%intialization matrices
kk=zeros(sdof,sdof);
mm=zeros(sdof,sdof);
k=zeros(4,4);
m=zeros(4,4);
tp=TP;
g12=G12;
```

```
g23=G23;
teta=teta1;
f55=f55mat(tp,g12,g23,teta);
th=npm+npta+1;
for iel=1:nel
    npt=npta+npm+npu;
    %n1=nodes(iel,1);     nr=nodes(iel,2);
    %x1=gcoord(n1);       xr=gcoord(nr);
    %AL=xr-x1;  %element lenght
    AL=L/nel;
    index=elindex(iel,nnel,ndof);
    a1=(npt)*TP*WID;
    a2=(npt-npm)*TP*WID;
    area=(a1+a2)/2;
    if it==1

[k]=kmidd1(E1,E2,NU12,NU21,G12,WID,TP,teta1,angle,AL,QXXi,npm,npta,npt,
th,nptm,npu,p);
m=mmidA(ro,area,AL);
    elseif it==2

[k]=kmiddt1(E1,E2,NU12,NU21,G12,WID,TP,teta1,angle,AL,QXXi,npm,npta,npt
,th,nptm,npu,p,MO,f55);
 [m]=(ro*area*AL/6)*[2 0 1 0;
            0 0 0 0;
            1 0 2 0;
            0 0 0 0];
    end
    [kk,mm]=elasmbl(kk,mm,m,k,index);
    if iel~=nel,
        th=th+6;
        npta=npta+3;
        npu=npu-6;
    else
    end
end

[kk,mm]=symcs(kk,mm,bcdof);
%solution of the system
%-----------------------------------------------------------------
[V,Q]=eig(kk,mm);
[LAMBDA,ITEM]=sort(diag(Q));
NEWV=V(:,ITEM);
fr=sqrt(LAMBDA)
```

---

fen2.m

This function gives the stiffness, mass and geometric matrices for tapered composite beams using advanced FEM

```
x=sym('x');
m=sym('m');
c=sym('c');
qb=sym('qb');
```

```
t=sym('t');
d1=sym('d1');
d2=sym('d2');
p=sym('p');
z=m*x+c;
H=sym('H');        %H is cos(alfa)
T=t/H;
d=qb*(T*z^2+T^3/12);
%d=qb*(t*c^2+t^3/12);
%d=sym('d');
l=sym('l');
ro=sym('ro');
%A=sym('A');
b=sym('b');
A=z*b;
i=[1 0 0 0 0 0 0 0 ;
    0 -1 0 0 0 0 0 0;
    0 0 0 6*d1 0 0 0 0;
    0 0 -2*d1 0 0 0 0 0;
    1 l l^2 l^3 l^4 l^5 l^6 l^7;
    0 -1 -2*l -3*l^2 -4*l^3 -5*l^4 -6*l^5 -7*l^6;
    0 0 0 6*d2 24*d2*l 60*d2*l^2 120*d2*l^3 210*d2*l^4;
    0 0 -2*d2 -6*d2*l -12*d2*l^2 -20*d2*l^3 -30*d2*l^4 -42*d2*l^5];
t=[1 x x^2 x^3 x^4 x^5 x^6 x^7];
n=t*inv(i);
for i=1:3
    for j=1:3
        n1=diff(n(1,i),2,x);
        n2=diff(n(1,j),2,x);
        n3=diff(n(1,i),x);
        n4=diff(n(1,j),x);
        k(i,j)=int(H^3*d*n1*n2,0,1);
        M(i,j)=int(ro*A*n(1,i)*n(1,j),0,1);
      M(i,j)=ro*A*M(i,j);
      G(i,j)=int(p*n3*n4,0,1);
    end
end
simplify(k)
simplify(M)
simplify(G)
```

Nad.m

This function gives the shape functions in advanced FEM

```
x=sym('x');
q=sym('q');
m=sym('m');
c=sym('c');
z=m*x+c;
d=q*t*(z^2+t^3/12);
l=sym('l');
i=[1 0 0 0 0 0 0 0 ;
    0 -1 0 0 0 0 0 0;
    0 0 0 6*d 0 0 0 0;
```

```
    0 0 -2*d 0 0 0 0 0;
    1 l l^2 l^3 l^4 l^5 l^6 l^7;
    0 -1 -2*l -3*l^2 -4*l^3 -5*l^4 -6*l^5 -7*l^6;
    0 0 0 6*d 24*d*l 60*d*l^2 120*d*l^3 210*d*l^4;
    0 0 -2*d -6*d*l -12*d*l^2 -20*d*l^3 -30*d*l^4 -42*d*l^5];
t=[1 x x^2 x^3 x^4 x^5 x^6 x^7];
n=t*inv(i);
```

Mad_uni

This function gives the mass matrix for uniform beam using advanced FEM

```
function [m]=mad_uni(ro,area,L,b,D)
D=D(1,1);
[m]=(ro*area*L/420)*[72940/429  4530*L/143  -383*L^2/(2574*b*D)
1370*L^2/(429*b*D)  17150/429  -1905*L/143  -521*L^3/(5148*b*D)  -
775*L^2/(429*b*D);

   4530*L/143  100*L^2/13  -6*L^4/(143*b*D) 245*L^3/(286*b*D)

  1905*L/143  -1865*L^2/429  -5*L^4/(156*b*D)  -995*L^3/(1716*b*D);

   -383*L^2/(2574*b*D)  -6*L^4/(143*b*D)  L^6/(3861*(b*D)^2) -
L^5/(198*(b*D)^2)  -521*L^3/(5148*b*D)  5*L^4/(156*b*D)
7*L^6/(30888*(b*D)^2) 43*L^5/10296;

   1370*L^2/(429*b*D)  245*L^3/(286*b*D)  -L^5/(198*(b*D)^2)
43*L^4/(429*(b*D)^2)  775*L^2/(429*b*D)  -995*L^3/(1716*b*D)  -
43*L^5/(10296*(b*D)^2)  131*L^4/(1716*(b*D)^2);

   17150/429  1905*L/143  -521*L^3/(5148*b*D)  775*L^2/(429*b*D)
72940/429  -4530*L/143  -383*L^2/(2574*b*D)  -1370*L^2/(429*b*D);

   -1905*L/143  -1865*L^2/429  5*L^4/(156*b*D)  -995*L^3/(1716*b*D)  -
4530*L/143  100*L^2/13  6*L^4/(143*b*D)  245*L^3/(286*b*D);

   -521*L^3/(5148*b*D)  -5*L^4/(156*b*D)  7*L^6/(30888*(b*D)^2)  -
43*L^5/(10296*(b*D)^2)  -383*L^3/(2574*b*D)  6*L^4/(143*b*D)
L^6/(3861*(b*D)^2)  L^5/(198*(b*D)^2);

   -775*L^2/(429*b*D)  -995*L^3/(1716*b*D)  43*L^5/(10296*(b*D)^2)  -
131*L^5/(1716*(b*D)^2)  -1370*L^2/(429*b*D)  245*L^3/(286*b*D)
L^5/(198*(b*D)^2)  43*L^4/(429*(b*D)^2)]
```

---

kad_uni

This function gives the stiffness matrix for uniform beam using advanced FEM

```
function [k]=kad_uni(D,L,b)
D=D(1,1);
```

```
k=(b*D/L^3)*[280/11  140*L/11  -L^3/(22*b*D)  40*L^2/(33*b*D)  -280/11
140*L/11  L^3/(22*b*D)  40*L^2/(33*b*D);

   140*L/11  600*L^2/77  -8*L^4/(231*b*D)  379*L^3/(462*b*D)  -140*L/11
380*L^2/77  5*L^4/(462*b*D)  181*L^3/(462*b*D);

   -L^3/(22*b*D)  -8*L^4/(231*b*D)  2*L^6/(3465*(b*D)^2)  -
L^5/(99*(b*D)^2)  L^3/(22*b*D)  -5*L^4/(462*b*D)  L^6/(4620*(b*D)^2)
5*L^6/(2772*(b*D)^2);

   40*L^2/(33*b*D)  379*L^3/(462*b*D)  -L^5/(99*(b*D)^2)
50*L^5/(231*(b*D)^2)  -40*L^2/(33*b*D)  181*L^3/(462*b*D)  -
5*L^5/(2772*(b*D)^2)  L^5/(462*(b*D)^2);

   -280/11  -140*L/11  L^3/(22*b*D)  -40*L^2/(33*b*D)  280/11  -
140*L/11  -L^3/(22*b*D)  -40*L^2/(33*b*D);

   140*L/11  380*L^2/77  -5*L^4/(462*b*D)  181*L^3/(462*b*D)  -140*L/11
600*L^2/77  8*L^4/(231*b*D)  379*L^3/(462*b*D);

   L^3/(22*b*D)  5*L^4/(462*b*D)  L^6/(4620*(b*D)^2)  -
5*L^5/(2772*(b*D)^2)  -L^3/(22*b*D)  8*L^4/(231*b*D)
2*L^6/(3465*(b*D)^2) L^5/(99*(b*D)^2);

    40*L^2/(33*b*D)  181*L^3/(462*b*D)  5*L^5/(2772*(b*D)^2)
L^4/(462*b*D)  -40*L^4/(462*b*D)  379*L^3/(462*b*D)  L^5/(99*(b*D)^2)
50*L^4/(231*(b*D)^2)]
```

---

adA

```
% This program calculates the modal vibration
%of a tapered composite beam made with model A using advanced FEM
%-------------------------------------------------------------------
%
%Material properties of the laminate
%
E1=113.9e9;E2=7.9856e9;r12=0.288;r21=0.0178;G12=3.138e9;

b=1;                % Width of the beam
tp=0.000125;         % Thickness of each ply
ro=1480;            % Material Density
npm=12;              %number of imaginary plies which are considered
for resin
npta=6;             % number of tapered  plies above the resin
alfa=-0.5;
ip=2;
alfa=alfa*pi/180;
L=(-12*0.000125)/(tan(alfa));

for II=1:2:18       % stacking sequences of laminate
   J=II+1;
   teta1(II)=0;
   teta1(J)=90;
end
```

```
teta1=teta1*pi/180;
Qr=4.288e9;             % Q for the resin
nel=3;                  %number of elements
nnode=nel+1;            % number of nodes
nnel=2;                 %number of nodes per element
ndof=4;                 %number of DOF per node
sdof=nnode*ndof;        % system DOF
%
%-----------------------------------------
%
%nodal connectivity
%-----------------------------------------------
for i=1:nel
   nodes(i,1)=i;
   nodes(i,2)=i+1;
end
% ------------------------------------------------
% Imposing boundary conditions
%
%-----------------------------------------------------------------
if ip==1
   bcdof=[1 4 sdof-3 sdof];
  elseif ip==2
bcdof=[1 2 sdof-1 sdof];
else
   bcdof=[1 2 sdof-3 sdof-2];

end
bcval=zeros(size(bcdof));
%intialization matrices
kk=zeros(sdof,sdof);
mm=zeros(sdof,sdof);
%k=zeros(8,8);
%m=zeros(8,8);
[Q]=Qmat(E1,E2,G12,r12,r21);
nn=npm/nel;
for iel=1:nel
   l=L/nel;
   npt=npta+npm;
   [d1,d2]=d1d2a(Q,Qr,npta,npm,teta1,tp,nn);

   % Calculating index for assembling the matrices
   index=elindex(iel,nnel,ndof);
   t=tp;
   a1=npt*tp*b;
   a2=(npt-nn)*tp*b;
   A=(a1+a2)/2;
   t=tp;
   [k1]=kadaf(d1,d2,Q,t,teta1,alfa,l,Qr,npt,npm,npta,nn);
   %k1=k1*2;           %for buckling
   %[Gb]=gbmatad(d1,d2,l);
   %[m]=[Gb];
   [m]=massad1(ro,A,l,d1,d2);

   % Assembling the matrices
```

```
   [kk,mm]=elasmbl(kk,mm,m,k1,index);

   if iel~=nel,
      npm=npm-nn;
   else
   end
end
% Applying boundary conditions

[kk,mm]=symbc(kk,mm,bcdof);
%
%Solution of the system
%--------------------------------------------------------------
[V,EV]=eig(kk,mm);
[LAMBDA,ITEM]=sort(diag(EV));
NEWV=V(:,ITEM);
fr=sqrt(LAMBDA)
```

---

adB

```
% This program calculates the modal vibration
%of a tapered composite beam made with model B using advanced FEM
%-------------------------------------------------------------------------

E1=113.9e9;E2=7.9856e9;r12=0.288;r21=0.0178;G12=3.138e9;

b=1.0;tp=0.000125;ro=1480;

p=0;npm=4;npta=6;nptm=18;npu=8;alfa=-3;alfa=alfa*pi/180;
L=12*0.000125/(tan(-alfa));
ip=2;

for II=1:2:18
   J=II+1;
   teta1(II)=0;
   teta1(J)=90;
   end

teta1=teta1*pi/180;
Qr=4.288e9;
nel=3;                  %number of elements
nnode=nel+1;            % number of nodes
nnel=2;                 %numbe of nodes per element
ndof=4;                 %number of DOF per node
sdof=nnode*ndof;        % system DOF
%
%----------------------------------------
%nodal connectivity
%-----------------------------------------------
for i=1:nel
   nodes(i,1)=i;
   nodes(i,2)=i+1;
end
if ip==1
   bcdof=[1 4 sdof-3 sdof];
```

```
  elseif ip==2
bcdof=[1 2 sdof-1 sdof];
else
   bcdof=[1 2 sdof-3 sdof-2];

end

bcval=zeros(size(bcdof));

%intialization matrices
kk=zeros(sdof,sdof);
mm=zeros(sdof,sdof);

[Q]=Qmat(E1,E2,G12,r12,r21);
th=npm+npta+1;
for iel=1:nel
       npt=npta+npm+npu;
 [d1,d2]=d1d2b(Q,b,tp,teta1,Qr,npm,npta,npt,th,nptm,npu);

   l=L/nel;
   index=feeldof1(iel,nnel,ndof);
   a1=(npt)*tp*b;
   a2=(npt-4)*tp*b;
   A=(a1+a2)/2;
   t=tp;
   [k1]=kaddB1(d1,d2,Q,t,alfa,l,Qr,teta1,npm,npta,npt,npu);
  %k1=k1*2;
    %[m]=mad3(ro,A,l,d1,d2);
    %[Gb]=gbmatad(d1,d2,l);
    %m=Gb;
     [m]=massad1(ro,A,l,d1,d2);
   [kk,mm]=feasmbl2(kk,mm,m,k1,index);
   if iel~=nel,
      th=th+4;
      npu=npu-4;
   else
   end
end

[kk,mm]=feaplycs(kk,mm,bcdof);
%solution of the system
%-----------------------------------------------------------------
[V,EV]=eig(kk,mm);
[LAMBDA,ITEM]=sort(diag(EV));
NEWV=V(:,ITEM);
fr=sqrt(LAMBDA)
```

---

adC

```
% This program calculates the modal vibration
%of a tapered composite beam made with model C using advanced FEM
%-----------------------------------------------------------------
```

```
E1=113.9e9;G12=4.48e9;E2=7.9856e9;r12=0.288;r21=0.0178;G12=3.138e9;

b=1.0;tp=0.000125;ro=1480;

npm=4;npta=14;alfa=-3;alfa=alfa*pi/180;
L=12*0.000125/(tan(-alfa));
ip=2;
for II=1:2:18
   J=II+1;
   teta1(II)=0;
   teta1(J)=90;
   end
teta1=teta1*pi/180;
Qr=4.288e9;
nel=3;                  %number of elements
nnode=nel+1;            % number of nodes
nnel=2;                 %numbe of nodes per element
ndof=4;                 %number of DOF per node
sdof=nnode*ndof;        % system DOF
%
%----------------------------------------
%nodal connectivity
%----------------------------------------------
for i=1:nel
   nodes(i,1)=i;
   nodes(i,2)=i+1;
end
if ip==1
   bcdof=[1 4 sdof-3 sdof];
  elseif ip==2
bcdof=[1 2 sdof-1 sdof];
else
   bcdof=[1 2 sdof-3 sdof-2];

end

bcval=zeros(size(bcdof));

%intialization matrices
kk=zeros(sdof,sdof);
mm=zeros(sdof,sdof);

[Q]=Qmat(E1,E2,G12,r12,r21);

for iel=1:nel
   npt=npm+npta;
   [d1,d2]=d1d2c(Q,Qr,npta,npm,teta1,tp)
   l=L/nel;
   index=elindex(iel,nnel,ndof);
   a1=(npt)*tp*b;
   a2=(npt-npm)*tp*b;
   A=(a1+a2)/2;
   t=tp;
    [k1]=kadC1(Q,t,teta1,alfa,l,Qr,npt,npm,npta,d1,d2);

   [m]=massad1(ro,A,l,d1,d2);
   [kk,mm]=elasmbl(kk,mm,m,k1,index);
```

```
   if iel~=nel,
      npta=npta-npm;
   else
   end
end
[kk,mm]=symbc(kk,mm,bcdof);
%solution of the system
%-----------------------------------------------------------------
[V,EV]=eig(kk,mm);
[LAMBDA,ITEM]=sort(diag(EV));
NEWV=V(:,ITEM);
fr=sqrt(LAMBDA)
```

---

adD

```
% This program calculates the modal vibration
%of a tapered composite beam made with model D using advanced FEM
%-----------------------------------------------------------------

E1=113.9e9;G12=4.48e9;E2=7.9856e9;r12=0.288;r21=0.0178;
G12=3.138e9;b=1.0;tp=0.000125;ro=1480;

p=0;
npm=4;npta=2;nptm=18;npu=12;alfa=-3;alfa=alfa*pi/180;
L=12*0.000125/(tan(-alfa));
ip=2;
for II=1:2:18
   J=II+1;
   teta1(II)=0;
   teta1(J)=90;
end
teta1=teta1*pi/180;
Qr=4.288e9;
nel=3;                  %number of elements
nnode=nel+1;            % number of nodes
nnel=2;                 %numbe of nodes per element
ndof=4;                 %number of DOF per node
sdof=nnode*ndof;        % system DOF
%
%-----------------------------------------
%nodal connectivity
%-----------------------------------------------
for i=1:nel
   nodes(i,1)=i;
   nodes(i,2)=i+1;
end
if ip==1
   bcdof=[1 4 sdof-3 sdof];
elseif ip==2
   bcdof=[1 2 sdof-1 sdof];
else
   bcdof=[1 2 sdof-3 sdof-2];
```

```
end
bcval=zeros(size(bcdof));
%intialization matrices
kk=zeros(sdof,sdof);
mm=zeros(sdof,sdof);
[Q]=Qmat(E1,E2,G12,r12,r21);
th=npm+npta+1;
for iel=1:nel
   npt=npta+npm+npu;
   [d1,d2]=d1d2d(Q,b,tp,teta1,Qr,npm,npta,npt,th,nptm,npu);

   l=L/nel;
   index=elindex(iel,nnel,ndof);
   a1=(npt)*tp*b;
   a2=(npt-4)*tp*b;
   A=(a1+a2)/2;
   t=tp;
   [k1]=kaddB1(d1,d2,Q,t,alfa,l,Qr,teta1,npm,npta,npt,npu);
   %k1=k1*2;                    % for buckling
   %[Gb]=gbmatad(d1,d2,l);
   %m=Gb;
   [m]=massad1(ro,A,l,d1,d2);
   [kk,mm]=elasmbl(kk,mm,m,k1,index);
   if iel~=nel,
      th=th+4;
      npta=npta+2;
      npu=npu-4;
   else
   end
end

[kk,mm]=symbc(kk,mm,bcdof);
%solution of the system
%-----------------------------------------------------------
[V,EV]=eig(kk,mm);
[LAMBDA,ITEM]=sort(diag(EV));
NEWV=V(:,ITEM);
fr=sqrt(LAMBDA)
```

---

gbmatad

```
% this function calculates the geometric stiffness matrix
% for advanced formulation
function [Gb]=gbmatad(d1,d2,l)

G(1,1)=700/429/l;G(1,2)=271/858;G(1,3)=-5/5148*l^2/d1;
G(1,4)=23/858*l/d1;G(1,5)=-700/429/l;G(1,6)=271/858;
G(1,7)=-5/5148*l^2/d2;G(1,8)=-23/858*l/d2;G(2,2)=300/1001*l;
G(2,3)=-25/18018*l^3/d1;G(2,4)=123/4004*l^2/d1;G(2,5)=-271/858;
G(2,6)=97/6006*l;G(2,7)=5/12012*l^3/d2;G(2,8)=47/12012*l^2/d2;
G(3,3)=1/90090/d1^2*l^5;G(3,4)=-37/180180/d1^2*l^4;
G(3,5)=5/5148*l^2/d1;G(3,6)=5/12012*l^3/d1;
G(3,7)=-1/144144/d1*l^5/d2;G(3,8)=-73/720720/d1*l^4/d2;
G(4,4)=73/18018/d1^2*l^3;G(4,5)=-23/858/d1*l;
```

```
G(4,6)=-47/12012/d1*l^2;G(4,7)=73/720720/d1*l^4/d2;
G(4,8)=7/5148/d1*l^3/d2;G(5,5)=700/429/l;G(5,6)=-271/858;
G(5,7)=5/5148*l^2/d2;G(5,8)=23/858*l/d2;
G(6,6)=300/1001*l;G(6,7)=-25/18018*l^3/d2;
G(6,8)=-123/4004*l^2/d2;G(7,7)=1/90090/d2^2*l^5;
G(7,8)=37/180180*l^4/d2^2;G(8,8)=73/18018/d2^2*l^3;

for i=1:8
   ii=i+1;
   for j=ii:8
      G(j,i)=G(i,j);
   end
end
[Gb]=[G];
```

---

kadtimo1

This function gives the stiffness matrix for uniform Timoshenko beam using advanced FEM

```
function [k]=kadtimo1(h55,d,l);
a=d/h55;

k(1,1)=6/5/l;k(1,2)=1/2;k(1,3)=1/10;k(1,4)=l/10*l;
k(1,5)=-6/5/l;k(1,6)=1/2;k(1,7)=1/10;k(1,8)=-l/10*l;%
k(2,2)=13/35*l+6/5/l*a;k(2,3)=-l/10*l;%k(2,4)=11/210*l^2+1/10*a;
k(2,5)=-1/2;k(2,6)=9/70*l-6/5/l*a;k(2,7)=l/10*l;
k(2,8)=-13/420*l^2+1/10*a;k(3,3)=2/15*l;k(3,4)=0;
k(3,5)=-1/10;k(3,6)=1/10*l;%k(3,7)=-l/30*l;
k(3,8)=-l^2/60;k(4,4)=1/105*l^3+2/15*l*a;k(4,5)=-l/10*l;
k(4,6)=13/420*l^2-1/10*a;k(4,7)=l/60*l^2;k(4,8)=-1/140*l^3-1/30*a;
k(5,5)=6/5/l;k(5,6)=-1/2;k(5,7)=-1/10;
k(5,8)=l/10*l;k(6,6)=13/35*l+5/6/l*a;k(6,7)=-1/10*l;
k(6,8)=-11/210*l^2-1/10*a;k(7,7)=2/15*l;k(7,8)=0;
k(8,8)=1/105*l^3+2/15*l*a;

for i=1:8
    ii=i+1;
    for j=ii:8
        k(j,i)=k(i,j);
    end
end
k=h55*k;
```

---

madtimo1

This function gives the mass matrix for uniform Timoshenko beam using advanced FEM

```
function [m]=madtimo1(ro,h,l);
m(1,1)=13/35;m(1,2)=0;m(1,3)=11/210*l;m(1,4)=0;m(1,5)=9/70;
m(1,6)=0;m(1,7)=-13/420*l;m(1,8)=0;m(2,2)=13/420*h^2;
m(2,3)=0;m(2,4)=11/2520*l*h^2;m(2,5)=0;m(2,6)=3/280*h^2;
```

```
m(2,7)=0;m(2,8)=-13/5040*h^2*l;m(3,3)=1/105*l^2;
m(3,4)=0;m(3,5)=13/420*l;m(3,6)=0;
m(3,7)=-1/140*l^2;m(3,8)=0;m(4,4)=1/1260*l^2*h^2;m(4,5)=0;
m(4,6)=13/5040*l*h^2;m(4,7)=0;m(4,8)=-1/1680*l^2*h^2;m(5,5)=13/35;
m(5,6)=0;m(5,7)=-11/210*l;m(5,8)=0;m(6,6)=13/420*h^2;
m(6,7)=0;m(6,8)=-11/2520*h^2*l;m(7,7)=1/105*l^2;
m(7,8)=0;m(8,8)=1/1260*h^2*l^2;
for i=1:8
    ii=i+1;
    for j=ii:8
        m(j,i)=m(i,j);
    end
end
m=ro*l*h*m;
```

---

tapered B

```
%This program calculates the vibration for a tapered beam
%with a thick section, tapered section and thin
section made of mode3l B
E1=113.9e9;E2=7.9856e9;r12=0.288;r21=0.0178;G12=3.138e9;
b=1.0;tp=0.000125;ro=1480;p=0;

npm=4;npta=2;nptm=18;npu=12;
L1=0.1278;
alfa=-2;
alfa=alfa*pi/180;
L2=-12*0.000125/tan(alfa);
L3=0.1278;
ip=3;
%for II=1:4
 %teta1(II)=0;
%end

for II=1:2:18
   J=II+1;
   teta(II)=0;
   teta(J)=90;
end
teta=teta*pi/180;
Qr=3.7e9/(1-0.37^2);

nel=5;                  %number of elements
nnode=nel+1;            % number of nodes
nnel=2;                 %numbe of nodes per element
ndof=4;                 %number of DOF per node
sdof=nnode*ndof;       % system DOF
%
%-----------------------------------------
%input data for nodal coordinates
%gcoord(1)=0.0;  gcoord(2)=0.03;  gcoord(3)=0.06;      gcoord(4)=0.09;
%gcoord=[0 0.2 0.2133 0.2266 0.24 0.44];
%
%nodal connectivity
```

```
%-----------------------------------------------
for i=1:nel
   nodes(i,1)=i;
   nodes(i,2)=i+1;
end
if ip==1
   bcdof=[1 4 sdof-3 sdof];
  elseif ip==2
bcdof=[1 2 sdof-1 sdof];
else
   bcdof=[1 2 sdof-3 sdof-2];
end
bcval=zeros(size(bcdof));
%intialization matrices
kk=zeros(sdof,sdof);
mm=zeros(sdof,sdof);
k=zeros(8,8);
m=zeros(8,8);
for iel=1:1
   %n1=nodes(iel,1);     nr=nodes(iel,2);
   %x1=gcoord(n1);       xr=gcoord(nr);
   %AL=xr-x1;  %element lenght
   l=L1/1;
   np=nptm;
   index=elindex(iel,nnel,ndof);
   [D]=dmatric(E1,E2,G12,teta,r12,r21,np,tp);
   d1=b*D;
   d2=b*D;
   d=b*D;
   A=np*tp;
   [k]=stiffad1(d,d1,d2,l);
   %[Gb]=gbmatad(d1,d2,l);
   [m]=massad1(ro,A,l,d1,d2);
   %stiffness matrix for taper part model A
   [kk,mm]=feasmbl2(kk,mm,m,k,index);
end
%nel1=nel-1;
%nel2=nel1+1;
th=npm+npta+1;
[Q]=Qmat(E1,E2,G12,r12,r21);
th=npm+npta+1;
for iel=2:4
   npt=npta+npm+npu;
   teta1=teta;
   [d1,d2]=d1d2d(Q,b,tp,teta1,Qr,npm,npta,npt,th,nptm,npu);
   l=L2/3;
   index=elindex(iel,nnel,ndof);
   a1=(npt)*tp*b;
   a2=(npt-npm)*tp*b;
   A=(a1+a2)/2;
   t=tp;
   [k1]=kaddB1(d1,d2,Q,t,alfa,l,Qr,teta1,npm,npta,npt,npu);
   %k1=k1*2;
   %[m]=mad3(ro,A,l,d1,d2);
   %[Gb]=gbmatad(d1,d2,l);
   %m=Gb;
   [m]=massad1(ro,A,l,d1,d2);
```

```
    [kk,mm]=feasmbl2(kk,mm,m,k1,index);
    if iel~=4,
       th=th+4
       npta=npta+2;
       npu=npu-4;
    else
    end
end
for iel=5:5
    %nl=nodes(iel,1);     nr=nodes(iel,2);
    %xl=gcoord(nl);       xr=gcoord(nr);
    %AL=xr-xl;  %element lenght
    l=L3/1;
    np=npta;
    index=elindex(iel,nnel,ndof);
    [D]=dmatric(E1,E2,G12,teta,r12,r21,np,tp);
    d1=b*D;
    d2=b*D;
    d=b*D;
    A=np*tp;
    [k]=stiffad1(d,d1,d2,l);
    %[Gb]=gbmatad(d1,d2,l);
    [m]=massad1(ro,A,l,d1,d2);
    [kk,mm]=elasmbl(kk,mm,m,k,index);
end

[kk,mm]=symbc(kk,mm,bcdof);
%
%solution of the system
%--------------------------------------------------------------
[V,Q]=eig(kk,mm);
[LAMBDA,ITEM]=sort(diag(Q));
NEWV=V(:,ITEM);
fr=sqrt(LAMBDA)
```

```
%This program calculates the vibration for a tapered beam
%with a thick section, tapered section and thin section
E2=7.9856e9;
r12=0.288;
r21=0.0178;
G12=3.138e9;
b=1.0;
tp=0.000125;
ro=1480;
p=0;
npm=4;    % note this program is changed to investigate the effects of
h1/h3
npta=14;
nptm=18;
L1=0.1278;
angle=-2;
angle=angle*pi/180;
L2=-12*0.000125/tan(angle);
```

```
%L2=Lt-L1-LTH;
L3=0.1278;
ip=1;
%for II=1:4
 %teta1(II)=0;
%end

for II=1:2:18
   J=II+1;
   teta(II)=0;
   teta(J)=90;
end
teta=teta*pi/180;
Qr=3.7e9/(1-0.37^2);

nel=5;              %number of elements
nnode=nel+1;         % number of nodes
nnel=2;              %numbe of nodes per element
ndof=4;              %number of DOF per node
sdof=nnode*ndof;     % system DOF
%
%----------------------------------------
%input data for nodal coordinates
%gcoord(1)=0.0;  gcoord(2)=0.03;  gcoord(3)=0.06;      gcoord(4)=0.09;
%gcoord=[0 0.2 0.2133 0.2266 0.24 0.44];
%
%nodal connectivity
%----------------------------------------------
for i=1:nel
   nodes(i,1)=i;
   nodes(i,2)=i+1;
end
if ip==1
   bcdof=[1 4 sdof-3 sdof];
  elseif ip==2
bcdof=[1 2 sdof-1 sdof];
else
   bcdof=[1 2 sdof-3 sdof-2];

end
bcval=zeros(size(bcdof));
%intialization matrices
kk=zeros(sdof,sdof);
mm=zeros(sdof,sdof);
k=zeros(8,8);
m=zeros(8,8);
for iel=1:1
   %n1=nodes(iel,1);     nr=nodes(iel,2);
   %x1=gcoord(n1);       xr=gcoord(nr);
   %AL=xr-x1;  %element lenght
   l=L1/1;
   np=nptm;
   index=elindex(iel,nnel,ndof);
   [D]=dmatric(E1,E2,G12,teta,r12,r21,np,tp);
   d1=b*D;
   d2=b*D;
   d=b*D;
```

```
   A=np*tp;
   [k]=stiffad1(d,d1,d2,l);
   %[Gb]=gbmatad(d1,d2,l);
   [m]=massad1(ro,A,l,d1,d2);

   %stiffness matrix for taper part model A
   [kk,mm]=elasmbl(kk,mm,m,k,index);
end
 [Q]=Qmat(E1,E2,G12,r12,r21);
for iel=2:4
   teta1=teta;
   npt=npm+npta;
   [d1,d2]=d1d2c(Q,Qr,npta,npm,teta1,tp);

   %n1=nodes(iel,1);    nr=nodes(iel,2);
   %x1=gcoord(n1);      xr=gcoord(nr);
   %AL=xr-x1;  %element lenght
   l=L2/3;
   index=feeldof1(iel,nnel,ndof);
   a1=(npt)*tp;
   a2=(npt-npm)*tp;
   A=(a1+a2)/2;
   t=tp;
   alfa=angle;
   [k1]=kadC1(Q,t,teta1,alfa,l,Qr,npt,npm,npta,d1,d2);
   [m]=massad1(ro,A,l,d1,d2);
   [kk,mm]=feasmbl2(kk,mm,m,k1,index);
   if iel~=4,
      npta=npta-npm;
   else
   end
end

for iel=5:5
   l=L3/1;
   np=npta;
   index=feeldof1(iel,nnel,ndof);
   [D]=dmatric(E1,E2,G12,teta,r12,r21,np,tp);
   d1=b*D;
   d2=b*D;
   d=b*D;
   A=np*tp;
   [k]=stiffad1(d,d1,d2,l);
   %[Gb]=gbmatad(d1,d2,l);
   [m]=massad1(ro,A,l,d1,d2);


   [kk,mm]=feasmbl2(kk,mm,m,k,index);
end

[kk,mm]=feaplycs(kk,mm,bcdof);

%
%solution of the system
%--------------------------------------------------------------
[V,Q]=eig(kk,mm);
[LAMBDA,ITEM]=sort(diag(Q));
```

```
NEWV=V(:,ITEM);
fr=sqrt(LAMBDA)
```
